The Application of Detrended Fluctuation Analysis and Adaptive Fractal Analysis on Center of Pressure Time Series in Parkinson's Disease

By

Melanie Weilert

Submitted to the graduate degree program in Bioengineering and the Graduate Faculty of the University of Kansas in partial fulfillment of the requirements for the degree of Master of Science.

_____

Chairperson Dr. Carl Luchies

_____

Dr. Huazhen Fang

_____

Dr. Suzanne Shontz

Date Defended: March 15th, 2017

The Thesis Committee for Melanie Weilert

certifies that this is the approved version of the following thesis:

The Application of Detrended Fluctuation Analysis and Adaptive Fractal Analysis on Center of Pressure Time Series in Parkinson's Disease

_____

Chairperson Dr. Carl Luchies

Date approved: March 15th, 2017

Abstract

The long term goal of this thesis is to create quantitative, clinically significant measures that allow for early detection of Parkinson's disease (PD) postural instability (PI), the progression of PI due to PD progression, and ultimately, fall risk in PD patients. Current clinical assessments in PD are not sufficiently sensitive to predict fall risk. Although biomechanical postural sway measures have provided quantitative characterization towards the progression of PI associated with PD progression, these methods are still not sufficiently sensitive to allow for early detection of PD and fall risk. Thus, a need arises for new quantitative methods to be established which can further describe PI progression in PD. This thesis had two overall goals:

- Evaluate the appropriate selection of input parameters of detrended fluctuation analysis (DFA) and adaptive fractal analysis (AFA) in simulated signals.
- Test the sensitivity of AFA, as compared to DFA, towards center of pressure velocity (COPv) time series towards characterization of postural instability (PI) progression in patients with Parkinson's disease.

Specific Aim 1 determined through iterative testing of input parameter combinations that both AFA and DFA are highly sensitive to input parameters when considering fractional Brownian motion (fBm) signals. Input parameter ranges for fBm-like signals in appropriately-large biological data should be examined at maximum window sizes (n_{max}) values between $N/6$ and $N/10$; minimum window sizes (n_{min}) values around 4 to 6 samples; and for fitted polynomial order (M) for AFA to remain first order.

Specific Aim 2 showed that fractal analysis methods may be sensitive towards detecting the development and progression of PI in PD. AFA and DFA were tested on postural sway data collected in a previous study that used mild PD patients (Hoehn and Yahr stage (H&Y) 2,

without postural deficits), moderate PD patients (H&Y 3, with postural deficits), and age-matched healthy controls (HC). AFA produced the most clinically significant measure, H_{fast}, which detected changes in COPv dynamics across smaller time scales than other parameters. These results suggest that components of fractal analysis on COPv time series could be used in concert with traditional quantitative and clinical measures to further enhance the sensitivity of clinical analysis, the understanding of PD PI dynamics and progression, and development of predictive computational simulations of motor and postural control in PD.

Acknowledgments

I am extraordinarily grateful to all of the people in my life who have helped me during my graduate career! Without their unconditional and unwavering support, I would not have succeeded in graduate school. I would like to thank a few people in particular for their help, guidance, and support:

- Dr. Carl Luchies, my advisor and committee chair. I could not have asked for a more encouraging, supportive, and knowledgeable advisor to help guide me through my graduate career. Your thoughtful approach to teaching, mentorship, and research has made me a better person, professionally and personally. I am heartened knowing that I will enter a new phase of my life having learned all I can from you.

- My committee members, Dr. Huazhen Fang and Dr. Suzanne Shontz. Their willingness to meet, discuss, and advise me was integral to my success in writing this thesis. My approach to this study and my research would not be the same without their expertise and advice.

- The Parkinson's disease patients and community members in this study. Without their dedication and volunteerism, this research would not be possible.

- My labmates and coworkers: Camilo, Ember, Mukui, Ednah, and Bhargavi—to name a few. Your friendship, support, encouragement, and help was essential to my life as a graduate student. Without you, I would not be the same person I am today. I am so grateful for the chance to get to know all of you!

- Dr. Jarod Hart for donating his time and expertise to help me hit the ground running with my research!

- My parents, Doris and John Weilert. Words cannot express how your love and support for me in every step of my life has impacted me. I couldn't have done this without you.

- My sister Martha Weilert. You've watched and protected me as I have stumbled through life, always knowing I could lean on you when I was down. Seeing myself through your eyes gave me the confidence to carry on in many situations.

- Finally, my fiancé Jarrett Kille. You are my best friend, my anchor, and my better half. You have been with me every step of the way, good or bad, and never wavered in unconditionally loving and supporting me, no matter the path I chose to take. Thank you for everything. I love you.

Table of Contents

List of Figures

List of Tables

Chapter 1: Introduction

Background and Motivation

Parkinson's disease (PD) is the second most common neurodegenerative disease in the world and is characterized by rigidity, resting tremor, bradykinesia, and postural instability (Alves, Forsaa et al. 2008). Caused by the degeneration of dopamine-producing cells in the basal ganglia (BG), PD interferes with healthy processing of motor, sensory and cognitive information (Centonze, Calabresi et al. 1999). There is no cure for PD, but there are successful treatment regimens used to help alleviate symptoms and improve quality of life. The most common of these is levodopa therapies (Jankovic and Aguilar, 2008).

It is well established that postural instability (PI) increases fall risk in people with PD as compared to aged matched healthy controls (HC) (Bloem and Grimbergen, et al. 2001; Wielinski, Erikson-Davis et al. 2005; McNeely, Duncan et al. 2012; Kim, Allen, et al. 2013). Falls can result in pain, limitation of movement, fear of falling, increased caregiver stress levels, loss of independence, and overall reduced quality of life (Bloem and Grimbergen, et al. 2001; Adkin, Frank et al. 2003; Kim, Allen, et al. 2013). There are two major rating scales used to evaluate PD and PI severity: Unified Parkinson's Disease Rating Scale (UPDRS) and Hoehn and Yahr (H&Y) (Simuni and Pahwa, 2009; Goetz, Poewe et al. 2004). While both are well-regarded and widely used, clinical evaluation measures such as the retropulsion test contain limitations such as unreliable history taking, inconsistent execution of assessments, and unreliable patient self-reporting (Bloem, Beckley et al. 1998; Visser, Marinus et al. 2003). More quantitative clinical assessment measures are needed in order to alleviate some of these limitations in order to accurately determine the severity of PI and fall risk.

Postural sway measures have been widely used in order to understand the relationship between fall risk, PI progression, and PD progression (Schmit, Riley et al. 2005; Chastan,

Debono et al. 2008; Stylianou, McVey et al. 2011; Mancini, Carlson-Kuhta et al. 2012). Common parameters extracted from the Center of pressure (COP) position time series are sway path length, sway area, sway range, peak velocity, and maximal direction (Stylianou, McVey, et al. 2011). COP has been used as a point of investigation to understand the postural control system in context of somatosensory, vestibular, visual, and auditory systems (Mancini, Horak et al. 2011; Hill, Stuart et al. 2016). In addition, recent investigations have been conducted showing that the COP time series s has time-varying statistical properties, indicating that it is a non-stationary signal (Collins and DeLuca, 1993; Schumann, Redfern et al. 1995; Vaillancourt and Newell, 2000; Delignieres, Deschamps et al. 2003; Loughlin, Redfern et al. 2003; Doyle, Newton et al. 2005; Schmit, Riley et al, 2005; Morrison, Kerr et al. 2008; Minamisawa, Takakura et al. 2009; Ramdani, Seigle et al. 2009; Kuznetsov, Bonnette et al. 2012; Harper, 2015). The COP velocity time series has also been identified as containing more valuable information than COP position or acceleration parameters, referencing a postural control model that is based on intermittent velocity-based control (Jeka, Kiemel et al. 2004; Ramdani, Seigle et al. 2009; Delignieres, Torre et al. 2011; Harper, 2015).

Investigations surrounding fractal analysis have yielded promising results in gait and posture research (Collins and DeLuca, 1993; Peng, Havlin et al. 1995; Delignieres, Deschamps et al. 2003; Doyle, Newton et al. 2005; Minamisawa, Takakura et al. 2009; Kuznetsov, Bonnette et al. 2012; Kirchner, Schubert et al. 2014; Harper, 2015). The most striking of these is the emergence of multiple scaling regions while using detrended fluctuation analysis (DFA) and adaptive fractal analysis (AFA) applied on the COP time series (Collins and DeLuca, 1993; Delignieres, Deschamps et al. 2003; Kuznetsov, Bonnette et al. 2012; Harper, 2015), which some have indicated represents an open- and closed- loop mechanism of neural networks relating to

postural control. However, because of the pilot nature of fractal application to COP parameters, care must be taken to correctly represent and translate fractal results from a mathematical to physiological context (Pincus and Goldberger, 1994; Likens, Fine et al. 2015). Both DFA and AFA are fractal methods reliant on input parameters in order to provide accurate results. While there has been some research towards appropriateness of input parameter selection (Caccia, Percival et al. 1997; Cannon, Percival et al. 1997; Riley, Bonnette et al. 2012; Schaefer, Brach et al. 2014), these heavily depend on the context, type, and size of the signal being investigated. To the best of our knowledge, no investigations have yet been conducted regarding appropriateness of input parameters in AFA and DFA towards fBm signals, which best characterize COP time series.

Specific Aims

The purpose of this study was twofold: (1) to evaluate appropriate parameter selection of DFA and AFA using simulated signals and (2) to test the sensitivity of AFA, as compared to DFA, towards COPv system parameters from PI measures in PD patients in order to characterize PI and PD progression. This will allow assessment of fall risk in PD patients and may provide a quantifiable binning method for PD severity. It is hypothesized that scaling behaviors in AFA will result in fractal characterization of postural sway and the strength of fractal behavior will modulate according to PD progression.

Applications of a new method of fractal analysis towards COPv measures and PI progression may help clinical assessments and quantitative characterization of PD progression, such as quantitative binning methods aimed towards diagnosing the severity of PD. It may also help contribute towards a computational model of developing PI in PD patient.

Thesis Content

This thesis contains five chapters. Chapter 1 contains an introduction to the field of studies being conducted. Chapter 2 contains a detailed background investigation of relevant and current literature by which these thesis studies are based. Chapter 3 contains a manuscript of the background, motivation, methods, and results of the study investigating appropriateness of DFA and AFA input parameters when considering fBm signals in context of evaluating PI parameters. Chapter 4 contains a manuscript of the background, motivation, methods, and results of the study on AFA and DFA sensitivity towards PI parameters that characterize PD severity. Chapter 5 summarizes the current studies and provides recommendation for future and related investigations.

References

Adkin, Allan L., James S. Frank, and Mandar S. Jog, 'Fear of Falling and Postural Control in Parkinson's Disease', *Movement Disorders*, 18 (2003), 496–502 <https://doi.org/10.1002/mds.10396>

Alves, Guido, Elin Bjelland Forsaa, Kenn Freddy Pedersen, Michaela Dreetz Gjerstad, and Jan Petter Larsen, 'Epidemiology of Parkinson's Disease', *Journal of Neurology*, 255 (2008), 18–32 <https://doi.org/10.1007/s00415-008-5004-3>

Bloem, Bastiaan R., Dennis J. Beckley, J. Gert van Dijk, Aeilko H. Zwinderman, Michael P. Remler, and Raymund A. C. Roos, 'Influence of Dopaminergic Medication on Automatic Postural Responses and Balance Impairment in Parkinson's Disease', *Movement Disorders*, 11 (1996), 509–21 <https://doi.org/10.1002/mds.870110506>

Bloem, Bastiaan R., Yvette A. M. Grimbergen, Monique Cramer, Mirjam Willemsen, and Aeilko H. Zwinderman, 'Prospective Assessment of Falls in Parkinson's Disease', *Journal of Neurology*, 248 (2001), 950–58 <https://doi.org/10.1007/s004150170047>

Caccia, David C., Donald Percival, Michael J. Cannon, Gary Raymond, and James B. Bassingthwaighte, 'Analyzing Exact Fractal Time Series: Evaluating Dispersional Analysis and Rescaled Range Methods', *Physica A: Statistical Mechanics and Its Applications*, 246 (1997), 609–32 <https://doi.org/10.1016/S0378-4371(97)00363-4>

Cannon, Michael J., Donald B. Percival, David C. Caccia, Gary M. Raymond, and James B. Bassingthwaighte, 'Evaluating Scaled Windowed Variance Methods for Estimating the Hurst Coefficient of Time Series', *Physica A: Statistical Mechanics and Its Applications*, 241 (1997), 606–26 <https://doi.org/10.1016/S0378-4371(97)00252-5>

Centonze, Diego, Paolo Calabresi, Patrizia Giacomini, and Giorgio Bernardi, 'Neurophysiology of Parkinson's Disease: From Basic Research to Clinical Correlates', *Clinical Neurophysiology*, 110 (1999), 2006–13 <https://doi.org/10.1016/S1388-2457(99)00173-X>

Chastan, Nathalie, Bertrand Debono, David Maltête, and Jacques Weber, 'Discordance between Measured Postural Instability and Absence of Clinical Symptoms in Parkinson's Disease Patients in the Early Stages of the Disease', *Movement Disorders*, 23 (2008), 366–72 <https://doi.org/10.1002/mds.21840>

Collins, J. J., and C. J. De Luca, 'Open-Loop and Closed-Loop Control of Posture: A Random-Walk Analysis of Center-of-Pressure Trajectories', *Experimental Brain Research*, 95 (1993), 308–18

Delignieres, Didier, Thibault Deschamps, Alexandre Legros, and Nicolas Caillou, 'A Methodological Note on Nonlinear Time Series Analysis: Is the Open-and Closed-Loop Model of Collins and De Luca (1993) a Statistical Artifact?', *Journal of Motor Behavior*, 35 (2003), 86

Delignières, Didier, Kjerstin Torre, and Pierre-Louis Bernard, 'Transition from Persistent to Anti-Persistent Correlations in Postural Sway Indicates Velocity-Based Control', *PLoS Computational Biology*, 7 (2011) <https://doi.org/10.1371/journal.pcbi.1001089>

Doyle, Tim L., Robert U. Newton, and Angus F. Burnett, 'Reliability of Traditional and Fractal Dimension Measures of Quiet Stance Center of Pressure in Young, Healthy People', *Archives of Physical Medicine and Rehabilitation*, 86 (2005), 2034–40 <https://doi.org/10.1016/j.apmr.2005.05.014>

Goetz, Christopher G., Werner Poewe, Olivier Rascol, Cristina Sampaio, Glenn T. Stebbins, Carl Counsell, and others, 'Movement Disorder Society Task Force Report on the Hoehn and Yahr Staging Scale: Status and Recommendations The Movement Disorder Society Task Force on Rating Scales for Parkinson's Disease', *Movement Disorders*, 19 (2004), 1020–28 <https://doi.org/10.1002/mds.20213>

Harper, Joshua Russell, 'Fractal Analysis of Center of Pressure Velocity Time Series in Parkinson's Disease' (unpublished Thesis, University of Kansas, 2015) <https://kuscholarworks.ku.edu/handle/1808/19412> [accessed 31 October 2016]

Hill, E., S. Stuart, S. Lord, S. Del Din, and L. Rochester, 'Vision, Visuo-Cognition and Postural Control in Parkinson's Disease: An Associative Pilot Study', *Gait & Posture*, 48 (2016), 74–76 <https://doi.org/10.1016/j.gaitpost.2016.04.024>

Jankovic, Joseph, and L Giselle Aguilar, 'Current Approaches to the Treatment of Parkinson's Disease', *Neuropsychiatric Disease and Treatment*, 4 (2008), 743–57

Jeka, John, Tim Kiemel, Robert Creath, Fay Horak, and Robert Peterka, 'Controlling Human Upright Posture: Velocity Information Is More Accurate Than Position or Acceleration', *Journal of Neurophysiology*, 92 (2004), 2368–79 <https://doi.org/10.1152/jn.00983.2003>

Kim, Samuel, Natalie Allen, Colleen Canning, and Victor Fung, 'Postural Instability in Patients with Parkinson's Disease', *CNS Drugs*, 27 (2013), 97–112

Kirchner, Marietta, Patric Schubert, Magnus Liebherr, and Christian T. Haas, 'Detrended Fluctuation Analysis and Adaptive Fractal Analysis of Stride Time Data in Parkinson's Disease: Stitching Together Short Gait Trials', *PLoS ONE*, 9 (2014) <https://doi.org/10.1371/journal.pone.0085787>

Kuznetsov, Nikita, Scott Bonnette, Jianbo Gao, and Michael A. Riley, 'Adaptive Fractal Analysis Reveals Limits to Fractal Scaling in Center of Pressure Trajectories', *Annals of Biomedical Engineering*, 41 (2012), 1646–60 <https://doi.org/10.1007/s10439-012-0646-9>

Likens, Aaron D., Justin M. Fine, Eric L. Amazeen, and Polemnia G. Amazeen, 'Experimental Control of Scaling Behavior: What Is Not Fractal?', *Experimental Brain Research*, 233 (2015), 2813–21 <https://doi.org/10.1007/s00221-015-4351-4>

Loughlin, P. J., M. S. Redfern, and J. M. Furman, 'Nonstationarities of Postural Sway', *IEEE Engineering in Medicine and Biology Magazine*, 22 (2003), 69–75 <https://doi.org/10.1109/MEMB.2003.1195699>

Mancini, Martina, Patricia Carlson-Kuhta, Cris Zampieri, John G. Nutt, Lorenzo Chiari, and Fay B. Horak, 'Postural Sway as a Marker of Progression in Parkinson's Disease: A Pilot Longitudinal Study', *Gait & Posture*, 36 (2012), 471–76 <https://doi.org/10.1016/j.gaitpost.2012.04.010>

Mancini, Martina, Fay B. Horak, Cris Zampieri, Patricia Carlson-Kuhta, John G. Nutt, and Lorenzo Chiari, 'Trunk Accelerometry Reveals Postural Instability in Untreated Parkinson's Disease', *Parkinsonism & Related Disorders*, 17 (2011), 557–62 <https://doi.org/10.1016/j.parkreldis.2011.05.010>

McNeely, Marie E., Ryan P. Duncan, and Gammon M. Earhart, 'Medication Improves Balance and Complex Gait Performance in Parkinson Disease', *Gait & Posture*, 36 (2012), 144–48 <https://doi.org/10.1016/j.gaitpost.2012.02.009>

Minamisawa, Tadayoshi, Kei Takakura, and Takashi Yamaguchi, 'Detrended Fluctuation Analysis of Temporal Variation of the Center of Pressure (COP) during Quiet Standing in Parkinsonian Patients', *Journal of Physical Therapy Science*, 21 (2009), 287–92 <https://doi.org/10.1589/jpts.21.287>

Morrison, S., G. Kerr, K. M. Newell, and P. A. Silburn, 'Differential Time- and Frequency-Dependent Structure of Postural Sway and Finger Tremor in Parkinson's Disease', *Neuroscience Letters*, 443 (2008), 123–28 <https://doi.org/10.1016/j.neulet.2008.07.071>

Peng, C.-K., Shlomo Havlin, and H. Eugene Stanley, 'Quantification of Scaling Exponents and Crossover Phenomena in Nonstationary Heartbeat Time Series', *Chaos*, 5 (1995), 82

Pincus, S. M., and A. L. Goldberger, 'Physiological Time-Series Analysis: What Does Regularity Quantify?', *American Journal of Physiology - Heart and Circulatory Physiology*, 266 (1994), H1643–56

Ramdani, Sofiane, Benoît Seigle, Julien Lagarde, Frédéric Bouchara, and Pierre Louis Bernard, 'On the Use of Sample Entropy to Analyze Human Postural Sway Data', *Medical Engineering & Physics*, 31 (2009), 1023–31 <https://doi.org/10.1016/j.medengphy.2009.06.004>

Schaefer, Alexander, Jennifer S. Brach, Subashan Perera, and Ervin Sejdić, 'A Comparative Analysis of Spectral Exponent Estimation Techniques for 1/fβ Processes with Applications to the Analysis of Stride Interval Time Series', *Journal of Neuroscience Methods*, 222 (2014), 118–30 <https://doi.org/10.1016/j.jneumeth.2013.10.017>

Schmit, Jennifer M., Michael A. Riley, Arif Dalvi, Alok Sahay, Paula K. Shear, Kevin D. Shockley, and others, 'Deterministic Center of Pressure Patterns Characterize Postural Instability in Parkinson's Disease', *Experimental Brain Research*, 168 (2005), 357–67 <https://doi.org/10.1007/s00221-005-0094-y>

Schumann, Timothy, Mark S. Redfern, Joseph M. Furman, Amro El-Jaroudi, and Luis F. Chaparro, 'Time-Frequency Analysis of Postural Sway', *Journal of Biomechanics*, 28 (1995), 603–7 <https://doi.org/10.1016/0021-9290(94)00113-I>

Simuni, Tanya, and Rajesh Pahwa, *Parkinson's Disease* (Cary, US: Oxford University Press, USA, 2009) <http://site.ebrary.com/lib/alltitles/docDetail.action?docID=10375051> [accessed 28 August 2016]

Stylianou, Antonis P., Molly A. McVey, Kelly E. Lyons, Rajesh Pahwa, and Carl W. Luchies, 'Postural Sway in Patients with Mild to Moderate Parkinson's Disease', *International Journal of Neuroscience*, 121 (2011), 614–21 <https://doi.org/10.3109/00207454.2011.602807>

Vaillancourt, David E, and Karl M Newell, 'The Dynamics of Resting and Postural Tremor in Parkinson's Disease', *Clinical Neurophysiology*, 111 (2000), 2046–56 <https://doi.org/10.1016/S1388-2457(00)00467-3>

Visser, Martine, Johan Marinus, Bastiaan R Bloem, Hannah Kisjes, Barbara M van den Berg, and Jacobus J van Hilten, 'Clinical Tests for the Evaluation of Postural Instability in Patients with Parkinson's disease1', *Archives of Physical Medicine and Rehabilitation*, 84 (2003), 1669–74 <https://doi.org/10.1053/S0003-9993(03)00348-4>

Wielinski, Catherine L., Cordelia Erickson-Davis, Rose Wichmann, Maria Walde-Douglas, and Sotirios A. Parashos, 'Falls and Injuries Resulting from Falls among Patients with Parkinson's Disease and Other Parkinsonian Syndromes', *Movement Disorders*, 20 (2005), 410–15 <https://doi.org/10.1002/mds.20347>

Chapter 2: Background

Parkinson's Disease

Epidemiology

Parkinson's disease (PD) is a progressive, neurodegenerative disorder that affects approximately 1 million people in the United States and 5 million people worldwide, to an estimated total of 0.3% of the world's population (Alves, Forsaa et al. 2008; Wirdefeldt, Adami et al. 2011). PD affects 1 to 2% of people older than 60, making it the second most common neurodegenerative disorder in the world (Olanow, Stern et al. 2009). This number increases to 3 to 5% in people aged 85 and older (Alves, Forsaa et al. 2008). Diagnosis usually occurs around the age of 60, with only 10% of diagnoses occurring when the patient is under the age of 40 (Wirdefeldt, Adami et al. 2011). The chances of being diagnosed increase as the population ages, with men 1.5 times more likely to be affected by PD than women (Lees, Hardy et al. 2009). PD has not been found to be related to race or ethnic origins, though due to methodological differences in studies, not much is known regarding geographic prevalence of PD (Alves, Forsaa et al. 2008). In 2010, estimates stated that 630,000 people in the United States had been diagnosed with PD, with an estimated national financial cost in 2010 dollars of over $14.4 billion and indirect costs exceeding $6 billion (Kowal, Dall et al. 2013).

Etiology and Neurophysiology

The etiology of PD is complex and has been investigated with respects to a wide range of genetic and environmental factors. However, it is well established that PD is characterized by four key attributes: resting tremor, bradykinesia, rigidity, and postural instability (PI) (Wirdefeldt, Adami et al. 2011). PD is caused by degeneration of dopaminergic neurons in the brain. The loss of these dopamine-containing cells results in decreased activity in the motor cortex. This occurs in the substantia nigra pars compacta (SNc), which is located in the basal

ganglia (BG). The BG is located in the forebrain, and is responsible for processing the flow of motor, sensory, and cognitive information (Centonze, Calabresi et al. 1999). Noticeable symptoms of PD start emerging when approximately 50 to 60% of the dopaminergic cells have died and more than 80% of the dopamine has been lost. There has been progress made in identifying genes relating to PD that shed light on different molecular mechanisms, but the pathogenesis of these mechanisms in relation to PD are still not well understood (Wirdefeldt, Adami et al. 2011).

Symptoms, Diagnosis, and Therapies of PD

Motor Symptoms

Once symptoms begin to appear in PD patients, there are four cardinal motor symptoms that begin to emerge: resting tremor, rigidity, bradykinesia, and postural instability (Simuni and Pahwa, 2009). Resting tremor is defined as an involuntary movement with approximate rhythmic and sinusoidal characteristics. These movements often have distinguishing amplitude and frequency profiles. In about 70% of PD patients, resting tremor exhibits a modal frequency of approximately 4 to 6 Hz (Vaillancourt and Newell, 2000). Resting tremor can affect one or more parts of the body such as the hands and arms, depending on the severity of PD. It is classified based off the circumstances of appearance, the frequency of the tremor, and the affected body area (Camara, Isasi, 2015). Rigidity, defined as stiffness in the muscles, most commonly seen in PD in the form of "cogwheeling", which presents as a "ratchety" sensation combined with passive joint movement (Simuni and Pahwa, 2009). Bradykinesia, or slowness of movement is a symptom associated with most BG disorders and can be observed in various motor activities. While largely thought to be a manifestation of motor slowness as a result of the degeneration of dopaminergic cells in the SNc, the physiological cause of bradykinesia is not well understood

(Shiner, Seymour, et al. 2012). Postural instability (PI) is the last cardinal motor symptom. PI can be present at diagnosis of PD and will worsen as PD progresses (Kim, Allen, et al. 2013). PI is one of the most debilitating symptoms of PD due to the high correlation of PI and fall risk, which can lead to considerable morbidity and mortality in PD patients (Wielinski, Erikson-Davis, et al. 2005). Even when patients are optimally medicated, there is a 40 to 70% chance PD patients will experience a fall. Upon experiencing a fall, fear of falling often develops (Kerr, Worringham, et al. 2010). Fear of falling, which results from PI as PD progresses, can have several negative impacts on a patient's quality of life including lack of confidence, depression, social isolation, loss of independence, and can provide a major barrier towards engaging in exercise (Kerr, Worringham, et al. 2010; Lindholm, Hagell, et al. 2013).

Non-Motor Symptoms

In addition to motor symptoms, other non-motor symptoms have become increasingly recognized to develop alongside or even before the four cardinal motor symptoms emerge. These non-motor symptoms can include sleep disorders, gastrointestinal disorders, orthostatic hypotension, and cognitive and neuropsychiatric disorders such as depression (Lim and Lang, 2010). Non-motor aspects of PD can be equally if not more disabling towards quality of life than motor-symptoms of PD and are often not identified in neurological consultations for PD (Simuni and Pahwa, 2009).

Diagnosis

PD is a neurodegenerative disorder that does not contain distinct neurological attributes able to be detected via neuroimaging or biomarker techniques. Because of this, it is difficult to determine when a patient is actually suffering from PD. The majority of clinical PD diagnoses

relies on the clinical observation of parkinsonian symptoms in combination with patient history and their response to dopaminergic therapy (Wirdefelt, Adamit, et al. 2011; Factor and Weiner, 2009). However, key non-motor symptoms related to parkinsonian-like conditions may be taken into consideration such as sleep disorders, sensory symptoms, depression, and gastrointestinal features. This is because some of these symptoms may precede the cardinal motor symptoms of PD and allow for an earlier diagnosis (Factor and Weiner, 2009; Gaig and Tolosa, 2009).

Therapies

There is no known cure for PD. However, there are several successful treatment strategies used to reduce parkinsonian symptoms. The most common of these is levodopa, though catechol-o-methyl transferase inhibitors and nondopaminergic agents can also be found (Jankovic and Aguilar, 2008). Levodopa is the most potent of these treatments, particularly towards bradykinesia. However, levodopa therapies have been associated with motor complications, raising the question about when in the course of PD is it appropriate to begin levodopa therapies (Jankovic and Aguilar, 2008; Lees, Hardy et al. 2009; McNeely, Duncan et al. 2012). There have been many contradicting reports in the role of "ON" levodopa medication and the role it plays in increasing PI and subsequently, fall risk. However, it has been observed that this is a hard symptom to quantify, since functional balance may improve with levodopa treatments while other balance and gait impairments may remain (McNeely, Duncan et al. 2012).

Rating of PD Progression

The two major rating scales used to evaluate and rank PD severity are the Unified Parkinson's Disease Rating Scale (UPDRS) and Hoehn and Yahr (H&Y) (Simuni and Pahwa,

2009; Goetz, Poewe et al. 2004). While both of these rating scales are widely used, they differ in some aspects in their approach to rating a patient.

The UPDRS scale takes a holistic approach to the functionality and quality of life of the patient by involving four scoring stages: 1) Mentation behavior and mood; 2) Activities of daily living; 3) Motor examination; and 4) Complications of therapy. The third stage is rated by the clinician and examines the cardinal symptoms of PD such as movement, balance, speech, and expression. The other three stages (one, two and four) are written examinations that address issues such as cognitive and mental health, ability to live independently, and complicating factors of the patient (Simuni and Pahwa, 2009).

The H&Y scale has a more acute focus on motor ability and balance. It is based on the concept that PD symptoms relate closely to PI and issues with bilateral motor involvement. Both the UPDRS and H&Y have been updated in the past 15 years by the Movement Disorder Society Task Force for Rating Scales in PD. Originally, the H&Y was designed to be a scale that descriptively characterized PD symptoms over a five point scale. However, since its conception in the 1990s, the H&Y has been updated. While maintaining an overall scale of 0 to 5, it now encompasses increments of 0.5 in order to help facilitate rating in clinical trials (Goetz, Poewe et al. 2004). Below is a summary of the stages of H&Y ratings.

Stage 0 – No signs of disease.

Stage 1 – Unilateral disease.

Stage 1.5 – Unilateral plus axial involvement.

Stage 2 – Bilateral disease, without impairment of balance.

Stage 2.5 – Mild bilateral disease with recovery on pull test.

Stage 3 – Mild to moderate bilateral disease; some postural instability; physically independent.

Stage 4 – Severe disability; still able to walk or stand unassisted.

Stage 5 – Wheelchair bound or bedridden unless aided. (Goetz, Poewe et al. 2004)

While both the UPDRS and H&Y scales are widely used and well regarded, concerns have been raised about whether these and other clinical rating methods contain the sensitivity required to accurately and quantitatively characterize the progression of PD. These rating scales, combined with clinical evaluation measures such as the retropulsion test contain limitations such as unreliable history taking, inconsistent execution of motor and balance examinations, and unreliable patient self-reporting of written examinations (Bloem, Beckley et al. 1998; Visser, Marinus et al. 2003). This raises a question of whether there exists a more quantitative and objective way to measure and rank PD such that progression is accurately characterized.

Postural Instability and Fall Risk in PD

It is well established that postural instability and fall risk increase as PD progresses. PI is consistently identified as one of the greatest risk factors for falls, which are nine times more likely to occur in PD patients than their healthy counterparts (Bloem and Grimbergen, et al. 2001; Wielinski, Erikson-Davis et al. 2005; McNeely, Duncan et al. 2012; Kim, Allen, et al. 2013). Both PI and falls have far-reaching consequences for the patient including pain, limitation, fear of falling, and high levels of caregiver stress. These result in a loss of independence for the patient and an overall reduced quality of life (Bloem and Grimbergen, et al. 2001; Adkin, Frank et al. 2003; Kim, Allen, et al. 2013). Many efforts have been made to identify the precise relationship between PI in people with PD and falls, however the characterization is more complex than that, with many other risk factors acting as modulators

such as: cognition, leg weakness, poor balance, freezing of gait, and others (Kim, Allen, et al. 2013).

Parkinson's and Postural Sway Analysis

Center of Pressure

PI progression in PD is a critical marker of disease progression in both UPDRS and H&Y (Goetz, Poewe et al. 2004; Simuni and Pahwa, 2009). Using postural sway as a quantifiable method of measurement of PI, investigators have been better able to understand the relationship between PI and postural sway and, consequently, PD progression (Schmit, Riley et al. 2005; Chastan, Debono et al. 2008; Stylianou, McVey et al. 2011; Mancini, Carlson-Kuhta et al. 2012). It has also been suggested that postural sway analysis is a method by which early clinical symptoms of PD could be detected due to a characteristic altered balance modulation strategy (Chastan, Debono et al. 2008; Mancini, Carlson-Kuhta et al. 2012).

The most common measure of postural sway that is used to quantify PI in PD patients is the center of pressure (COP) time series. It has been shown that there is a stark difference in the parameters extracted to describe the COP time series of healthy older adults versus older adults with PD (Schmit, Riley et al. 2005). The location of the COP as a function of time is a calculation based on the measurement of the forces and moments that the base of support (in this case, feet) exerts on the floor. The combination of moments and forces in this COP equation results in the location of the resultant force of the base of support during stance. Over time, this point-location of the resultant force forms a path that is dependent on the placement of foot as well as muscular and neuromotor control of the body, particularly the legs and feet. Because of this, the COP time series is often interpreted as the neuromuscular response of the body with respects to inner and outer perturbations or changes of the center of mass (COM) location. COP

is most commonly collected though a patient standing on a force plate in a quiet, quasi-static stance. The surface of the force plate is usually treated as the x-y plane in 3-dimensional space, so the equation for COP in the x-y plane can be expressed as:

$$COPx = \frac{M_y + F_x \times d_z}{F_z}$$

$$COPy = \frac{M_x + F_y \times d_z}{F_z}$$

where COPx is the COP position in the x-direction, COPy is the COP position in the y-direction, F_x and F_y are forces parallel to the top of the force plate, F_z is the normal force with respects to the force plate surface, M_x and M_y are the moments parallel to the force plate and d_z is the distance below the surface of the force plate at which the origin of its coordinate system is located.

COP and Postural Control Systems

COP is also well regarded as an indicator for a postural control system that includes somatosensory, vestibular, visual and auditory systems. The postural control system is a combination of these systems and the integration of the central nervous system (CNS), which processes these different signals (Mancini, Horak et al. 2011; Hill, Stuart et al. 2016). This makes it an ideal candidate for investigations regarding characterization of PI in PD and fall risk in PD. Much progress has been made investigating how COP characterizes key features in PD using measures such as sway path length, sway area, sway range, velocity, accelerations, and directional sway of COP (Horak, Dimitrova, et al. 2005; Mancini, Horak et al. 2011; Stylianou, McVey, et al. 2011; McNeely, Duncan, et all 2012). These investigations have found that PD, compared to healthy controls (HC) have been found to produce larger sway path lengths, larger sway areas, larger ranges, and larger velocities and accelerations.

However, though these results are fairly intuitive, much research has been done regarding the development of control systems, models, and the integration of other cardinal symptoms of PD in the use of characterizing PD though COP measures. Rigidity, resting tremor, and bradykinesia have all been shown to have a significant effect on the postural control system of a PD patient (Vaillancourt and Newell 2000; Morrison, Kerr et al. 2008; Kerr, Morrison et al. 2008; Bartolic, Pirtosek et al. 2010; Park, Roemmich et al. 2016). Bartolic et al. posited in 2009 that increased activity and increased synchronization of central oscillators in the basal ganglia (BG) in the CNS is the reason for clinically evident tremor. However, if only one of these features is present, tremor is not apparent on a clinical level. Bartolic et al. tested this by measuring amplitude and frequency of tremor over time. The results indicate that detectable amplitude of parkinsonian tremor is indeed a product on synchronization and activity of central oscillators in the BG (Bartolic, Pirtosek et al. 2010). Upon dopaminergic treatment of PD, the synchronization is de-coupled, and tremor becomes clinically unapparent. This sheds light on physiological bases for postural control and the effects of PD on their neurological systems as well as the effects of medication in detection and diagnosis of worsening parkinsonian symptoms.

Park et al. recently demonstrated that PD patients have decreased complexity of hip and ankle joint movements and an increased rate of asymmetry between limb-couplings while walking at a self-selected speed on a treadmill for three to five minutes. These findings correlate with a previous study using postural sway and kinematic marker data from quiet standing with eyes open (EO) and eyes closed conditions (EC) by Sasagawa et al. showing similar effects in PD. Sasagawa et al. noted that this could have a substantial effect on the measurements

pertaining to body kinematics, especially rigidity (Sasagawa, Ushiyama et al. 2009; Park, Roemmich et al. 2016).

Investigations regarding parkinsonian tremor have also produced interesting results regarding postural control and a nonlinear, stochastic structure of organization. Kerr et al. investigated the effects of limb tremor and postural sway in PD. They found that PD participants in the study had a single prominent peak of tremor frequency between 4 and 7 Hz, which contrasted with young and older participants with smaller peaks between 1 to 4 and 7 to 12 Hz, but lacked the 4 to 7 Hz peak that was characteristic for the PD participants. No prominent peaks were seen in young and older participants. This study showed that tremor can be manifested in COP measures and dynamics (Kerr, Morrison et al. 2008).

While these patterns prove useful tools in detection and diagnosis of PD, they also raise the question of whether the collection of these cardinal motor symptoms—bradykinesia, resting tremor, and rigidity—are the reason for the differences in HC and PD patients in COP measures. Morrison et al. addressed this through investigations of postural sway and finger tremor in PD patients, showing that there was a lack of correlation between inter-limb tremor in parkinsonian patients (Morrison, Kerr et al. 2008).

Non-Stationarity of COP

Based on the previous section, analysis of the COP time series clearly provides valuable information regarding the effect that PD has on the ability to maintain balance during quiet standing. However, recently more documentation has been published regarding the non-stationary and nonlinear nature of the COP time series and thus, postural dynamics. This is because measures of postural sway are a time series—data obtained at successive times, often with equal intervals between them. They result from a dynamical system that is evolving over

time, not a constant measure that can simply be averaged over time or across multiple trials. A popular method is to low-pass filter the COP time series in an effort to eliminate frequencies above the cutoff frequency, which are considered "noise". Two concerns have been raised regarding this approach. First, the COP time series may not be stationary, which is an assumption behind the frequently used filtering methods. Second, the variability removed from the signal during the filtering process may contain valuable information regarding the dynamical system being studied. Therefore, more attention has been given to postural sway as a time series, including its non-stationary nature and inherent variability as a dynamical system.

A non-stationary signal is a signal that has time-varying statistical properties, such as mean and standard deviation. Investigations have been conducted on a wide range of nonstationary (also known as "nonlinear") methods in order to discern patterns of non-stationarity in COP measures. Some of these methods include time frequency analysis (Schumann, Redfern et al. 1995; Loughlin, Redfern et al. 2003), entropy (Cavanaugh, Mercer et al. 2007; Vaillancourt and Newell, 2000; Morrison, Kerr et al. 2008; Ramdani, Seigle et al. 2009), regression quantification analysis (RQA) (Schmit, Riley et al, 2005), fractal analysis (Collins and DeLuca, 1993; Delignieres, Deschamps et al. 2003; Doyle, Newton et al. 2005; Minamisawa, Takakura et al. 2009; Kuznetsov, Bonnette et al. 2012; Harper, 2015) and investigated the nonstationary properties of motor mechanisms (Cavanaugh, Guskiewicz et al. 2005; Stergiou and Decker, 2011). These nonlinear methods of analysis do not rely on traditional assumptions of single stationarity and often use nonlinear systems of equations or recurrence relations to characterize the signal.

An excellent example of the value of nonstationary methods is a study mentioned above. In 2000, Vaillancourt et al. demonstrated that tremor displays time-dependent organization and

that despite no clinical observations of tremor, PD patients show increased regularity and redistribution of power in their tremor patterns. This time-dependent organizational structure was characterized by using approximate entropy (ApEn), a nonlinear analysis method by which entropic regularity is exhibited. As opposed to HC, PD patients exhibited greater regularity in their tremors, drawing a correlation between activities in neural control with regularity of seemingly "passive" tremors. The investigators also display that these characteristics of postural and resting tremor are indicative of a method by which earlier assessments and diagnosis of PD symptoms may be made, since regularity was detected in patients that, clinically, were not noted to have significant parkinsonian tremor (Vaillancourt and Newell, 2000).

Morrison et. al. also exhibited the nonstationary properties of COP in parkinsonian patients. ApEn, time-frequency analysis and synchrony analysis, time- and frequency-dependent patterns of COP were investigated. Increased regularity in parkinsonian tremor was found, supporting Vaillancourt's study published in 2000. In addition to this, COP measures were deemed to have a greater degree of complexity in PD patients as compared to HC. Synchrony was also investigated between inter-limb tremor and no correlation was found (Vaillancourt and Newell, 2000; Morrison, Kerr et al. 2008). This implies that both postural tremor and postural sway, as characterized by COP measures, are likely resulting from neural control signals and not mechanical wave transmissions brought upon by parkinsonian motor symptoms such as bradykinesia, rigidity, and tremor. These findings emphasize the relationship of PD and the stochastic, underlying neural mechanisms surrounding postural control as well as highlight the value of COP and postural control measures in characterizing these mechanisms to help with both physiological and clinical assessments of PD.

COP Velocity

In addition to an increase in regard for the non-stationary properties of COP position, more attention has also been given to COP velocity (COPv) and the non-stationary properties that this signal exhibits (Jeka, Kiemel et al. 2004; Ramdani, Seigle et al. 2009; Delignieres, Torre et al. 2011; Harper, 2015). Jeka et al. describes velocity measures as the most sensitive signal towards postural sway feedback control when considering position, velocity, and acceleration (Jeka, Kiemel et al. 2004). Feedback from velocity-based mechanisms are now being regarded as the most accurate and sensitive signals that the neural controller mediates.

This claim is further supported by Delignieres in 2011, where it is argued that velocity feedback's sensitivity stems from a velocity-based, intermittent neural controller (Delignieres, Torre et al. 2011). This claim is also supported from several previous investigations of Delignieres in 2003 and 2006 that took a critical look at fractal analysis of COP measures to determine the appropriate use of non-stationary methodologies when looking at postural control mechanisms (Delignieres, Deschamps et al. 2003; Delignieres, Ramdani et al. 2006). This effort was based off of previous assertions by the pioneering study in 1993 by Collins and De Luca in which postural control mechanisms were characterized with open- and closed-loop systems based off of the results of fractal investigations using COP measures. This approach will be discussed later in this chapter (Collins and De Luca, 1993).

Fractal Analysis of Postural Instability Measures

Through the development and refinement of different nonlinear analysis techniques, it has been revealed that physiological processes exhibit strong fractal behavior. Furthermore, through the use of fractal analysis, this behavior can be characterized to reveal new insights

about nonstationary stochastic patterns that were unavailable to us before. For example, scientific studies have used fractal analysis to reveal new insights into forest fire progression (Turcotte, Malamud et al. 2002), gene expression (Aldrich, Horsley et al. 2010), DNA coding patterns, space-filling properties of tumors, and viral infections (Cross, 1997).

There are two kinds of fractal processes that are discretely sampled: 1) fractional Gaussian noise (fGn) and 2) fractional Brownian motion (fBm). fGn is considered to be a stationary signal while fBm is considered to be non-stationary with time-dependent variance (Delignieres, Torre et al. 2011). It is important to note that both fGn and fBm are related signals. The integration of fGn noise will exhibit fBm signal properties. This means that the identification of the signal as fGn or fBm is important when beginning to analyze data using fractal methods (Eke, Herman et al. 2000). Both fGn and fBm processes are considered "long memory" processes, which means that they will exhibit statistical correlations over long time scales, as opposed to adjacent (or nearly adjacent) correlations (Riley, Bonnette et al. 2012). The variance of displacement for a fBm process is a power function that follows the scaling law:

$$SD(\Delta x) \propto \Delta t^{H}$$

where $SD(\Delta x)$ is a variance of the displacement of the time series and Δt^{H} represents the power scaling law over various time intervals and scales. H is the Hurst exponent, and is considered the power law scaling parameter.

Ranging from 0 to 1, H represents the diffusion property specific to fBm processes. As H increases, the more "diffusive" the behavior of the fBm "long memory" signal (Delignieres, Torre et al. 2011). Since the fBm system of H scaling is centered on 0.5, the resultant H value can tell an investigator much about the system that is being investigated. An H value of $0 < 0.5$ indicates an anti-correlated (also referenced as "anti-persistent") process. This means that

increases of the signal are likely to be followed by decreases, and vice versa. An H value of $0.5 < 1$ indicates a correlated (also referenced as "persistent") process. This means that increases of a signal are likely to be followed by further increases, and vice versa. Persistent processes are associated with positive "long memory" correlations and anti-persistent processes are associated with negative "long memory" correlations (Riley, Bonnette et al. 2012).

Detrended Fluctuation Analysis

Detrended Fluctuation Analysis (DFA) is a widespread application of fractal analysis that is useful in determining statistical patterns not available through conventional means. DFA uses a detrending algorithm by which fluctuations are analyzed through residual scaling of first-order polynomial regression of "windows" in the signal that increase in size. There are many applications of DFA, including in the field of biological data and gait and posture research (Collins and DeLuca, 1993; Peng, Havlin et al. 1995; Delignieres, Deschamps et al. 2003; Doyle, Newton et al. 2005; Minamisawa, Takakura et al. 2009; Kuznetsov, Bonnette et al. 2012; Kirchner, Schubert et al. 2014; Harper, 2015).

DFA made its debut in applications towards biological data in 1995 in order to analyze the fluctuations of heartbeat intervals between healthy and non-healthy patients. The interbeat segment of a heartbeat cycle is well-known to be an irregular, non-stationary process. The estimation of H, which is the resultant value of DFA, comes from the slope of the power scaling law described above. In Peng et al, it was discovered that multiple scaling regions—and therefore, multiple H values—were displayed in this power scaling logarithmic plot, with a "crossover point" on the log scale indicating the separation between these two regions.

This result is interesting, since purely fBm and fGn signals should only show one scaling region. The existence of more than one scaling region is indicative of additional mechanisms

existing in biological data and are not immediately apparent. Peng et al. drew the correlation between these multiple scaling regions to long- and short- range scaling indicators of healthy and unhealthy heart interbeat values (Peng, Havlin et al. 1995). This analysis of multiple scaling regions and crossover points in DFA was further explored by Collins and De Luca in 1993 with respects to COP position time series. The bi-logarithmic plot comparing fluctuation versus scale also showed two scaling regions for H, which Collins and De Luca compared to the open- and closed-loop neural circuitry of the brain in motor control (Collins and DeLuca, 1993). The short- and long- range phenomenon has also been exhibited for COP velocity time series (Delignieres, Torre et al. 2011).

Adaptive Fractal Analysis

Adaptive fractal analysis (AFA) is a relatively new fractal analysis method that has gained popularity in recent years. Utilizing an adaptive detrending algorithm, AFA extracts globally smooth trend signals to analyze the scaling of residuals to the fit of the original signal. AFA differs from DFA in that it provides a globally smooth fit across the signal, providing a "stitching" step that DFA does not (Riley, Bonnette et al. 2012). AFA has been proposed as an alternative to DFA because it is believed to handle arbitrary, non-linear trends with more efficiency, provides better resolution of fractal behavior over smaller signal lengths, and provides direct interpretation of spectral energy, while DFA does not (Gao, Hu et al. 2011; Riley, Bonnette et al. 2012). AFA has successfully been applied towards biological signals that more robustly describe the nonlinear patterns, such as heart rate variability in the field of cardiology (Gao, Gurbaxani et al. 2013).

Because of the pilot-nature of this method, there has not been a significant amount of literature published on AFA in the field of gait and posture research (Kuznetsov, Bonnette et al.

2012; Riley, Bonnette et al. 2012; Kirchner, Schubert et al. 2014). However, none of these studies has investigated COP velocity time series or applications of AFA towards PD patients. Because it is predicted that AFA is better suited to handling smaller timer series and processing more "arbitrary" signals due to the globally smooth stitching step, there is value in testing the sensitivity of AFA to COP velocity time series of PD patients. It is well documented that as PD severity increases, postural parameters begin to act more erratically, with a wider, more variable sway path than healthy counterparts (Mancini, Horak et al. 2011; Stylianou, McVey, et al. 2011). Therefore, it is hypothesized is the present study that AFA will be sensitive to the increase in unpredictability and provide further insight into the changing motor control patterns observed in PD patients.

Parameter Selection in Fractal Methods

Although DFA and AFA provide excellent tools for nonlinear interpretations of data, it is important that these tools be used correctly. There is not a clear consensus on the appropriate selection of the input parameters used in these tools. Often the parameters are selected without published justification. Several studies have noted that both DFA and AFA exhibit a high dependence on input parameters and that care should be used when selecting these parameters (Caccia, Percival et al. 1997; Cannon, Percival et al. 1997; Riley, Bonnette et al. 2012; Schaefer, Brach et al. 2014).

Several input parameters need to be considered when setting up fractal methods for application on biological data. Three major input parameters of DFA are: data length (N), minimum window size (n_{min}) and maximum window size (n_{max}) (Caccia, Percival et al. 1997; Cannon, Percival et al. 1997). It is advised to reduce estimate bias and variance by excluding certain window sizes when performing fractal analysis. The variance of displacement, depicted

in the power scaling law discussed above, indicates that the size of the window is subject to statistical artifacts and might result in misleading measures. Small windows sizes may not capture relevant attributes of a correlated signal and tend to calculate standard deviation with too few number of samples to be statistically reliable. Conversely, when windows are too large, fewer windows remain to average out the variance of displacement, reducing the variance that the H exponent estimates (Cannon, Percival et al. 1997).

Four major input parameters of AFA are: data length (N), minimum window size (n_{min}), maximum window size (n_{max}), and order of polynomial fit towards residual fluctuation (M) (Riley, Bonnette et al. 2012). As described above, N, n_{min}, and n_{max} are subject to strict considerations similar to DFA. The order of polynomial fit used (M) is a unique parameter to AFA, and has not been subject to parameter investigations.

These input parameters stated above all provide different challenges and considerations. The most commonly discussed of these parameters is length of the data (i.e. signal length, data length, data size, time series length). Estimates for short time series can be unreliable in fractal analysis; for example, Cannon et al. advised that N remain over 215 "significant" samples in order to have a 95% probability of differentiating true H values by a resolution of 0.1 (Cannon, Percival et al. 1997). Samples smaller than these are unreliable and not appropriate for fractal analysis. The "significance" of these samples should be enough to fully characterize the intrinsic dynamics of the signal, regardless of the frequency of data collection. Oversampling will not enhance the results of fractal analysis and is not an appropriate substitute when addressing the issue of short data series and the proper application of fractal methods (Stergiou, 2016). Cannon et al. also addresses the ambiguity of window size selection. Maximum and minimum window sizes have typically been selected at the discretion of the investigator, but inappropriate selection

could lead to either misleading or missing patterns. If too many window sizes are deemed inappropriate, underlying signals could be lost due to overly conservative selection. If too few window sizes are deemed inappropriate, putative patterns in the data could emerge that are merely statistical artifacts (Cannon, Percival et al. 1997). Caccia et al. suggests that the Hurst exponent estimated by fractal methods exhibits bias at certain H ranges, thereby reducing accuracy of the estimation. They uncovered that for an fGn process, dispersional analysis (a common form of fractal analysis) is unbiased for $H < 0.9$ and series length $N > 1024$. However, when $H > 0.9$, dispersional analysis begins to underestimate H. Rescaled range analysis methods overestimates H for signals with $H<0.7$ and underestimates H for $H>0.7$ (Caccia, Percival et al. 1997). This variability in accuracy raises a question of whether certain parameters are better suited towards estimation of certain H exponent ranges. Additionally, because of the bi-logarithmic nature of the plots, it can be confusing on how to best handle H exponent estimates derived from these plots. Literature has also been published suggesting guidelines on how best to approach calculating slope estimates in order to help clarify ambiguities in the calculation process (Almurad and Delignieres, 2016). Finally, Riley et al. cautions that *M* typically should remain either first or second order, because higher orders of residual calculations could lead to "overfitting", or an inflation of the Hurst exponent (Riley, Bonnette et al. 2012).

These studies provide helpful guidelines on general appropriateness of applications of fractal methods. However, depending on the type of signal being considered, the nature of the experimental data, and the input parameters used on AFA and DFA, the circumstances can change. This is particularly true when the experimental data collected in a biological field results in multiple scaling regions from fractal analysis. Chapter 3 in this thesis seeks to provide insight regarding the effect of parameter selection on the results of AFA and DFA when applied to fBm

signals. The selection of appropriate parameters for the analysis of COPv time series is of special interest for this study. Similar parameter investigations have been done on approximate entropy and sample entropy nonlinear methods (Yentes, Hunt et al. 2012).

Limitations to Fractal Methods

With the use of nonlinear analysis tools becoming more widespread, it is also important to clearly define what the results of these methods mean in a physiological context. As Pincus and Goldberger commented in 1994, applications of nonlinear methods may be made incorrectly, or without justifiable basis. The transition of mathematical results to physiological interpretations can sometimes become "lost in translation" and incorrect assumptions made about the phenomena being observed (Pincus and Goldberger, 1994; Likens, Fine et al. 2015). In fractal analysis, it is important to understand that H does not clearly determine patterns such as "randomness of a signal", "chaos of a signal" or other such cut-and-dry assertions. Delignieres raised such concerns regarding Collins and De Luca's 1993 study, in which they proposed that the transition of persistent to anti-persistent signal in fractal methods was representative of an open- and closed-loop mechanism in postural control by which the neural controller could be characterized (Collins and DeLuca, 1993; Delignieres, Torre et al. 2011). The analysis of the COP position time series using fractal methods have, at times, resulted in up to three scaling regions in the resulting bi-logarithmic plot. Because of this, certain fractal methods were suggested as potentially unsuitable for analyzing COP position time series (Kuznetsov, Bonnette, et al. 2012). Because of this, it is important to be deliberate about the results surrounding fractal methods in order to avoid ambiguity and "fuzziness" of interpretation.

While this interpretation of fractal scaling regions described above has been well received by the scientific community, criticisms of these interpretations also exist. As Likens et al.

investigated in 2015, fractal scaling behavior may not be indicative of simultaneous persistent and anti-persistent behavior (i.e. long and short range processes or open- and closed-loop processes). Through investigations of various motor control tasks correlating to the strength of fractal behavior, investigators indicated that the nature of the external task, the level of control during the task, and the engagement level of the task drastically affects the strength of fractal exhibitions, claiming "…as participants stop attending and participating cognitively, fractal patterns may weaken or disappear", resulting in scaling regions or abnormal results (Likens, Fine et al. 2015). Another interesting interpretation of scaling regions was proposed in 1992 by Lipsitz and Goldberger. In this paper, it was discussed that processes such as cardiovascular control, pulsatile hormone release, and electroencephalographic potentials display a loss of "complexity" as a patient ages, which leads to new potential applications of fractals and chaos theory (Lipsitz and Goldberger, 1992). Complex variability, loss of control, and highly variable fluctuations surrounding physiological processes could be related to loss of strong fractal behavior in these processes and other neural mechanisms. Instead of an open- and closed-loop explanation, fractal scaling behavior could also be considered as representative of the complexity of a signal.

Summary

Parkinson's disease (PD) is the second-most common neurodegenerative disease in the world. PD is characterized by rigidity, bradykinesia, resting tremor, and postural instability. Postural instability is of particular interest in motor control investigations, because of its close association with fall risk. The subjectivity of current clinical methods in determining PD diagnosis and severity lead to inadequate information about fall risk and its link to PD progression. Traditional methods of detecting postural instability—such as sway and gait

parameters—are promising, but do not take into account the nonlinear, stochastic nature of physiological systems.

Fractal analysis methods are applicable to biological processes and are able to describe the non-stationary behavior in order to understand the underlying mechanisms that may lead to an improvement in clinical assessments. Using velocity information of COP measures, there is potential to further understand the neural circuitry behind PD in an attempt to characterize PI progression and link it to PD severity. While fractal methods are an excellent tool, it is also important to consider their high dependence on input parameters. The appropriate selection of such parameters combined with the nature of the existing data can greatly influence the result of fractal analysis methods. To the best of our knowledge, fractal methods such as adaptive fractal analysis (AFA) and detrended fluctuation analysis (DFA) have not been subject to a parameter study focusing on the appropriateness of fBm signal input. Therefore, in Chapter 3 of this thesis, we will investigate the sensitivity of Hurst estimates derived from AFA and DFA towards input parameter combinations. There has also been no comparison conducted to the best of our knowledge between the sensitivity of AFA and DFA towards PD COP velocity measures. In Chapter 4 of this thesis, we will investigate the sensitivity of AFA and DFA methods towards detecting the progression of PD through COPv time series that will act as a characterization motor control and balance in study participants.

References

Adkin, Allan L., James S. Frank, and Mandar S. Jog, 'Fear of Falling and Postural Control in Parkinson's Disease', *Movement Disorders*, 18 (2003), 496–502 <https://doi.org/10.1002/mds.10396>

Aldrich, Preston R., Horsley, Robert K, Ahmed, Yousuf A., Williamson, Joseph J, Turcic, Stefan M. "Fractal Topology of Gene Promoter Networks at Phase Transitions." *Gene Regulation and Systems Biology* 4 (2010): 75–82. Print.

Almurad, Zainy M. H., and Didier Delignières, 'Evenly Spacing in Detrended Fluctuation Analysis', *Physica A: Statistical Mechanics and Its Applications*, 451 (2016), 63–69 <https://doi.org/10.1016/j.physa.2015.12.155>

Alves, Guido, Elin Bjelland Forsaa, Kenn Freddy Pedersen, Michaela Dreetz Gjerstad, and Jan Petter Larsen, 'Epidemiology of Parkinson's Disease', *Journal of Neurology*, 255 (2008), 18–32 <https://doi.org/10.1007/s00415-008-5004-3>

Bartolić, Andrej, Zvezdan Pirtošek, Janez Rozman, and Samo Ribarič, 'Tremor Amplitude and Tremor Frequency Variability in Parkinson's Disease Is Dependent on Activity and Synchronisation of Central Oscillators in Basal Ganglia', *Medical Hypotheses*, 74 (2010), 362–65 <https://doi.org/10.1016/j.mehy.2009.06.057>

Bloem, B. R., Dennis J. Beckley, Bob J. van Hilten, and Raymund A. C. Roos, 'Clinimetrics of Postural Instability in Parkinson's Disease', *Journal of Neurology*, 245 (1998), 669–73 <https://doi.org/10.1007/s004150050265>

Bloem, Bastiaan R., Dennis J. Beckley, J. Gert van Dijk, Aeilko H. Zwinderman, Michael P. Remler, and Raymund A. C. Roos, 'Influence of Dopaminergic Medication on Automatic Postural Responses and Balance Impairment in Parkinson's Disease', *Movement Disorders*, 11 (1996), 509–21 <https://doi.org/10.1002/mds.870110506>

Bloem, Bastiaan R., Yvette A. M. Grimbergen, Monique Cramer, Mirjam Willemsen, and Aeilko H. Zwinderman, 'Prospective Assessment of Falls in Parkinson's Disease', *Journal of Neurology*, 248 (2001), 950–58 <https://doi.org/10.1007/s004150170047>

Caccia, David C., Donald Percival, Michael J. Cannon, Gary Raymond, and James B. Bassingthwaighte, 'Analyzing Exact Fractal Time Series: Evaluating Dispersional Analysis and Rescaled Range Methods', *Physica A: Statistical Mechanics and Its Applications*, 246 (1997), 609–32 <https://doi.org/10.1016/S0378-4371(97)00363-4>

Camara, Carmen, Pedro Isasi, Kevin Warwick, Virginie Ruiz, Tipu Aziz, John Stein, and others, 'Resting Tremor Classification and Detection in Parkinson's Disease Patients', *Biomedical Signal Processing and Control*, 16 (2015), 88–97 <https://doi.org/10.1016/j.bspc.2014.09.006>

Cannon, Michael J., Donald B. Percival, David C. Caccia, Gary M. Raymond, and James B. Bassingthwaighte, 'Evaluating Scaled Windowed Variance Methods for Estimating the Hurst Coefficient of Time Series', *Physica A: Statistical Mechanics and Its Applications*, 241 (1997), 606–26 <https://doi.org/10.1016/S0378-4371(97)00252-5>

Cavanaugh, James T., Kevin M. Guskiewicz, and Nicholas Stergiou, 'A Nonlinear Dynamic Approach for Evaluating Postural Control', *Sports Medicine*, 35 (2005), 935–50 <https://doi.org/10.2165/00007256-200535110-00002>

Cavanaugh, James T, Vicki S Mercer, and Nicholas Stergiou, 'Approximate Entropy Detects the Effect of a Secondary Cognitive Task on Postural Control in Healthy Young Adults: A Methodological Report', *Journal of NeuroEngineering and Rehabilitation*, 4 (2007), 42 <https://doi.org/10.1186/1743-0003-4-42>

Centonze, Diego, Paolo Calabresi, Patrizia Giacomini, and Giorgio Bernardi, 'Neurophysiology of Parkinson's Disease: From Basic Research to Clinical Correlates', *Clinical Neurophysiology*, 110 (1999), 2006–13 <https://doi.org/10.1016/S1388-2457(99)00173-X>

Chastan, Nathalie, Bertrand Debono, David Maltête, and Jacques Weber, 'Discordance between Measured Postural Instability and Absence of Clinical Symptoms in Parkinson's Disease Patients in the Early Stages of the Disease', *Movement Disorders*, 23 (2008), 366–72 <https://doi.org/10.1002/mds.21840>

Cross, S. S. "Fractals in Pathology." *The Journal of Pathology* 182.1 (1997): 1–8. *PubMed*. Web.

Collins, J. J., and C. J. De Luca, 'Open-Loop and Closed-Loop Control of Posture: A Random-Walk Analysis of Center-of-Pressure Trajectories', *Experimental Brain Research*, 95 (1993), 308–18

Delignieres, Didier, Thibault Deschamps, Alexandre Legros, and Nicolas Caillou, 'A Methodological Note on Nonlinear Time Series Analysis: Is the Open-and Closed-Loop Model of Collins and De Luca (1993) a Statistical Artifact?', *Journal of Motor Behavior*, 35 (2003), 86

Delignieres, Didier, Sofiane Ramdani, Loïc Lemoine, Kjerstin Torre, Marina Fortes, and Grégory Ninot, 'Fractal Analyses for "short" Time Series: A Re-Assessment of Classical Methods', *Journal of Mathematical Psychology*, 50 (2006), 525–44 <https://doi.org/10.1016/j.jmp.2006.07.004>

Delignières, Didier, Kjerstin Torre, and Pierre-Louis Bernard, 'Transition from Persistent to Anti-Persistent Correlations in Postural Sway Indicates Velocity-Based Control', *PLoS Computational Biology*, 7 (2011) <https://doi.org/10.1371/journal.pcbi.1001089>

Doyle, Tim L., Robert U. Newton, and Angus F. Burnett, 'Reliability of Traditional and Fractal Dimension Measures of Quiet Stance Center of Pressure in Young, Healthy People', *Archives of Physical Medicine and Rehabilitation*, 86 (2005), 2034–40 <https://doi.org/10.1016/j.apmr.2005.05.014>

Eke, A., P. Hermán, J. B. Bassingthwaighte, G. M. Raymond, D. B. Percival, M. Cannon, and others, 'Physiological Time Series: Distinguishing Fractal Noises from Motions', *Pflugers Archiv: European Journal of Physiology*, 439 (2000), 403–15

Factor, Stewart, and William Weiner, *Parkinson's Disease : Diagnosis and Clinical Management : Diagnosis and Clinical Management (2)* (New York, US: Demos, 2008)

<http://site.ebrary.com/lib/alltitles/docDetail.action?docID=10210545> [accessed 4 September 2016]

Gaig, Carles, and Eduardo Tolosa, 'When Does Parkinson's Disease Begin?', *Movement Disorders*, 24 (2009), S656–64 <https://doi.org/10.1002/mds.22672>

Gao, Jianbo, Brian M. Gurbaxani, Jing Hu, Keri J. Heilman, Vincent A. Emanuele II, Greg F. Lewis, and others, 'Multiscale Analysis of Heart Rate Variability in Non-Stationary Environments', *Frontiers in Physiology*, 4 (2013), 1–8 <https://doi.org/10.3389/fphys.2013.00119>

Gao, Jianbo, Jing Hu, and Wen-wen Tung, 'Facilitating Joint Chaos and Fractal Analysis of Biosignals through Nonlinear Adaptive Filtering', *PLoS ONE*, 6 (2011) <https://doi.org/10.1371/journal.pone.0024331>

Goetz, Christopher G., Werner Poewe, Olivier Rascol, Cristina Sampaio, Glenn T. Stebbins, Carl Counsell, and others, 'Movement Disorder Society Task Force Report on the Hoehn and Yahr Staging Scale: Status and Recommendations The Movement Disorder Society Task Force on Rating Scales for Parkinson's Disease', *Movement Disorders*, 19 (2004), 1020–28 <https://doi.org/10.1002/mds.20213>

Harper, Joshua Russell, 'Fractal Analysis of Center of Pressure Velocity Time Series in Parkinson's Disease' (unpublished Thesis, University of Kansas, 2015) <https://kuscholarworks.ku.edu/handle/1808/19412>

Hill, E., S. Stuart, S. Lord, S. Del Din, and L. Rochester, 'Vision, Visuo-Cognition and Postural Control in Parkinson's Disease: An Associative Pilot Study', *Gait & Posture*, 48 (2016), 74–76 <https://doi.org/10.1016/j.gaitpost.2016.04.024>

Horak, Fay B., Diana Dimitrova, and John G. Nutt, 'Direction-Specific Postural Instability in Subjects with Parkinson's Disease', *Experimental Neurology*, 193 (2005), 504–21 <https://doi.org/10.1016/j.expneurol.2004.12.008>

Jankovic, Joseph, and L Giselle Aguilar, 'Current Approaches to the Treatment of Parkinson's Disease', *Neuropsychiatric Disease and Treatment*, 4 (2008), 743–57

Jeka, John, Tim Kiemel, Robert Creath, Fay Horak, and Robert Peterka, 'Controlling Human Upright Posture: Velocity Information Is More Accurate Than Position or Acceleration', *Journal of Neurophysiology*, 92 (2004), 2368–79 <https://doi.org/10.1152/jn.00983.2003>

Kerr, G. K., C. J. Worringham, M. H. Cole, P. F. Lacherez, J. M. Wood, and P. A. Silburn, 'Predictors of Future Falls in Parkinson Disease', *Neurology*, 75 (2010), 116–24 <https://doi.org/10.1212/WNL.0b013e3181e7b688>

Kerr, Graham, Steven Morrison, and Peter Silburn, 'Coupling between Limb Tremor and Postural Sway in Parkinson's Disease', *Movement Disorders*, 23 (2008), 386–94 <https://doi.org/10.1002/mds.21851>

Kim, Samuel, Natalie Allen, Colleen Canning, and Victor Fung, 'Postural Instability in Patients with Parkinson's Disease', *CNS Drugs*, 27 (2013), 97–112

Kirchner, Marietta, Patric Schubert, Magnus Liebherr, and Christian T. Haas, 'Detrended Fluctuation Analysis and Adaptive Fractal Analysis of Stride Time Data in Parkinson's Disease: Stitching Together Short Gait Trials', *PLoS ONE*, 9 (2014) <https://doi.org/10.1371/journal.pone.0085787>

Kowal, Stacey L., Timothy M. Dall, Ritashree Chakrabarti, Michael V. Storm, and Anjali Jain, 'The Current and Projected Economic Burden of Parkinson's Disease in the United States', *Movement Disorders*, 28 (2013), 311–18 <https://doi.org/10.1002/mds.25292>

Kuznetsov, Nikita, Scott Bonnette, Jianbo Gao, and Michael A. Riley, 'Adaptive Fractal Analysis Reveals Limits to Fractal Scaling in Center of Pressure Trajectories', *Annals of Biomedical Engineering*, 41 (2012), 1646–60 <https://doi.org/10.1007/s10439-012-0646-9>

Lees, Andrew J, John Hardy, and Tamas Revesz, 'Parkinson's Disease', *The Lancet*, 373 (2009), 2055–66 <https://doi.org/10.1016/S0140-6736(09)60492-X>

Likens, Aaron D., Justin M. Fine, Eric L. Amazeen, and Polemnia G. Amazeen, 'Experimental Control of Scaling Behavior: What Is Not Fractal?', *Experimental Brain Research*, 233 (2015), 2813–21 <https://doi.org/10.1007/s00221-015-4351-4>

Lim, Shen-Yang, and Anthony E. Lang, 'The Nonmotor Symptoms of Parkinson's disease—An Overview', *Movement Disorders*, 25 (2010), S123–30 <https://doi.org/10.1002/mds.22786>

Lindholm, Beata, Peter Hagell, Oskar Hansson, and Maria H. Nilsson, 'Factors Associated with Fear of Falling in People with Parkinson's Disease', *BMC Neurology*, 14 (2014), 19 <https://doi.org/10.1186/1471-2377-14-19>

Lipsitz LA, and Goldberger AL, 'Loss of "Complexity" and Aging: Potential Applications of Fractals and Chaos Theory to Senescence', *JAMA*, 267 (1992), 1806–9 <https://doi.org/10.1001/jama.1992.03480130122036>

Loughlin, P. J., M. S. Redfern, and J. M. Furman, 'Nonstationarities of Postural Sway', *IEEE Engineering in Medicine and Biology Magazine*, 22 (2003), 69–75 <https://doi.org/10.1109/MEMB.2003.1195699>

Mancini, Martina, Patricia Carlson-Kuhta, Cris Zampieri, John G. Nutt, Lorenzo Chiari, and Fay B. Horak, 'Postural Sway as a Marker of Progression in Parkinson's Disease: A Pilot Longitudinal Study', *Gait & Posture*, 36 (2012), 471–76 <https://doi.org/10.1016/j.gaitpost.2012.04.010>

Mancini, Martina, Fay B. Horak, Cris Zampieri, Patricia Carlson-Kuhta, John G. Nutt, and Lorenzo Chiari, 'Trunk Accelerometry Reveals Postural Instability in Untreated Parkinson's Disease', *Parkinsonism & Related Disorders*, 17 (2011), 557–62 <https://doi.org/10.1016/j.parkreldis.2011.05.010>

McNeely, Marie E., Ryan P. Duncan, and Gammon M. Earhart, 'Medication Improves Balance and Complex Gait Performance in Parkinson Disease', *Gait & Posture*, 36 (2012), 144–48 <https://doi.org/10.1016/j.gaitpost.2012.02.009>

Minamisawa, Tadayoshi, Kei Takakura, and Takashi Yamaguchi, 'Detrended Fluctuation Analysis of Temporal Variation of the Center of Pressure (COP) during Quiet Standing in Parkinsonian Patients', *Journal of Physical Therapy Science*, 21 (2009), 287–92 <https://doi.org/10.1589/jpts.21.287>

Morrison, S., G. Kerr, K. M. Newell, and P. A. Silburn, 'Differential Time- and Frequency-Dependent Structure of Postural Sway and Finger Tremor in Parkinson's Disease', *Neuroscience Letters*, 443 (2008), 123–28 <https://doi.org/10.1016/j.neulet.2008.07.071>

Olanow, C. W., M. B. Stern, and K. Sethi, 'The Scientific and Clinical Basis for the Treatment of Parkinson Disease (2009)', *Neurology*, 72 (2009), S1–136 <https://doi.org/10.1212/WNL.0b013e3181a1d44c>

Park, Kiwon, Ryan T. Roemmich, Jonathan M. Elrod, Christopher J. Hass, and Elizabeth T. Hsiao-Wecksler, 'Effects of Aging and Parkinson's Disease on Joint Coupling, Symmetry, Complexity and Variability of Lower Limb Movements during Gait', *Clinical Biomechanics*, 33 (2016), 92–97 <https://doi.org/10.1016/j.clinbiomech.2016.02.012>

Peng, C.-K., Shlomo Havlin, and H. Eugene Stanley, 'Quantification of Scaling Exponents and Crossover Phenomena in Nonstationary Heartbeat Time Series', *Chaos*, 5 (1995), 82

Pincus, S. M., and A. L. Goldberger, 'Physiological Time-Series Analysis: What Does Regularity Quantify?', *American Journal of Physiology - Heart and Circulatory Physiology*, 266 (1994), H1643–56

Ramdani, Sofiane, Benoît Seigle, Julien Lagarde, Frédéric Bouchara, and Pierre Louis Bernard, 'On the Use of Sample Entropy to Analyze Human Postural Sway Data', *Medical Engineering & Physics*, 31 (2009), 1023–31 <https://doi.org/10.1016/j.medengphy.2009.06.004>

Riley, Michael A., Scott Bonnette, Nikita Kuznetsov, Sebastian Wallot, and Jianbo Gao, 'A Tutorial Introduction to Adaptive Fractal Analysis', *Fractal Physiology*, 3 (2012), 371 <https://doi.org/10.3389/fphys.2012.00371>

Sasagawa, Shun, Junichi Ushiyama, Motoki Kouzaki, and Hiroaki Kanehisa, 'Effect of the Hip Motion on the Body Kinematics in the Sagittal Plane during Human Quiet Standing', *Neuroscience Letters*, 450 (2009), 27–31 <https://doi.org/10.1016/j.neulet.2008.11.027>

Schaefer, Alexander, Jennifer S. Brach, Subashan Perera, and Ervin Sejdić, 'A Comparative Analysis of Spectral Exponent Estimation Techniques for 1/fβ Processes with Applications to the Analysis of Stride Interval Time Series', *Journal of Neuroscience Methods*, 222 (2014), 118–30 <https://doi.org/10.1016/j.jneumeth.2013.10.017>

Schmit, Jennifer M., Michael A. Riley, Arif Dalvi, Alok Sahay, Paula K. Shear, Kevin D. Shockley, and others, 'Deterministic Center of Pressure Patterns Characterize Postural

Instability in Parkinson's Disease', *Experimental Brain Research*, 168 (2005), 357–67 <https://doi.org/10.1007/s00221-005-0094-y>

Schumann, Timothy, Mark S. Redfern, Joseph M. Furman, Amro El-Jaroudi, and Luis F. Chaparro, 'Time-Frequency Analysis of Postural Sway', *Journal of Biomechanics*, 28 (1995), 603–7 <https://doi.org/10.1016/0021-9290(94)00113-I>

Shiner, Tamara, Ben Seymour, Mkael Symmonds, Peter Dayan, Kailash P. Bhatia, and Raymond J. Dolan, 'The Effect of Motivation on Movement: A Study of Bradykinesia in Parkinsons Disease: e47138', *PLoS One*, 7 (2012) <https://doi.org/http://dx.doi.org.www2.lib.ku.edu/10.1371/journal.pone.0047138>

Simuni, Tanya, and Rajesh Pahwa, *Parkinson's Disease* (Cary, US: Oxford University Press, USA, 2009) <http://site.ebrary.com/lib/alltitles/docDetail.action?docID=10375051> [accessed 28 August 2016]

Stergiou, Nicholas. Editor. *Nonlinear Analysis for Human Movement Variability*. Boca Raton: Taylor & Francis, CRC Press, 2016. Print.

Stergiou, Nicholas, and Leslie M. Decker, 'Human Movement Variability, Nonlinear Dynamics, and Pathology: Is There a Connection?', *Human Movement Science*, EWOMS 2009: The European Workshop on Movement Science, 30 (2011), 869–88 <https://doi.org/10.1016/j.humov.2011.06.002>

Stylianou, Antonis P., Molly A. McVey, Kelly E. Lyons, Rajesh Pahwa, and Carl W. Luchies, 'Postural Sway in Patients with Mild to Moderate Parkinson's Disease', *International Journal of Neuroscience*, 121 (2011), 614–21 <https://doi.org/10.3109/00207454.2011.602807>

Turcotte, Donald L. Malamud, Bruce D, Guzzetti, Fausto, Reichenbach, Paola. "Self-Organization, the Cascade Model, and Natural Hazards." *Proceedings of the National Academy of Sciences of the United States of America* 99 Suppl 1 (2002): 2530–2537. *PubMed*. Web.

Vaillancourt, David E, and Karl M Newell, 'The Dynamics of Resting and Postural Tremor in Parkinson's Disease', *Clinical Neurophysiology*, 111 (2000), 2046–56 <https://doi.org/10.1016/S1388-2457(00)00467-3>

Visser, Martine, Johan Marinus, Bastiaan R Bloem, Hannah Kisjes, Barbara M van den Berg, and Jacobus J van Hilten, 'Clinical Tests for the Evaluation of Postural Instability in Patients with Parkinson's disease1', *Archives of Physical Medicine and Rehabilitation*, 84 (2003), 1669–74 <https://doi.org/10.1053/S0003-9993(03)00348-4>

Wielinski, Catherine L., Cordelia Erickson-Davis, Rose Wichmann, Maria Walde-Douglas, and Sotirios A. Parashos, 'Falls and Injuries Resulting from Falls among Patients with Parkinson's Disease and Other Parkinsonian Syndromes', *Movement Disorders*, 20 (2005), 410–15 <https://doi.org/10.1002/mds.20347>

Wirdefeldt, Karin, Hans-Olov Adami, Philip Cole, Dimitrios Trichopoulos, and Jack Mandel, 'Epidemiology and Etiology of Parkinson's Disease: A Review of the Evidence', *European Journal of Epidemiology*, 26 (2011), 1 <https://doi.org/10.1007/s10654-011-9581-6>

Yentes, Jennifer M., Nathaniel Hunt, Kendra K. Schmid, Jeffrey P. Kaipust, Denise McGrath, and Nicholas Stergiou, 'The Appropriate Use of Approximate Entropy and Sample Entropy with Short Data Sets', *Annals of Biomedical Engineering*, 41 (2012), 349–65 <https://doi.org/10.1007/s10439-012-0668-3>

Chapter 3: Parameter Study

Abstract

Background: Fractal methods are an emerging nonlinear analysis tool that can identify stochastic patterns that are undetectable through conventional analysis. Detrended fluctuation analysis (DFA) is a fractal method that is commonly used in such analysis. Adaptive fractal analysis (AFA) is a fairly new method developed to overcome known limitations with fractal methods. Both DFA and AFA are highly sensitive to input parameters and there is very little existing consensus on appropriateness of parameter selection. This study investigates the accuracy of AFA and DFA across combinations of input parameters in order to provide insight on how changing parameters affects fractal method results.

Methods: Fractional Brownian motion (fBm) signals were generated based off of a desired Hurst exponent (H). Parameter ranges were identified for (1) data length (N): 500, 1000, 2500, and 5000 samples; (2) minimum window size (n_{min}): 2, 4, 6, and 8 samples; (3) maximum window size (n_{max}): $\frac{N}{2}$, $\frac{N}{4}$, $\frac{N}{6}$, $\frac{N}{8}$, and $\frac{N}{10}$ samples; and (4) order of the fitted polynomial for AFA (M): 1st or 2nd order polynomial fits. AFA and DFA were conducted for every combination of these parameters. Each combination was conducted on twenty different generated signals (n=20). Repeated measures ANOVA and Tukey post hoc tests were conducted in order to determine the effects of changing input parameter combinations as well as identify interactions between input parameters.

Findings: AFA and DFA were verified to be highly sensitive to input parameters. Significance was found for N, n_{min}, and n_{max} using DFA. Significance was found for N, n_{min}, n_{max}, and M using AFA. Multiple interactions were found for both methods.

Interpretation: The selection of input parameters can have a large impact on the accuracy of AFA and DFA. Based off the characteristics of data and experimental design, investigators should demonstrate care when selecting the appropriate parameters for fractal methods. The results suggest parameter ranges for fBm-like signals in appropriately-large biological data to be examined at n_{max} values between $N/6$ and $N/10$, n_{min} values should remain around 4 to 6 samples, and that the fitted polynomial order M for AFA should remain first order.

Introduction

In recent years, the application of fractal analysis used to explore datasets has become more widespread over a range of biological fields. Fractals are any type of infinitely scaled and repeated pattern. Fractal analysis is defined as assessing the complexity of fractals using nonlinear mathematical analysis methods as opposed to traditional Euclidean concepts. Fractal analysis has been used to uncover a host of patterns and complex geometries in a broad range of scientific topics such as forest fire progression (Turcotte, Malamud et al. 2002), gene expression (Aldrich, Horsley et al. 2010), DNA coding patterns, space-filling properties of tumors, and viral infections (Cross, 1997).

Detrended fluctuation analysis (DFA) is one such fractal analysis method. By breaking time series into windows and analyzing the properties of each window individually, DFA provides a fluctuations versus window bi-logarithmic plot that reveals the scaling properties of the time series. DFA is based off of power law scaling behavior shown below:

$$SD(\Delta x) \propto \Delta t^{H}$$

where $SD(\Delta x)$ is a variance of the displacement of the time series and Δt^H represents the power scaling law over various time intervals and scales. H is the Hurst exponent, and is considered the power law scaling parameter.

First applied towards heartbeat interval variations by Peng in 1995 (Peng, Havlin et al. 1995), DFA was able to differentiate between heart rate time series from patients with severe congestive heart failure and healthy patients. In addition to this characterization of healthy versus diseased patients, DFA was also sensitive to what was first referenced as a "crossover phenomenon". Peng et al. suggested that DFA was able to discriminate between short- and long-range scaling exponents, and that these scaling exponents were indicative of complex physiological dynamics that may not be detected through traditional linear methods that assume the time series to be stationary. There have been other instances of detection in crossover phenomenon, particularly in the field of gait and posture research. Correlations were also drawn towards short- and long-range scaling exponents and their relationship to open and closed loop postural dynamics related with motor control and an intermittent velocity-based control system (Collins and De Luca, 1993; Delignieres, Torre et al. 2011).

Another fractal analysis method that has been developed in recent years is called adaptive fractal analysis (AFA). It is similar to DFA in that it is a nonlinear detrending algorithm that focuses on the power scaling law in order to provide a bi-logarithmic comparison between fluctuations of displacement of a time series with the size of window being investigated. AFA differentiates from DFA in that it uses a globally smooth trend signal by patching together local polynomial fits of the time series in overlapping window sets. The order of the polynomial can also be controlled. DFA only uses a first order polynomials and does not stitch together the window sets, providing instead a "piecewise" trend signal by which the fluctuations of the time

series can be estimated (Riley, Bonnette et al 2012). Developed in 2011 by Gao et al. AFA was applied towards heart rate variability and found to be a useful tool in extracting nonlinear properties from times series data (Gao, Hu et al 2011; Gao, Gurbaxani et al 2013). Gao also argues that AFA possesses intrinsic advantages over DFA due to (1) better resolution of fractal behavior for shorter time series, (2) can more robustly deal with arbitrary, strong non-linear trends, and (3) possesses a built in proof on why AFA yields the correct H while DFA does not (Gao, Hu et al 2011; Riley, Bonnette et al. 2012).

Both AFA and DFA provide powerful tools for nonlinear analysis of stochastic systems. However, while fractal analysis is a useful tool in understanding previously hidden phenomena in data exhibiting fractal characteristics, it is also important to note that there are limitations to this fractal method. The results of fractal methods are highly dependent on input parameters and lacks relative consistency (Cannon, Percival et al. 1997). The reliability of fractal analysis is also highly dependent on the range of resultant Hurst exponents being investigated (Caccia, Percival et al. 1997). The appropriateness of fractal analysis depends heavily on the nature of the signal being investigated, the type of fractal method used, the range of resultant generated Hurst exponents, and most importantly, the selected input parameters. Both AFA and DFA have been noted to be sensitive to key input parameters: (1) data length (N), (2) minimum window size (n_{min}), and (3) maximum window size (n_{max}) (Caccia, Percival et al. 1997; Cannon, Percival et al. 1997; Riley, Bonnette et al. 2012; Stergiou, 2016). AFA also possesses an additional input parameter: order of the fitted polynomial (M). DFA traditionally only extrapolates variance of the displacement with first order polynomials.

There is not a clear consensus on appropriate selection of most of these parameters and popular selection trends often are selected without published justification. The purpose of this

study was to investigate the effect of changing N, n_{min}, n_{max}, and M input parameters on results of AFA and DFA analysis applied to fBm signals. fBm signals are often found in physiological systems, particularly in gait and posture research with respects to center of pressure (COP) signals (Collins and De Luca, 1993; Eke, Herman et al. 2000; Delignieres, Torre et al. 2011; Kuznetsov, Bonette, et al. 2012). Analysis of generated fBm signals can provide an excellent theoretical threshold by which a baseline of appropriate parameters can be drawn. It is clear that there is a need to investigate (1) the effects and interactions of parameter combinations on the resultant H value, (2) the effect of the resultant H ranges on the accuracy of estimations, and (3) which detrending algorithm more accurately estimates the resultant H. These three facets of the study will be analyzed in order to provide recommendations on appropriate input parameters selections by which investigators can address fBm and fBm-like signals in physiological systems. We hypothesize that the Hurst exponent from both AFA and DFA will be sensitive towards the selection of N, n_{min}, n_{max}, and M. Further understanding of the effects of input parameters on resultant H values and how the detrending algorithms (AFA vs DFA) compare will provide investigators with more information on appropriateness of fractal analysis parameter design.

Methods

Data Preparation and Generation

In order to investigate the effect of parameter selection on the results of AFA and DFA applied to fBm signals, it was essential to generate a well-understood signal datasets by which comparisons can be drawn. Both AFA and DFA fractal methods provide an estimate of the Hurst exponent (H) of the signal being analyzed. If the "true" resultant H is not known for a signal prior to conducting AFA or DFA, then estimation accuracy cannot be calculated. Therefore, a

method is required to generate an fBm signal based off a known Hurst exponent, so that the accuracy of the AFA and DFA estimation of H can be determined. This was accomplished using approximations of a stochastic integral, which derives from the work of Mandelbrot and Ness in 1968 and an extension of this work by Coerujolly in 2000 (Mandelbrot and Ness, 1968; Coeurjolly, 2000). A code was developed that uses the desired Hurst exponent and signal length as input parameters. Hurst exponent estimations using fractal methods risk bias as they approach certain H ranges (Caccia, Percival et al. 1997). Therefore, it is necessary to generate fBm signals utilizing Hurst exponent values over the range of 0.1 to 0.9, with increment resolution of 0.1. This strategy provides the opportunity to investigate the sensitivity of parameter selection on fBm signals generated using a range of H values and helps to determine whether AFA or DFA provide a more consistent estimation of H at each increment of H generated data. The signal length (N) is also a well-documented influencing factor on the accuracy of H estimation by DFA and AFA (Cannon, Percival et al. 1997; Riley, Bonnette et al. 2012; Stergiou, 2016). For each selected Hurst exponent value, signals were generated at N=500, 1000, 2500, and 5000 in order to simulate a range of typical data lengths in posture and gait studies previously conducted (Caccia, Percival et al. 1997; Cavanaugh, Guskiewicz et al. 2005; Stergiou, 2016). Twenty signals were generated for each combination of signal length and H. These generated fBm signals were produced using MATLAB (MATLAB, Natick, MA, USA).

Data Analysis

Each individual signal was analyzed using DFA(N, n_{min}, n_{max}) and AFA(N, n_{min}, n_{max}, M). The calculation of the Hurst exponent using DFA and AFA is described below.

Detrended Fluctuation Analysis

DFA was performed on each generated fBm signal to estimate H. The method used was consistent with Peng et al. and Delignieres et al. (Peng, Havlin et al. 1995; Delignieres, Torre et al. 2011). DFA applies the power scaling law in order to compare variance of displacement against increments of discrete time scales, with the size of the time scales defined by the user. In the present study, multiple time scales were used for DFA and their interactions with other input parameters were investigated. The steps below were derived from Delignieres et al.:

1. Integrate the signal using the equation: $y(k) = \sum_{i=1}^{k}[B(i) - B_{ave}]$, where *B(i)* is the i^{th} interval and B_{ave} is the average interval. The integrated time series is expressed as *y(k).*

2. Partition the integrated time series into non-overlapping windows of equal length (*n*).

3. Fit a first-order, least squares line to the data in each box. The line represents the trend inside each window. The y coordinates of each trend can be expressed as $y_n(k)$.

4. Detrend the integrated time series, *y(k)*, by subtracting the local trend, $y_n(k)$, for each window.

5. Calculate the RMS fluctuation using the following equation:

$$F(n) = \sqrt{\frac{1}{N}\sum_{k=1}^{N}[y(k) - y_n(k)]^2}$$

6. Plot *F(n)* versus *n* (fluctuation versus scale) on a bi-logarithmic plot.

The resulting plot should provide a linear relationship between *F(n)* and *n*. The slope of the first-order, least squares fit regression line of this linear relationship is analogous to the Hurst exponent (H) and the relationship can be expressed using the power law scaling behavior:

$$SD(\Delta x) \propto \Delta t^H$$

where $SD(\Delta x)$ is a variance of the displacement of the time series and Δt^H represents the power scaling law over various time intervals and scales.

Adaptive Fractal Analysis

AFA was performed on each generated fBm signal to estimate H. AFA was introduced by Gao et al. in 2011 and also applies power law scaling behavior in order to compare fluctuation versus scale analysis (Gao, Hu et al 2011). AFA differs from DFA in that it integrates a step that creates a globally smooth detrending signal using overlapping window intervals rather than non-overlapping windows containing first-order, least square signals (Riley, Bonnette et al. 2012). In the present study, multiple window scales were used for AFA and their interactions with other input parameters were investigated. The steps below were derived from Riley et al.:

1. a. If the data represents a fractional Gaussian process (fGn), integrate the signal.

1. b. If the data represents a fractional Brownian process (fBm), integration of the signal is not advised.

2. Partition the time series (*u(i)*) into windows of length: $w = 2n + 1$, with windows overlapping by $n + 1$ points. Note that the user will set the window sizes, so *n* is not a free parameter (i.e. $n = \frac{(w-1)}{2}$.

3. Within each window, the least squares polynomial of order *M* is identified. *M* is an input parameter that is selected by the user.

4. The local fits of each window then need to be "stitched" together in order to provide a smooth global fit to the time series. This is done by taking a weighted combination of the fits of two adjacent windows and can be expressed mathematically as:

$$y^{(c)}(l) = w_1 y^{(i)}(l+n) + w_2 y^{(i+1)}(l), \qquad l = 1,2,\dots,n+1$$

where $w_1 = 1 - \frac{l-1}{n}$ and $w_2 = \frac{l-1}{n}$.

4. Once a globally smooth trend(*v(i)*) has been created from overlapping windows, detrend the time series (*u(i)*) from the globally smooth trend in order to examine how the variance of the residuals of fit compare to the window scales. Calculate using the following equation:

$$F(w) = \sqrt{\frac{1}{N}\sum_{i=1}^{N}[u(i) - v(i)]^2}$$

6. Plot *F(n)* versus *n* (fluctuation versus scale) on a bi-logarithmic plot. Riley et al. quantified this relation in a plot of $\log_2(F(w))$ versus $\log_2(w)$, as opposed to a logarithmic base of ten used in DFA (Riley, Bonnette et al. 2012). The resulting plot should provide a linear relationship between *F(w)* and *w*. Similar to DFA, the slope of the resultant least squares fit regression line in analogous to the Hurst exponent (H).

Experimental Design

The effect of input parameters was investigated on the estimation of H using AFA and DFA applied to fBm signals generated using a range of H values. For both AFA and DFA, input parameters included: (1) data length (N), (2) minimum window size (n_{min}), (3) maximum window size (n_{max}), and only in the case of AFA, (4) order of the fitted polynomial (M). Each fBm signal, generated using Hurst exponent values of 0.1 to 0.9 in increments of 0.1, was subjected to the estimation of the Hurst exponent for combinations of N=500, 1000, 2500, and 5000; n_{min}=4, 6, 8, and 10; $n_{max} = \frac{N}{2}, \frac{N}{4}, \frac{N}{6}, \frac{N}{8}$, and $\frac{N}{10}$; and M=1 and 2 for a total of 1440 combinations of AFA parameters and 720 combinations of DFA parameters. Each combination was tested with twenty trials in order to provide a more robust estimation of the efficacy of each combination at accurately predicting H. Generated signal lengths were also selected based off recommendations in previously published literature for gait and posture research that also addressed appropriateness of nonlinear methods (Caccia, Percival et al. 1997; Stergiou, 2016). The minimum and maximum windows were selected based off recommendations in previously published literature. Cannon et al. cautions against overly small windows that do not provide reliable calculation of variance of residuals as well as overly large windows introducing bias because of the inability of a first- or second-order trend to characterize the window (Cannon, Percival et al. 1997). Minimum window size did not contain $n_{min} = 2$ in this parameter study (which would theoretically be the smallest window size possible) due to variance of the residuals of fit being biased if only 2 samples are within each window. Order of the fitted polynomial parameters were selected based off the recommendations of investigation from Riley et al. (Riley, Bonnette et al, 2012). All data analysis methods were coded and calculated in MATLAB (MATLAB, Natick, MA, USA).

Statistical Analysis

Group means and standard deviations for the estimated AFA and DFA Hurst exponents from generated fBm signals, their differences from the theoretical H values by which the fBm signals were generated, and the resulting percent errors were calculated for all combinations of parameters. A repeated measures ANOVA was conducted to determine the effect of input parameter combinations of N, n_{min}, and n_{max} input parameters towards DFA and the effect of changing N, n_{min}, n_{max}, and M input parameters towards AFA. The effect of fractal method used (DFA vs. AFA), input parameter combinations, and H range on the accuracy of H estimation was also investigated. In DFA, if a significant 3-way interaction was found between N, n_{min}, and n_{max}, this indicated that the estimation of H dependent on the selection of all three input parameters. If a significant 2-way interaction was found, then the estimate of H dependent on the selection of two of the parameters, but independent of the third parameter. In AFA, if a significant 4-way interaction was found between N, n_{min}, n_{max}, and M, this indicated that the estimation of H was dependent on all four input parameters. If a significant 3-way interaction was found, then H is different depending on three of the parameters, and so on and so forth. Significant main effects and interaction effects were investigated using Tukey-Kramer's post hoc tests to further investigate parametric effects on accuracy of Hurst exponent estimates. Significance was considered for $p<0.05$. All statistical analyses were calculated in R 3.2.3.

Results

DFA

Significant main effects differences were found across generated Hurst exponent ranges ($F_{8,13680}$: 12927.02, $p<0.001$), N ($F_{3,13680}$: 8.54, $p<0.0001$), n_{min} ($F_{3,13680}$: 3.19, $p<0.05$), and n_{max} ($F_{4,13680}$: 141.92, $p<0.0001$). Significant two-way interactions were found between generated

Hurst exponent ranges and N ($F_{3,13680}$: 10.01, p<0.0001); and between generated Hurst exponent ranges and n_{max} ($F_{3,13680}$: 2.03, p<0.0001). DFA also had different accuracies of H estimation depending on generated H exponent ranges (Table 1.1).

Main effects post-hoc Tukey tests showed that N=2500 differed significantly from pairwise comparisons to N=500 (p<0.01) and to N=1000 (p<0.05). All pairwise comparisons of n_{max} groups were significant (p <0.05) except between pairwise comparisons N/6 – N/8 and N/8 – N/10. Generated H ranges differed significantly for all pairwise comparisons (p <0.001). Tukey post-hoc tests also revealed that all pairwise comparisons of n_{min} increments did not show significance within 95% confidence intervals.

AFA

Significant main effects differences were found across generated H ranges ($F_{8,27360}$: 16513.87, p<0.001), n_{min} ($F_{3,27360}$: 62.82, p<0.001), n_{max} ($F_{4,27360}$: 711.21, p<0.001), and M ($F_{1,27360}$: 370.14, p<0.001). Significant two-way interactions were found between generated H ranges and N ($F_{24,27360}$: 33.95, p<0.001); between generated H ranges and n_{min} ($F_{24,27360}$: 5.98, p<0.001); between N and n_{min} ($F_{9,27360}$: 6.16, p<0.001); between generated H ranges and n_{max} ($F_{32,27360}$: 67.94, p<0.001); between N and n_{max} ($F_{12,27360}$: 15.70, p<0.001); and between n_{max} and M ($F_{4,27360}$: 7.32, p<0.001). Significant three-way interactions were found between generated H ranges, N, and n_{max} ($F_{96,27360}$: 6.30, p<0.001). AFA was consistent across values of N, but different depending on the values of n_{min}, n_{max}, and M. AFA also had different accuracies of H estimation depending on generated H exponent value (Table 1.2).

Main effects post-hoc Tukey tests revealed significance between all pairwise comparisons of n_{max} groups (p<0.05), the pairwise comparison of M (p<0.001), and all pairwise

comparisons of generated H range groups (p<0.001). All pairwise comparisons of n_{min} groups were significant (p <0.01) except between pairwise comparisons 6 – 8 and 8 – 10. Tukey post-hoc tests also revealed that all pairwise comparisons of N did not show significance.

Discussion

The purpose of this study was to investigate the effects of input parameters on the accuracy of DFA and AFA towards fBm signals. Physiological process often display both fBm and fractal characteristics. Fractal analysis methods are highly sensitive towards input parameters. Because of this, there is a clear need to analyze (1) the effects and interactions of changing input parameters, (2) the effect of H range values on fractal estimation accuracy, and (2) which detrending algorithm provides accurate and reliable estimations of H. Through the careful investigation of parameter combinations and their resulting accuracies across different spectrums of the Hurst exponent, recommendations may be provided on appropriateness of parameter selection when considering experimental signals similar to fBm noise. The results of this study can be used as a reference for investigators interested in using AFA or DFA for their data analysis. This study can also provide more perspective in the context of appropriateness of data selection and input parameter selection when considering other signals, such as fractional Gaussian noise (fGn).

It is important to note that main analysis of these results were conducted by way of raw differencing of the generated H to the estimated H and percent differencing of the generated H to the estimated H. These two methods provide different forms of information that can, in combination, be used to provide a more holistic perspective of parametric combinations. Raw differencing is useful to determine inflation or deflation trends in H calculation, which percent differencing is unable to do. Percent differencing provides an estimation of relative consistency

between trials and also acts as a check to ensure that raw differencing results that appear to be more accurate may simply be due to averaging a combination of overestimated and underestimated Hurst exponents in order to provide a seemingly "perfect" parameter combination.

Detrended Fluctuation Analysis (DFA)

Data length (*N*): Tukey Kramer post hoc tests verified that DFA shows sensitivity towards data length. Data lengths of 2500 samples provided the most accurate estimations of H and differed significantly from N=500 (p<0.01) and N=1000 (p<0.05). This indicates that larger data lengths are desirable when performing DFA. However, all data length increments investigated summarily estimated the correct H value within ±0.1 ranges. These findings are consistent with Cannon et al. which recommended data length sizes exceed 2^8 samples prior to considering fractal investigations as an appropriate analysis methods (Cannon, Percival et al. 1997). Smaller data lengths may provide more inaccurate estimates, but for the purposes of this study, we can confirm that larger data lengths tend to provide more reliable results (Figures 2.1, 2.4, and 3).

Maximum window size (n_{max}): This parameter proved to be the most parametrically significant measure considered when evaluating accuracy of H estimates. This is to be expected, since larger window sizes are traditionally worse estimates of fluctuation (Cannon, Percival et al. 1997). Elimination of larger window sizes has, up to now, usually occurred at the discretion of the investigator, who must face two problems: (1) elimination of too many window sizes can hide existing patterns in the data and (2) including window sizes that are too large can reveal false patterns that are merely statistical artifacts of the method. The results of this study show that all pairwise comparisons were significant (p <0.05) except between pairwise comparisons

$N/6 - N/8$ and $N/8 - N/10$. Fig. 2.1 clearly shows that $N/2$ and $N/4$ provide generally unreliable estimates of H and are inappropriate parameter selections for fBm signals using DFA. Figure 3 shows that once Hurst exponent ranges exceed 0.3, the previous statement is true. Interestingly, when Hurst exponent ranges are 0.2 and smaller, the opposite trend is apparent— n_{max} values that provide a larger window range (such as $N/2$ and $N/4$) show more accurate estimations of H over these low ranges. This is perhaps due to larger maximum window sizes indicate more window sizes are being analyzed as a whole, which provides the fluctuation versus window size bi-logarithmic plot with more information by which to estimate a more "arbitrary" signal. It is also important to note that investigators will rarely encounter physiological signals around $0 < H < 0.2$ range and that visual inspection and characterization of these signals appear to be more Gaussian in nature, rather than Brownian (Figure 1). Signals that appear to be fBm noise will provide more accurate estimation of H when using DFA n_{max} values between $N/6$ and $N/10$.

Minimum window size (n_{min}): Repeated measures ANOVA indicated that n_{min} increments were significant ($p<0.05$). However, closer inspection using Tukey Kramer post hoc tests showed that no pairwise comparison was sufficiently significant within 95% confidence range, though significance was found within a 90% confidence range. This shows that selection of n_{min} increments using DFA is unlikely to affect the accuracy of the Hurst exponent estimation, though should still be carefully selected. Referencing Figs. 2.1 and 3, it is apparent that as n_{min} increases, it promotes slight overestimation or underestimation of *H*, depending on the H range it is estimating. This is most apparent around Hurst exponent ranges of 0.3 to 0.8 and data lengths of N=500 and N=1000, though observable under other parameter combinations as well (Fig. 2.1). This parameter also seems to provide a more pronounced influence as n_{max} becomes more unreliable. As the n_{max} ranges become smaller, approaching $N/10$, n_{min} ranges become more

unreliable. This is perhaps due to the fact that as n_{max} ranges become smaller, there are fewer numbers of windows by which to conduct a bi-logarithmic fluctuation versus scale plot. By also selecting a larger n_{min} value, an investigator further decreases the scale of investigation—thereby reducing the scope of the resulting DFA. Therefore, while n_{min} is not the most impactful parameter selection choice (in terms of resulting accuracy in estimating H), when n_{max} values are between $N/6$ and $N/10$, n_{min} values should remain around 4 to 6 samples.

Hurst exponent ranges: It has been previously noted that fractal methods show different reliabilities when estimating a variety of ranges of the Hurst exponent (Caccia, Percival et al. 1997). The findings of this study are consistent with these claims, with significance found between every pairwise comparison of H ranges using Tukey post hoc analysis ($p<0.001$). DFA showed high unreliability in H calculation at various Hurst exponent ranges. When H signals were between 0.1 and 0.2, DFA consistently overestimated H and provided inflated results (Figure 3, Appendix 2.1). When H signals were between 0.3 and 0.9, DFA consistently underestimated H and provided results that were smaller than the actual H values (Figure 3). There is a stark contrast between consistent overestimation of H values around 0.2 and consistent underestimation of H values around 0.3. The implication of these results are not immediately apparent. Tukey post hoc tests show that there is a 2-way interaction between the selected H signal range and *N*. This means that the estimated H accuracy is different depending on the combinations of the generated H range and *N* (and as discussed above, a larger *N* provides more reliable estimates of H) (Figure 2.1 and 3). There is also a 2-way interaction between the selected H signal range and n_{max}. This 2-way interaction make sense, since n_{max} is derived from *N*. Because of these variances in accuracy between estimating certain ranges of H, investigators applying experimental data should conduct preliminary investigations in order to anticipate

resultant H ranges and account for obstacles that DFA may provide in terms of overestimation or underestimation.

Adaptive Fractal Analysis (AFA)

Data length (*N*): Repeated measures ANOVA and Tukey Kramer post hoc tests verified that AFA did not show sensitivity towards data length. This is perhaps due to the selection of data lengths to be tested, as none challenge Cannon et al.'s recommendation of data lengths remaining above 2^8 samples (Cannon, Percival, et al. 1997). AFA's unique characteristic of overlapping windows may provide a more robust framework by which residuals of fit may be calculated, therefore handling smaller data lengths with the same clout as larger data lengths. Statistical analysis revealed 2-way interactions between *N* and n_{min} and between *N* and n_{max}. This means that data length changes as maximum window size changes and as minimum window size changes. Because of these interactions, care should be taken when selecting appropriate window sizes to complement data length to provide the most accurate results.

Maximum window size (n_{max}): As discussed above with DFA, n_{max} revealed itself to be the most parametrically significant input parameter when evaluating fractal methods. The results of parametric investigations of n_{max} revealed similar results to DFA—that larger maximum window ranges produced significantly poorer results than that of more conservative n_{max} values. Post hoc tests revealed all pairwise comparisons were significant (p <0.001) except between pairwise comparisons $N/8 - N/10$, which were still significant, but to a power of p<0.05. In this way, AFA seems to be more dependent on maximum window size selection than DFA. In reference to Figures 2.2, 2.3, 2.5, and 2.6, it can be seen that as the maximum window size decreases, the accuracy of the estimates improve. This can be also seen in Appendix 2, which additionally showcases how $N/2$ is consistently an inappropriate parameter selection. This trend

occurs fairly consistently through the parameters combinations. It is also important to note on Figures 2.5 and 2.6 that AFA seems to consistently inflate their H calculation throughout the entire parametric combination spectrum, except in specific situations where: (1) *N* is shorter—500 or 1000 samples in length, (2) n_{min} is shorter—4 or 6 samples in length, (3) n_{max} is short—N/8 or N/10 samples in length, and (4) Hurst exponent ranges tend to be persistent signals—over 0.5 up to 0.9. This could be due to similar reasons as discussed in the n_{max} parametric results of DFA. These are interesting combinations, initially suggesting that as the parametric combinations "trim down" the data (and subsequently the dynamics of the signal), AFA is more likely to underestimate the actual H value. However, n_{min} actually providing the most information at 4 and 6 samples contradicts that theory—especially because the underestimation peaks at n_{min}=4. This underestimation is perhaps due to a "translation" of the signal to the left on the bi-logarithmic plot. Put in a different way, considering windows at smaller intervals using both n_{max} and n_{min}, while additionally selecting data lengths that are not as powerful (i.e. shorter), creates a pattern of consistently small windows by which to analyze fluctuations versus scale. Statistically, variance of residuals tend to provide smaller values when the windows by which a regression line is plotted is smaller. Therefore, underestimation of these signals implies that the window frame is consistently subject to small windows and the intrinsic bias that comes with this parameter selection. This is evident in persistent signal ranges of H due to the signals being less "arbitrary" and easier to represent. Investigators considering AFA as a potential fractal method to use on experimental data are recommended to consider n_{max} values between *N*/6 and *N*/10.

Minimum window size (n_{min}): All pairwise comparisons of n_{min} were significant (p <0.01) except between pairwise comparisons 6 – 8 and 8 – 10. This implies that AFA is sensitive towards the selection of the minimum window size input parameter. Figures 2.2 and 2.3 show

that as n_{min} increases, it promotes slight overestimation of H. As discussed in the DFA section, this trend implies that selecting larger n_{min} values decreases the number of window sizes examined and reduces the power and analytical scope of AFA. The trend of n_{min} relating to the underestimation of signals at certain parametric combinations is discussed in the n_{max} analysis above (Figures 2.5 and 2.6). Based on these results, it is recommended that n_{min} values should be selected between 4 to 6 samples in length while using AFA.

Hurst exponent ranges: The findings of AFA results are consistent with Caccia et al. who reports that Hurst exponents are less accurately estimated at certain levels (Caccia, Percival et al. 1997). As with DFA, significance was found between every pairwise comparison of H ranges using Tukey post hoc analysis (p<0.001). AFA consistently inflated the Hurst exponent throughout each Hurst exponent range that was evaluated. The largest overestimation occurred at the tail ends of each spectrum, being highest from 0.1 - 0.3 and also tending to show inflation around 0.8 and 0.9 ranges. However, unlike DFA, AFA did not usually underestimate the results. This consistency points out that while AFA has a more predictable results when estimating fBm signals, care should be taken when addressing overfitting and inflation of H. Post hoc tests also reveal that there are 2-way interactions between the selected H signal range and N; between the selected H signal range and n_{max}; and between the selected H signal range and n_{min}. There is also a 3-way interaction between the selected H signal range, N and n_{max}. This means that the estimated H accuracy is different depending on these combinations of parameters. Because of these variances in accuracy between estimating certain ranges of H, investigators applying experimental data should conduct preliminary investigations in order to anticipate resultant H ranges and account for obstacles that AFA may provide. Additional attention should be provided to address inflation and overestimation of H.

Order of residual calculation (*M*): Tukey Kramer post hoc tests and the summary results in Figures 2.2, 2.3, 2.4, and 2.5 show that *M*=1 and *M*=2 differ significantly. *M*=1 is a more appropriate parameter selection than *M*=2, and consistently outperforms across both percent differences and raw differencing. By comparing Figures 2.4 and 2.5, it is evident that the parameter selection of *M*=2 introduces overfitting a second-order polynomial by which variance of the residuals will be calculated. This inflates Hurst exponent estimations in AFA, and indicates that first-order polynomial residual calculations is a more appropriate parameter selection when considering fBm signals. These findings are consistent with results in Riley et al.'s introduction to AFA where AFA produced slightly more accurate estimates for pink and white (fGn) noise, but slightly worse estimates for brown noise (fBm) (Riley, Bonnette et al. 2012). Note that a 2-way interaction between n_{max} and *M* was detected. This is likely due to the order of the residual of fit "overfitting" over larger window sizes. When selecting an *M* that is not first order, care should be taken to select appropriate n_{max} parameter limits.

Comparison of Key Parameter Characteristics of AFA and DFA

The results of this study showcase how both DFA and AFA are highly sensitive to input parameters and characteristics of the data (such as length and selected Hurst exponent range). Both have similarities and differences in both the methodology of calculation and how the parameters should be selected and appropriateness of data should be evaluated.

AFA provided more resistance to inconsistencies when considering data length (N). Graphical summaries (Figure 2 and Figure 3), review of statistical summaries (Appendix 1), and statistical analysis and post hoc evaluation (Table 1.1 and Table 1.2) showed that *N* differed very little amongst AFA results but DFA showed that *N* holds a larger influence over the accuracy of estimations. This verifies Gao et al.'s prediction that AFA is a more robust method in terms of

data length and accuracy of estimation (Gao, Hu et al 2011; Riley, Bonnette et al. 2012). Investigators concerned with smaller data lengths interfering with their fractal estimates should consider these differences. It is also relevant to note that this study did not seek to identify or quantify specific data appropriateness, only to investigate the effects of changing data characteristics and changing parameters on accuracy of fractal analysis using AFA and DFA. Data sets that are smaller than N=500 are not necessarily inappropriate selections, but should be treated with caution.

Maximum window size should be similarly treated with respects to AFA and DFA, with recommended selections ranging from about $N/6 - N/10$. Similarity of results show that both AFA and DFA are highly dependent on this parameter, likely due to the fact that higher window sizes increase the chance of emerging statistical artifacts, which can appear as scaling regions or additional patterns of the data that may not necessarily be appropriate. Depending on the complexity of the data, the length of the data, and the fractal method used investigators should select maximum window size based off of these varying properties.

One last distinction that AFA and DFA possess is their contrast in consistency of results across the H spectrum. AFA is highly consistent in its trends, either accurately estimating H or overestimating H (Figures 2.5 and 2.6). Overestimation tends to occur at the "tail ends" of the H spectra around 0.1 and around 0.9. Because of this, investigators can predict that if inaccuracies occur, they are largely due to "overfitting" and can adjust parameters accordingly. DFA, however, provides an overall more reliable raw differencing estimate of H (Figure 2.4) as compared to raw differencing of H with AFA (Figures 2.5 and 2.6). Upon closer inspection, DFA is subject to more unpredictable inflation or deflation of H estimates (Figure 3), but over smaller scales. It shows marked sensitivity to certain parameter combinations with no distinct

overall pattern. Percent differencing also lends insight to these distinctions by showcasing how DFA may overall provide more accurate estimates, but the relative consistency of those estimates is less than AFA. Averaging over a raw differencing table can seem accurate if trials provide overestimation and underestimation in equal measure. Percent differencing each measure before averaging shows us in Figure 2.1 that DFA provides worse estimates overall than AFA at selected H ranges of 0.3 or less. DFA provides better estimates overall than AFA at selected H ranges of 0.5 or less. Therefore, if investigators anticipate working in either of these regions, perhaps one method might be more suitable than the other. Both DFA and AFA are excellent tools to use when discerning patterns not available through stationary analysis methods, but they are both highly and uniquely sensitive to input parameters and should be treated with deliberate care.

Conclusion

AFA and DFA are fractal analysis methods that possess high sensitivity to input parameters. Combinations of (1) data length (N), (2) minimum window size (n_{min}), (3) maximum window size (n_{max}), and in the case of AFA, order of the fitted polynomial (M). The accuracy of both AFA and DFA in estimating the Hurst exponent at selected Hurst exponent ranges were analyzed at every combination for generated fBm signals. For both AFA and DFA, n_{max} was found to be the most significant parameter ($p<0.001$) that could affect H estimations up to an inaccuracy of 0.3, depending on other parameter combinations. Careful selection of n_{max} could make a great difference in the accuracy of H estimations when using experimental data. Avoidance of higher order M values is also highly recommended in order to avoid overfitting with AFA. DFA showed greater sensitivity to data length than AFA and greater inconsistency in overestimation and underestimation trends. However, DFA, compared to AFA, also showed

overall more precise estimation, particularly higher along the H spectrum. Depending on the approximate H range the experimental data lies within, the data size, and the nature of the signal, the appropriateness of input parameters and fractal methods will change.

This study serves to highlight how two fractal methods perform under combinations of input parameters with varying data characteristics. In fractal analysis, input parameters often go unreported in literature and selection of these parameters are often made at the discretion of the investigator. Very little consensus has been established on appropriateness of fractal measures or their input parameters on different experimental data signals. Parametric analysis of combinations in fBm signals, which appear often in physiological data, may provide insight and allow for recommendations about appropriate selection and experimental design using fractal methods.

Limitations: There are limitations to this study which should be considered. Due to the pilot nature of this study, parametric ranges of different input conditions were selected based off of preexisting literature. Other range values and parametric combinations were excluded based off of computational limitations (i.e. generation of longer data lengths). Shorter data lengths were excluded from generation because of the incompatibility with certain selected parametric combinations. Further studies should investigate wider ranges of each parametric input and seek to determine whether other variations of fractal analysis provide equivalent sensitivity to input parameters. It would also be relevant to investigate the effects of input parameter combinations in fractal analysis on other signals often found in physiological experimental data such as Gaussian noise or pink noise.

References

Aldrich, Preston R., Robert K. Horsley, Yousuf A. Ahmed, Joseph J. Williamson, and Stefan M. Turcic, 'Fractal Topology of Gene Promoter Networks at Phase Transitions', *Gene Regulation and Systems Biology*, 4 (2010), 75–82

Barnds, Annaria, 'BIOMECHANICAL MARKERS AS INDICATORS OF POSTURAL INSTABILITY PROGRESSION IN PARKINSON'S DISEASE', 2015 <https://kuscholarworks.ku.edu/handle/1808/19425> [accessed 21 November 2016]

Caccia, David C., Donald Percival, Michael J. Cannon, Gary Raymond, and James B. Bassingthwaighte, 'Analyzing Exact Fractal Time Series: Evaluating Dispersional Analysis and Rescaled Range Methods', *Physica A: Statistical Mechanics and Its Applications*, 246 (1997), 609–32 <https://doi.org/10.1016/S0378-4371(97)00363-4>

Cannon, Michael J., Donald B. Percival, David C. Caccia, Gary M. Raymond, and James B. Bassingthwaighte, 'Evaluating Scaled Windowed Variance Methods for Estimating the Hurst Coefficient of Time Series', *Physica A: Statistical Mechanics and Its Applications*, 241 (1997), 606–26 <https://doi.org/10.1016/S0378-4371(97)00252-5>

Cavanaugh, James T., Kevin M. Guskiewicz, and Nicholas Stergiou, 'A Nonlinear Dynamic Approach for Evaluating Postural Control', *Sports Medicine*, 35 (2005), 935–50 <https://doi.org/10.2165/00007256-200535110-00002>

Coeurjolly, Jean-Francois, 'Simulation and Identification of the Fractional Brownian Motion: A Bibliographical and Comparative Study', *ResearchGate*, 5 (2000) <https://doi.org/10.18637/jss.v005.i07>

Collins, J. J., and C. J. De Luca, 'Open-Loop and Closed-Loop Control of Posture: A Random-Walk Analysis of Center-of-Pressure Trajectories', *Experimental Brain Research*, 95 (1993), 308–18

Cross, S. S., 'Fractals in Pathology', *The Journal of Pathology*, 182 (1997), 1–8 <https://doi.org/10.1002/(SICI)1096-9896(199705)182:1<1::AID-PATH808>3.0.CO;2-B>

Delignières, Didier, Kjerstin Torre, and Pierre-Louis Bernard, 'Transition from Persistent to Anti-Persistent Correlations in Postural Sway Indicates Velocity-Based Control', *PLoS Computational Biology*, 7 (2011) <https://doi.org/10.1371/journal.pcbi.1001089>

Eke, A., P. Hermán, J. B. Bassingthwaighte, G. M. Raymond, D. B. Percival, M. Cannon, and others, 'Physiological Time Series: Distinguishing Fractal Noises from Motions', *Pflugers Archiv: European Journal of Physiology*, 439 (2000), 403–15

Gao, Jianbo, Brian M. Gurbaxani, Jing Hu, Keri J. Heilman, Vincent A. Emanuele II, Greg F. Lewis, and others, 'Multiscale Analysis of Heart Rate Variability in Non-Stationary Environments', *Frontiers in Physiology*, 4 (2013), 1–8 <https://doi.org/10.3389/fphys.2013.00119>

Gao, Jianbo, Jing Hu, and Wen-wen Tung, 'Facilitating Joint Chaos and Fractal Analysis of Biosignals through Nonlinear Adaptive Filtering', *PLoS ONE*, 6 (2011) <https://doi.org/10.1371/journal.pone.0024331>

Kuznetsov, Nikita, Scott Bonnette, Jianbo Gao, and Michael A. Riley, 'Adaptive Fractal Analysis Reveals Limits to Fractal Scaling in Center of Pressure Trajectories', *Annals of Biomedical Engineering*, 41 (2012), 1646–60 <https://doi.org/10.1007/s10439-012-0646-9>

Mandelbrot, Benoit B., and John W. Van Ness, 'Fractional Brownian Motions, Fractional Noises and Applications', *SIAM Review*, 10 (1968), 422–37

Peng, C.-K., Shlomo Havlin, and H. Eugene Stanley, 'Quantification of Scaling Exponents and Crossover Phenomena in Nonstationary Heartbeat Time Series', *Chaos*, 5 (1995), 82

Riley, Michael A., Scott Bonnette, Nikita Kuznetsov, Sebastian Wallot, and Jianbo Gao, 'A Tutorial Introduction to Adaptive Fractal Analysis', *Fractal Physiology*, 3 (2012), 371 <https://doi.org/10.3389/fphys.2012.00371>

Stergiou, Nicholas. Editor. *Nonlinear Analysis for Human Movement Variability*. Boca Raton: Taylor & Francis, CRC Press, 2016. Print.

Turcotte, Donald L., Bruce D. Malamud, Fausto Guzzetti, and Paola Reichenbach, 'Self-Organization, the Cascade Model, and Natural Hazards', *Proceedings of the National Academy of Sciences of the United States of America*, 99 Suppl 1 (2002), 2530–37 <https://doi.org/10.1073/pnas.012582199>

Figure 1

Depiction of sample fBm signals generated at N=1000 at each Hurst exponent range between 0.1 and 0.9. Note that as the input H parameter increases for each generated signal, deterministic patterns become visually evident.

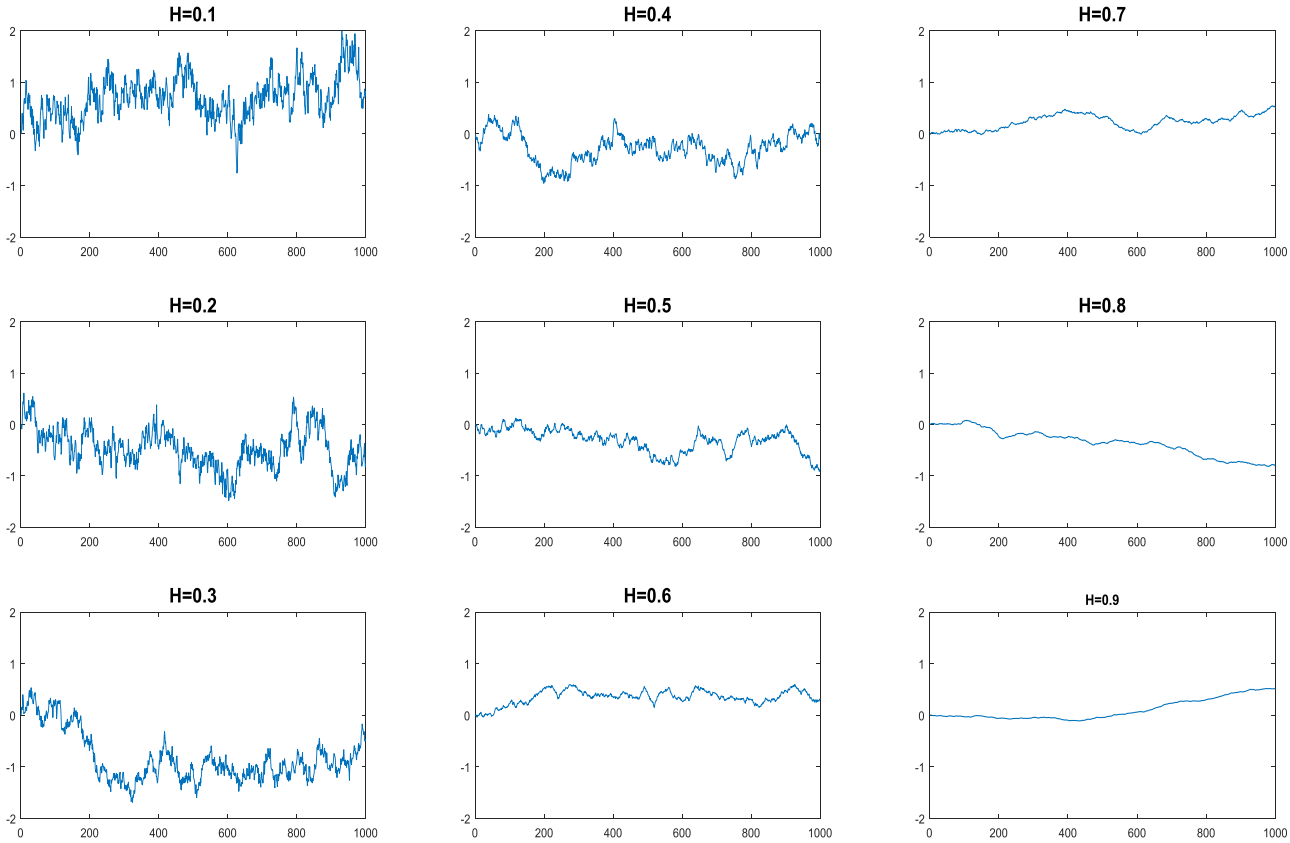

Figure 2: Heatmaps depicting differences between the generated Hurst exponent from the fBm signals and the Hurst exponent estimated using DFA and AFA. In each plot, certain parameters and ranges were excluded in order to enhance resolution of appropriate parameters. For the overall depiction of ranges and parameters, refer to Appendix 2.

Figure 2.1: Heatmap showing percent difference using DFA with generated H ranges H=0.1 and H=0.2 eliminated. This was done in order to provide a consistent resolution over each DFA and AFA chart to show relative accuracies of each method. Every other parameter investigated is shown in the heat map.

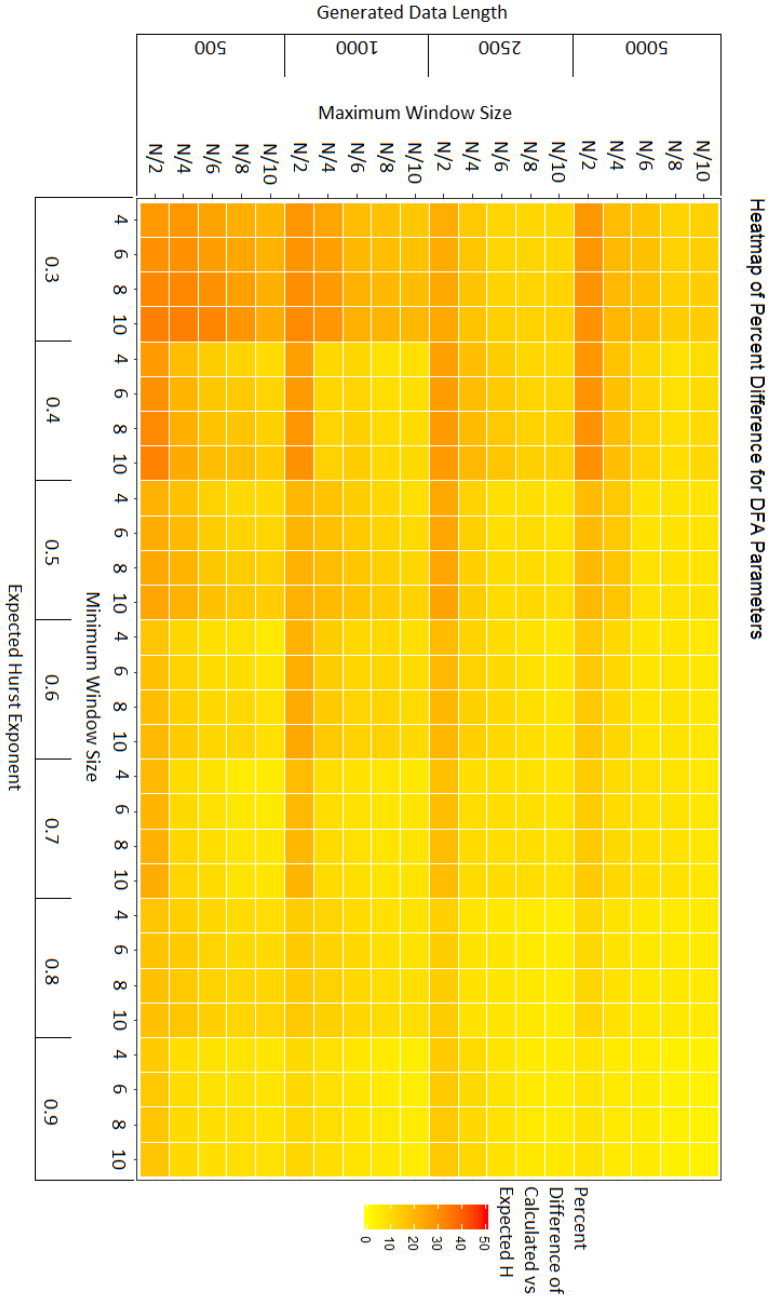

Figure 2.2: Heatmap showing percent difference using AFA (*M*=1), with generated H ranges H=0.1 and H=0.2 eliminated. This was done in order to provide a consistent resolution over each DFA and AFA chart to show relative accuracies of each method. Every other parameter investigated is shown in the heat map.

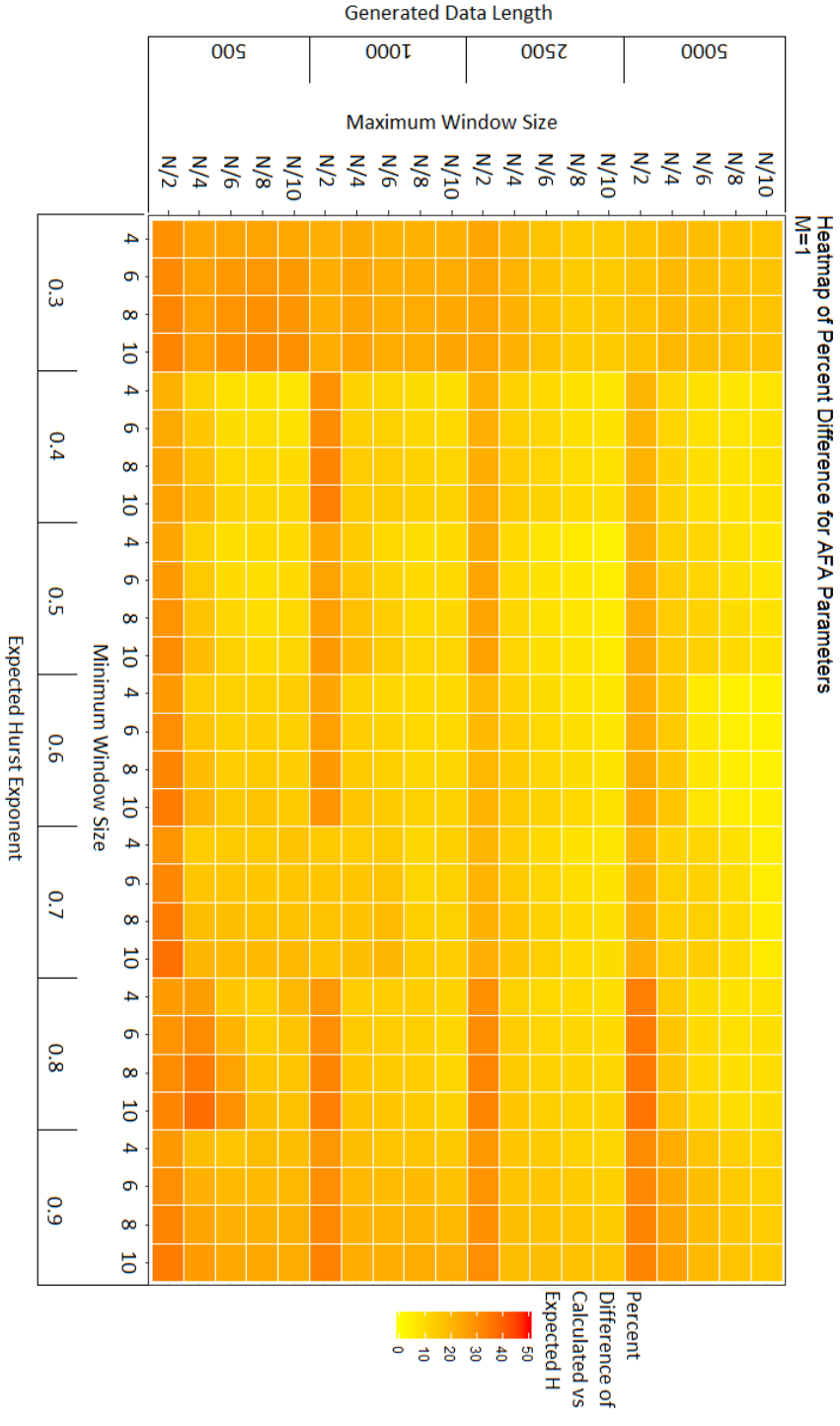

Figure 2.3: Heatmap showing percent difference using AFA (*M*=2), with generated H ranges H=0.1 and H=0.2 eliminated. This was done in order to provide a consistent resolution over each DFA and AFA chart to show relative accuracies of each method. Every other parameter investigated is shown in the heat map.

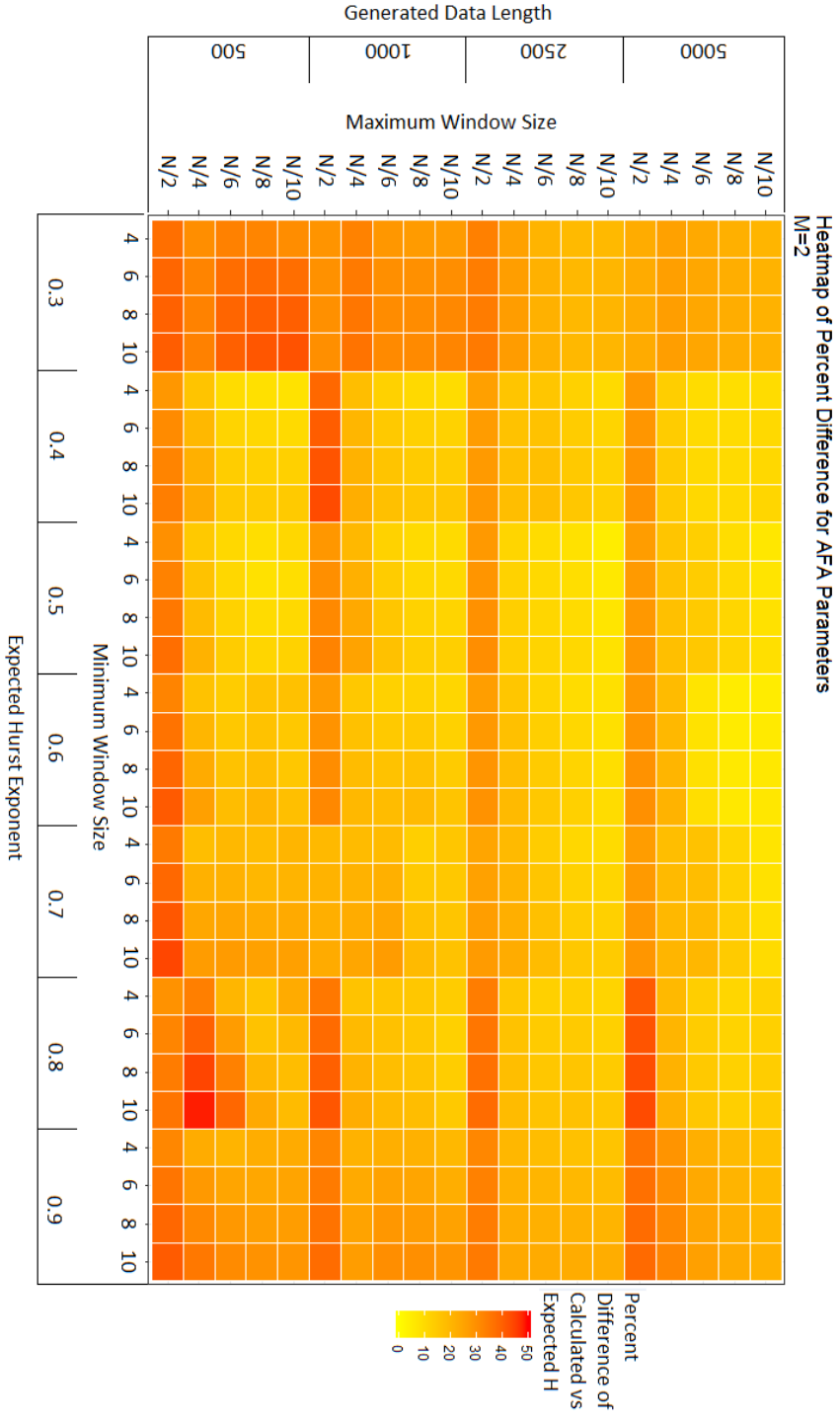

Figure 2.4: Heatmap showing differences between generated and estimated H using DFA. The n_{max} parameter N/2 was eliminated. This was done in order to provide a consistent resolution over each DFA and AFA chart to show relative accuracies of each method. Every other parameter investigated is shown in the heat map.

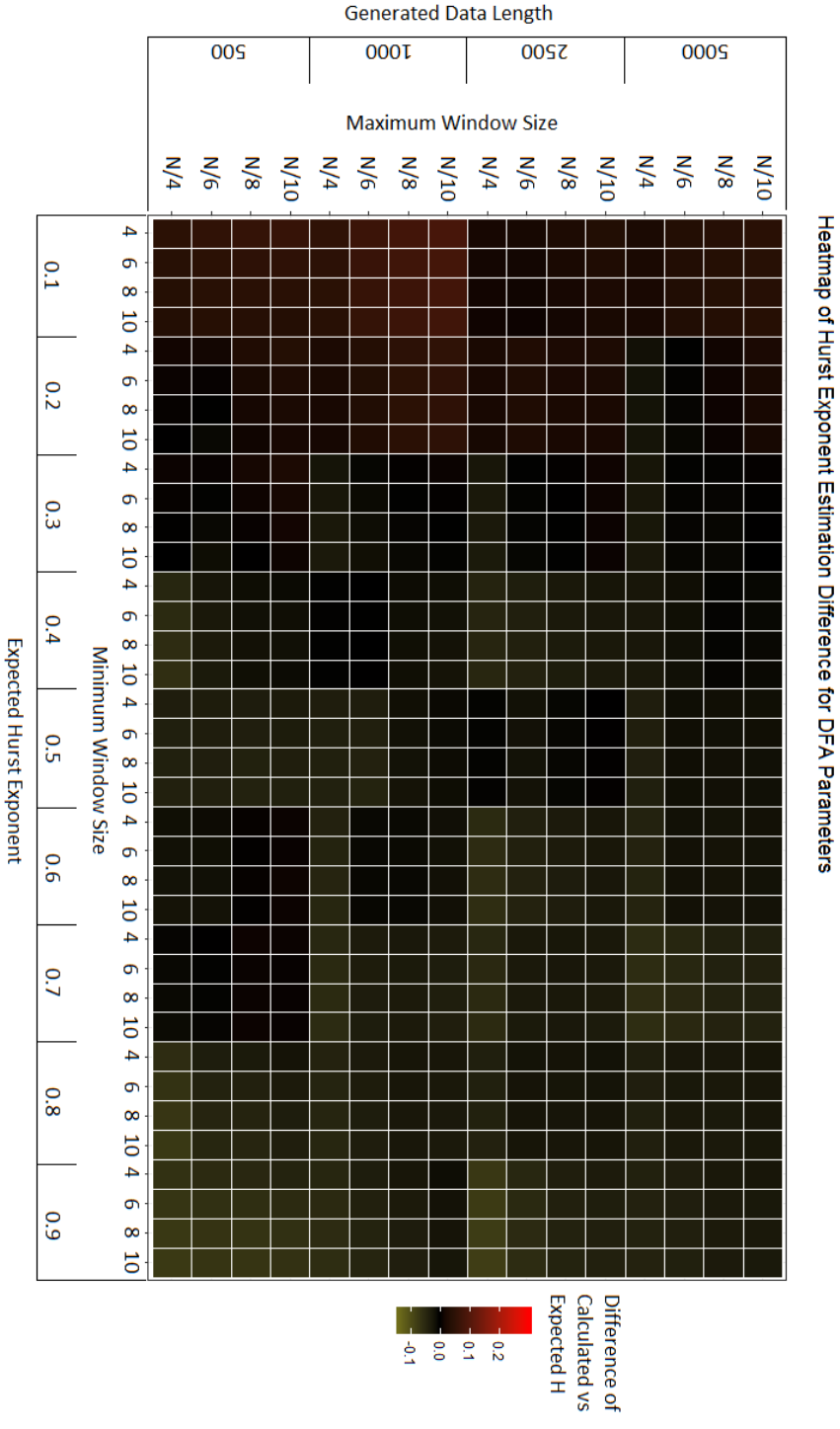

Figure 2.5: Heatmap showing differences between generated and estimated H using AFA (*M*=1). The n_{max} parameter N/2 was eliminated. This was done in order to provide a consistent resolution over each DFA and AFA chart to show relative accuracies of each method. Every other parameter investigated is shown in the heat map.

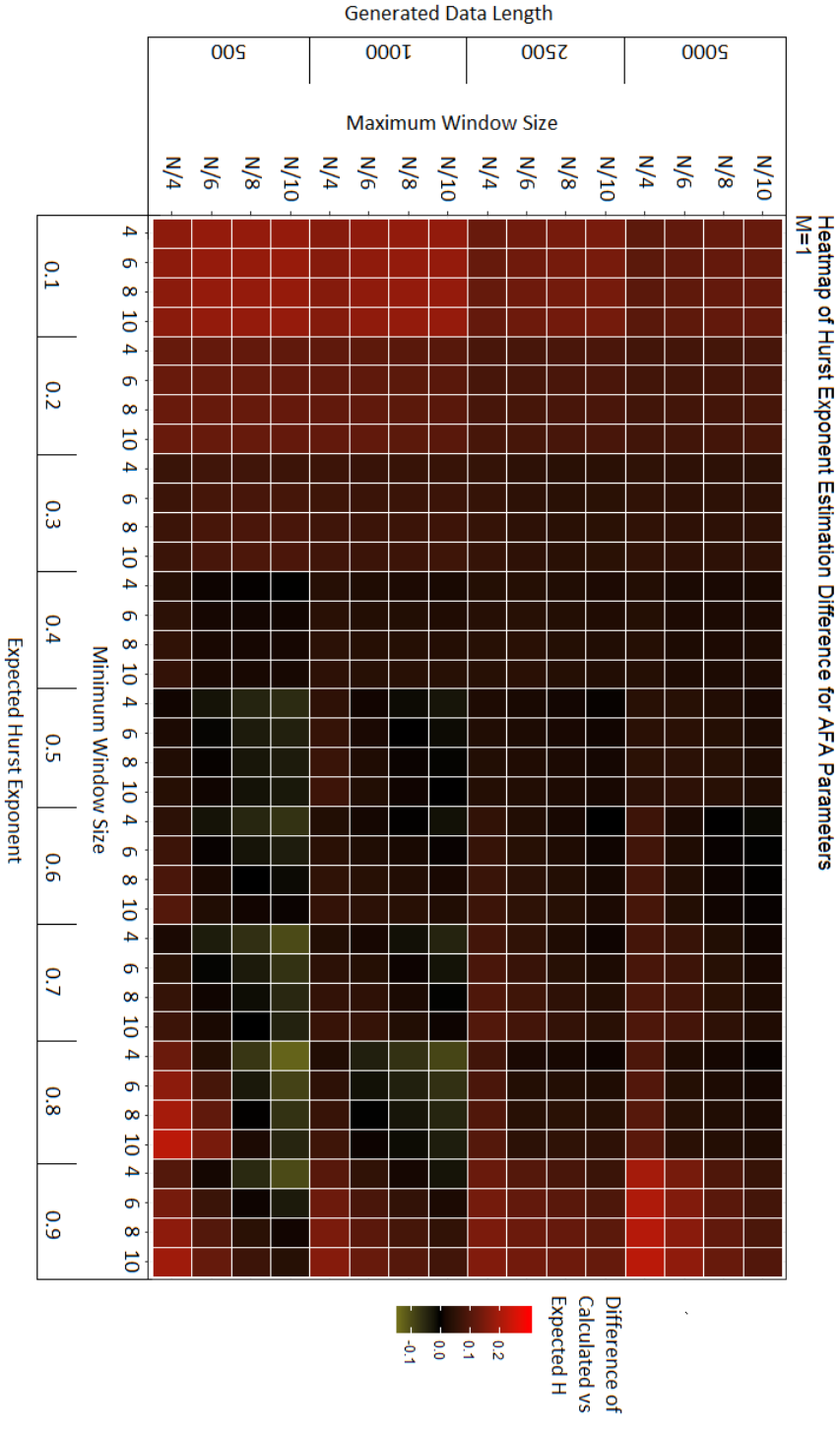

Figure 2.6: Heatmap showing differences between generated and estimated H using AFA (*M*=2). The n_{max} parameter N/2 was eliminated. This was done in order to provide a consistent resolution over each DFA and AFA chart to show relative accuracies of each method. Every other parameter investigated is shown in the heat map.

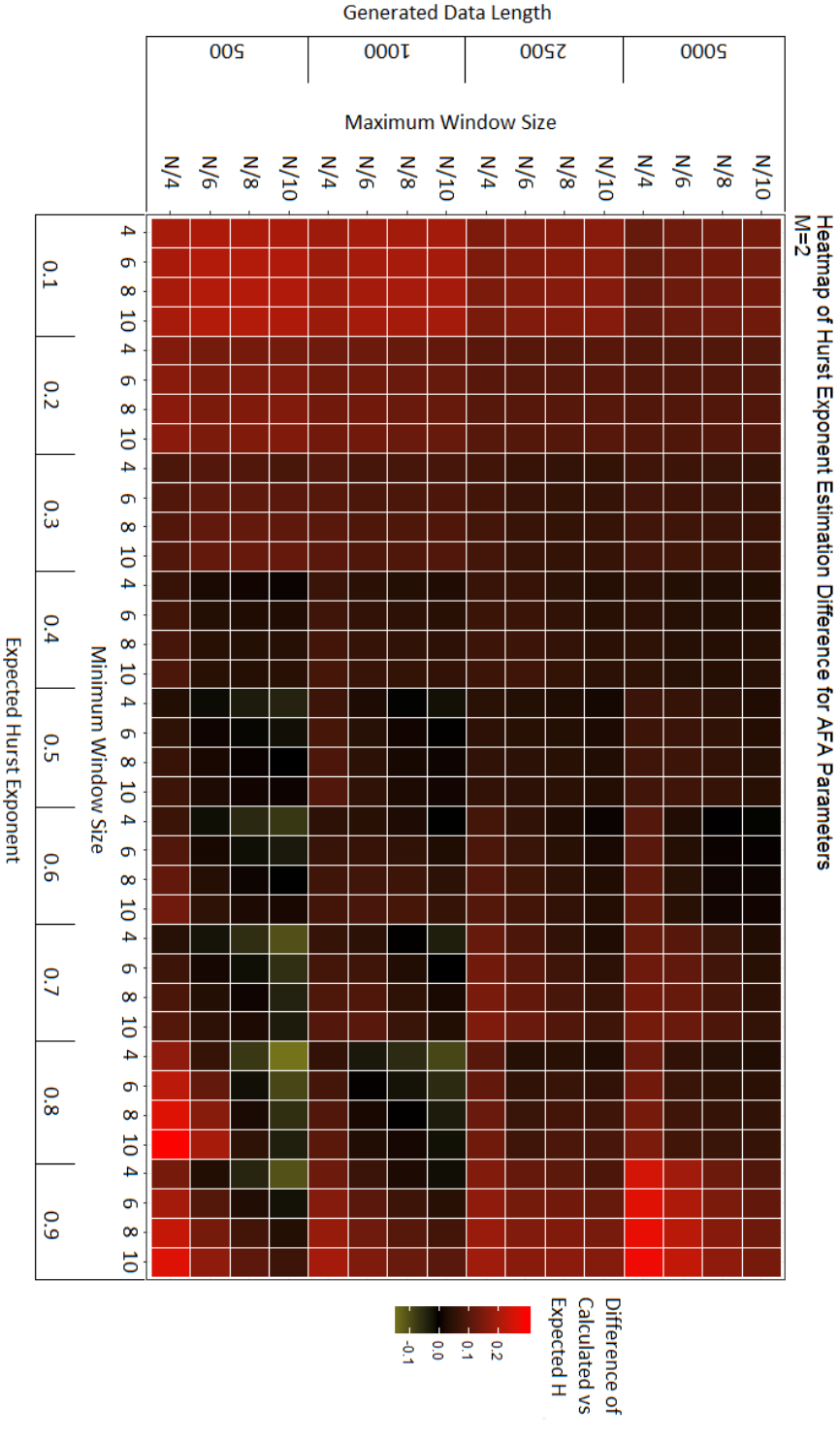

Figure 3: Heatmap depicting differences between the generated Hurst exponent from the fBm signals and the Hurst exponent estimated using DFA. The n_{max} parameter N/2 was eliminated. This was done in order enhance resolution of appropriate parameters. The range over which these differences are shown is rescaled to provide the best view of DFA parameters, since Figure 2.4 does not provide this information when considered across the same scaling ranges as AFA.

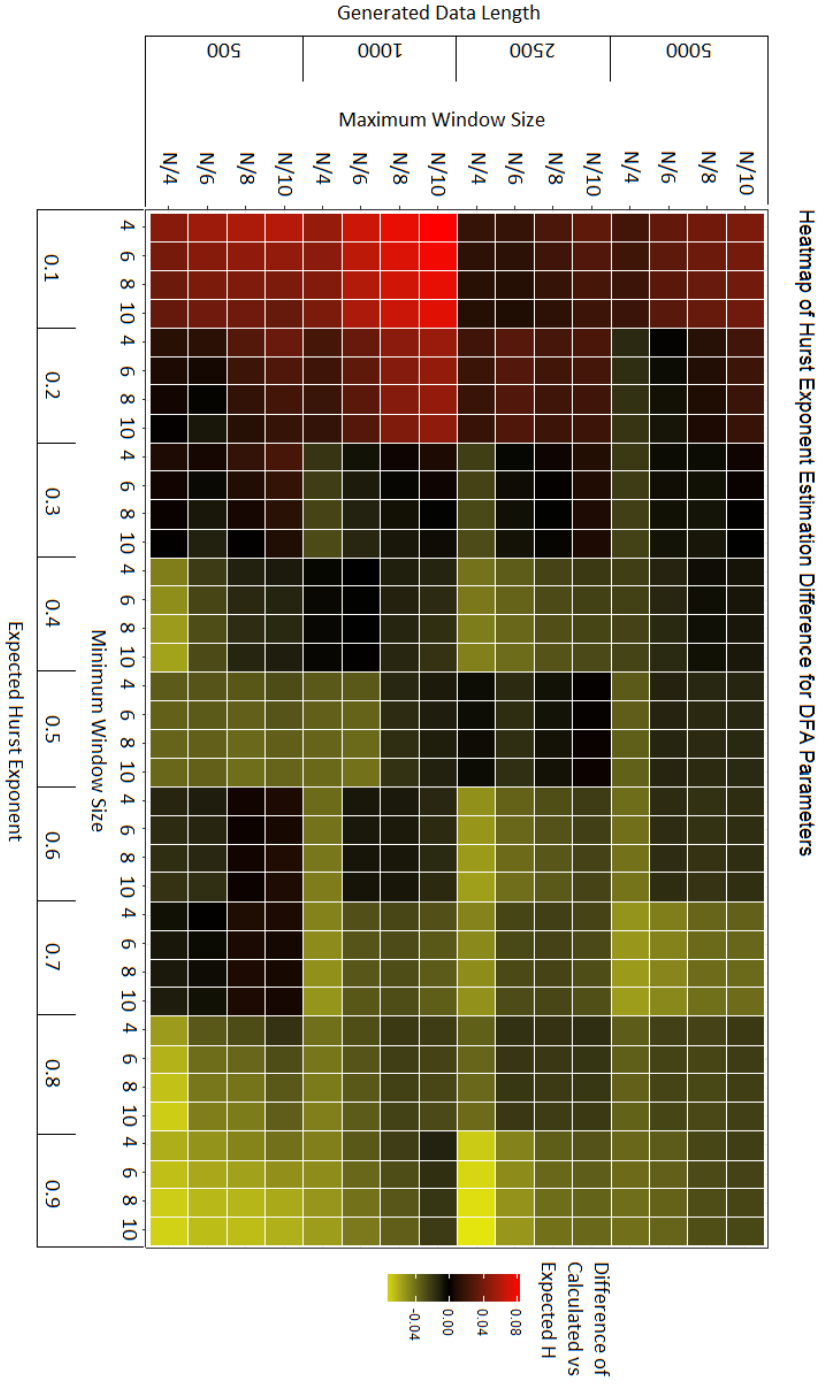

Table 1: Repeated Measures ANOVA for combinations of each possible group using DFA and AFA.

Table 1.1
Repeated Measures ANOVA for combinations of each possible group using DFA. Degrees of freedom (Df), sums of squares (Sum Sq), means of squares (Mean Sq), F statistics (F value) and p statistics (Pr(>F)) are reported below for significance values of 0-0.001 (***). 0.001-0.01 (**), 0.01-0.05 (*) and 0.05-0.1 (.). Groups can be identified as generated H ranges (H_exp), length of data (N), minimum window size (nmin), and maximum window size(nmax).

	Df	Sum Sq	Mean Sq	F value	Pr(>F)	
H_exp	8	794.47	99.308	12927.0198	< 2.2e-16	***
N	3	0.20	0.066	8.5415	1.156e-05	***
nmin	3	0.07	0.025	3.1894	0.0226474	*
nmax	4	4.36	1.090	141.9166	< 2.2e-16	***
H_exp:N	24	1.86	0.077	10.0788	< 2.2e-16	***
H_exp:nmin	24	0.01	0.000	0.0632	1.0000000	
N:nmin	9	0.02	0.002	0.2694	0.9828340	
H_exp:nmax	32	0.50	0.016	2.0309	0.0005126	***
N:nmax	12	0.07	0.006	0.7464	0.7066026	
nmin:nmax	12	0.00	0.000	0.0027	1.0000000	
H_exp:N:nmin	72	0.01	0.000	0.0160	1.0000000	
H_exp:N:nmax	96	0.82	0.009	1.1113	0.2152078	
H_exp:nmin:nmax	96	0.00	0.000	0.0058	1.0000000	
N:nmin:nmax	36	0.00	0.000	0.0026	1.0000000	
H_exp:N:nmin:nmax	288	0.01	0.000	0.0033	1.0000000	
Residuals	13680	105.09	0.008			

Table 1.2
Repeated Measures ANOVA for combinations of each possible group using AFA. Degrees of freedom (Df), sums of squares (Sum Sq), means of squares (Mean Sq), F statistics (F value) and p statistics (Pr(>F)) are reported below for significance values of 0-0.001 (***). 0.001-0.01 (**), 0.01-0.05 (*) and 0.05-0.1 (.). Groups can be identified as generated H ranges (H_exp), length of data (N), minimum window size (nmin), maximum window size(nmax) and order of variance polynomial fits (order).

	Df	Sum Sq	Mean Sq	F value	Pr(>F)	
H_exp	8	1878.81	234.851	16513.8724	< 2.2e-16	***
N	3	0.08	0.026	1.8271	0.13979	
nmin	3	2.68	0.893	62.8214	< 2.2e-16	***
nmax	4	40.46	10.114	711.2083	< 2.2e-16	***
order	1	5.26	5.264	370.1430	< 2.2e-16	***
H_exp:N	24	11.59	0.483	33.9527	< 2.2e-16	***
H_exp:nmin	24	2.04	0.085	5.9846	< 2.2e-16	***
N:nmin	9	0.79	0.088	6.1632	1.013e-08	***
H_exp:nmax	32	30.92	0.966	67.9363	< 2.2e-16	***
N:nmax	12	2.68	0.223	15.6968	< 2.2e-16	***
nmin:nmax	12	0.12	0.010	0.6879	0.76489	
H_exp:order	8	0.21	0.027	1.8715	0.05974	.
N:order	3	0.01	0.003	0.2371	0.87053	
nmin:order	3	0.06	0.019	1.3443	0.25797	
nmax:order	4	0.42	0.104	7.3243	6.850e-06	***
H_exp:N:nmin	72	0.48	0.007	0.4710	0.99996	
H_exp:N:nmax	96	8.61	0.090	6.3042	< 2.2e-16	***
H_exp:nmin:nmax	96	0.12	0.001	0.0910	1.00000	
N:nmin:nmax	36	0.03	0.001	0.0576	1.00000	
H_exp:N:order	24	0.21	0.009	0.6076	0.93235	
H_exp:nmin:order	24	0.02	0.001	0.0631	1.00000	
N:nmin:order	9	0.02	0.002	0.1552	0.99784	
H_exp:nmax:order	32	0.14	0.004	0.3160	0.99992	
N:nmax:order	12	0.02	0.002	0.1200	0.99989	
nmin:nmax:order	12	0.00	0.000	0.0285	1.00000	
H_exp:N:nmin:nmax	288	0.09	0.000	0.0217	1.00000	
H_exp:N:nmin:order	72	0.01	0.000	0.0056	1.00000	
H_exp:N:nmax:order	96	0.17	0.002	0.1223	1.00000	
H_exp:nmin:nmax:order	96	0.00	0.000	0.0020	1.00000	
N:nmin:nmax:order	36	0.00	0.000	0.0039	1.00000	
H_exp:N:nmin:nmax:order	288	0.00	0.000	0.0005	1.00000	
Residuals	27360	389.10	0.014			

Chapter 4: PD Study

Abstract

Background: Postural instability (PI), characterized by quantitative analysis of center of pressure (COP), is a cardinal motor symptom of Parkinson's disease (PD) associated with high fall risk and a decrease in quality of life. No current clinical method provides adequate sensitivity to detect and quantify PI and fall risk as PD progresses. Non-stationary fractal methods have been proposed as a quantifiable analysis tool by which COP and PI can be characterized in PD patients. The study investigates and compares the sensitivity of these fractal methods applied towards COP velocity (COPv) in mild (without PI) and moderate PD (with PI) and age-range matched healthy controls to quantify the development of PI.

Methods: Data was analyzed from a previous study that measured quiet stance postural sway in mild PD (n=13), moderate PD (n=10) and age-range matched healthy controls (n=21) in eyes open (EO) and eyes closed (EC) sensory conditions. Reaction forces and moments were measured on a force plate and used to calculate COP and COPv. Detrended fluctuation analysis (DFA) and adaptive fractal analysis (AFA) were calculated and a small sample Bayesian correlation criterion model (SICc) was applied to verify scaling region results. A 2-way ANOVA with blocking conditions was used to determine the effects of Group, Condition, and the interaction effects on all parameters.

Findings: 1- and 2-region models for DFA and 2- and 3-region models for AFA characterized scaling behavior in PD. Significant Group effects were found for both DFA and AFA, particularly within the parameter H_{fast}, indicating that both fractal methods were sensitive towards PI and PD progression. AFA also produced more anti-persistent patterns across most conditions and was resistant to inter-participant variability.

Interpretation: Both AFA and DFA are sensitive to the progression of PI and PD. While AFA found fewer significant measures than DFA, it provided a more consistent characterization of PI in PD and was more resistant to inter-participant variability. The emergence of highly variable scaling regions in both AFA and DFA also suggest that postural dynamics characterized by velocity-based neural controllers possess a complexity that reaches past traditional intermittent fGn-fBm frameworks.

Introduction

Parkinson's disease (PD) is the second most common neurodegenerative disorder in the world (Alves, Forsaa et al. 2008). PD is characterized by four motor cardinal traits: tremor, rigidity, bradykinesia, and postural instability (PI) (Wirdefeldt, Adami et al. 2011). The loss of dopaminergic cells in the basal ganglia during PD results in degenerating motor control. As the degeneration of motor function progresses, PI intensifies and an increase in fall risk emerges in PD patients (Wielinski, Erikson-Davis et al. 2005; McNeely, Duncan et al. 2012). Falls can lead to an overall decrease in quality of life from resulting pain, limitation, fear of falling, and high levels of caregiver stress (Bloem and Grimbergen, et al. 2001; Adkin, Frank et al. 2003; Kim, Allen, et al. 2013). There is no known cure for PD, but treatment options exist in order to alleviate symptoms, the most common of which is levodopa.

PD diagnosis is primarily evaluated through two major rating scales: the Unified Parkinson's Disease Rating Scale (UPDRS) and Hoehn and Yahr (H&Y) (Simuni and Pahwa, 2009; Goetz, Poewe et al. 2004). Through written examinations, motor assessments, and interactions with the patient, clinicians are able to identify key symptoms of PD. This can often be a challenging process, since noticeable symptoms of PD usually start emerging when approximately 50 to 60% of the dopaminergic cells have died and more than 80% of dopamine has been lost (Wirdefeldt, Adami et al. 2011). For this reason, there is a need for a deeper understanding and characterization of PD progression in order to provide an opportunity for identification of early markers for PD diagnosis. Current clinical measures and assessments are not suitable for quantifiable early detection of PD (Doyle, Newton et al. 2005; Barnds, 2015; Harper, 2015).

Because of the close association of PI and fall risk, postural sway measures are being used as a quantifiable measure of motor control and progression of PD **(**Schmit, Riley et al. 2005; Chastan, Debono et al. 2008; Stylianou, McVey et al. 2011; Mancini, Carlson-Kuhta et al. 2012). Center of pressure (COP) is a time series that has been used as an indicator for somatosensory, vestibular, visual and auditory contributions towards a postural control system in the central nervous system (CNS) (Mancini, Horak et al. 2011; Hill, Stuart et al. 2016). Analysis of COP time series has brought about useful characterization of the motor control system in terms of PI and PD progression (Horak, Dimitrova, et al. 2005; Mancini, Horak et al. 2011; Stylianou, McVey, et al. 2011; McNeely, Duncan, et al. 2012).

COP time series is often assumed to be a stationary signal. However, there is a growing consensus amongst investigators that the COP time series exhibits non-stationary properties—meaning statistical measures such as mean and standard deviation vary over time (Collins and DeLuca, 1993; Schumann, Redfern et al. 1995; Vaillancourt and Newell, 2000; Delignieres, Deschamps et al. 2003; Loughlin, Redfern et al. 2003; Doyle, Newton et al. 2005; Schmit, Riley et al, 2005; Cavanaugh, Mercer et al. 2007; Morrison, Kerr et al. 2008; Minamisawa, Takakura et al. 2009; Ramdani, Seigle et al. 2009; Kuznetsov, Bonnette et al. 2012; Harper, 2015; Stergiou, 2016). Non-stationary characteristics of COP signals indicate that while stationary patterns may provide useful information, analysis adhering towards non-stationary assumptions reveal embedded patterns in the data that were not previously apparent. Both COP position and COP velocity (COPv) time series have been noted for their non-stationary properties (Jeka, Kiemel et al. 2004; Ramdani, Seigle et al. 2009; Delignieres, Torre et al. 2011; Harper, 2015). Additional analysis of postural sway feedback mechanisms reveal that COPv provides the most sensitive and pertinent information when considering motor control systems, as compared to

COP position or COP acceleration time series (Jeka, Kiemel et al. 2004). Some argue that this sensitivity derives from a velocity-based, intermittent neural controller embedded in the schema of motor control (Delignieres, Torre et al. 2011). Using detrended fluctuation analysis (DFA) first introduced by Peng et al. in 1995, Delignieres et al. also characterized unique properties of COPv with power law scaling behavior (Peng, Havlin et al. 1995; Delignieres, Torre et al. 2011). Bi-logarithmic plots of fluctuation versus time exhibited multiple scaling regions, indicative of open loop and closed loop postural control (Collins and De Luca, 1993). The presence of multiple scaling regions has also been suggested to be a sign of deterioration of complexity in a signal, rather than a direct relation towards neural mechanisms (Lipsitz and Goldberger, 1992). Strong fractal behavior is usually associated with a single scaling region, whereas multiple scaling regions could represent complex variability, loss of control, and highly variable fluctuations in a pattern.

Applying DFA towards PD COPv signals, correlations between open loop (reflexive feedforward) and closed loop (somatosensory feedback) mechanisms and intermittent velocity-based control support the idea of COPv sensitivity towards detection of a neural controller (Harper, 2015). However, due to limitations in signal length and sample size, alternative fractal analysis methods should be considered in order to provide a more robust characterization of physiological results. Adaptive fractal analysis (AFA) is one such recently developed fractal method. Similar to DFA, AFA extracts a globally smooth trend signal in order to apply power law scaling towards estimation of the Hurst exponent (H), which acts as a measure of long-term memory of a time series through correlation of signal fluctuations and time scales. AFA is believed to handle arbitrary, non-linear trends with more efficiency than DFA, provides higher resolution of fractal behavior over smaller signal lengths than DFA, and provides direct

interpretation of spectral energy, while DFA does not (Gao, Hu et al. 2011; Riley, Bonnette et al. 2012).

The purpose of this study was to investigate whether AFA and DFA parameters demonstrate sensitivity towards COPv time series in PD patients, compared to HC, in order to further understand and characterize the development of balance problems (i.e. PI) in persons with PD. The presence and progression of PD and the presence of PI were determined through standard current clinical assessments in order to provide a comparison towards the effectiveness of AFA and DFA in detecting the presence and progression of PD and the presence of PI. Hypothesis #1: AFA, compared to DFA, will show more robust sensitivity towards the presence of postural instability and with more consistent results regarding Group and Condition comparisons.

A secondary goal of this study is to better understand the effect that the presence of PD has on the scaling regions (HC versus mild PD) and the effect that the presence of PI, associated with PD progression, has on scaling regions (mild PD versus moderate PD). Hypothesis #2: AFA, compared to DFA, will show greater sensitivity towards scaling regions, depicting a higher scaling resolution by which to draw conclusions regarding PI characterization using fractal methods. Further understanding of AFA as an applicable tool towards COPv analysis may widen our understanding of postural controls systems and could benefit clinical assessments of PD, with an emphasis on early detection using PI as a quantifiable marker of progression.

Methods

Participants

As reported previously by Barnds et al. (Barnds, 2015), twenty-three patients with PD and twenty-one age matched healthy controls (HC) participated in a postural sway task study. These participants were included in two previously conducted studies investigating the differences between HC and PD over varying severity ranges in postural sway measures (Stylianou et al., 2011; Barnds, 2015). All participants with PD were recruited from the University of Kansas Medical Center (KUMC) Parkinson's disease and Movement Disorder Center. All individuals were informed and gave written consent as approved by the University's Institutional Review Board.

Participants with PD were divided into two sub-categories: Mild PD (PD-Mi) in which there were no apparent postural deficits and Moderate PD (PD-Mo) in which postural deficits were present. Placement into the two PD groups and all PD diagnoses were based on clinical assessment performed by a movement disorders neurologist (RP), as discussed in Barnds et al. All participants with PD were able to walk without assistance, were without severe depression (BDI<30/63), dementia (MMSE>24/30), and musculoskeletal or neurologic impairments unrelated to PD, had an H&Y score of 2 (PD-Mi) or 3 (PD-Mo) and had not had neurosurgery for PD. HC participants were recruited from the surrounding community and were without any significant cognitive, musculoskeletal or neurologic impairment.

Task

As reported by Stylianou et al. (Stylianou et al, 2011), participants wearing standardized footwear were asked to stand quietly on a force plate with self-selected stance width, with their arms at their side and looking forward. Participants with PD were instructed to maintain their

normal medication schedule and were tested *on* medication. The mean (SD) time since the last antiparkinsonian dosage was 2.1 (1.0) hours. Six trials of postural sway data were collected, each in periods of 30 seconds. There were two standing conditions: Eyes Open (EO) and Eyes Closed (EC) and three trials of each were performed in randomly selected order. Further details on the task are described in Stylianou et al.

Experimental Measurements

Postural sway kinetic data was collected using AMTI six-channel force plates (Advanced Mechanical Technology Inc., Watertown, MA, USA) and sampled at 1000 Hz using a 16-bit A/D data acquisition system (National Instruments, Austin, TX, USA). Video data was used in order to ensure subject compliance with postural sway task instructions.

Kinetic data was low-pass filtered with a fourth-order, zero phase shift, Butterworth filter with a cut-off frequency of 10 Hz. COP path (COPp) was then calculated in the anterior-posterior (AP) direction. COPp was not calculated in the mediolateral (ML) direction because stance width of the base of support was not a controlled parameter in task instructions. COP velocity (COPv) in the AP direction was calculated using a fourth order accuracy numerical derivative of the COPp. The COPv time series was down-sampled to 100 Hz. Each trial was analyzed separately. Trials within a participant were blocked to allow for the assessment of variability between subjects within each group. All data analysis was conducted using MATLAB (MATLAB, Natick, MA, USA).

Data Analysis

Detrended Fluctuation Analysis

DFA was performed on each participant trial (to a total of 6 trials per participant) as consistent with Peng et al. and Delignieres et al. (Peng, Havlin et al. 1995; Delignieres, Torre et al. 2011). DFA applies the power scaling law in order to compare variance of displacement against increments of discrete time scales. The size of the time scales is defined by the user. In the present study, multiple time scales were used for DFA and their interactions with other input parameters were investigated. The steps below were derived from Delignieres et al.:

1. Integrate the signal using the equation: $y(k) = \sum_{i=1}^{k}[B(i) - B_{ave}]$, where *B(i)* is the i^{th} interval and B_{ave} is the average interval. The integrated time series is expressed as *y(k)*.

2. Partition the integrated time series into non-overlapping windows of equal length (*n*).

3. Fit a first-order, least squares line to the data in each window. The line represents the trend inside each window. The y coordinates of each trend can be expressed as $y_n(k)$.

4. Detrend the integrated time series, *y(k)*, by subtracting the local trend, $y_n(k)$, for each window.

5. Calculate the RMS fluctuation using the following equation:

$$F(n) = \sqrt{\frac{1}{N}\sum_{k=1}^{N}[y(k) - y_n(k)]^2}$$

6. Plot *F(n)* versus *n* (fluctuation versus scale) on a bi-logarithmic plot.

The resulting plot should provide a linear relationship between *F(n)* and *n*. The slope of the first-order, least squares fit regression line of this linear relationship is analogous to the Hurst exponent (H) and the relationship can be expressed using the power law scaling behavior:

$$SD(\Delta x) \propto \Delta t^{H}$$

where $SD(\Delta x)$ is a variance of the displacement of the time series and Δt^{H} represents the power scaling law over various time intervals and scales.

Each of the participant trials was analyzed using DFA with signal lengths of N=3000, minimum window size of n_{min} =4, and maximum window size of n_{max} =N/10=300. These input parameters were based on the appropriate parameter specifications and findings in Chapter 3 of this thesis.

Adaptive Fractal Analysis

AFA was performed on each participant trial (to a total of 6 trials per participant) as a pilot investigation towards an alternative additional fractal method to DFA. AFA was introduced by Gao et al. in 2011 and also applies power law scaling behavior in order to compare fluctuation versus scale analysis (Gao, Hu et al 2011). AFA differs from DFA in that it includes a step that creates a globally smooth detrending signal using overlapping window intervals rather than non-overlapping windows containing first-order, least square signals (Riley, Bonnette et al. 2012). In the present study, multiple window scales were used for AFA and their interactions with other input parameters were investigated. The steps below were derived from Riley et al.:

1. a. If the data represents a fractional Gaussian process (fGn), integrate the signal.

1. b. If the data represents a fractional Brownian process (fBm), integration of the signal is not advised.

2. Partition the time series (*u(i)*) into windows of length: $w = 2n + 1$, with windows overlapping by $n + 1$ points. Note that the user will set the window sizes, so *n* is not a free parameter (i.e. $n = \frac{(w-1)}{2}$.

3. Within each window, the least squares polynomial of order *M* is identified. *M* is an input parameter that is selected by the user.

4. The local fits of each window then need to be "stitched" together in order to provide a smooth global fit to the time series. This is done by taking a weighted combination of the fits of two adjacent windows and can be expressed mathematically as:

$$y^{(c)}(l) = w_1 y^{(i)}(l + n) + w_2 y^{(i+1)}(l), \qquad l = 1,2, \dots, n + 1$$

where $w_1 = 1 - \frac{l-1}{n}$ and $w_2 = \frac{l-1}{n}$.

5. Once a globally smooth trend (*v(i)*) has been created from overlapping windows, detrend the time series (*u(i)*) from the globally smooth trend in order to examine how the variance of the residuals of fit compare to the window scales. Calculate using the following equation:

$$F(w) = \sqrt{\frac{1}{N}\sum_{i=1}^{N}[u(i) - v(i)]^2}$$

6. Plot *F(n)* versus *n* (fluctuation versus scale) on a bi-logarithmic plot. Riley et al. quantified this relation in a plot of $\log_2(F(w))$ versus $\log_2(w)$, as opposed to a logarithmic base of ten used in DFA (Riley, Bonnette et al. 2012). The resulting plot should provide a linear relationship between *F(w)* and *w*. Similar to DFA, the slope of the resultant least squares fit regression line in analogous to the Hurst exponent (H).

Each of the participant trials was analyzed using AFA with signal lengths of N=3000, minimum window size of n_{min}= 4, maximum window size of n_{max}=N/10=300, and order of residual polynomial fit of M=1. These input parameters were based on the appropriate parameter specifications and findings in Chapter 3 of this thesis.

Calculation and Validation of Scaling Regions

After performing AFA and DFA on each of the participant trials, each bi-logarithmic plot was visually inspected for the presence of scaling regions and the number of possible linear scaling regions that the data displayed. For DFA, visual inspection indicated in most cases that 1 to 2 regions were present for intermediate and long time scales. For AFA, visual inspection indicated in most cases that 2 to 3 regions were present for short, intermediate, and long time scales.

However, visual inspection introduces ambiguity in the decision-making process for determining both how many scaling regions are present and where the crossover points (i.e. the point at which one scaling region ends and another begins) lie for each plot. The following quantitative model fitting routine is derived from Kuznetsov et al. and based on the small-sample Bayesian information criterion (SICc). It provides a formal procedure that was applied to each participant trial (Kuznetsov, Bonnette et al. 2012). Minor changes were made to refine the goodness of fit process and to accommodate both the scaling region estimates of AFA and DFA. The steps below were derived from Kuznetsov et al. 2012:

1. Given a bi-logarithmic plot, model a single scaling region fit onto the bi-logarithmic plot. To do this, fit a first-order polynomial to the bi-logarithmic plot of fluctuation versus window scale. Calculate and store the quantified goodness of fit, defined as the residual sum of squares (RSS), which can be expressed as:

$$RSS = \sum (y_i - \hat{y})^2$$

2. Model a 2-region scaling model fit onto the bi-logarithmic plot. To do this, fit the following piecewise linear model with two regions and one breakpoint (*k*) between them to the plot:

$$y = b_1 x + a_1 \quad for\ x < k$$

$$y = b_2 x + a_2 \quad for\ x > k$$

In order to determine the best-fitting 2-region model, evaluate global goodness of fit for all possible breakpoint locations between logarithmic values from 5 to 80% of all possible options. These boundaries were determined from typical ranges of breakpoint locations. Each region must have at least three window scaling separations in order to ensure that fits were well-placed. Calculate goodness of fit for each iteration of breakpoint locations using the RSS equation in (1). Select the smallest RSS value as the "idyllic" breakpoint location for the 2-region model of the bi-logarithmic plot.

3. Model a 3-region scaling model fit onto the bi-logarithmic plot. To do this, fit the following piecewise linear model with three regions and two breakpoints (k_1 and k_2) between them to the plot:

$$y = b_1 x + a_1 \quad for\ x < k_1$$

$$y = b_2 x + a_2 \quad for\ k_2 < x < k_1$$

$$y = b_3 x + a_3 \quad for\ x > k_2$$

In order to determine the best-fitting 3-region model, a more involved process is required. Typical breakpoint locations for k_1 and $k_2$were identified and it was determined to be

appropriate to divide the bi-logarithmic plot in half and repeat step (2) for both k_1 and k_2 in their respective halves of the plot, thus breaking a 3-region model down into two 2-region models. For both k_1 and k_2, evaluate global goodness of fit for all possible breakpoint locations between logarithmic values from 5 to 80% of all possible options for the respective data halves. Certain criteria must also be met: (a) each region must have at least three window scaling separations; (b) the first (fast) scaling region begins at the first considered *w*; and (c) the last (slow) scaling region ends at the maximum *w*. Calculate goodness of fit for each iteration of breakpoint locations for both k_1 and k_2 using the RSS equation in (1). Select the smallest RSS value as the "idyllic" breakpoint location for that component of the bi-logarithmic plot. Using this method, this allows the investigator to identify k_1, k_2, b_1 and b_3 (i.e. both breakpoint locations and the slopes of the short and long scaling regions). The intermediate scaling region can be determined by fitting a first-order polynomial to the bi-logarithmic plot between the window values of k_1 and k_2 to determine the slope of b_2.

4. Steps (1)-(3) were performed in order to calculate a goodness of fit value for 1-, 2-, and 3-region scaling models. Using a small-sample Bayesian information criterion (SICc) which penalized increased goodness of fit as additional parameters are added to the model, one can determine which of these three scaling models is the most appropriate fit for the bi-logarithmic plot. This criterion can be expressed as:

$$SICc = \ln\left(\frac{RSS}{S}\right) + \frac{p\ln(S)}{S-p-2}$$

where *S* is the number of fitted scales, RSS is the residual sum of squares, and *p* is the number of model parameters. For the 1-region model *p*=3 (starting position, slope, and intercept), for the 2-region model *p*=6 (starting position, breakpoint, two slopes, and two intercepts), and for the 3-

region model p=8 (two breakpoints, three slopes, and three intercepts). Starting position was included in the 1- and 2-region models because a couple initial points in the data hinted at a fast scaling region (usually only apparent in 3-region models). These points could influence the fitting procedures while only existing as statistical artifacts. Calculate SICc for 1-, 2-, and 3-region scaling models for the bi-logarithmic plot.

5. Choose the model with the lowest SICc value as the best-fitting model and calculate the slopes (i.e. H), intercepts, and boundaries for each region of the model.

Each bi-logarithmic plot was subject to the scaling region validation procedure outlined above for both AFA and DFA.

In order to clarify between differences of scale, of the three possible scaling regions identified, the first scaling region observed at fast time scales is expressed henceforth by H_{fast}, the second scaling region observed at intermediate time scales is expressed as H_{int}, and the third scaling region observed at slow time scales is expressed as H_{slow}. Based off of the nature and position of the scaling regions on the bi-logarithmic plot: 1-region scaling models will express single resultant slope as H; 2-region scaling models will express the resultant slopes as H_{fast} (first region) and H_{int} (second region) and will express the resultant breakpoint as Cr; and 3-region scaling models will express the resultant slopes as H_{fast} (first region), H_{int} (second region), and H_{slow} (third region) and will express the resultant breakpoints as Cr1 and Cr2.

Statistical Analysis

Summary statistics of 1-, 2-, and 3-region bi-logarithmic plots for AFA and DFA were calculated. Main effects and interactions were investigated using a blocked 2-way ANOVA of Group (HC, PD-Mi, PD-Mo) and Condition (EO, EC) for 1-, 2-, and 3-region models for both

AFA and DFA. Participants were each treated as a separate block with independently regarded trials. Blocking validity was tested between participants. For 1-region models, 2-way ANOVA was conducted on H, the single existing slope. For 2-region models, 2-way ANOVA was conducted on H_{fast}, H_{fint}, and Cr. For 3-region models, 2-way ANOVA was conducted on H_{fast}, H_{int}, H_{slow}, Cr1 and Cr2. Significant main effects and interaction parameters were investigated using Tukey-Kramer's post hoc tests to further investigate parametric effects on accuracy of Hurst exponent estimates and breakpoint locations. Significance was considered for $p<0.05$. All statistical analyses were calculated in R 3.2.3.

Results

Anthropometric data such as age, height, and mass of participants were analyzed in a previous study (Barnds et al., 2015) and no significant group differences were found.

Scaling Region Distribution

Analysis revealed that DFA produced 1- and 2-region model scaling. No significant effects were found in the number of scaling regions/region distribution using DFA (Table 2.a). AFA produced 2- and 3-region scaling models. No single-region scaling models were found in any trial using AFA. No significant Condition effect was found in the scaling region distribution. A significant Group effect was found in the 2-region AFA model, with an increase in the 2-region model distribution as PD progresses (Table 2.b). Intra-participant variability in scaling region models was present, but was not significant across either Condition or Group.

DFA (Detrended Fluctuation Analysis)

1-region scaling models: The estimated Hurst exponent was the only parameter investigated in the single-region model. A significant Group effect was found (i.e. HC, Mi, and Mo) ($F_{2,160}$:

7.7971, $p<0.001$) (Table 3.a). Post-hoc analysis revealed that no individual pairwise comparison of Group could produce enough significance to meet the 95% confidence interval criteria.

2-region scaling models: Three output parameters were investigated in the 2-region model: two resultant slopes (H_{fast} and H_{int}) and the crossover point between the slopes (Cr). A significant Group-by-Condition effect was found in H_{fast} ($F_{2, 31}$: 3.9932, $p<0.01$) (Table 3.a). The crossover (Cr) point was significant with respect to Condition ($F_{1, 31}$: 8.9542, $p<0.01$) and the Group-by-Condition interaction ($F_{2, 31}$: 5.5386, $p<0.01$) (Table 3.a). Post hoc analysis of both H_{fast} and Cr revealed that the interaction effect between Condition and Group was significant ($p<0.001$). In HC, the Condition has no effect, but when the interactions of Condition and Group are compared between HC and either PD-Mi or PD-Mo, removing visual feedback affected both H_{fast} and Cr values.

In every scaling region model and output investigated, DFA showed a high sensitivity towards differentiating participants (i.e. the blocking factor) ($p<0.001$) validating the experimental design and confirming that inter-participant sway can be highly variable.

AFA (Adaptive Fractal Analysis)

2-region scaling models: Three output parameters were investigated in the 2-region: two resultant slopes (H_{fast} and H_{int}) and the crossover point between the slopes (Cr). H_{fast} analysis revealed a significant Group effect ($F_{2, 5}$: 11.5498, $p<0.05$) and sensitivity towards inter-participant variability ($p<0.05$) (Table 3.b). H_{int} and Cr analysis did not reveal any significant effects.

3-region scaling models: Five output parameters were investigated in the 3-region models: three resultant slopes (H_{fast}, H_{int}, and H_{slow}) and two crossover points between each slope pair (Cr1 and

Cr2). H_{fast} analysis revealed a significant Group effect ($F_{2, 188}$: 17.5343, $p<0.001$) and blocking factor ($p<0.001$) (Table 3.b). H_{int} results revealed a significant Condition effect ($F_{1, 188}$: 9.1041, $p<0.01$) and the blocking factor ($p<0.001$) (Table 3.b). Cr1 results show significant a Group effect ($F_{2, 188}$: 3.5369, $p<0.05$) and blocking factor ($p<0.001$) (Table 3.b). No post hoc pairwise comparisons between Group levels for H_{fast} and Cr1 provided enough significance to reject the null.

Discussion

The purpose of this study was to test the sensitivity of AFA, compared to DFA, on COPv time series parameters in order to further understand the onset and progression of postural instability (PI) associated with PD progression. AFA and DFA are fractal methods that employ non-stationary principles towards signal analysis and do not rely on assumptions of stationarity. For these reasons, AFA and DFA are likely to detect patterns that are not apparent using traditional clinical assessment or stationary COP position analysis (e.g. sway path, range, peak velocity). These nonstationary characteristics may be detectable at an earlier stage of PD induced PI or may provide information that can enhance clinical assessment and diagnosis of PD before falls occur as a result of progression of PI. A combination of quantitative stationary and non-stationary signal analysis methods may offer a more effective tool for detection of fall risk patients, and allow clinicians to intervene with therapeutic or compensatory prevention strategies.

The results of this study also provide insight into the sensitivity of AFA towards complex sway data. AFA is a relatively new method, introduced within the last ten years. Through this study, the usefulness of AFA can be evaluated in context of sway parameters and the role of this tool in neural control analysis as compared to DFA. DFA has been used as a method by which to

characterize postural sway as a velocity-based intermittent controller, with a combination of open and closed loop processes modulating sway parameters (Collins and De Luca, 1993; Delignieres, Torre et al. 2011; Harper, 2015). Exploration of this topic might not be directly useful for a clinical setting, however, it may help guide future research into modeling and simulation of parkinsonian sway, which could pave the road to an effective detection tool.

DFA (Detrended Fluctuation Analysis)

In reference to Table 2.a, distribution of scaling regions shows little significance. In DFA measures, no significant patterns were observed between either Condition (EO and EC) or Group (HC, PD-Mi, and PD-Mo). DFA ranged between 18% and 28% of trials displaying a 2-region scaling model, while the remaining trials displayed a single-region scaling model (Figure 4 and Figure 5.a).

1-region scaling models of DFA showed sensitivity towards Group in H_{fast} analysis (Table 4.a). However, post hoc analysis did not reveal significant pairwise comparisons. This is perhaps due to the pilot nature of the study with a small number of participants. With more data and patients, significance between pairwise comparisons of the different Group levels might be found. Group means revealed a tendency towards persistent signals, indicative of a deterministic pattern residing within 1-region signals (Figure 6.a.i). 2-region scaling models revealed statistical significance and sensitivity towards Condition and Group interactions when analyzing H_{fast} and Cr results (Table 4.a). Post hoc analysis showed that these interactions characterized detection of significance between HC/PD-Mi and HC/PD-Mo results across each Condition combination. However, this interaction effect was unable to detect significance between PD-Mi and PD-Mo comparisons and is therefore a poor tool to use as a characterization of PI and PD progression. Group means indicated that H_{fast} signals tended to be persistent and displayed deterministic

trends. H_{int} signals produced high amounts of variability between both Group and Condition measures, which indicates that any correlations from these results are likely to be unreliable (Figure 6.a.ii).

A blocking factor was added to the statistical design in anticipation that trials may drastically vary between participants. Because Parkinson's disease is often present in a patient for approximately 6 to 8 years before clinical symptoms are diagnosable, there is a chance that the clinically diagnosed PD rating might not be accurate. Hence, variability between participants was accounted for. In every analyzed measure of single and 2-region scaling models, significance was shown between the results of participants (Table 4.a). Statistical summaries also verify that in single-region and 2-region summary of results, variance of Hurst exponent measures are widely spread, indicating that outliers (i.e. differences in participant's postural sway) exist (Figure 6.a.i and Figure 6.a.ii).

This variability between patients and the inconsistency of 1- versus 2-region scaling models contradicts previously conducted investigations, in which 2-region scaling of DFA was observed to be the standard result when applied towards a COPv signal (Collins and De Luca, 1993; Delignieres, Torre et al. 2011; Harper, 2015). These studies maintained that the 2-region scaling of DFA was representative of a velocity-based intermittent controller modulating between open (fast time scale) and closed loop (slow time scale) in neural control of postural sway. Existence and prevalence of a single-scaling region contradicts that theory. A likely explanation for this contradiction lies in the input parameters selected for DFA, specifically, selection of an appropriate maximum window size. Consistent with the findings in Chapter 3, a maximum window size (n_{max}) was selected to be $N/10$, where N is the total length of the signal. Previous literature often does not report the selected n_{max} value or uses the maximum possible

value, *N*/2 (to a total of two windows) at the last fluctuation versus time scale plotted point on the bi-logarithmic plot. The findings in Chapter 3 maintain that this is a poor selection and results with liberally selected maximum window ranges usually are derived from statistical artifacts of the method, not underlying data patterns. It is possible that the existence of a second scaling region may be due to these statistical artifacts of residual-based analysis.

Another explanation for the contradiction between present and previous results lies in an alternate interpretation of fractal results on physiological data. Complex variability, loss of control, and highly variable fluctuations surrounding physiological processes could be related to loss of strong fractal behavior, which relies on deterministic chaos, not randomness to be effective (Lipsitz and Goldberger, 1992). Fractal analysis traditionally provides a single scaling region by which to analysis the Hurst exponent, the result of power law scaling. Existence of multiple scaling regions may be indicative of a loss of strong fractal behavior and complexity in a signal degrading towards randomness. Instead of an open and closed loop explanation of scaling regions, this alternative hints that the strength of the fractal scaling could be considered as representative of complexity of a signal and the robustness of complex neural control. Loss of fractal strength could indicate loss of complex neural control and represent PD progression, as an alternative explanation to the traditional open and closed loop neural controller that requires only 2-region models to exist.

AFA (Adaptive Fractal Analysis)

Scaling regions were distributed along 2-region and 3-region scaling models when AFA was applied (Table 3.b). The emergence of a 3-region scaling model is interesting, though not unique—Kuznetsov et al. observed almost exclusively 3-region scaling models when analyzing young, healthy participant COP parameters with AFA (Kuznetsov, Bonnette et al. 2012). 3-

region models conflict with COP fractal scaling representing open and closed loop neural systems, indicating that other models should be considered when explaining COP postural dynamics. AFA was subject to the same input parameter limitations as DFA based off the analysis conducted in Chapter 3, so it is unlikely that the Hurst measures are statistical artifacts of the method.

Approximately 8-18% of trials displayed 2-region characteristics, while the remaining trials displayed a 3-region scaling model (Figures 4 and 5.b). There was little significance found between these distributions versus either Condition or Group, though an increase in 2-region distributions was observed in the EO trials as patient PD severity increased. This was not the case for the EO Condition (Table 3.b). AFA 3-region models were sensitive towards differences across participants, while the 2-region models were not (Table 4.b). Statistical summaries also mirror this observation, with 2-region models (Figure 6.b.i) producing far fewer ranges of variability between Hurst measures than 3-region models (Figure 6.b.ii).

AFA, compared to DFA, found far fewer statistically significant effects and interactions across scaling models, though the results were more consistent across scaling models. H_{fast} for both 2- and 3-region models was found to be significant across Group, with post hoc analysis marking sensitivity towards PD progression. Cr1 in the 3-region model was also sensitive to Group categories, but did not provide the strength of response comparable to H_{fast} (Table 4.b). Persistence versus anti-persistence in a signal across a condition was hard to judge, since the high degree of variability obstructed the reliability of group means (Figure 6.b.i and Figure 6.b.ii). There was a greater tendency towards anti-persistence as a whole, which contradicts the findings of DFA in which deterministic patterns were indicated by Hurst measures and raises questions about the appropriateness of AFA versus DFA as a fractal method to use in PD.

While measures such as H_{fast} and Cr1 provide significance towards Group (i.e. PD severity) and are therefore a potential marker for PD progression, several issues exist within the AFA methods and results that could indicate inadequate sensitivity towards PI and PD progression. The high degree of variance between participants shown in Figure 3 makes conclusions on persistence of a signal in context of summary statistics very unreliable. Because of the degree of variance and inability of an investigator to rely on group means, the spread of results cannot be combined towards any conclusive result across conditions. Another issue exists in the results themselves. Table 2 shows that in many of the measures, several results exceed a value of 1. This challenges the assumption of a fGn-fBm framework of postural control. The theoretical upper limit for an fBm signal is a Hurst value of 1 and literature suggests that COP parameters display fBm tendencies. Integration of a fGn process should only increase the Hurst measures by a total value of 1, therefore values above this indicate issues with underlying assumptions of COP signals. Also, the emergence of multiple scaling regions call into question velocity acting as an intermittent neural controller between a 2-region scaling model of open and closed loop systems. DFA showed a greater adherence to fBm characteristics and might prove to be a more appropriate fractal method to apply towards postural sway analysis.

Conclusion

The results of this study in part support Hypothesis #1. In general, fractal analysis methods may be sensitive towards detecting the development and progression of PI in PD. AFA produced the most clinically significant Group measure, H_{fast}, which detected changes in COP dynamics across smaller time scales than other parameters. However, while H_{fast} contributed the most information about changes in COP indicative of PI and PD progression across PD Groups,

high levels of variance and inconsistent characterization of previously understood fBm patterns make AFA results harder to interpret and more unreliable than DFA.

The results of this study did not support Hypothesis #2. While we did find variability across scaling regions for both DFA and AFA, they did not characterize PI development or PD progression. The distribution of scaling regions in both AFA and DFA did not show significance towards Group or Condition. However, the presence of multiple scaling regions across both AFA and DFA indicates that changes in COP dynamics may not be adequately summarized through an intermittent velocity-based controller operating between open and closed loop neural systems, as that assumption relies on 2-region model results only. AFA showed greater sensitivity towards detecting scaling regions, but provided more variable results than DFA. This heightened sensitivity is likely the reason behind the emergence of the AFA 3-region model of fractal scaling, which conflicts with the traditional assumption of an fGn-fBm framework. Other models should be considered which better explain fractal scaling results.

This study serves as a pilot attempt to apply AFA towards investigations surrounding COP dynamics in the context of Parkinson's disease progression and motor control deterioration. Applications of non-stationary methods towards PD progression will help in developing quantitative clinical assessments of PI that could more accurately track disease progression and fall risk. The results of this study show that non-stationary fractal methods may provide new insight on previous understanding of postural control systems, which can enhance development of models and computer simulations that better characterize postural sway and fall risk in PD patients.

Limitations: This study represents a pilot effort to test the sensitivity of AFA as compared to DFA to COP signals in Parkinson's disease patients using both PD severity and sensory input as conditions for experimental results. Condition factors, cognitive factors, and other individual factors were not examined in the context of AFA sensitivity. There is a need to identify whether AFA exhibits sensitivity towards other changes in COP dynamics in order to further investigate the role of multiple scaling regions in postural dynamics. Due to the pilot nature of this study, there were a relatively small number of subjects considered. Mediolateral direction in COP measures were also not considered in the analysis because the experimental methods allowed participants to select a natural stance width, resulting in an inconsistent mediolateral base of support across the participants. Further studies should be conducted over larger time intervals, with more subjects, and with control stance width in order to improve the resolution of the fractal methods investigated. For each investigation conducted using any kind of fractal analysis, careful consideration of appropriate input parameter selection needs to take place, as fractal methods are highly reliant on the initial conditions set.

References

Adkin, Allan L., James S. Frank, and Mandar S. Jog, 'Fear of Falling and Postural Control in Parkinson's Disease', *Movement Disorders*, 18 (2003), 496–502 <https://doi.org/10.1002/mds.10396>

Alves, Guido, Elin Bjelland Forsaa, Kenn Freddy Pedersen, Michaela Dreetz Gjerstad, and Jan Petter Larsen, 'Epidemiology of Parkinson's Disease', *Journal of Neurology*, 255 (2008), 18–32 <https://doi.org/10.1007/s00415-008-5004-3>

Barnds, A. (2015). *Biomechanical Markers as Indicators of Postural Instability Progression in Parkinson's Disease*. (Dissertation, University of Kansas, 2015)

Bloem, Bastiaan R., Yvette A. M. Grimbergen, Monique Cramer, Mirjam Willemsen, and Aeilko H. Zwinderman, 'Prospective Assessment of Falls in Parkinson's Disease', *Journal of Neurology*, 248 (2001), 950–58 <https://doi.org/10.1007/s004150170047>

Cavanaugh, James T, Vicki S Mercer, and Nicholas Stergiou, 'Approximate Entropy Detects the Effect of a Secondary Cognitive Task on Postural Control in Healthy Young Adults: A Methodological Report', *Journal of NeuroEngineering and Rehabilitation*, 4 (2007), 42 <https://doi.org/10.1186/1743-0003-4-42>

Chastan, Nathalie, Bertrand Debono, David Maltête, and Jacques Weber, 'Discordance between Measured Postural Instability and Absence of Clinical Symptoms in Parkinson's Disease Patients in the Early Stages of the Disease', *Movement Disorders*, 23 (2008), 366–72 <https://doi.org/10.1002/mds.21840>

Collins, J. J., and C. J. De Luca, 'Open-Loop and Closed-Loop Control of Posture: A Random-Walk Analysis of Center-of-Pressure Trajectories', *Experimental Brain Research*, 95 (1993), 308–18

Delignières, Didier, Kjerstin Torre, and Pierre-Louis Bernard, 'Transition from Persistent to Anti-Persistent Correlations in Postural Sway Indicates Velocity-Based Control', *PLoS Computational Biology*, 7 (2011) <https://doi.org/10.1371/journal.pcbi.1001089>

Doyle, Tim L., Robert U. Newton, and Angus F. Burnett, 'Reliability of Traditional and Fractal Dimension Measures of Quiet Stance Center of Pressure in Young, Healthy People', *Archives of Physical Medicine and Rehabilitation*, 86 (2005), 2034–40 <https://doi.org/10.1016/j.apmr.2005.05.014>

Gao, Jianbo, Jing Hu, and Wen-wen Tung, 'Facilitating Joint Chaos and Fractal Analysis of Biosignals through Nonlinear Adaptive Filtering', *PLoS ONE*, 6 (2011) <https://doi.org/10.1371/journal.pone.0024331>

Goetz, Christopher G., Werner Poewe, Olivier Rascol, Cristina Sampaio, Glenn T. Stebbins, Carl Counsell, and others, 'Movement Disorder Society Task Force Report on the Hoehn and Yahr Staging Scale: Status and Recommendations The Movement Disorder Society Task Force on Rating Scales for Parkinson's Disease', *Movement Disorders*, 19 (2004), 1020–28 <https://doi.org/10.1002/mds.20213>

Harper, Joshua Russell, 'Fractal Analysis of Center of Pressure Velocity Time Series in Parkinson's Disease' (Thesis, University of Kansas, 2015) <https://kuscholarworks.ku.edu/handle/1808/19412>

Hill, E., S. Stuart, S. Lord, S. Del Din, and L. Rochester, 'Vision, Visuo-Cognition and Postural Control in Parkinson's Disease: An Associative Pilot Study', *Gait & Posture*, 48 (2016), 74–76 <https://doi.org/10.1016/j.gaitpost.2016.04.024>

Horak, Fay B., Diana Dimitrova, and John G. Nutt, 'Direction-Specific Postural Instability in Subjects with Parkinson's Disease', *Experimental Neurology*, 193 (2005), 504–21 <https://doi.org/10.1016/j.expneurol.2004.12.008>

Jeka, John, Tim Kiemel, Robert Creath, Fay Horak, and Robert Peterka, 'Controlling Human Upright Posture: Velocity Information Is More Accurate Than Position or Acceleration', *Journal of Neurophysiology*, 92 (2004), 2368–79 <https://doi.org/10.1152/jn.00983.2003>

Kim, Samuel, Natalie Allen, Colleen Canning, and Victor Fung, 'Postural Instability in Patients with Parkinson's Disease', *CNS Drugs*, 27 (2013), 97–112

Kuznetsov, Nikita, Scott Bonnette, Jianbo Gao, and Michael A. Riley, 'Adaptive Fractal Analysis Reveals Limits to Fractal Scaling in Center of Pressure Trajectories', *Annals of Biomedical Engineering*, 41 (2012), 1646–60 <https://doi.org/10.1007/s10439-012-0646-9>

Lipsitz LA, and Goldberger AL, 'Loss of "Complexity" and Aging: Potential Applications of Fractals and Chaos Theory to Senescence', *JAMA*, 267 (1992), 1806–9 <https://doi.org/10.1001/jama.1992.03480130122036>

Loughlin, P. J., M. S. Redfern, and J. M. Furman, 'Nonstationarities of Postural Sway', *IEEE Engineering in Medicine and Biology Magazine*, 22 (2003), 69–75 <https://doi.org/10.1109/MEMB.2003.1195699>

Mancini, Martina, Patricia Carlson-Kuhta, Cris Zampieri, John G. Nutt, Lorenzo Chiari, and Fay B. Horak, 'Postural Sway as a Marker of Progression in Parkinson's Disease: A Pilot Longitudinal Study', *Gait & Posture*, 36 (2012), 471–76 <https://doi.org/10.1016/j.gaitpost.2012.04.010>

Mancini, Martina, Fay B. Horak, Cris Zampieri, Patricia Carlson-Kuhta, John G. Nutt, and Lorenzo Chiari, 'Trunk Accelerometry Reveals Postural Instability in Untreated Parkinson's Disease', *Parkinsonism & Related Disorders*, 17 (2011), 557–62 <https://doi.org/10.1016/j.parkreldis.2011.05.010>

McNeely, Marie E., Ryan P. Duncan, and Gammon M. Earhart, 'Medication Improves Balance and Complex Gait Performance in Parkinson Disease', *Gait & Posture*, 36 (2012), 144–48 <https://doi.org/10.1016/j.gaitpost.2012.02.009>

Minamisawa, Tadayoshi, Kei Takakura, and Takashi Yamaguchi, 'Detrended Fluctuation Analysis of Temporal Variation of the Center of Pressure (COP) during Quiet Standing in Parkinsonian Patients', *Journal of Physical Therapy Science*, 21 (2009), 287–92 <https://doi.org/10.1589/jpts.21.287>

Morrison, S., G. Kerr, K. M. Newell, and P. A. Silburn, 'Differential Time- and Frequency-Dependent Structure of Postural Sway and Finger Tremor in Parkinson's Disease', *Neuroscience Letters*, 443 (2008), 123–28 <https://doi.org/10.1016/j.neulet.2008.07.071>

Peng, C.-K., Shlomo Havlin, and H. Eugene Stanley, 'Quantification of Scaling Exponents and Crossover Phenomena in Nonstationary Heartbeat Time Series', *Chaos*, 5 (1995), 82

Ramdani, Sofiane, Benoît Seigle, Julien Lagarde, Frédéric Bouchara, and Pierre Louis Bernard, 'On the Use of Sample Entropy to Analyze Human Postural Sway Data', *Medical Engineering & Physics*, 31 (2009), 1023–31 <https://doi.org/10.1016/j.medengphy.2009.06.004>

Riley, Michael A., Scott Bonnette, Nikita Kuznetsov, Sebastian Wallot, and Jianbo Gao, 'A Tutorial Introduction to Adaptive Fractal Analysis', *Fractal Physiology*, 3 (2012), 371 <https://doi.org/10.3389/fphys.2012.00371>

Schmit, Jennifer M., Michael A. Riley, Arif Dalvi, Alok Sahay, Paula K. Shear, Kevin D. Shockley, and others, 'Deterministic Center of Pressure Patterns Characterize Postural Instability in Parkinson's Disease', *Experimental Brain Research*, 168 (2005), 357–67 <https://doi.org/10.1007/s00221-005-0094-y>

Schumann, Timothy, Mark S. Redfern, Joseph M. Furman, Amro El-Jaroudi, and Luis F. Chaparro, 'Time-Frequency Analysis of Postural Sway', *Journal of Biomechanics*, 28 (1995), 603–7 <https://doi.org/10.1016/0021-9290(94)00113-I>

Simuni, Tanya, and Rajesh Pahwa, *Parkinson's Disease* (Cary, US: Oxford University Press, USA, 2009) <http://site.ebrary.com/lib/alltitles/docDetail.action?docID=10375051> [accessed 28 August 2016]

Stergiou, Nicholas. Editor. *Nonlinear Analysis for Human Movement Variability*. Boca Raton: Taylor & Francis, CRC Press, 2016. Print.

Stylianou, Antonis P., Molly A. McVey, Kelly E. Lyons, Rajesh Pahwa, and Carl W. Luchies, 'Postural Sway in Patients with Mild to Moderate Parkinson's Disease', *International Journal of Neuroscience*, 121 (2011), 614–21 <https://doi.org/10.3109/00207454.2011.602807>

Vaillancourt, David E, and Karl M Newell, 'The Dynamics of Resting and Postural Tremor in Parkinson's Disease', *Clinical Neurophysiology*, 111 (2000), 2046–56 <https://doi.org/10.1016/S1388-2457(00)00467-3>

Wielinski, Catherine L., Cordelia Erickson-Davis, Rose Wichmann, Maria Walde-Douglas, and Sotirios A. Parashos, 'Falls and Injuries Resulting from Falls among Patients with Parkinson's Disease and Other Parkinsonian Syndromes', *Movement Disorders*, 20 (2005), 410–15 <https://doi.org/10.1002/mds.20347>

Wirdefeldt, Karin, Hans-Olov Adami, Philip Cole, Dimitrios Trichopoulos, and Jack Mandel, 'Epidemiology and Etiology of Parkinson's Disease: A Review of the Evidence', *European Journal of Epidemiology*, 26 (2011), 1 <https://doi.org/10.1007/s10654-011-9581-6>

Figure 4: Depiction of 1-, 2-, and 3-region scaling model sample construction plots.

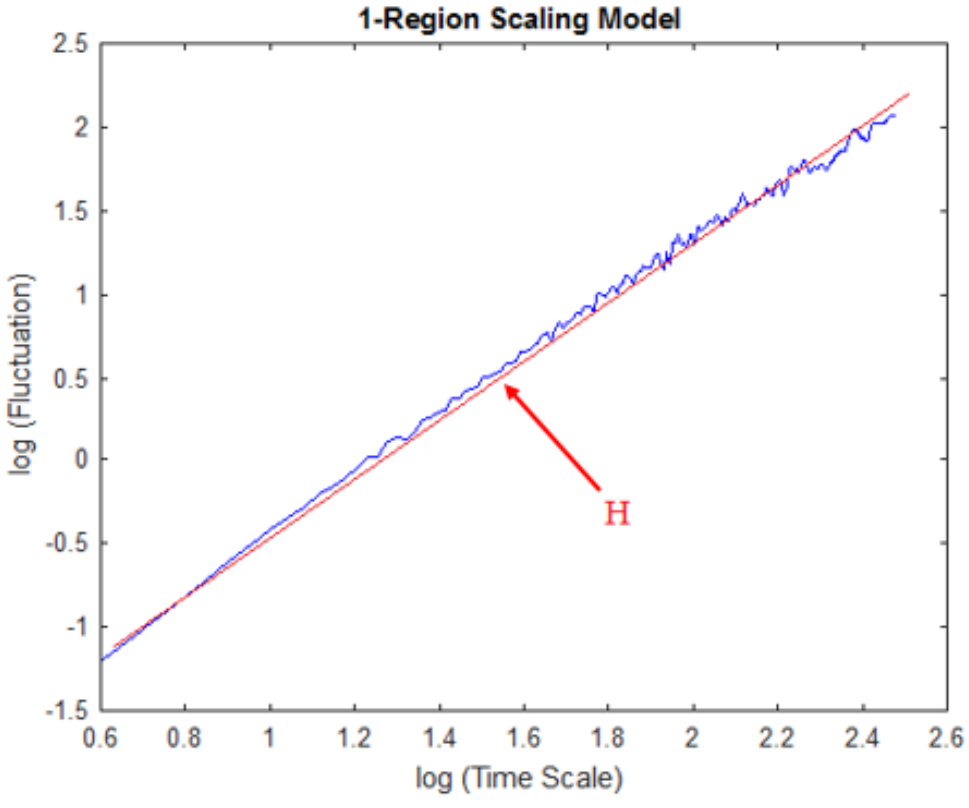

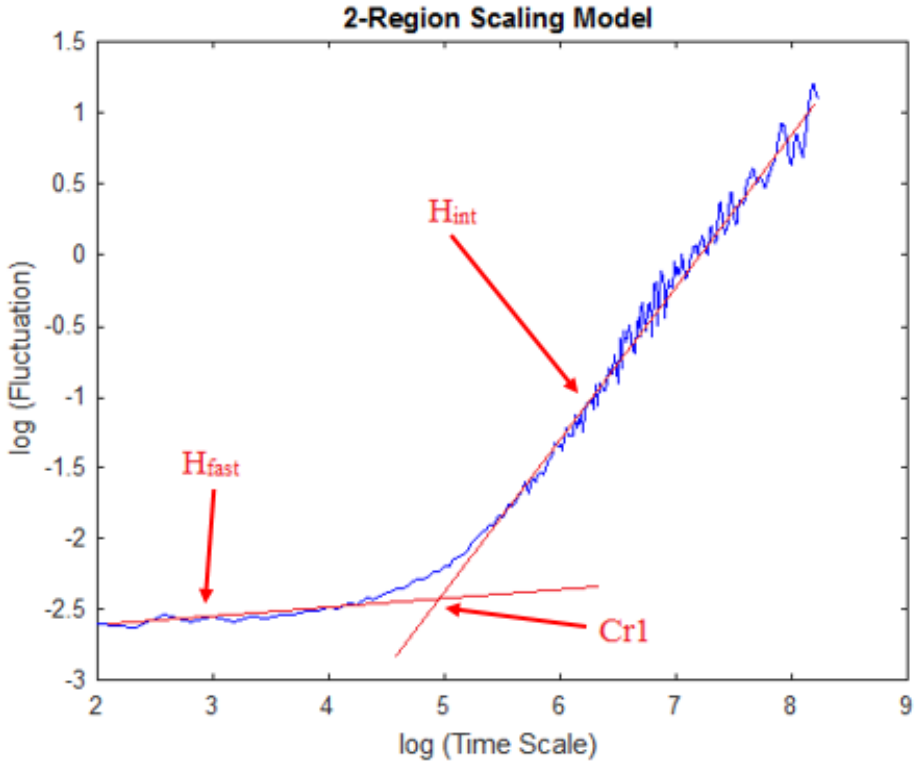
2-Region Scaling Model
log (Fluctuation)
log (Time Scale)
Hint
Hfast
Cr1

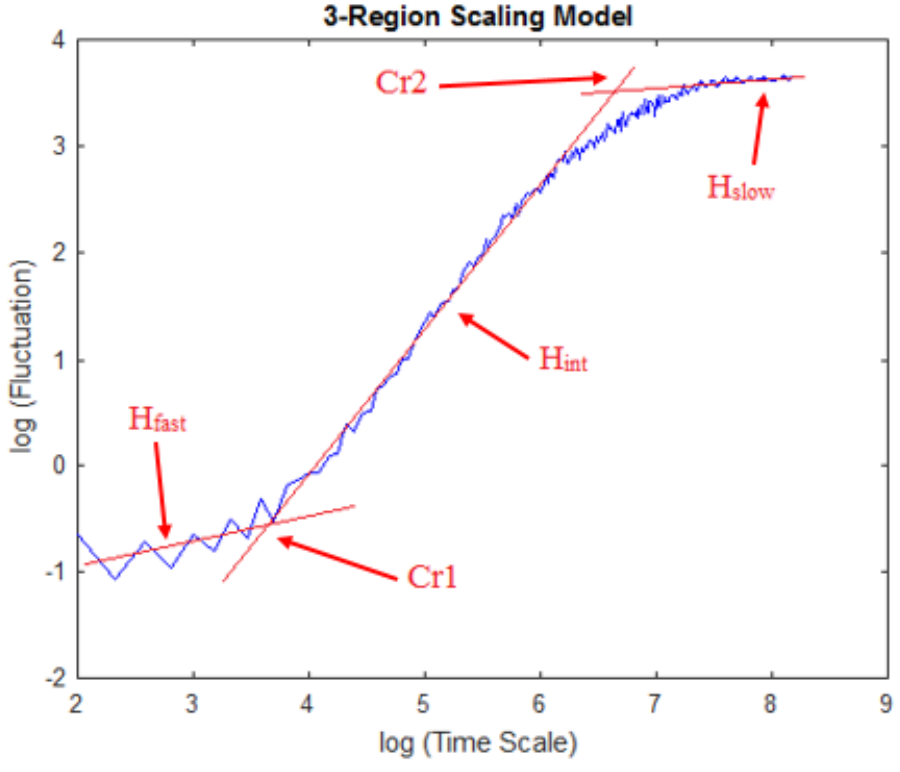
3-Region Scaling Model
log (Fluctuation)
log (Time Scale)
Cr2
Hslow
Hint
Hfast
Cr1

Figure 5: Depiction of typical bi-logarithmic fluctuation vs. scale plots for each combination of trials. Healthy controls (HC), mild Parkinson's disease (PD-Mi), and moderate Parkinson's disease (PD-Mo) are reported with two Conditions of eyes open (EO) sway and eyes closed (EC sway).

(a) Typical bi-logarithmic plot using DFA. 1-region scaling models were assumed to be typical because of the high distribution of occurrences (Table 3.a).

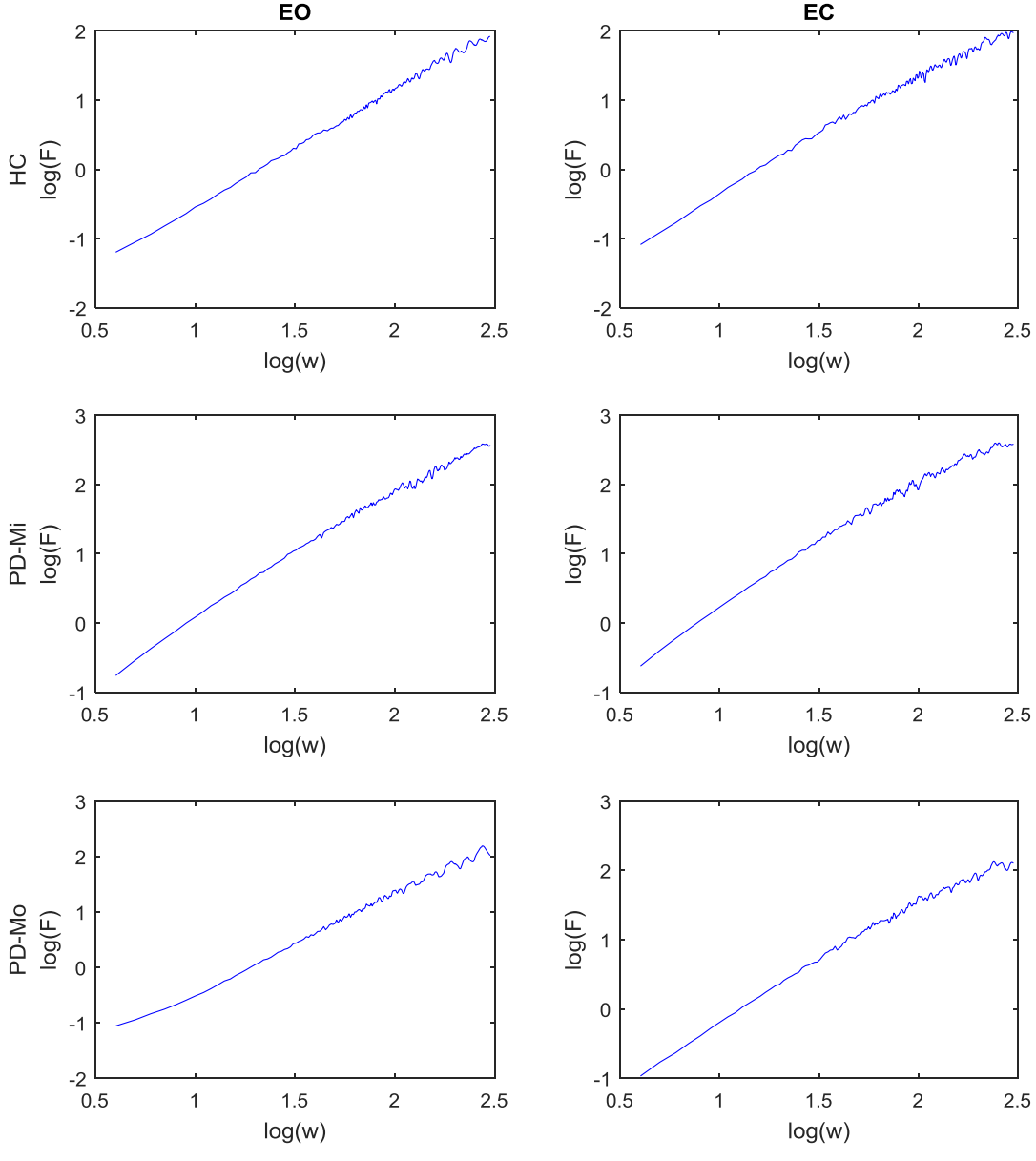

(b) Typical bi-logarithmic plot using AFA. 3-region scaling models were assumed to be typical because of the high distribution of occurrences (Table 3.b).

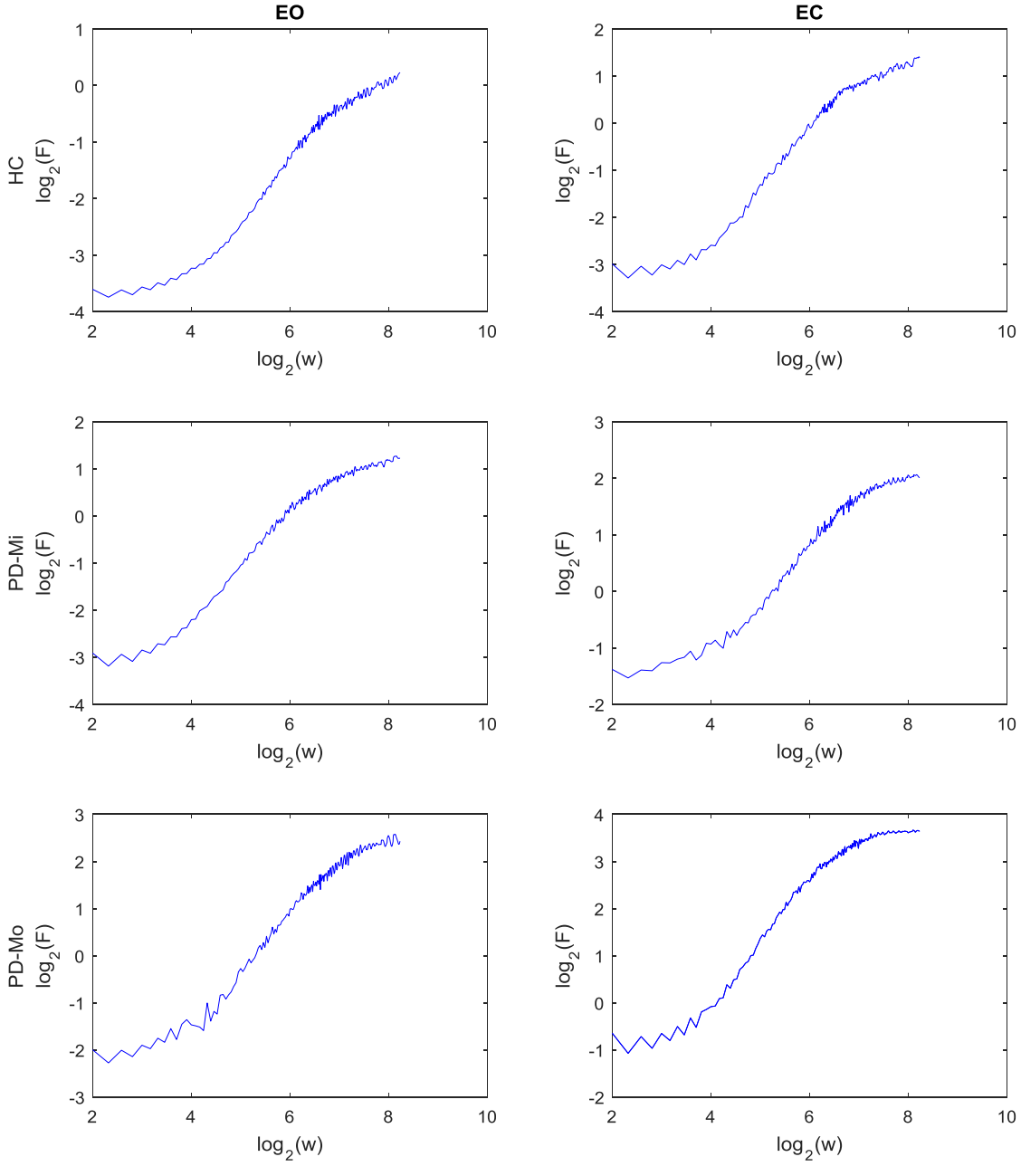

Figure 6: Graphical summary of group means and standard deviations (error bars) for (a) DFA and (b) AFA for each measure and condition. Healthy controls (HC), mild Parkinson's disease (PD-Mi), and moderate Parkinson's disease (PD-Mo) are reported with two Conditions of eyes open (EO) sway and eyes closed (EC sway).

(a) Graphical summary of group means and standard deviations (error bars) for DFA. For 1-region scaling models, H is the Hurst exponent. For 2-region scaling models, H_{fast} is the first scaling region observed at fast time intervals, H_{int} is the second scaling region observed around intermediate time intervals, and Cr is the crossover point between the two along the time interval scale.

(i) 1-Region Summary Graph for DFA

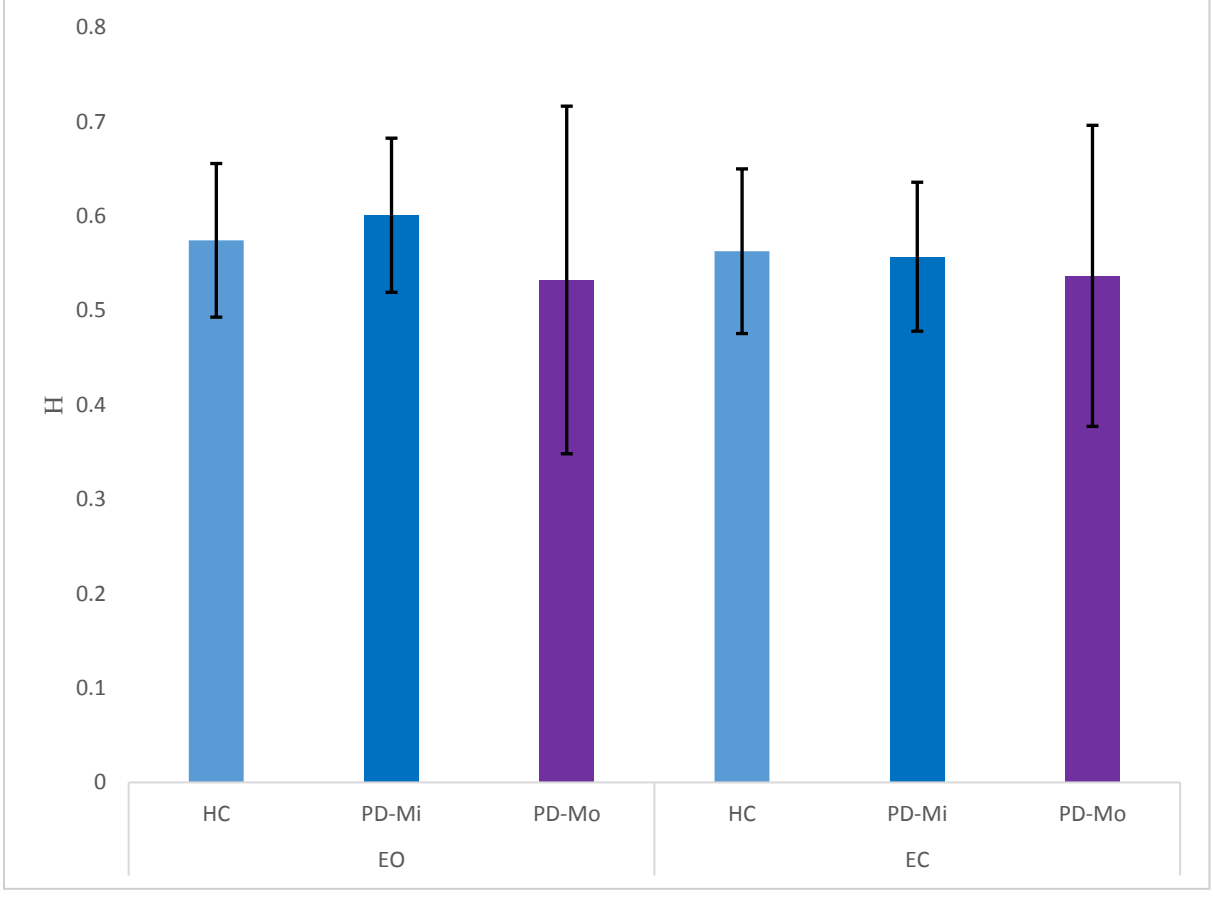

(ii) 2-Region Summary Graphs for DFA

2-Region Summary of Hurst Estimates

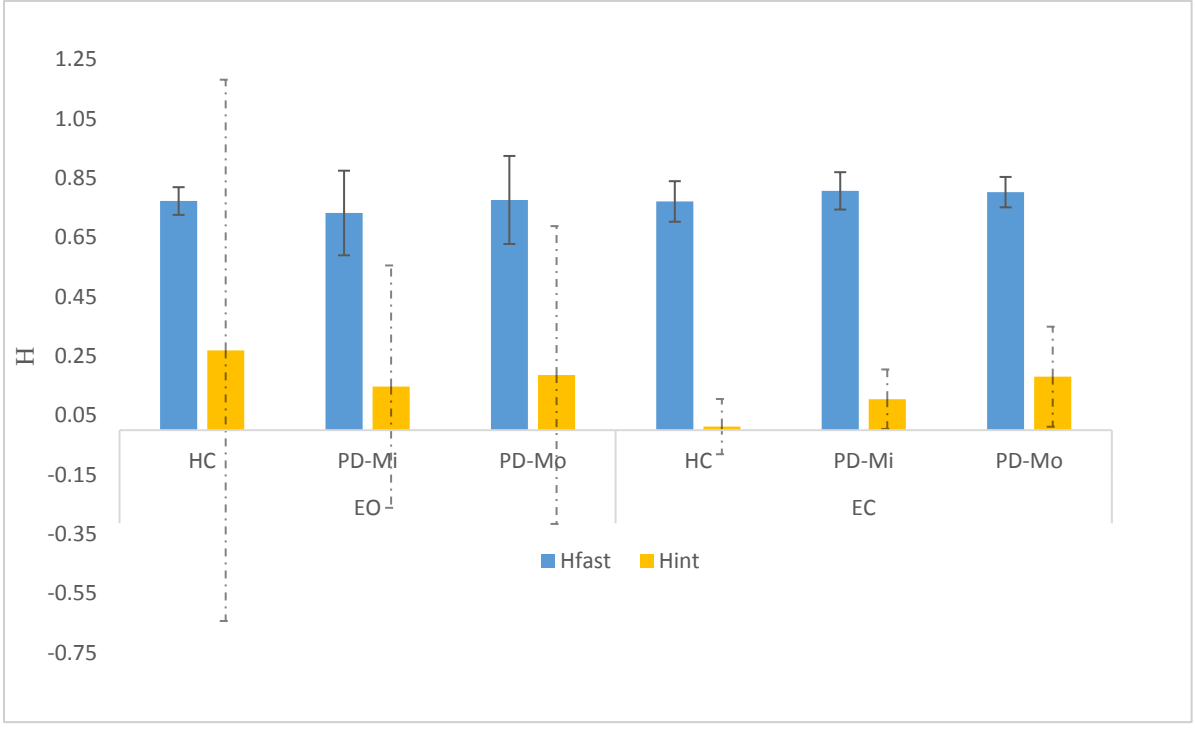

2-Region Summary of Crossover Point

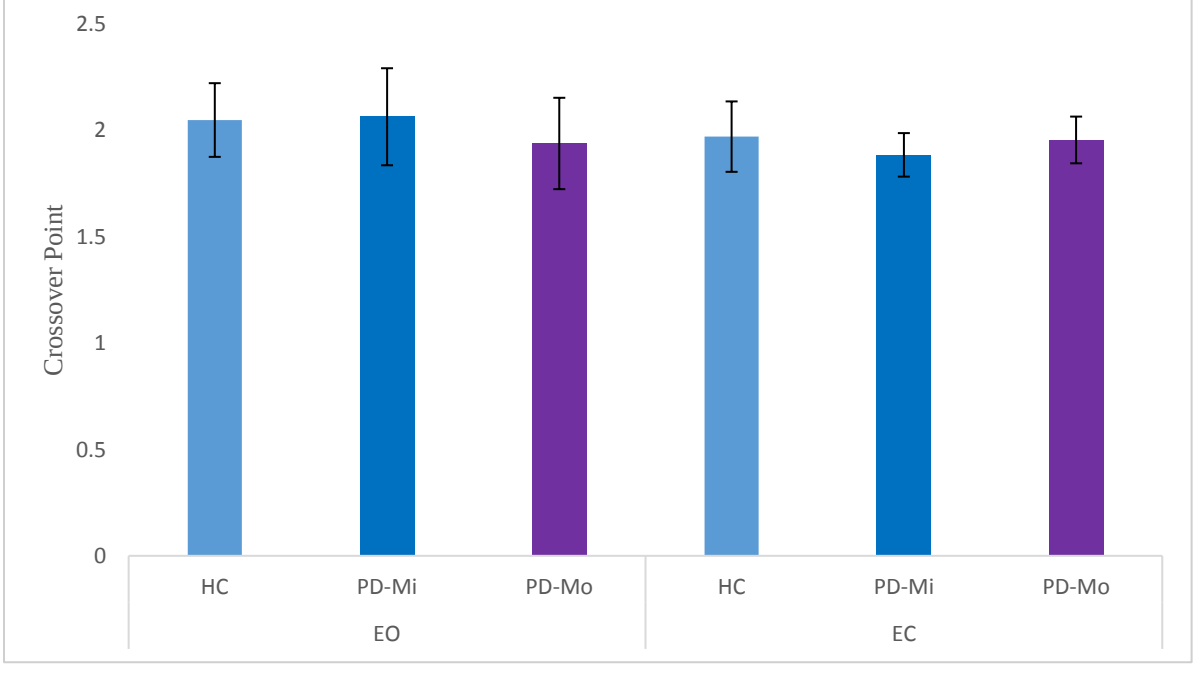

(b) Graphical summary of group means and standard deviations (error bars) for AFA. For 2-region scaling models, H_{fast} is the first scaling region observed at fast time intervals, H_{int} is the second scaling region observed around intermediate time intervals, and Cr is the crossover point between the two along the time interval scale. For 3-region scaling models, H_{fast} is the first scaling region observed at fast time intervals, H_{int} is the second scaling region observed around intermediate time intervals, H_{slow} is the third csaling region observed around slow time intervals, Cr1 is the crossover point between H_{fast} and H_{int}, and Cr 2 is the crossover point between H_{int} and H_{slow}.

(i) 2-Region Summary Graphs for AFA

2-Region Summary of Hurst Estimates

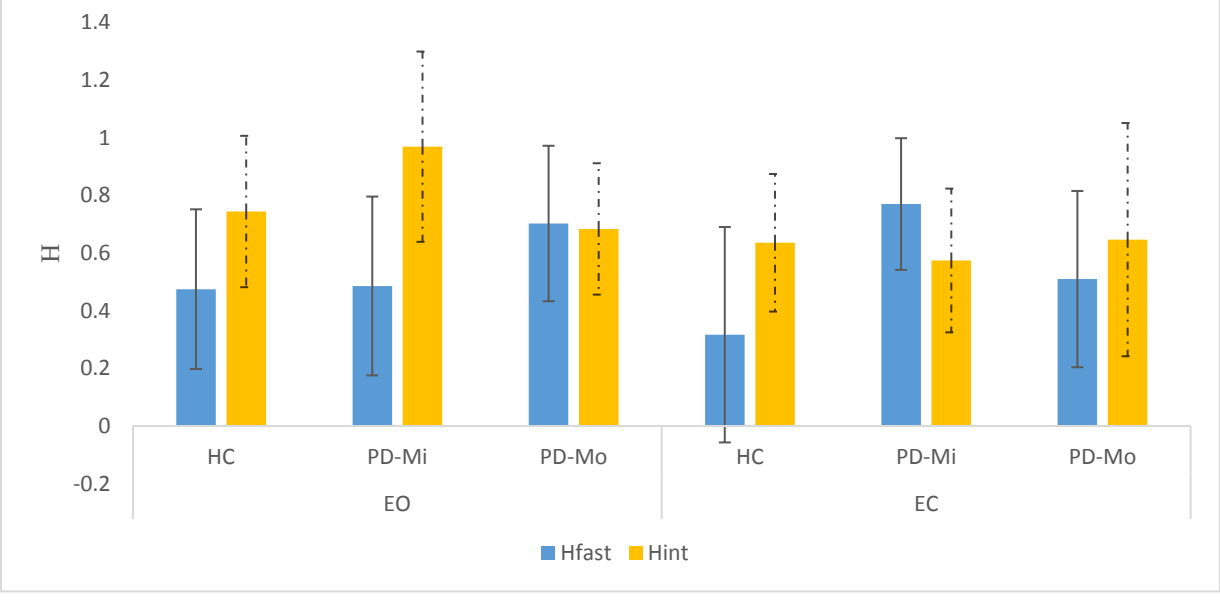

2-Region Summary of Crossover Point

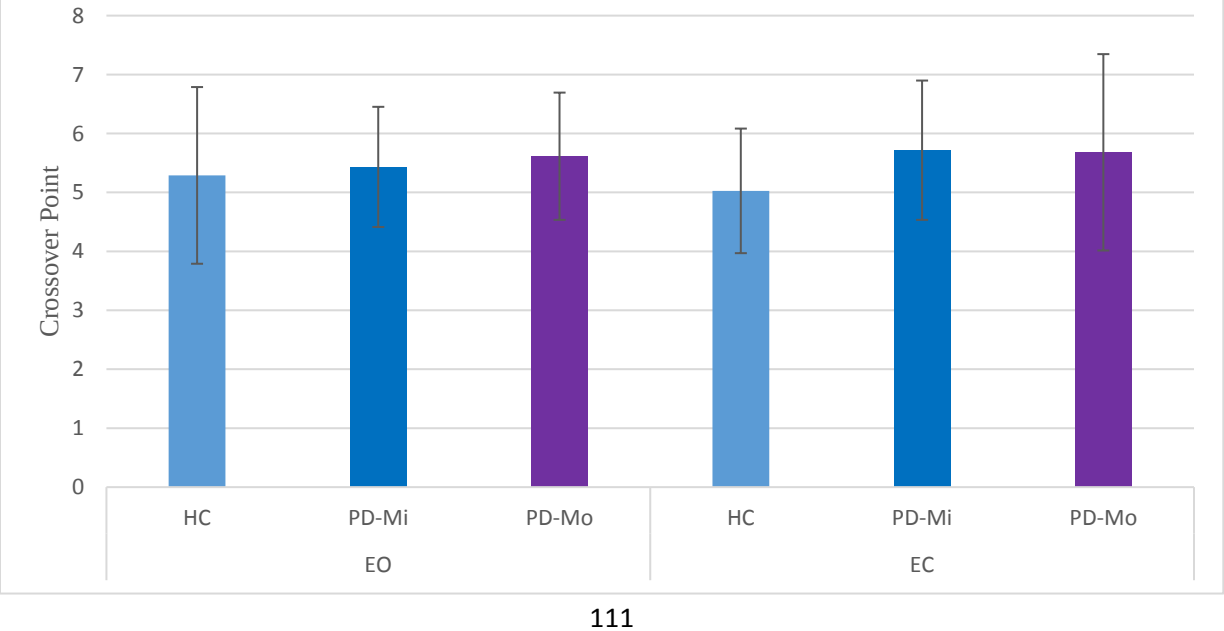

(ii) 3-Region Summary Graphs for AFA

3-Region Summary of Hurst Estimates

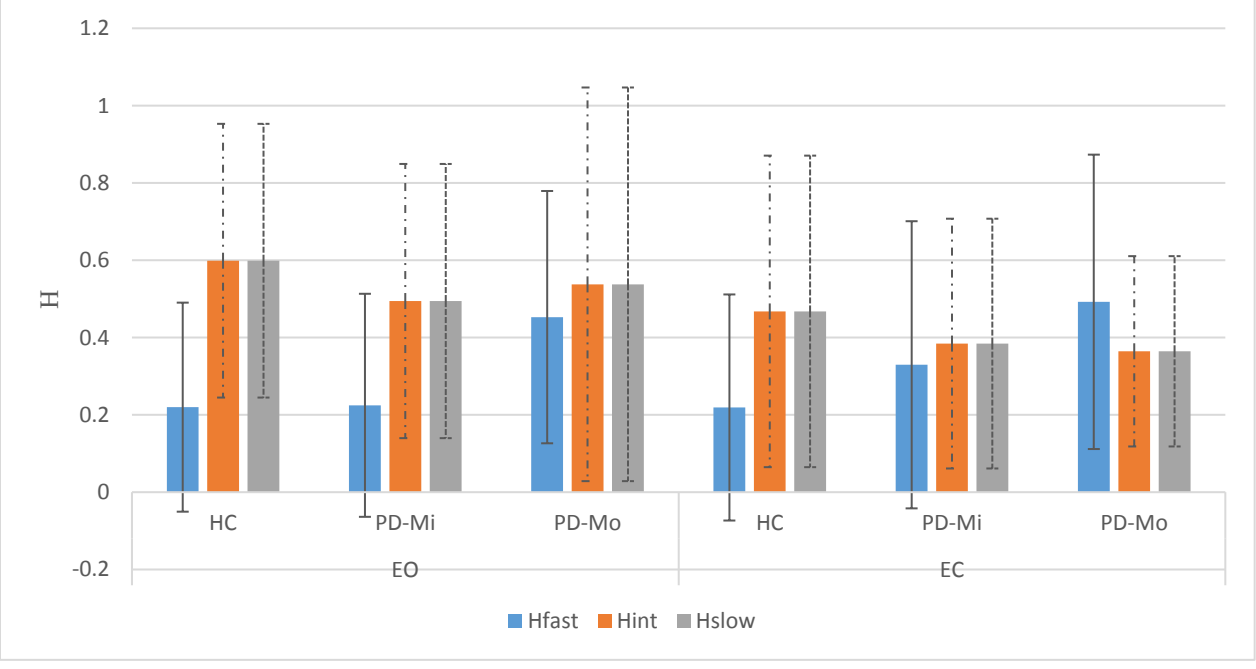

3-Region Summary of Crossover Points

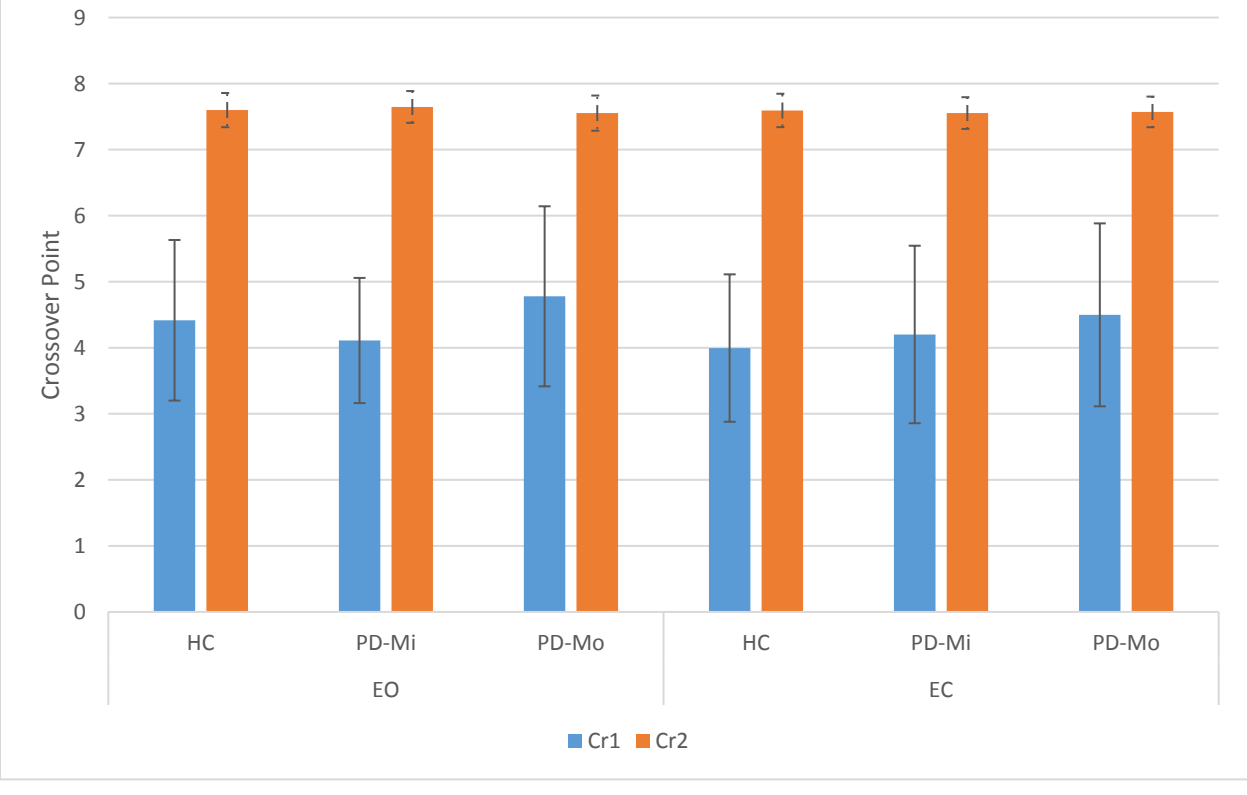

Table 2: Summary Statistics for (a) DFA and (b) AFA

(a) Group means (standard deviations) for each measure and each condition across 1-region and 2-region scaling models for DFA. Healthy controls (HC), mild Parkinson's disease (PD-Mi), and moderate Parkinson's disease (PD-Mo) are reported with two Conditions of eyes open (EO) sway and eyes closed (EC sway). For 1-region scaling models, H is the Hurst exponent. For 2-region scaling models, H_{fast} is the first scaling region observed at fast time intervals, H_{int} is the second scaling region observed around intermediate time intervals, and Cr is the crossover point between the two along the time interval scale.

	Condition	Group	H	-	-
1-region	EO	HC	0.574 (0.081)	-	-
		PD-Mi	0.601 (0.082)	-	-
		PD-Mo	0.532 (0.184)	-	-
	EC	HC	0.563 (0.087)	-	-
		PD-Mi	0.557 (0.079)	-	-
		PD-Mo	0.537 (0.160)	-	-
2-region	Condition	Group	H_{fast}	H_{int}	Cr
	EO	HC	0.772 (0.047)	0.269 (0.912)	2.049 (0.173)
		PD-Mi	0.732 (0.143)	0.147 (0.408)	2.064 (0.228)
		PD-Mo	0.776 (0.148)	0.186 (0.502)	1.938 (0.215)
	EC	HC	0.771 (0.068)	0.012 (0.093)	1.971 (0.166)
		PD-Mi	0.807 (0.063)	0.105 (0.100)	1.885 (0.102)
		PD-Mo	0.802 (0.051)	0.180 (0.169)	1.955 (0.110)

(b) Group means (standard deviations) for each measure and each condition across 2-region and 3-region scaling models for AFA. Healthy controls (HC), mild Parkinson's disease (PD-Mi), and moderate Parkinson's disease (PD-Mo) are reported with two Conditions of eyes open (EO) sway and eyes closed (EC sway). For 2-region scaling models, H_{fast} is the first scaling region observed at fast time intervals, H_{int} is the second scaling region observed around intermediate time intervals, and Cr is the crossover point between the two along the time interval scale. For 3-region scaling models, H_{fast} is the first scaling region observed at fast time intervals, H_{int} is the second scaling region observed around intermediate time intervals, H_{slow} is the third csaling region observed around slow time intervals, Cr1 is the crossover point between H_{fast} and H_{int}, and Cr 2 is the crossover point between H_{int} and H_{slow}.

	Condition	Group	H_{fast}	H_{int}	Cr	-	-
2-region	EO	HC	0.474 (0.277)	0.744 (0.263)	5.289 (1.499)	-	-
		PD-Mi	0.486 (0.310)	0.969 (0.330)	5.433 (1.019)	-	-
		PD-Mo	0.702 (0.270)	0.684 (0.228)	5.614 (1.079)	-	-
	EC	HC	0.316 (0.374)	0.635 (0.239)	5.027 (1.057)	-	-
		PD-Mi	0.770 (0.228)	0.574 (0.249)	5.716 (1.182)	-	-
		PD-Mo	0.510 (0.306)	0.646 (0.405)	5.681 (1.666)	-	-
	Condition	**Group**	**H_{fast}**	**H_{int}**	**H_{slow}**	**Cr1**	**Cr2**
3-region	EO	HC	0.220 (0.270)	0.599 (0.354)	0.599 (0.354)	4.416 (1.216)	7.598 (0.259)
		PD-Mi	0.225 (0.288)	0.494 (0.355)	0.494 (0.355)	4.110 (0.948)	7.646 (0.241)
		PD-Mo	0.453 (0.326)	0.538 (0.509)	0.538 (0.509)	4.779 (1.363)	7.553 (0.266)
	EC	HC	0.219 (0.292)	0.468 (0.403)	0.468 (0.403)	3.995 (1.116)	7.593 (0.253)
		PD-Mi	0.330 (0.371)	0.384 (0.323)	0.384 (0.323)	4.201 (1.344)	7.553 (0.240)
		PD-Mo	0.492 (0.381)	0.364 (0.246)	0.364 (0.246)	4.498 (1.385)	7.571 (0.232)

Table 3

Summary of scaling region models determined by SICc quantitative fitting in terms of percentages for both (a) DFA and (b) AFA. Healthy controls (HC), mild Parkinson's disease (PD-Mi), and moderate Parkinson's disease (PD-Mo) are reported with two Conditions of eyes open (EO) sway and eyes closed (EC sway).

(a) Percentages of DFA Scaling Region Models

Condition	**EO**		**EC**	
Scaling Regions	**1**	**2**	**1**	**2**
HC	19	81	25	75
PD-Mi	25	75	28	72
PD-Mo	18	82	18	82

(b) Percentages of AFA Scaling Region Models

Condition	**EO**		**EC**	
Scaling Regions	**2**	**3**	**2**	**3**
HC	8	92	6	94
PD-Mi	11	89	17	83
PD-Mo	18	82	12	88

Table 4

Results for 2-way ANOVA with blocking for both (a) DFA and (b) AFA.

(a) 2-way ANOVA results for DFA containing 1-region and 2-region scaling models. For 1-region scaling models, H is the Hurst exponent. For 2-region scaling models, H_{fast} is the first scaling region observed at fast time intervals, H_{int} is the second scaling region observed around intermediate time intervals, and Cr is the crossover point between the two along the time interval scale.

	Response: H						
		Df	**Sum Sq**	**Mean Sq**	**F value**	**Pr(>F)**	**Sig.**
1-region	**Condition**	1	0.01334	0.013341	3.4329	0.065751	.
	Group	2	0.0606	0.030301	7.7971	0.000587	***
	Participant (Block)	39	1.92624	0.049391	12.7094	<2.2e-16	***
	Condition: Group	2	0.02189	0.010945	2.8165	0.062787	.
	Residuals	160	0.62178	0.003886	-	-	
	Response: H_{fast}						
		Df	**Sum Sq**	**Mean Sq**	**F value**	**Pr(>F)**	**Sig.**
2-region	**Condition**	1	0.011955	0.011955	3.5434	0.069199	.
	Group	2	0.003421	0.00171	0.05069	0.060724	
	Participant (Block)	21	0.282925	0.013473	3.9932	0.000255	***
	Condition: Group	2	0.039533	0.019767	5.8587	0.006946	**
	Residuals	31	0.010459	0.003374	-	-	
	Response: H_{int}						
		Df	**Sum Sq**	**Mean Sq**	**F value**	**Pr(>F)**	**Sig.**
	Condition	1	0.2645	0.26452	3.9758	0.05502	.
	Group	2	0.0258	0.01289	0.1937	0.82486	
	Participant (Block)	21	10.0973	0.48083	7.2269	5.81E-07	***
	Condition: Group	2	0.1319	0.06593	0.991	0.38267	
	Residuals	31	2.0625	0.06653	-	-	
	Response: Cr						
		Df	**Sum Sq**	**Mean Sq**	**F value**	**Pr(>F)**	**Sig.**
	Condition	1	0.11534	0.115338	8.9542	0.005392	**
	Group	2	0.03811	0.019057	1.4795	0.24339	
	Participant (Block)	21	1.04547	0.049784	3.865	0.000341	***
	Condition: Group	2	0.14268	0.071342	5.5386	0.008778	**
	Residuals	31	0.39931	0.012881	-	-	
	Significance codes: 0 ‘***’ 0.001 ‘**’ 0.01 ‘*’ 0.05 ‘.’ 0.1 ‘ ’ 1						

(b) 2-way ANOVA results for AFA containing 2-region and 3-region scaling models. For 2-region scaling models, H_{fast} is the first scaling region observed at fast time intervals, H_{int} is the second scaling region observed around intermediate time intervals, and Cr is the crossover point between the two along the time interval scale. For 3-region scaling models, H_{fast} is the first scaling region observed at fast time intervals, H_{int} is the second scaling region observed around intermediate time intervals, H_{slow} is the third csaling region observed around slow time intervals, Cr1 is the crossover point between H_{fast} and H_{int}, and Cr 2 is the crossover point between H_{int} and H_{slow}.

	Response: H_{fast}						
		Df	**Sum Sq**	**Mean Sq**	**F value**	**Pr(>F)**	**Sig.**
	Condition	1	0.00005	0.000048	0.0031	0.95749	
	Group	2	0.35428	0.17714	11.5498	0.01336	*
	Participant (Block)	19	2.17838	0.114652	734755	0.01745	*
	Condition: Group	1	0.00061	0.000611	0.0398	0.84967	
	Residuals	5	0.07669	0.015337	-	-	
	Response: H_{int}						
		Df	**Sum Sq**	**Mean Sq**	**F value**	**Pr(>F)**	**Sig.**
	Condition	1	0.20319	0.203189	4.2314	0.09479	.
2-region	**Group**	2	0.04952	0.024761	0.05156	0.062575	
	Participant (Block)	19	1.71709	0.090373	1.882	0.2501	
	Condition: Group	1	0.04856	0.048565	1.0113	0.36074	
	Residuals	5	0.2401	0.04802	-	-	
	Response: Cr						
		Df	**Sum Sq**	**Mean Sq**	**F value**	**Pr(>F)**	**Sig.**
	Condition	1	0.0193	0.01927	0.0088	0.0088	
	Group	2	1.2512	0.6256	0.2869	0.2869	
	Participant (Block)	19	25.6055	1.34766	0.6181	0.6181	
	Condition: Group	1	0.4255	0.42549	0.1951	0.1951	
	Residuals	5	10.9017	2.18035	-	-	
	Signif. codes: 0 ‘***’ 0.001 ‘**’ 0.01 ‘*’ 0.05 ‘.’ 0.1 ‘ ’ 1						

3-region	**Response: H_{fast}**						
		Df	**Sum Sq**	**Mean Sq**	**F value**	**Pr(>F)**	**Sig.**
	Condition	1	0.091	0.09098	1.2978	0.2561	
	Group	2	2.4585	1.22923	17.5343	1.04E-07	***
	Participant (Block)	41	9.314	0.22717	3.2405	2.90E-08	***
	Condition: Group	2	0.1552	0.0776	1.107	0.3327	
	Residuals	188	13.1796	0.0701	-	-	
	Response: H_{int}						
		Df	**Sum Sq**	**Mean Sq**	**F value**	**Pr(>F)**	**Sig.**
	Condition	1	1.0713	1.07132	9.1041	0.002904	**
	Group	2	0.4676	0.23381	1.9869	0.139984	
	Participant (Block)	41	9.8166	0.23943	2.0347	0.000755	***
	Condition: Group	2	0.0131	0.00653	0.0555	0.946013	
	Residuals	188	22.1228	0.11767	-	-	
	Response: H_{slow}						
		Df	**Sum Sq**	**Mean Sq**	**F value**	**Pr(>F)**	**Sig.**
	Condition	1	2.384	2.38356	2.5393	0.113	
	Group	2	0.76	0.37987	0.4047	0.6679	
	Participant (Block)	41	39.321	0.95904	1.0217	0.4459	
	Condition: Group	2	0.503	0.25158	0.268	0.7652	
	Residuals	162	152.063	0.93866	-	-	
	Response: Cr1						
		Df	**Sum Sq**	**Mean Sq**	**F value**	**Pr(>F)**	**Sig.**
	Condition	1	3.521	3.5215	2.818	0.094873	.
	Group	2	8.84	4.4199	3.5369	0.031055	*
	Participant (Block)	41	104.21	2.5417	3.03	0.000759	***
	Condition: Group	2	2.295	1.1473	0.9181	0.40107	
	Residuals	188	234.931	1.2496	-	-	
	Response: Cr2						
		Df	**Sum Sq**	**Mean Sq**	**F value**	**Pr(>F)**	**Sig.**
	Condition	1	0.0316	0.031638	0.6244	0.4304	
	Group	2	0.0536	0.02681	0.5291	0.59	
	Participant (Block)	41	4.8044	0.117181	2.3127	7.89E-05	***
	Condition: Group	2	0.1299	0.064927	1.2814	0.2801	
	Residuals	188	9.5255	0.050668	-	-	
	Signif. codes: 0 ‘***’ 0.001 ‘**’ 0.01 ‘*’ 0.05 ‘.’ 0.1 ‘ ’ 1						

Chapter 5: Summary

Summary of Study

The primary objective of this thesis was to investigate the utilization of fractal analysis towards the development of quantitative, clinically significant measures that allow for early detection of Parkinson's disease (PD) postural instability (PI), the progression of PI due to PD progression, and ultimately, fall risk in PD patients.

Chapter 3 evaluated the effect of input parameter combinations of DFA and AFA in simulated fBm signals in an attempt to provide recommendations on appropriate parameter selection for fractal methods. Using approximations of stochastic integrals, fBm signals of desired length and Hurst exponent (H) were generated. Input parameter ranges were identified for (1) data length (N): 500, 1000, 2500, and 5000 samples; (2) minimum window size (n_{min}): 2, 4, 6, and 8 samples; (3) maximum window size (n_{max}): $\frac{N}{2}$, $\frac{N}{4}$, $\frac{N}{6}$, $\frac{N}{8}$, and $\frac{N}{10}$ samples; and (4) order of the fitted polynomial for AFA (M): 1st or 2nd order polynomial fits. AFA and DFA were conducted for every combination of these parameters for twenty trials (n=20) per combination. Both AFA and DFA were found to be highly sensitive to input parameter combinations. Parameter ranges for fBm-like signals in appropriately-large biological data are recommended to be examined at n_{max} values between N/6 and N/10, n_{min} values should remain around 4 to 6 samples, and that the fitted polynomial order M for AFA should remain first order.

Chapter 4 tested the sensitivity of AFA, as compared to DFA, towards center of pressure velocity (COPv) time series in the characterization of postural instability (PI) progression in patients with Parkinson's disease. A secondary goal was to investigate the relationship between fractal scaling behavior and the development of PI in PD. Postural sway data were analyzed that were previously collected on mild PD patients (Hoehn and Yahr stage (H&Y) 2, without postural deficits), moderate PD patients (H&Y 3, with postural deficits), and age-matched healthy

controls (HC). Ground reaction forces and moments were collected from subjects standing quality on a force plate in eyes open (EO) and eyes closed (EC) conditionals. COPv was calculated and analyzed with respects to both AFA and DFA. Scaling region properties of each trial were verified using a small sample Bayesian correlation criterion model (SICc). Both AFA and DFA were sensitive to the progression of PI and PD, however, AFA provided the most clinically significant measure H_{fast}. H_{fast} was found to be sensitive to PI and PD progression, regardless of scaling region model, which was not the case for other fractal parameters. 1- and 2-region models for DFA and 2- and 3-region models for AFA described scaling behavior in PD. However, scaling region distribution and variability results did not significantly characterize PI development or PD progression. The presence of multiple scaling regions across both AFA and DFA does indicate that changes in COP dynamics may not be adequately summarized through an intermittent velocity-based controller operating between open and closed loop neural systems, as that assumption relies on 2-region model results only. Other models should be considered which better explain fractal scaling results.

Limitations and Future Studies

Due to the pilot nature of this study's two primary goals, several limitations exist. In reference to Chapter 3, parametric ranges of different input conditions were selected off of preexisting literature. Other range values and parametric combinations were excluded based off of computational limitations (i.e. generation of longer data lengths). Shorter data lengths were excluded from generation due to incompatibility with the selected parametric combinations. Future studies should investigate wider ranges of each parametric input and seek to determine whether other variations of fractal analysis provide equivalent sensitivity to input parameters. It would also be relevant to investigate the effects of input parameter combinations in fractal

analysis on other signals often found in physiological experimental data such as pink noise, which is not well understood in the context of fractal analysis.

Chapter 4 limitations are largely due to the pilot nature of the subject pool and experimental methodology. The relatively small number of subjects limited the statistical power of the analysis. In addition, self-selected stance width as part of the experimental protocol prevented the COP measures in the mediolateral direction from being included in the analysis due to inconsistent mediolateral base of support across the participants. In addition, condition factors, cognitive factors, and other individual factors were not examined in the context of AFA or DFA sensitivity. There is a need to investigate whether fractal methods exhibit sensitivity towards other changes in COP dynamics in order to further investigate and understand the role of multiple scaling regions in postural dynamics. Also, while SICc model fitting routines were conducted in order to quantitatively determine the number of scaling regions, other model fitting routines should be considered to verify which protocol provides the most robust analysis of scaling behavior, particularly with an experimental subject pool such as parkinsonian patients. Further studies should be conducted over larger time intervals, with more subjects, and with controlled stance width in order to improve the scope of fractal methods investigated. Lastly, the study should be safely extended to both PD populations who are *off* medication and who already possess a history of falls in order to further assess the sensitivity of fractal methods towards PD progression.

Appendix A: Summary Statistics: Group means and standard deviations for each combination of *N*, n_{min}, n_{max} and *M* using AFA and DFA across all generated H signal ranges. These means are displayed as raw data (Appendices 1.1-1.8), differences of H estimation versus generated H value (Appendices 1.9-1.16), and percent differences of H estimation versus generated H value (Appendices 1.17-1.24).

Appendix 1.1: Raw data group means and standard deviations for each combination of $n_{min,}$ and n_{max} using DFA across all generated H signal ranges when N=500 (depicted blue**)**.

Window Sizes		H								
Min	Max	0.1	0.2	0.3	0.4	0.5	0.6	0.7	0.8	0.9
4	N/2	0.099 (0.112)	0.199 (0.108)	0.274 (0.105)	0.329 (0.159)	0.465 (0.130)	0.568 (0.123)	0.634 (0.145)	0.741 (0.180)	0.785 (0.140)
	N/4	0.147 (0.061)	0.213 (0.081)	0.308 (0.097)	0.355 (0.094)	0.467 (0.113)	0.587 (0.086)	0.696 (0.092)	0.745 (0.141)	0.839 (0.089)
	N/6	0.154 (0.059)	0.213 (0.086)	0.305 (0.090)	0.379 (0.072)	0.469 (0.073)	0.591 (0.073)	0.700 (0.072)	0.768 (0.116)	0.848 (0.080)
	N/8	0.159 (0.050)	0.229 (0.069)	0.317 (0.076)	0.389 (0.061)	0.468 (0.063)	0.604 (0.068)	0.708 (0.055)	0.772 (0.101)	0.853 (0.075)
	N/10	0.162 (0.047)	0.237 (0.065)	0.324 (0.073)	0.392 (0.050)	0.472 (0.062)	0.607 (0.063)	0.707 (0.054)	0.782 (0.098)	0.859 (0.076)
6	N/2	0.093 (0.120)	0.196 (0.115)	0.269 (0.112)	0.325 (0.171)	0.464 (0.138)	0.565 (0.132)	0.628 (0.155)	0.737 (0.187)	0.779 (0.145)
	N/4	0.141 (0.067)	0.207 (0.087)	0.304 (0.105)	0.349 (0.104)	0.465 (0.123)	0.585 (0.093)	0.693 (0.100)	0.738 (0.150)	0.834 (0.092)
	N/6	0.147 (0.065)	0.204 (0.097)	0.298 (0.098)	0.375 (0.082)	0.467 (0.081)	0.587 (0.080)	0.698 (0.078)	0.761 (0.124)	0.841 (0.082)
	N/8	0.150 (0.057)	0.221 (0.081)	0.309 (0.083)	0.386 (0.072)	0.465 (0.070)	0.602 (0.075)	0.706 (0.060)	0.763 (0.108)	0.843 (0.077)
	N/10	0.151 (0.053)	0.227 (0.080)	0.317 (0.079)	0.388 (0.058)	0.469 (0.070)	0.606 (0.070)	0.704 (0.059)	0.772 (0.106)	0.849 (0.078)
8	N/2	0.088 (0.128)	0.193 (0.122)	0.266 (0.118)	0.321 (0.180)	0.463 (0.144)	0.563 (0.139)	0.623 (0.163)	0.735 (0.194)	0.773 (0.151)
	N/4	0.138 (0.073)	0.204 (0.093)	0.302 (0.113)	0.345 (0.111)	0.464 (0.132)	0.584 (0.100)	0.692 (0.108)	0.733 (0.158)	0.830 (0.095)
	N/6	0.143 (0.071)	0.199 (0.106)	0.293 (0.105)	0.372 (0.089)	0.465 (0.089)	0.586 (0.088)	0.697 (0.086)	0.757 (0.132)	0.836 (0.085)
	N/8	0.145 (0.064)	0.216 (0.091)	0.305 (0.090)	0.384 (0.080)	0.462 (0.079)	0.604 (0.082)	0.707 (0.066)	0.758 (0.117)	0.837 (0.081)
	N/10	0.143 (0.058)	0.223 (0.093)	0.313 (0.086)	0.386 (0.063)	0.466 (0.078)	0.608 (0.078)	0.705 (0.065)	0.768 (0.117)	0.841 (0.083)
10	N/2	0.084 (0.136)	0.191 (0.128)	0.263 (0.124)	0.319 (0.189)	0.463 (0.150)	0.561 (0.147)	0.618 (0.170)	0.733 (0.200)	0.769 (0.155)
	N/4	0.135 (0.078)	0.201 (0.097)	0.300 (0.120)	0.343 (0.119)	0.463 (0.140)	0.582 (0.106)	0.691 (0.113)	0.730 (0.165)	0.828 (0.098)
	N/6	0.139 (0.075)	0.193 (0.113)	0.289 (0.113)	0.373 (0.098)	0.465 (0.096)	0.583 (0.096)	0.696 (0.090)	0.755 (0.139)	0.835 (0.086)
	N/8	0.139 (0.068)	0.211 (0.099)	0.300 (0.098)	0.387 (0.091)	0.460 (0.087)	0.602 (0.085)	0.707 (0.068)	0.755 (0.123)	0.834 (0.082)
	N/10	0.136 (0.061)	0.217 (0.102)	0.309 (0.093)	0.391 (0.071)	0.464 (0.086)	0.607 (0.083)	0.705 (0.067)	0.766 (0.125)	0.839 (0.084)

Appendix 1.2: Raw data group means and standard deviations for each combination of $n_{min,}$ and n_{max} using DFA across all generated H signal ranges when N=1000 (depicted green**)**.

Window Sizes		H								
Min	Max	0.1	0.2	0.3	0.4	0.5	0.6	0.7	0.8	0.9
4	N/2	0.103 (0.101)	0.208 (0.090)	0.282 (0.102)	0.362 (0.122)	0.456 (0.142)	0.501 (0.134)	0.587 (0.121)	0.745 (0.134)	0.849 (0.118)
	N/4	0.153 (0.074)	0.224 (0.086)	0.281 (0.086)	0.398 (0.060)	0.468 (0.092)	0.561 (0.101)	0.653 (0.071)	0.760 (0.102)	0.855 (0.089)
	N/6	0.169 (0.058)	0.236 (0.056)	0.295 (0.069)	0.400 (0.062)	0.468 (0.077)	0.593 (0.084)	0.671 (0.061)	0.772 (0.090)	0.868 (0.071)
	N/8	0.179 (0.038)	0.249 (0.052)	0.303 (0.065)	0.390 (0.042)	0.487 (0.066)	0.592 (0.079)	0.674 (0.057)	0.779 (0.083)	0.878 (0.060)
	N/10	0.186 (0.035)	0.253 (0.048)	0.307 (0.059)	0.388 (0.041)	0.492 (0.061)	0.587 (0.068)	0.671 (0.051)	0.778 (0.080)	0.889 (0.053)
6	N/2	0.099 (0.106)	0.205 (0.095)	0.280 (0.106)	0.360 (0.128)	0.454 (0.148)	0.497 (0.140)	0.582 (0.127)	0.743 (0.139)	0.846 (0.122)
	N/4	0.149 (0.080)	0.221 (0.091)	0.278 (0.091)	0.398 (0.064)	0.465 (0.097)	0.559 (0.106)	0.651 (0.074)	0.757 (0.106)	0.850 (0.093)
	N/6	0.165 (0.065)	0.233 (0.060)	0.292 (0.074)	0.400 (0.067)	0.464 (0.082)	0.593 (0.089)	0.669 (0.064)	0.769 (0.094)	0.862 (0.074)
	N/8	0.174 (0.043)	0.246 (0.056)	0.299 (0.070)	0.388 (0.046)	0.485 (0.072)	0.592 (0.084)	0.673 (0.060)	0.777 (0.087)	0.872 (0.062)
	N/10	0.181 (0.040)	0.251 (0.053)	0.303 (0.065)	0.385 (0.045)	0.491 (0.067)	0.585 (0.073)	0.668 (0.053)	0.775 (0.084)	0.883 (0.054)
8	N/2	0.095 (0.110)	0.204 (0.099)	0.279 (0.110)	0.358 (0.133)	0.453 (0.154)	0.494 (0.146)	0.578 (0.131)	0.742 (0.143)	0.844 (0.125)
	N/4	0.145 (0.085)	0.219 (0.096)	0.275 (0.096)	0.398 (0.068)	0.464 (0.102)	0.557 (0.110)	0.649 (0.076)	0.756 (0.109)	0.847 (0.096)
	N/6	0.162 (0.070)	0.232 (0.065)	0.289 (0.078)	0.400 (0.073)	0.462 (0.087)	0.594 (0.094)	0.669 (0.066)	0.768 (0.097)	0.859 (0.077)
	N/8	0.171 (0.047)	0.246 (0.060)	0.296 (0.075)	0.387 (0.050)	0.484 (0.077)	0.593 (0.090)	0.672 (0.063)	0.777 (0.091)	0.868 (0.064)
	N/10	0.178 (0.045)	0.251 (0.057)	0.299 (0.070)	0.383 (0.048)	0.490 (0.071)	0.586 (0.077)	0.667 (0.055)	0.774 (0.088)	0.881 (0.056)
10	N/2	0.092 (0.114)	0.202 (0.102)	0.278 (0.114)	0.357 (0.137)	0.451 (0.158)	0.490 (0.150)	0.575 (0.135)	0.740 (0.147)	0.843 (0.128)
	N/4	0.143 (0.091)	0.217 (0.100)	0.273 (0.100)	0.399 (0.072)	0.462 (0.106)	0.555 (0.114)	0.647 (0.078)	0.754 (0.113)	0.845 (0.099)
	N/6	0.159 (0.076)	0.229 (0.069)	0.287 (0.081)	0.400 (0.079)	0.459 (0.092)	0.594 (0.097)	0.668 (0.068)	0.767 (0.101)	0.856 (0.080)
	N/8	0.169 (0.052)	0.245 (0.065)	0.294 (0.079)	0.387 (0.054)	0.482 (0.082)	0.594 (0.094)	0.672 (0.065)	0.776 (0.094)	0.866 (0.066)
	N/10	0.176 (0.049)	0.250 (0.061)	0.297 (0.074)	0.382 (0.052)	0.489 (0.076)	0.585 (0.080)	0.666 (0.057)	0.773 (0.093)	0.879 (0.057)

Appendix 1.3: Raw data group means and standard deviations for each combination of $n_{min,}$ and n_{max} using DFA across all generated H signal ranges when N=2500 (depicted yellow**)**.

Window Sizes		H								
Min	Max	0.1	0.2	0.3	0.4	0.5	0.6	0.7	0.8	0.9
4	N/2	0.091 (0.078)	0.177 (0.092)	0.279 (0.086)	0.327 (0.112)	0.467 (0.156)	0.514 (0.111)	0.599 (0.117)	0.736 (0.134)	0.789 (0.136)
	N/4	0.117 (0.078)	0.221 (0.069)	0.278 (0.057)	0.359 (0.086)	0.497 (0.090)	0.549 (0.078)	0.653 (0.077)	0.765 (0.070)	0.830 (0.096)
	N/6	0.118 (0.061)	0.230 (0.053)	0.299 (0.046)	0.367 (0.061)	0.485 (0.065)	0.564 (0.065)	0.675 (0.073)	0.782 (0.073)	0.853 (0.075)
	N/8	0.126 (0.050)	0.225 (0.043)	0.303 (0.042)	0.375 (0.053)	0.495 (0.060)	0.572 (0.059)	0.677 (0.068)	0.782 (0.058)	0.866 (0.061)
	N/10	0.133 (0.044)	0.226 (0.036)	0.310 (0.039)	0.379 (0.054)	0.501 (0.053)	0.578 (0.050)	0.675 (0.059)	0.784 (0.052)	0.870 (0.056)
6	N/2	0.088 (0.080)	0.175 (0.095)	0.278 (0.088)	0.325 (0.115)	0.466 (0.159)	0.512 (0.113)	0.596 (0.120)	0.734 (0.138)	0.786 (0.139)
	N/4	0.114 (0.081)	0.220 (0.072)	0.275 (0.059)	0.357 (0.090)	0.497 (0.093)	0.547 (0.081)	0.651 (0.079)	0.763 (0.071)	0.827 (0.099)
	N/6	0.114 (0.065)	0.229 (0.056)	0.297 (0.048)	0.364 (0.065)	0.484 (0.067)	0.563 (0.068)	0.674 (0.076)	0.781 (0.075)	0.850 (0.078)
	N/8	0.121 (0.053)	0.222 (0.046)	0.301 (0.044)	0.373 (0.056)	0.495 (0.063)	0.570 (0.061)	0.676 (0.071)	0.780 (0.060)	0.863 (0.062)
	N/10	0.128 (0.047)	0.223 (0.039)	0.308 (0.042)	0.377 (0.057)	0.501 (0.056)	0.577 (0.052)	0.673 (0.062)	0.781 (0.053)	0.866 (0.058)
8	N/2	0.087 (0.081)	0.174 (0.097)	0.277 (0.090)	0.323 (0.118)	0.466 (0.163)	0.510 (0.116)	0.594 (0.122)	0.732 (0.141)	0.784 (0.142)
	N/4	0.112 (0.084)	0.219 (0.074)	0.274 (0.061)	0.355 (0.093)	0.497 (0.096)	0.545 (0.083)	0.650 (0.081)	0.762 (0.073)	0.824 (0.101)
	N/6	0.111 (0.068)	0.228 (0.059)	0.296 (0.050)	0.363 (0.067)	0.484 (0.070)	0.561 (0.070)	0.673 (0.078)	0.780 (0.078)	0.848 (0.080)
	N/8	0.118 (0.056)	0.221 (0.048)	0.300 (0.046)	0.371 (0.058)	0.495 (0.066)	0.569 (0.063)	0.675 (0.073)	0.779 (0.062)	0.861 (0.064)
	N/10	0.124 (0.051)	0.221 (0.042)	0.308 (0.044)	0.375 (0.060)	0.502 (0.059)	0.576 (0.054)	0.672 (0.065)	0.780 (0.055)	0.864 (0.059)
10	N/2	0.085 (0.083)	0.172 (0.099)	0.276 (0.091)	0.322 (0.120)	0.465 (0.166)	0.509 (0.118)	0.592 (0.125)	0.731 (0.143)	0.782 (0.144)
	N/4	0.111 (0.087)	0.218 (0.077)	0.273 (0.063)	0.354 (0.095)	0.497 (0.098)	0.544 (0.085)	0.649 (0.083)	0.761 (0.074)	0.822 (0.103)
	N/6	0.108 (0.071)	0.228 (0.061)	0.295 (0.052)	0.361 (0.070)	0.483 (0.072)	0.560 (0.072)	0.673 (0.080)	0.780 (0.080)	0.846 (0.082)
	N/8	0.115 (0.059)	0.220 (0.051)	0.299 (0.048)	0.370 (0.060)	0.495 (0.068)	0.568 (0.065)	0.674 (0.076)	0.778 (0.064)	0.859 (0.065)
	N/10	0.121 (0.053)	0.220 (0.044)	0.307 (0.046)	0.373 (0.063)	0.502 (0.061)	0.575 (0.055)	0.671 (0.067)	0.779 (0.056)	0.863 (0.061)

Appendix 1.4: Raw data group means and standard deviations for each combination of $n_{min,}$ and n_{max} using DFA across all generated H signal ranges when N=5000 (depicted red**)**.

Window Sizes		H								
Min	Max	0.1	0.2	0.3	0.4	0.5	0.6	0.7	0.8	0.9
4	N/2	0.089 (0.118)	0.169 (0.154)	0.278 (0.114)	0.356 (0.125)	0.433 (0.104)	0.534 (0.092)	0.633 (0.096)	0.764 (0.127)	0.841 (0.082)
	N/4	0.123 (0.066)	0.186 (0.082)	0.279 (0.069)	0.377 (0.076)	0.467 (0.086)	0.561 (0.062)	0.648 (0.065)	0.766 (0.082)	0.862 (0.064)
	N/6	0.134 (0.047)	0.199 (0.059)	0.297 (0.060)	0.388 (0.060)	0.488 (0.048)	0.585 (0.050)	0.655 (0.065)	0.777 (0.067)	0.867 (0.053)
	N/8	0.140 (0.041)	0.211 (0.057)	0.297 (0.053)	0.397 (0.048)	0.487 (0.045)	0.583 (0.049)	0.663 (0.056)	0.776 (0.059)	0.875 (0.041)
	N/10	0.143 (0.033)	0.222 (0.050)	0.303 (0.054)	0.394 (0.046)	0.487 (0.040)	0.584 (0.042)	0.665 (0.044)	0.779 (0.054)	0.878 (0.038)
6	N/2	0.088 (0.120)	0.168 (0.157)	0.277 (0.116)	0.355 (0.127)	0.432 (0.106)	0.533 (0.094)	0.632 (0.097)	0.763 (0.129)	0.839 (0.083)
	N/4	0.121 (0.068)	0.184 (0.084)	0.278 (0.070)	0.377 (0.079)	0.466 (0.088)	0.560 (0.063)	0.647 (0.067)	0.766 (0.083)	0.861 (0.065)
	N/6	0.133 (0.049)	0.197 (0.061)	0.296 (0.062)	0.387 (0.062)	0.488 (0.050)	0.585 (0.052)	0.653 (0.067)	0.776 (0.068)	0.865 (0.054)
	N/8	0.138 (0.043)	0.209 (0.059)	0.296 (0.054)	0.396 (0.049)	0.486 (0.046)	0.582 (0.051)	0.662 (0.058)	0.775 (0.061)	0.873 (0.042)
	N/10	0.141 (0.035)	0.220 (0.052)	0.302 (0.056)	0.394 (0.048)	0.487 (0.041)	0.584 (0.043)	0.663 (0.046)	0.778 (0.056)	0.876 (0.039)
8	N/2	0.086 (0.122)	0.167 (0.159)	0.276 (0.117)	0.355 (0.129)	0.431 (0.108)	0.532 (0.095)	0.632 (0.099)	0.763 (0.130)	0.839 (0.084)
	N/4	0.120 (0.070)	0.182 (0.086)	0.277 (0.072)	0.376 (0.081)	0.465 (0.091)	0.559 (0.064)	0.646 (0.068)	0.765 (0.084)	0.860 (0.066)
	N/6	0.132 (0.050)	0.196 (0.062)	0.296 (0.063)	0.386 (0.064)	0.488 (0.051)	0.584 (0.053)	0.652 (0.068)	0.775 (0.069)	0.864 (0.055)
	N/8	0.137 (0.044)	0.208 (0.061)	0.295 (0.056)	0.396 (0.051)	0.486 (0.048)	0.582 (0.052)	0.661 (0.060)	0.774 (0.062)	0.872 (0.043)
	N/10	0.140 (0.036)	0.219 (0.054)	0.301 (0.058)	0.393 (0.050)	0.486 (0.042)	0.584 (0.044)	0.662 (0.047)	0.778 (0.057)	0.875 (0.039)
10	N/2	0.085 (0.124)	0.166 (0.161)	0.276 (0.119)	0.354 (0.131)	0.430 (0.109)	0.532 (0.096)	0.631 (0.100)	0.763 (0.132)	0.838 (0.085)
	N/4	0.119 (0.071)	0.181 (0.087)	0.276 (0.073)	0.375 (0.082)	0.465 (0.093)	0.558 (0.065)	0.645 (0.069)	0.765 (0.085)	0.860 (0.067)
	N/6	0.131 (0.052)	0.194 (0.064)	0.295 (0.064)	0.386 (0.066)	0.487 (0.052)	0.584 (0.054)	0.651 (0.070)	0.775 (0.070)	0.864 (0.056)
	N/8	0.136 (0.046)	0.207 (0.063)	0.294 (0.057)	0.396 (0.053)	0.485 (0.049)	0.582 (0.054)	0.660 (0.061)	0.774 (0.063)	0.871 (0.043)
	N/10	0.139 (0.038)	0.218 (0.056)	0.300 (0.059)	0.393 (0.052)	0.486 (0.043)	0.583 (0.045)	0.661 (0.049)	0.777 (0.058)	0.874 (0.040)

Appendix 1.5: Raw data group means and standard deviations for each combination of n_{min}, n_{max}, and M using AFA across all generated H signal ranges when N=500 (depicted blue).

Window Size			H								
Min	Max	Order	0.1	0.2	0.3	0.4	0.5	0.6	0.7	0.8	0.9
4	N/2	1	0.209 (0.048)	0.269 (0.057)	0.349 (0.058)	0.479 (0.069)	0.591 (0.109)	0.709 (0.125)	0.824 (0.124)	1.069 (0.143)	1.174 (0.192)
		2	0.225 (0.046)	0.293 (0.058)	0.368 (0.057)	0.511 (0.076)	0.630 (0.114)	0.747 (0.139)	0.879 (0.141)	1.130 (0.163)	1.222 (0.229)
	N/4	1	0.212 (0.019)	0.279 (0.031)	0.353 (0.040)	0.435 (0.053)	0.542 (0.080)	0.672 (0.077)	0.781 (0.088)	0.892 (0.142)	1.100 (0.142)
		2	0.225 (0.020)	0.298 (0.030)	0.376 (0.045)	0.449 (0.058)	0.568 (0.088)	0.701 (0.096)	0.826 (0.107)	0.930 (0.160)	1.152 (0.179)
	N/6	1	0.219 (0.018)	0.279 (0.021)	0.351 (0.033)	0.423 (0.039)	0.541 (0.061)	0.624 (0.042)	0.764 (0.095)	0.829 (0.115)	1.045 (0.126)
		2	0.235 (0.019)	0.297 (0.019)	0.372 (0.033)	0.436 (0.032)	0.562 (0.065)	0.631 (0.054)	0.807 (0.125)	0.857 (0.140)	1.095 (0.161)
	N/8	1	0.224 (0.017)	0.282 (0.021)	0.349 (0.031)	0.422 (0.034)	0.533 (0.045)	0.600 (0.036)	0.733 (0.078)	0.817 (0.094)	0.995 (0.116)
		2	0.240 (0.016)	0.298 (0.019)	0.366 (0.031)	0.434 (0.033)	0.547 (0.044)	0.601 (0.043)	0.766 (0.097)	0.840 (0.122)	1.032 (0.159)
	N/10	1	0.226 (0.015)	0.286 (0.020)	0.349 (0.026)	0.421 (0.034)	0.520 (0.041)	0.593 (0.035)	0.711 (0.049)	0.806 (0.088)	0.964 (0.119)
		2	0.243 (0.014)	0.300 (0.018)	0.362 (0.023)	0.434 (0.039)	0.529 (0.035)	0.597 (0.045)	0.731 (0.065)	0.832 (0.120)	0.999 (0.162)
6	N/2	1	0.208 (0.049)	0.269 (0.058)	0.349 (0.059)	0.480 (0.070)	0.593 (0.111)	0.712 (0.127)	0.828 (0.126)	1.077 (0.145)	1.181 (0.195)
		2	0.225 (0.047)	0.293 (0.059)	0.369 (0.058)	0.513 (0.077)	0.633 (0.116)	0.751 (0.142)	0.884 (0.143)	1.139 (0.166)	1.230 (0.233)
	N/4	1	0.211 (0.020)	0.278 (0.032)	0.354 (0.041)	0.436 (0.055)	0.545 (0.082)	0.677 (0.079)	0.786 (0.090)	0.899 (0.146)	1.110 (0.147)
		2	0.224 (0.021)	0.298 (0.031)	0.377 (0.046)	0.451 (0.060)	0.572 (0.090)	0.707 (0.099)	0.834 (0.110)	0.939 (0.165)	1.165 (0.184)
	N/6	1	0.217 (0.018)	0.279 (0.022)	0.351 (0.034)	0.425 (0.041)	0.545 (0.063)	0.629 (0.044)	0.772 (0.099)	0.836 (0.119)	1.059 (0.131)
		2	0.234 (0.019)	0.297 (0.020)	0.373 (0.034)	0.439 (0.033)	0.568 (0.068)	0.637 (0.056)	0.817 (0.130)	0.867 (0.146)	1.111 (0.167)
	N/8	1	0.223 (0.018)	0.281 (0.022)	0.350 (0.033)	0.424 (0.035)	0.537 (0.047)	0.606 (0.038)	0.741 (0.082)	0.826 (0.098)	1.009 (0.122)
		2	0.238 (0.017)	0.298 (0.019)	0.368 (0.033)	0.436 (0.034)	0.553 (0.046)	0.607 (0.044)	0.778 (0.102)	0.853 (0.128)	1.051 (0.167)
	N/10	1	0.224 (0.016)	0.285 (0.021)	0.350 (0.027)	0.424 (0.035)	0.525 (0.043)	0.598 (0.037)	0.720 (0.052)	0.816 (0.093)	0.980 (0.126)
		2	0.241 (0.015)	0.300 (0.019)	0.364 (0.024)	0.438 (0.041)	0.536 (0.037)	0.605 (0.047)	0.743 (0.069)	0.846 (0.126)	1.020 (0.172)
8	N/2	1	0.208 (0.050)	0.269 (0.058)	0.349 (0.060)	0.482 (0.072)	0.595 (0.113)	0.714 (0.129)	0.831 (0.128)	1.082 (0.147)	1.187 (0.198)
		2	0.224 (0.048)	0.293 (0.060)	0.369 (0.059)	0.515 (0.078)	0.636 (0.118)	0.754 (0.144)	0.888 (0.146)	1.146 (0.169)	1.237 (0.237)
	N/4	1	0.210 (0.020)	0.278 (0.032)	0.354 (0.042)	0.437 (0.057)	0.547 (0.084)	0.680 (0.081)	0.790 (0.093)	0.905 (0.149)	1.118 (0.150)
		2	0.223 (0.021)	0.297 (0.031)	0.377 (0.047)	0.452 (0.061)	0.575 (0.093)	0.712 (0.102)	0.839 (0.113)	0.945 (0.169)	1.175 (0.189)
	N/6	1	0.216 (0.019)	0.278 (0.023)	0.351 (0.035)	0.426 (0.042)	0.547 (0.065)	0.632 (0.046)	0.777 (0.102)	0.841 (0.123)	1.068 (0.136)
		2	0.232 (0.020)	0.296 (0.020)	0.374 (0.035)	0.440 (0.034)	0.571 (0.070)	0.641 (0.058)	0.825 (0.135)	0.873 (0.150)	1.123 (0.173)
	N/8	1	0.221 (0.018)	0.280 (0.023)	0.350 (0.034)	0.425 (0.036)	0.540 (0.048)	0.609 (0.039)	0.747 (0.086)	0.832 (0.102)	1.019 (0.127)
		2	0.237 (0.017)	0.297 (0.020)	0.368 (0.034)	0.438 (0.036)	0.557 (0.048)	0.611 (0.046)	0.786 (0.106)	0.861 (0.133)	1.064 (0.174)
	N/10	1	0.222 (0.017)	0.285 (0.022)	0.350 (0.028)	0.425 (0.037)	0.528 (0.045)	0.602 (0.038)	0.726 (0.054)	0.823 (0.097)	0.991 (0.132)
		2	0.239 (0.015)	0.299 (0.019)	0.364 (0.025)	0.440 (0.043)	0.540 (0.038)	0.609 (0.049)	0.751 (0.072)	0.856 (0.131)	1.034 (0.181)
10	N/2	1	0.207 (0.051)	0.268 (0.059)	0.349 (0.060)	0.483 (0.073)	0.597 (0.115)	0.716 (0.131)	0.833 (0.130)	1.087 (0.149)	1.191 (0.201)
		2	0.223 (0.049)	0.293 (0.060)	0.369 (0.059)	0.516 (0.080)	0.638 (0.120)	0.757 (0.146)	0.891 (0.148)	1.151 (0.171)	1.242 (0.241)
	N/4	1	0.209 (0.021)	0.277 (0.033)	0.354 (0.043)	0.438 (0.058)	0.548 (0.085)	0.683 (0.083)	0.794 (0.095)	0.909 (0.152)	1.125 (0.154)
		2	0.222 (0.022)	0.297 (0.032)	0.378 (0.048)	0.453 (0.063)	0.577 (0.095)	0.716 (0.104)	0.844 (0.116)	0.950 (0.173)	1.182 (0.193)
	N/6	1	0.215 (0.019)	0.278 (0.023)	0.351 (0.036)	0.426 (0.043)	0.550 (0.067)	0.635 (0.047)	0.781 (0.105)	0.845 (0.127)	1.075 (0.140)
		2	0.231 (0.021)	0.296 (0.021)	0.374 (0.036)	0.441 (0.035)	0.574 (0.072)	0.644 (0.060)	0.831 (0.139)	0.878 (0.154)	1.133 (0.179)
	N/8	1	0.220 (0.019)	0.280 (0.023)	0.350 (0.035)	0.426 (0.037)	0.543 (0.050)	0.611 (0.040)	0.751 (0.089)	0.836 (0.106)	1.027 (0.132)
		2	0.235 (0.018)	0.296 (0.021)	0.369 (0.035)	0.439 (0.037)	0.560 (0.050)	0.614 (0.047)	0.792 (0.110)	0.866 (0.137)	1.074 (0.181)
	N/10	1	0.221 (0.017)	0.284 (0.022)	0.350 (0.029)	0.426 (0.038)	0.531 (0.046)	0.605 (0.039)	0.730 (0.057)	0.828 (0.100)	0.999 (0.138)
		2	0.237 (0.016)	0.298 (0.020)	0.364 (0.026)	0.441 (0.045)	0.543 (0.039)	0.612 (0.050)	0.758 (0.075)	0.863 (0.136)	1.044 (0.189)

Appendix 1.6: Raw data group means and standard deviations for each combination of n_{min}, n_{max}, and M using AFA across all generated H signal ranges when N=1000 (depicted green**)**.

Window Size			H								
Min	Max	Order	0.1	0.2	0.3	0.4	0.5	0.6	0.7	0.8	0.9
4	N/2	1	0.252 (0.036)	0.338 (0.079)	0.364 (0.056)	0.511 (0.125)	0.600 (0.126)	0.699 (0.153)	0.760 (0.118)	1.016 (0.241)	1.115 (0.268)
		2	0.280 (0.036)	0.369 (0.080)	0.380 (0.059)	0.552 (0.130)	0.641 (0.137)	0.737 (0.163)	0.805 (0.131)	1.061 (0.273)	1.152 (0.290)
	N/4	1	0.264 (0.026)	0.317 (0.034)	0.371 (0.053)	0.439 (0.047)	0.551 (0.104)	0.633 (0.084)	0.733 (0.122)	0.831 (0.161)	1.006 (0.187)
		2	0.290 (0.028)	0.335 (0.034)	0.400 (0.058)	0.467 (0.051)	0.571 (0.124)	0.650 (0.096)	0.761 (0.159)	0.856 (0.193)	1.031 (0.219)
	N/6	1	0.274 (0.021)	0.314 (0.033)	0.364 (0.044)	0.429 (0.049)	0.512 (0.073)	0.616 (0.088)	0.717 (0.125)	0.764 (0.142)	0.954 (0.188)
		2	0.298 (0.024)	0.333 (0.035)	0.385 (0.040)	0.446 (0.039)	0.527 (0.078)	0.642 (0.101)	0.748 (0.157)	0.775 (0.171)	0.968 (0.244)
	N/8	1	0.278 (0.022)	0.309 (0.026)	0.363 (0.038)	0.425 (0.043)	0.491 (0.063)	0.602 (0.088)	0.686 (0.101)	0.739 (0.113)	0.917 (0.178)
		2	0.298 (0.022)	0.325 (0.024)	0.383 (0.037)	0.437 (0.041)	0.498 (0.069)	0.627 (0.105)	0.702 (0.127)	0.748 (0.141)	0.924 (0.234)
	N/10	1	0.279 (0.024)	0.306 (0.023)	0.364 (0.031)	0.420 (0.039)	0.479 (0.058)	0.585 (0.081)	0.658 (0.103)	0.712 (0.086)	0.880 (0.166)
		2	0.297 (0.023)	0.320 (0.021)	0.382 (0.035)	0.430 (0.043)	0.485 (0.068)	0.599 (0.096)	0.666 (0.132)	0.711 (0.110)	0.888 (0.214)
6	N/2	1	0.251 (0.038)	0.340 (0.083)	0.365 (0.058)	0.517 (0.131)	0.607 (0.131)	0.708 (0.161)	0.769 (0.125)	1.035 (0.255)	1.134 (0.282)
		2	0.280 (0.038)	0.372 (0.084)	0.382 (0.062)	0.560 (0.137)	0.651 (0.144)	0.749 (0.171)	0.817 (0.139)	1.084 (0.288)	1.175 (0.306)
	N/4	1	0.264 (0.029)	0.319 (0.036)	0.373 (0.056)	0.444 (0.050)	0.560 (0.112)	0.645 (0.090)	0.748 (0.130)	0.850 (0.173)	1.032 (0.201)
		2	0.291 (0.030)	0.338 (0.036)	0.405 (0.062)	0.476 (0.055)	0.584 (0.134)	0.664 (0.103)	0.781 (0.170)	0.882 (0.207)	1.063 (0.234)
	N/6	1	0.275 (0.022)	0.317 (0.035)	0.368 (0.048)	0.435 (0.053)	0.523 (0.079)	0.631 (0.095)	0.737 (0.137)	0.785 (0.156)	0.988 (0.206)
		2	0.300 (0.026)	0.337 (0.038)	0.391 (0.044)	0.456 (0.043)	0.541 (0.085)	0.663 (0.110)	0.776 (0.174)	0.803 (0.188)	1.008 (0.267)
	N/8	1	0.279 (0.025)	0.311 (0.028)	0.368 (0.042)	0.433 (0.048)	0.501 (0.070)	0.620 (0.097)	0.708 (0.112)	0.763 (0.126)	0.956 (0.199)
		2	0.301 (0.024)	0.330 (0.026)	0.390 (0.041)	0.449 (0.046)	0.512 (0.076)	0.654 (0.116)	0.733 (0.142)	0.782 (0.159)	0.972 (0.262)
	N/10	1	0.280 (0.026)	0.308 (0.024)	0.369 (0.035)	0.430 (0.045)	0.491 (0.065)	0.605 (0.091)	0.683 (0.116)	0.740 (0.098)	0.925 (0.188)
		2	0.301 (0.026)	0.325 (0.024)	0.392 (0.040)	0.444 (0.049)	0.502 (0.077)	0.629 (0.108)	0.700 (0.148)	0.748 (0.126)	0.943 (0.244)
8	N/2	1	0.250 (0.039)	0.341 (0.087)	0.365 (0.061)	0.522 (0.137)	0.613 (0.136)	0.714 (0.168)	0.775 (0.131)	1.050 (0.266)	1.147 (0.295)
		2	0.279 (0.039)	0.374 (0.088)	0.382 (0.065)	0.567 (0.143)	0.658 (0.150)	0.757 (0.179)	0.825 (0.146)	1.101 (0.301)	1.191 (0.320)
	N/4	1	0.263 (0.031)	0.319 (0.038)	0.375 (0.060)	0.447 (0.053)	0.567 (0.120)	0.652 (0.096)	0.757 (0.138)	0.863 (0.184)	1.050 (0.213)
		2	0.290 (0.032)	0.339 (0.037)	0.407 (0.065)	0.480 (0.058)	0.592 (0.143)	0.673 (0.110)	0.793 (0.181)	0.898 (0.221)	1.084 (0.247)
	N/6	1	0.275 (0.024)	0.317 (0.038)	0.369 (0.051)	0.439 (0.057)	0.529 (0.086)	0.641 (0.101)	0.750 (0.149)	0.798 (0.168)	1.010 (0.221)
		2	0.300 (0.028)	0.338 (0.041)	0.393 (0.047)	0.461 (0.047)	0.549 (0.093)	0.677 (0.117)	0.794 (0.189)	0.820 (0.204)	1.035 (0.287)
	N/8	1	0.280 (0.027)	0.311 (0.030)	0.369 (0.046)	0.438 (0.052)	0.507 (0.077)	0.633 (0.105)	0.723 (0.122)	0.779 (0.138)	0.983 (0.218)
		2	0.301 (0.026)	0.330 (0.029)	0.393 (0.045)	0.455 (0.051)	0.519 (0.083)	0.671 (0.126)	0.752 (0.155)	0.802 (0.175)	1.004 (0.288)
	N/10	1	0.281 (0.029)	0.309 (0.026)	0.372 (0.039)	0.436 (0.049)	0.497 (0.072)	0.620 (0.100)	0.698 (0.127)	0.756 (0.109)	0.955 (0.209)
		2	0.300 (0.028)	0.326 (0.026)	0.396 (0.044)	0.451 (0.055)	0.509 (0.085)	0.647 (0.119)	0.721 (0.163)	0.770 (0.141)	0.981 (0.272)
10	N/2	1	0.249 (0.041)	0.343 (0.090)	0.365 (0.063)	0.526 (0.143)	0.617 (0.141)	0.720 (0.175)	0.779 (0.137)	1.062 (0.277)	1.158 (0.307)
		2	0.278 (0.041)	0.376 (0.091)	0.382 (0.067)	0.572 (0.149)	0.664 (0.155)	0.763 (0.186)	0.830 (0.152)	1.115 (0.313)	1.202 (0.333)
	N/4	1	0.262 (0.033)	0.320 (0.040)	0.375 (0.063)	0.450 (0.056)	0.572 (0.127)	0.658 (0.101)	0.764 (0.146)	0.874 (0.193)	1.063 (0.224)
		2	0.289 (0.034)	0.339 (0.039)	0.409 (0.069)	0.484 (0.061)	0.598 (0.151)	0.679 (0.117)	0.801 (0.191)	0.910 (0.233)	1.099 (0.260)
	N/6	1	0.274 (0.025)	0.318 (0.040)	0.370 (0.055)	0.442 (0.061)	0.533 (0.092)	0.648 (0.108)	0.761 (0.160)	0.808 (0.180)	1.027 (0.236)
		2	0.299 (0.030)	0.339 (0.044)	0.394 (0.050)	0.465 (0.050)	0.554 (0.100)	0.687 (0.123)	0.808 (0.205)	0.832 (0.219)	1.054 (0.307)
	N/8	1	0.280 (0.029)	0.312 (0.031)	0.370 (0.050)	0.442 (0.056)	0.511 (0.083)	0.643 (0.112)	0.734 (0.132)	0.790 (0.150)	1.003 (0.236)
		2	0.301 (0.028)	0.330 (0.031)	0.394 (0.048)	0.460 (0.055)	0.524 (0.090)	0.684 (0.135)	0.766 (0.170)	0.817 (0.192)	1.028 (0.313)
	N/10	1	0.281 (0.031)	0.309 (0.027)	0.373 (0.042)	0.441 (0.054)	0.500 (0.079)	0.631 (0.108)	0.709 (0.139)	0.768 (0.121)	0.978 (0.230)
		2	0.300 (0.030)	0.325 (0.028)	0.398 (0.048)	0.457 (0.061)	0.513 (0.093)	0.661 (0.130)	0.735 (0.180)	0.785 (0.158)	1.008 (0.301)

Appendix 1.7: Raw data group means and standard deviations for each combination of n_{min}, n_{max}, and M using AFA across all generated H signal ranges when N=2500 (depicted yellow**)**.

Window Size			H								
Min	Max	Order	0.1	0.2	0.3	0.4	0.5	0.6	0.7	0.8	0.9
4	N/2	1	0.230 (0.041)	0.289 (0.049)	0.372 (0.053)	0.449 (0.101)	0.593 (0.111)	0.697 (0.088)	0.784 (0.149)	1.010 (0.186)	1.126 (0.197)
		2	0.254 (0.047)	0.306 (0.044)	0.401 (0.060)	0.487 (0.105)	0.626 (0.116)	0.753 (0.096)	0.830 (0.163)	1.051 (0.214)	1.173 (0.208)
	N/4	1	0.227 (0.028)	0.286 (0.031)	0.359 (0.048)	0.437 (0.067)	0.527 (0.070)	0.655 (0.082)	0.779 (0.094)	0.878 (0.143)	1.029 (0.133)
		2	0.252 (0.027)	0.306 (0.032)	0.378 (0.051)	0.465 (0.069)	0.545 (0.069)	0.682 (0.092)	0.825 (0.103)	0.906 (0.170)	1.058 (0.164)
	N/6	1	0.238 (0.022)	0.286 (0.025)	0.349 (0.032)	0.438 (0.034)	0.521 (0.043)	0.633 (0.067)	0.754 (0.066)	0.822 (0.122)	1.002 (0.144)
		2	0.262 (0.021)	0.304 (0.023)	0.363 (0.032)	0.463 (0.034)	0.537 (0.050)	0.655 (0.075)	0.792 (0.079)	0.840 (0.151)	1.022 (0.180)
	N/8	1	0.245 (0.019)	0.288 (0.022)	0.343 (0.023)	0.431 (0.025)	0.513 (0.038)	0.619 (0.062)	0.728 (0.066)	0.819 (0.110)	0.986 (0.134)
		2	0.265 (0.018)	0.305 (0.021)	0.358 (0.023)	0.448 (0.032)	0.528 (0.046)	0.629 (0.075)	0.755 (0.087)	0.844 (0.139)	1.011 (0.168)
	N/10	1	0.248 (0.020)	0.290 (0.021)	0.345 (0.023)	0.425 (0.023)	0.504 (0.030)	0.600 (0.061)	0.710 (0.066)	0.810 (0.102)	0.968 (0.120)
		2	0.266 (0.021)	0.306 (0.019)	0.359 (0.026)	0.437 (0.031)	0.516 (0.034)	0.606 (0.078)	0.729 (0.090)	0.831 (0.130)	0.992 (0.153)
6	N/2	1	0.230 (0.042)	0.289 (0.050)	0.373 (0.055)	0.451 (0.104)	0.597 (0.114)	0.701 (0.090)	0.789 (0.153)	1.020 (0.192)	1.137 (0.203)
		2	0.253 (0.049)	0.306 (0.046)	0.403 (0.062)	0.489 (0.108)	0.631 (0.119)	0.760 (0.098)	0.837 (0.168)	1.063 (0.220)	1.185 (0.214)
	N/4	1	0.226 (0.029)	0.286 (0.033)	0.360 (0.049)	0.439 (0.070)	0.531 (0.073)	0.662 (0.085)	0.788 (0.098)	0.889 (0.149)	1.042 (0.139)
		2	0.252 (0.028)	0.306 (0.033)	0.380 (0.053)	0.468 (0.072)	0.551 (0.071)	0.691 (0.096)	0.838 (0.108)	0.920 (0.178)	1.075 (0.171)
	N/6	1	0.237 (0.024)	0.285 (0.026)	0.350 (0.033)	0.441 (0.036)	0.526 (0.045)	0.641 (0.071)	0.766 (0.069)	0.835 (0.130)	1.020 (0.152)
		2	0.261 (0.022)	0.305 (0.024)	0.365 (0.034)	0.469 (0.036)	0.544 (0.053)	0.666 (0.080)	0.808 (0.083)	0.856 (0.161)	1.044 (0.190)
	N/8	1	0.243 (0.020)	0.288 (0.023)	0.344 (0.025)	0.435 (0.026)	0.520 (0.040)	0.629 (0.066)	0.741 (0.070)	0.835 (0.117)	1.009 (0.144)
		2	0.264 (0.019)	0.305 (0.022)	0.360 (0.024)	0.454 (0.035)	0.537 (0.049)	0.642 (0.080)	0.774 (0.093)	0.866 (0.149)	1.039 (0.179)
	N/10	1	0.246 (0.021)	0.289 (0.023)	0.346 (0.024)	0.429 (0.024)	0.511 (0.032)	0.611 (0.065)	0.725 (0.070)	0.829 (0.111)	0.994 (0.129)
		2	0.266 (0.022)	0.307 (0.020)	0.362 (0.027)	0.444 (0.033)	0.526 (0.037)	0.620 (0.084)	0.750 (0.096)	0.857 (0.141)	1.024 (0.166)
8	N/2	1	0.229 (0.043)	0.289 (0.051)	0.373 (0.056)	0.452 (0.106)	0.600 (0.117)	0.705 (0.093)	0.793 (0.156)	1.027 (0.197)	1.144 (0.207)
		2	0.252 (0.050)	0.306 (0.047)	0.404 (0.063)	0.491 (0.110)	0.635 (0.122)	0.765 (0.101)	0.842 (0.172)	1.071 (0.226)	1.193 (0.219)
	N/4	1	0.224 (0.030)	0.285 (0.034)	0.361 (0.051)	0.441 (0.073)	0.534 (0.075)	0.667 (0.088)	0.795 (0.102)	0.897 (0.155)	1.051 (0.143)
		2	0.250 (0.029)	0.305 (0.034)	0.381 (0.055)	0.471 (0.075)	0.554 (0.074)	0.697 (0.100)	0.847 (0.112)	0.930 (0.184)	1.086 (0.177)
	N/6	1	0.235 (0.025)	0.285 (0.028)	0.350 (0.035)	0.443 (0.038)	0.530 (0.047)	0.647 (0.074)	0.774 (0.073)	0.843 (0.136)	1.032 (0.159)
		2	0.260 (0.023)	0.304 (0.026)	0.365 (0.035)	0.472 (0.038)	0.548 (0.055)	0.674 (0.083)	0.820 (0.087)	0.866 (0.169)	1.058 (0.199)
	N/8	1	0.242 (0.021)	0.287 (0.024)	0.344 (0.026)	0.437 (0.028)	0.524 (0.042)	0.635 (0.070)	0.751 (0.073)	0.845 (0.124)	1.023 (0.152)
		2	0.262 (0.020)	0.304 (0.023)	0.360 (0.025)	0.457 (0.036)	0.542 (0.052)	0.651 (0.084)	0.787 (0.097)	0.880 (0.158)	1.057 (0.190)
	N/10	1	0.244 (0.022)	0.288 (0.024)	0.346 (0.025)	0.431 (0.025)	0.516 (0.034)	0.618 (0.068)	0.736 (0.074)	0.841 (0.119)	1.011 (0.138)
		2	0.264 (0.024)	0.305 (0.021)	0.362 (0.028)	0.447 (0.034)	0.531 (0.039)	0.629 (0.088)	0.764 (0.101)	0.874 (0.150)	1.046 (0.177)
10	N/2	1	0.228 (0.044)	0.288 (0.053)	0.374 (0.057)	0.453 (0.108)	0.603 (0.120)	0.708 (0.095)	0.796 (0.160)	1.033 (0.201)	1.149 (0.211)
		2	0.252 (0.051)	0.305 (0.048)	0.405 (0.065)	0.492 (0.113)	0.638 (0.125)	0.769 (0.103)	0.846 (0.176)	1.078 (0.231)	1.200 (0.223)
	N/4	1	0.223 (0.031)	0.285 (0.035)	0.361 (0.053)	0.441 (0.076)	0.536 (0.078)	0.670 (0.091)	0.800 (0.105)	0.902 (0.160)	1.058 (0.148)
		2	0.249 (0.030)	0.305 (0.036)	0.381 (0.057)	0.472 (0.078)	0.556 (0.076)	0.702 (0.103)	0.854 (0.116)	0.937 (0.191)	1.093 (0.183)
	N/6	1	0.233 (0.026)	0.284 (0.029)	0.350 (0.036)	0.445 (0.040)	0.532 (0.049)	0.652 (0.077)	0.781 (0.075)	0.848 (0.142)	1.040 (0.165)
		2	0.258 (0.024)	0.303 (0.027)	0.365 (0.037)	0.474 (0.040)	0.551 (0.058)	0.680 (0.087)	0.829 (0.090)	0.873 (0.177)	1.068 (0.208)
	N/8	1	0.240 (0.022)	0.286 (0.025)	0.344 (0.027)	0.439 (0.029)	0.527 (0.044)	0.641 (0.073)	0.758 (0.076)	0.853 (0.131)	1.034 (0.159)
		2	0.261 (0.021)	0.303 (0.024)	0.360 (0.026)	0.460 (0.038)	0.546 (0.054)	0.657 (0.088)	0.797 (0.101)	0.891 (0.167)	1.070 (0.200)
	N/10	1	0.242 (0.023)	0.287 (0.025)	0.346 (0.026)	0.433 (0.026)	0.519 (0.035)	0.624 (0.071)	0.744 (0.078)	0.851 (0.126)	1.024 (0.146)
		2	0.261 (0.025)	0.304 (0.022)	0.361 (0.029)	0.449 (0.036)	0.536 (0.041)	0.636 (0.093)	0.776 (0.106)	0.887 (0.160)	1.062 (0.188)

Appendix 1.8: Raw data group means and standard deviations for each combination n_{min}, n_{max}, and M using AFA across all generated H signal ranges when N=5000 (depicted red**)**.

Window Size			H								
Min	Max	Order	0.1	0.2	0.3	0.4	0.5	0.6	0.7	0.8	0.9
4	N/2	1	0.209 (0.048)	0.269 (0.057)	0.349 (0.058)	0.479 (0.069)	0.591 (0.109)	0.709 (0.125)	0.824 (0.124)	1.069 (0.143)	1.174 (0.192)
		2	0.225 (0.046)	0.293 (0.058)	0.368 (0.057)	0.511 (0.076)	0.630 (0.114)	0.747 (0.139)	0.879 (0.141)	1.130 (0.163)	1.222 (0.229)
	N/4	1	0.212 (0.019)	0.279 (0.031)	0.353 (0.040)	0.435 (0.053)	0.542 (0.080)	0.672 (0.077)	0.781 (0.088)	0.892 (0.142)	1.100 (0.142)
		2	0.225 (0.020)	0.298 (0.030)	0.376 (0.045)	0.449 (0.058)	0.568 (0.088)	0.701 (0.096)	0.826 (0.107)	0.930 (0.160)	1.152 (0.179)
	N/6	1	0.219 (0.018)	0.279 (0.021)	0.351 (0.033)	0.423 (0.039)	0.541 (0.061)	0.624 (0.042)	0.764 (0.095)	0.829 (0.115)	1.045 (0.126)
		2	0.235 (0.019)	0.297 (0.019)	0.372 (0.033)	0.436 (0.032)	0.562 (0.065)	0.631 (0.054)	0.807 (0.125)	0.857 (0.140)	1.095 (0.161)
	N/8	1	0.224 (0.017)	0.282 (0.021)	0.349 (0.031)	0.422 (0.034)	0.533 (0.045)	0.600 (0.036)	0.733 (0.078)	0.817 (0.094)	0.995 (0.116)
		2	0.240 (0.016)	0.298 (0.019)	0.366 (0.031)	0.434 (0.033)	0.547 (0.044)	0.601 (0.043)	0.766 (0.097)	0.840 (0.122)	1.032 (0.159)
	N/10	1	0.226 (0.015)	0.286 (0.020)	0.349 (0.026)	0.421 (0.034)	0.520 (0.041)	0.593 (0.035)	0.711 (0.049)	0.806 (0.088)	0.964 (0.119)
		2	0.243 (0.014)	0.300 (0.018)	0.362 (0.023)	0.434 (0.039)	0.529 (0.035)	0.597 (0.045)	0.731 (0.065)	0.832 (0.120)	0.999 (0.162)
6	N/2	1	0.208 (0.049)	0.269 (0.058)	0.349 (0.059)	0.480 (0.070)	0.593 (0.111)	0.712 (0.127)	0.828 (0.126)	1.077 (0.145)	1.181 (0.195)
		2	0.225 (0.047)	0.293 (0.059)	0.369 (0.058)	0.513 (0.077)	0.633 (0.116)	0.751 (0.142)	0.884 (0.143)	1.139 (0.166)	1.230 (0.233)
	N/4	1	0.211 (0.020)	0.278 (0.032)	0.354 (0.041)	0.436 (0.055)	0.545 (0.082)	0.677 (0.079)	0.786 (0.090)	0.899 (0.146)	1.110 (0.147)
		2	0.224 (0.021)	0.298 (0.031)	0.377 (0.046)	0.451 (0.060)	0.572 (0.090)	0.707 (0.099)	0.834 (0.110)	0.939 (0.165)	1.165 (0.184)
	N/6	1	0.217 (0.018)	0.279 (0.022)	0.351 (0.034)	0.425 (0.041)	0.545 (0.063)	0.629 (0.044)	0.772 (0.099)	0.836 (0.119)	1.059 (0.131)
		2	0.234 (0.019)	0.297 (0.020)	0.373 (0.034)	0.439 (0.033)	0.568 (0.068)	0.637 (0.056)	0.817 (0.130)	0.867 (0.146)	1.111 (0.167)
	N/8	1	0.223 (0.018)	0.281 (0.022)	0.350 (0.033)	0.424 (0.035)	0.537 (0.047)	0.606 (0.038)	0.741 (0.082)	0.826 (0.098)	1.009 (0.122)
		2	0.238 (0.017)	0.298 (0.019)	0.368 (0.033)	0.436 (0.034)	0.553 (0.046)	0.607 (0.044)	0.778 (0.102)	0.853 (0.128)	1.051 (0.167)
	N/10	1	0.224 (0.016)	0.285 (0.021)	0.350 (0.027)	0.424 (0.035)	0.525 (0.043)	0.598 (0.037)	0.720 (0.052)	0.816 (0.093)	0.980 (0.126)
		2	0.241 (0.015)	0.300 (0.019)	0.364 (0.024)	0.438 (0.041)	0.536 (0.037)	0.605 (0.047)	0.743 (0.069)	0.846 (0.126)	1.020 (0.172)
8	N/2	1	0.208 (0.050)	0.269 (0.058)	0.349 (0.060)	0.482 (0.072)	0.595 (0.113)	0.714 (0.129)	0.831 (0.128)	1.082 (0.147)	1.187 (0.198)
		2	0.224 (0.048)	0.293 (0.060)	0.369 (0.059)	0.515 (0.078)	0.636 (0.118)	0.754 (0.144)	0.888 (0.146)	1.146 (0.169)	1.237 (0.237)
	N/4	1	0.210 (0.020)	0.278 (0.032)	0.354 (0.042)	0.437 (0.057)	0.547 (0.084)	0.680 (0.081)	0.790 (0.093)	0.905 (0.149)	1.118 (0.150)
		2	0.223 (0.021)	0.297 (0.031)	0.377 (0.047)	0.452 (0.061)	0.575 (0.093)	0.712 (0.102)	0.839 (0.113)	0.945 (0.169)	1.175 (0.189)
	N/6	1	0.216 (0.019)	0.278 (0.023)	0.351 (0.035)	0.426 (0.042)	0.547 (0.065)	0.632 (0.046)	0.777 (0.102)	0.841 (0.123)	1.068 (0.136)
		2	0.232 (0.020)	0.296 (0.020)	0.374 (0.035)	0.440 (0.034)	0.571 (0.070)	0.641 (0.058)	0.825 (0.135)	0.873 (0.150)	1.123 (0.173)
	N/8	1	0.221 (0.018)	0.280 (0.023)	0.350 (0.034)	0.425 (0.036)	0.540 (0.048)	0.609 (0.039)	0.747 (0.086)	0.832 (0.102)	1.019 (0.127)
		2	0.237 (0.017)	0.297 (0.020)	0.368 (0.034)	0.438 (0.036)	0.557 (0.048)	0.611 (0.046)	0.786 (0.106)	0.861 (0.133)	1.064 (0.174)
	N/10	1	0.222 (0.017)	0.285 (0.022)	0.350 (0.028)	0.425 (0.037)	0.528 (0.045)	0.602 (0.038)	0.726 (0.054)	0.823 (0.097)	0.991 (0.132)
		2	0.239 (0.015)	0.299 (0.019)	0.364 (0.025)	0.440 (0.043)	0.540 (0.038)	0.609 (0.049)	0.751 (0.072)	0.856 (0.131)	1.034 (0.181)
10	N/2	1	0.207 (0.051)	0.268 (0.059)	0.349 (0.060)	0.483 (0.073)	0.597 (0.115)	0.716 (0.131)	0.833 (0.130)	1.087 (0.149)	1.191 (0.201)
		2	0.223 (0.049)	0.293 (0.060)	0.369 (0.059)	0.516 (0.080)	0.638 (0.120)	0.757 (0.146)	0.891 (0.148)	1.151 (0.171)	1.242 (0.241)
	N/4	1	0.209 (0.021)	0.277 (0.033)	0.354 (0.043)	0.438 (0.058)	0.548 (0.085)	0.683 (0.083)	0.794 (0.095)	0.909 (0.152)	1.125 (0.154)
		2	0.222 (0.022)	0.297 (0.032)	0.378 (0.048)	0.453 (0.063)	0.577 (0.095)	0.716 (0.104)	0.844 (0.116)	0.950 (0.173)	1.182 (0.193)
	N/6	1	0.215 (0.019)	0.278 (0.023)	0.351 (0.036)	0.426 (0.043)	0.550 (0.067)	0.635 (0.047)	0.781 (0.105)	0.845 (0.127)	1.075 (0.140)
		2	0.231 (0.021)	0.296 (0.021)	0.374 (0.036)	0.441 (0.035)	0.574 (0.072)	0.644 (0.060)	0.831 (0.139)	0.878 (0.154)	1.133 (0.179)
	N/8	1	0.220 (0.019)	0.280 (0.023)	0.350 (0.035)	0.426 (0.037)	0.543 (0.050)	0.611 (0.040)	0.751 (0.089)	0.836 (0.106)	1.027 (0.132)
		2	0.235 (0.018)	0.296 (0.021)	0.369 (0.035)	0.439 (0.037)	0.560 (0.050)	0.614 (0.047)	0.792 (0.110)	0.866 (0.137)	1.074 (0.181)
	N/10	1	0.221 (0.017)	0.284 (0.022)	0.350 (0.029)	0.426 (0.038)	0.531 (0.046)	0.605 (0.039)	0.730 (0.057)	0.828 (0.100)	0.999 (0.138)
		2	0.237 (0.016)	0.298 (0.020)	0.364 (0.026)	0.441 (0.045)	0.543 (0.039)	0.612 (0.050)	0.758 (0.075)	0.863 (0.136)	1.044 (0.189)

Appendix 1.9: Differenced from generated H value group means and standard deviations for each combination of $n_{min,}$ and n_{max} using DFA across all generated H signal ranges when N=500 (depicted blue**)**.

Window Sizes		H								
Min	Max	0.1	0.2	0.3	0.4	0.5	0.6	0.7	0.8	0.9
4	N/2	-0.001 (0.112)	-0.001 (0.108)	-0.026 (0.105)	-0.071 (0.159)	-0.035 (0.130)	-0.032 (0.123)	-0.066 (0.145)	-0.059 (0.180)	-0.115 (0.140)
	N/4	0.047 (0.061)	0.013 (0.081)	0.008 (0.097)	-0.045 (0.094)	-0.033 (0.113)	-0.013 (0.086)	-0.004 (0.092)	-0.055 (0.141)	-0.061 (0.089)
	N/6	0.054 (0.059)	0.013 (0.086)	0.005 (0.090)	-0.021 (0.072)	-0.031 (0.073)	-0.009 (0.073)	0.000 (0.072)	-0.032 (0.116)	-0.052 (0.080)
	N/8	0.059 (0.050)	0.029 (0.069)	0.017 (0.076)	-0.011 (0.061)	-0.032 (0.063)	0.004 (0.068)	0.008 (0.055)	-0.028 (0.101)	-0.047 (0.075)
	N/10	0.062 (0.047)	0.037 (0.065)	0.024 (0.073)	-0.008 (0.050)	-0.028 (0.062)	0.007 (0.063)	0.007 (0.054)	-0.018 (0.098)	-0.041 (0.076)
6	N/2	-0.007 (0.120)	-0.004 (0.115)	-0.031 (0.112)	-0.075 (0.171)	-0.036 (0.138)	-0.035 (0.132)	-0.072 (0.155)	-0.063 (0.187)	-0.121 (0.145)
	N/4	0.041 (0.067)	0.007 (0.087)	0.004 (0.105)	-0.051 (0.104)	-0.035 (0.123)	-0.015 (0.093)	-0.007 (0.100)	-0.062 (0.150)	-0.066 (0.092)
	N/6	0.047 (0.065)	0.004 (0.097)	-0.002 (0.098)	-0.025 (0.082)	-0.033 (0.081)	-0.013 (0.080)	-0.002 (0.078)	-0.039 (0.124)	-0.059 (0.082)
	N/8	0.050 (0.057)	0.021 (0.081)	0.009 (0.083)	-0.014 (0.072)	-0.035 (0.070)	0.002 (0.075)	0.006 (0.060)	-0.037 (0.108)	-0.057 (0.077)
	N/10	0.051 (0.053)	0.027 (0.080)	0.017 (0.079)	-0.012 (0.058)	-0.031 (0.070)	0.006 (0.070)	0.004 (0.059)	-0.028 (0.106)	-0.051 (0.078)
8	N/2	-0.012 (0.128)	-0.007 (0.122)	-0.034 (0.118)	-0.079 (0.180)	-0.037 (0.144)	-0.037 (0.139)	-0.077 (0.163)	-0.065 (0.194)	-0.127 (0.151)
	N/4	0.038 (0.073)	0.004 (0.093)	0.002 (0.113)	-0.055 (0.111)	-0.036 (0.132)	-0.016 (0.100)	-0.008 (0.108)	-0.067 (0.158)	-0.070 (0.095)
	N/6	0.043 (0.071)	-0.001 (0.106)	-0.007 (0.105)	-0.028 (0.089)	-0.035 (0.089)	-0.014 (0.088)	-0.003 (0.086)	-0.043 (0.132)	-0.064 (0.085)
	N/8	0.045 (0.064)	0.016 (0.091)	0.005 (0.090)	-0.016 (0.080)	-0.038 (0.079)	0.004 (0.082)	0.007 (0.066)	-0.042 (0.117)	-0.063 (0.081)
	N/10	0.043 (0.058)	0.023 (0.093)	0.013 (0.086)	-0.014 (0.063)	-0.034 (0.078)	0.008 (0.078)	0.005 (0.065)	-0.032 (0.117)	-0.059 (0.083)
10	N/2	-0.016 (0.136)	-0.009 (0.128)	-0.037 (0.124)	-0.081 (0.189)	-0.037 (0.150)	-0.039 (0.147)	-0.082 (0.170)	-0.067 (0.200)	-0.131 (0.155)
	N/4	0.035 (0.078)	0.001 (0.097)	0.000 (0.120)	-0.057 (0.119)	-0.037 (0.140)	-0.018 (0.106)	-0.009 (0.113)	-0.070 (0.165)	-0.072 (0.098)
	N/6	0.039 (0.075)	-0.007 (0.113)	-0.011 (0.113)	-0.027 (0.098)	-0.035 (0.096)	-0.017 (0.096)	-0.004 (0.090)	-0.045 (0.139)	-0.065 (0.086)
	N/8	0.039 (0.068)	0.011 (0.099)	0.000 (0.098)	-0.013 (0.091)	-0.040 (0.087)	0.002 (0.085)	0.007 (0.068)	-0.045 (0.123)	-0.066 (0.082)
	N/10	0.036 (0.061)	0.017 (0.102)	0.009 (0.093)	-0.009 (0.071)	-0.036 (0.086)	0.007 (0.083)	0.005 (0.067)	-0.034 (0.125)	-0.061 (0.084)

Appendix 1.10: Differenced from generated H value group means and standard deviations for each combination of $n_{min,}$ and n_{max} using DFA across all generated H signal ranges when N=1000 (depicted green**)**.

Window Sizes		H								
Min	Max	0.1	0.2	0.3	0.4	0.5	0.6	0.7	0.8	0.9
4	N/2	0.003 (0.101)	0.008 (0.090)	-0.018 (0.102)	-0.038 (0.122)	-0.044 (0.142)	-0.099 (0.134)	-0.113 (0.121)	-0.055 (0.134)	-0.051 (0.118)
	N/4	0.053 (0.074)	0.024 (0.086)	-0.019 (0.086)	-0.002 (0.060)	-0.032 (0.092)	-0.039 (0.101)	-0.047 (0.071)	-0.040 (0.102)	-0.045 (0.089)
	N/6	0.069 (0.058)	0.036 (0.056)	-0.005 (0.069)	0.000 (0.062)	-0.032 (0.077)	-0.007 (0.084)	-0.029 (0.061)	-0.028 (0.090)	-0.032 (0.071)
	N/8	0.079 (0.038)	0.049 (0.052)	0.003 (0.065)	-0.010 (0.042)	-0.013 (0.066)	-0.008 (0.079)	-0.026 (0.057)	-0.021 (0.083)	-0.022 (0.060)
	N/10	0.086 (0.035)	0.053 (0.048)	0.007 (0.059)	-0.012 (0.041)	-0.008 (0.061)	-0.013 (0.068)	-0.029 (0.051)	-0.022 (0.080)	-0.011 (0.053)
6	N/2	-0.001 (0.106)	0.005 (0.095)	-0.020 (0.106)	-0.040 (0.128)	-0.046 (0.148)	-0.103 (0.140)	-0.118 (0.127)	-0.057 (0.139)	-0.054 (0.122)
	N/4	0.049 (0.080)	0.021 (0.091)	-0.022 (0.091)	-0.002 (0.064)	-0.035 (0.097)	-0.041 (0.106)	-0.049 (0.074)	-0.043 (0.106)	-0.050 (0.093)
	N/6	0.065 (0.065)	0.033 (0.060)	-0.008 (0.074)	0.000 (0.067)	-0.036 (0.082)	-0.007 (0.089)	-0.031 (0.064)	-0.031 (0.094)	-0.038 (0.074)
	N/8	0.074 (0.043)	0.046 (0.056)	-0.001 (0.070)	-0.012 (0.046)	-0.015 (0.072)	-0.008 (0.084)	-0.027 (0.060)	-0.023 (0.087)	-0.028 (0.062)
	N/10	0.081 (0.040)	0.051 (0.053)	0.003 (0.065)	-0.015 (0.045)	-0.009 (0.067)	-0.015 (0.073)	-0.032 (0.053)	-0.025 (0.084)	-0.017 (0.054)
8	N/2	-0.005 (0.110)	0.004 (0.099)	-0.021 (0.110)	-0.042 (0.133)	-0.047 (0.154)	-0.106 (0.146)	-0.122 (0.131)	-0.058 (0.143)	-0.056 (0.125)
	N/4	0.045 (0.085)	0.019 (0.096)	-0.025 (0.096)	-0.002 (0.068)	-0.036 (0.102)	-0.043 (0.110)	-0.051 (0.076)	-0.044 (0.109)	-0.053 (0.096)
	N/6	0.062 (0.070)	0.032 (0.065)	-0.011 (0.078)	0.000 (0.073)	-0.038 (0.087)	-0.006 (0.094)	-0.031 (0.066)	-0.032 (0.097)	-0.041 (0.077)
	N/8	0.071 (0.047)	0.046 (0.060)	-0.004 (0.075)	-0.013 (0.050)	-0.016 (0.077)	-0.007 (0.090)	-0.028 (0.063)	-0.023 (0.091)	-0.032 (0.064)
	N/10	0.078 (0.045)	0.051 (0.057)	-0.001 (0.070)	-0.017 (0.048)	-0.010 (0.071)	-0.014 (0.077)	-0.033 (0.055)	-0.026 (0.088)	-0.019 (0.056)
10	N/2	-0.008 (0.114)	0.002 (0.102)	-0.022 (0.114)	-0.043 (0.137)	-0.049 (0.158)	-0.110 (0.150)	-0.125 (0.135)	-0.060 (0.147)	-0.057 (0.128)
	N/4	0.043 (0.091)	0.017 (0.100)	-0.027 (0.100)	-0.001 (0.072)	-0.038 (0.106)	-0.045 (0.114)	-0.053 (0.078)	-0.046 (0.113)	-0.055 (0.099)
	N/6	0.059 (0.076)	0.029 (0.069)	-0.013 (0.081)	0.000 (0.079)	-0.041 (0.092)	-0.006 (0.097)	-0.032 (0.068)	-0.033 (0.101)	-0.044 (0.080)
	N/8	0.069 (0.052)	0.045 (0.065)	-0.006 (0.079)	-0.013 (0.054)	-0.018 (0.082)	-0.006 (0.094)	-0.028 (0.065)	-0.024 (0.094)	-0.034 (0.066)
	N/10	0.076 (0.049)	0.050 (0.061)	-0.003 (0.074)	-0.018 (0.052)	-0.011 (0.076)	-0.015 (0.080)	-0.034 (0.057)	-0.027 (0.093)	-0.021 (0.057)

Appendix 1.11: Differenced from generated H value group means and standard deviations for each combination of $n_{min,}$ and n_{max} using DFA across all generated H signal ranges when N=2500 (depicted yellow**)**.

Window Sizes		H								
Min	Max	0.1	0.2	0.3	0.4	0.5	0.6	0.7	0.8	0.9
4	N/2	-0.009 (0.078)	-0.023 (0.092)	-0.021 (0.086)	-0.073 (0.112)	-0.033 (0.156)	-0.086 (0.111)	-0.101 (0.117)	-0.064 (0.134)	-0.111 (0.136)
	N/4	0.017 (0.078)	0.021 (0.069)	-0.022 (0.057)	-0.041 (0.086)	-0.003 (0.090)	-0.051 (0.078)	-0.047 (0.077)	-0.035 (0.070)	-0.070 (0.096)
	N/6	0.018 (0.061)	0.030 (0.053)	-0.001 (0.046)	-0.033 (0.061)	-0.015 (0.065)	-0.036 (0.065)	-0.025 (0.073)	-0.018 (0.073)	-0.047 (0.075)
	N/8	0.026 (0.050)	0.025 (0.043)	0.003 (0.042)	-0.025 (0.053)	-0.005 (0.060)	-0.028 (0.059)	-0.023 (0.068)	-0.018 (0.058)	-0.034 (0.061)
	N/10	0.033 (0.044)	0.026 (0.036)	0.010 (0.039)	-0.021 (0.054)	0.001 (0.053)	-0.022 (0.050)	-0.025 (0.059)	-0.016 (0.052)	-0.030 (0.056)
6	N/2	-0.012 (0.080)	-0.025 (0.095)	-0.022 (0.088)	-0.075 (0.115)	-0.034 (0.159)	-0.088 (0.113)	-0.104 (0.120)	-0.066 (0.138)	-0.114 (0.139)
	N/4	0.014 (0.081)	0.020 (0.072)	-0.025 (0.059)	-0.043 (0.090)	-0.003 (0.093)	-0.053 (0.081)	-0.049 (0.079)	-0.037 (0.071)	-0.073 (0.099)
	N/6	0.014 (0.065)	0.029 (0.056)	-0.003 (0.048)	-0.036 (0.065)	-0.016 (0.067)	-0.037 (0.068)	-0.026 (0.076)	-0.019 (0.075)	-0.050 (0.078)
	N/8	0.021 (0.053)	0.022 (0.046)	0.001 (0.044)	-0.027 (0.056)	-0.005 (0.063)	-0.030 (0.061)	-0.024 (0.071)	-0.020 (0.060)	-0.037 (0.062)
	N/10	0.028 (0.047)	0.023 (0.039)	0.008 (0.042)	-0.023 (0.057)	0.001 (0.056)	-0.023 (0.052)	-0.027 (0.062)	-0.019 (0.053)	-0.034 (0.058)
8	N/2	-0.013 (0.081)	-0.026 (0.097)	-0.023 (0.090)	-0.077 (0.118)	-0.034 (0.163)	-0.090 (0.116)	-0.106 (0.122)	-0.068 (0.141)	-0.116 (0.142)
	N/4	0.012 (0.084)	0.019 (0.074)	-0.026 (0.061)	-0.045 (0.093)	-0.003 (0.096)	-0.055 (0.083)	-0.050 (0.081)	-0.038 (0.073)	-0.076 (0.101)
	N/6	0.011 (0.068)	0.028 (0.059)	-0.004 (0.050)	-0.037 (0.067)	-0.016 (0.070)	-0.039 (0.070)	-0.027 (0.078)	-0.020 (0.078)	-0.052 (0.080)
	N/8	0.018 (0.056)	0.021 (0.048)	0.000 (0.046)	-0.029 (0.058)	-0.005 (0.066)	-0.031 (0.063)	-0.025 (0.073)	-0.021 (0.062)	-0.039 (0.064)
	N/10	0.024 (0.051)	0.021 (0.042)	0.008 (0.044)	-0.025 (0.060)	0.002 (0.059)	-0.024 (0.054)	-0.028 (0.065)	-0.020 (0.055)	-0.036 (0.059)
10	N/2	-0.015 (0.083)	-0.028 (0.099)	-0.024 (0.091)	-0.078 (0.120)	-0.035 (0.166)	-0.091 (0.118)	-0.108 (0.125)	-0.069 (0.143)	-0.118 (0.144)
	N/4	0.011 (0.087)	0.018 (0.077)	-0.027 (0.063)	-0.046 (0.095)	-0.003 (0.098)	-0.056 (0.085)	-0.051 (0.083)	-0.039 (0.074)	-0.078 (0.103)
	N/6	0.008 (0.071)	0.028 (0.061)	-0.005 (0.052)	-0.039 (0.070)	-0.017 (0.072)	-0.040 (0.072)	-0.027 (0.080)	-0.020 (0.080)	-0.054 (0.082)
	N/8	0.015 (0.059)	0.020 (0.051)	-0.001 (0.048)	-0.030 (0.060)	-0.005 (0.068)	-0.032 (0.065)	-0.026 (0.076)	-0.022 (0.064)	-0.041 (0.065)
	N/10	0.021 (0.053)	0.020 (0.044)	0.007 (0.046)	-0.027 (0.063)	0.002 (0.061)	-0.025 (0.055)	-0.029 (0.067)	-0.021 (0.056)	-0.037 (0.061)

Appendix 1.12: Differenced from generated H value group means and standard deviations for each combination of $n_{min,}$ and n_{max} using DFA across all generated H signal ranges when N=5000 (depicted red**)**.

Window Sizes		H								
Min	Max	0.1	0.2	0.3	0.4	0.5	0.6	0.7	0.8	0.9
4	N/2	-0.011 (0.118)	-0.031 (0.154)	-0.022 (0.114)	-0.044 (0.125)	-0.067 (0.104)	-0.066 (0.092)	-0.067 (0.096)	-0.036 (0.127)	-0.059 (0.082)
	N/4	0.023 (0.066)	-0.014 (0.082)	-0.021 (0.069)	-0.023 (0.076)	-0.033 (0.086)	-0.039 (0.062)	-0.052 (0.065)	-0.034 (0.082)	-0.038 (0.064)
	N/6	0.034 (0.047)	-0.001 (0.059)	-0.003 (0.060)	-0.012 (0.060)	-0.012 (0.048)	-0.015 (0.050)	-0.045 (0.065)	-0.023 (0.067)	-0.033 (0.053)
	N/8	0.040 (0.041)	0.011 (0.057)	-0.003 (0.053)	-0.003 (0.048)	-0.013 (0.045)	-0.017 (0.049)	-0.037 (0.056)	-0.024 (0.059)	-0.025 (0.041)
	N/10	0.043 (0.033)	0.022 (0.050)	0.003 (0.054)	-0.006 (0.046)	-0.013 (0.040)	-0.016 (0.042)	-0.035 (0.044)	-0.021 (0.054)	-0.022 (0.038)
6	N/2	-0.012 (0.120)	-0.032 (0.157)	-0.023 (0.116)	-0.045 (0.127)	-0.068 (0.106)	-0.067 (0.094)	-0.068 (0.097)	-0.037 (0.129)	-0.061 (0.083)
	N/4	0.021 (0.068)	-0.016 (0.084)	-0.022 (0.070)	-0.023 (0.079)	-0.034 (0.088)	-0.040 (0.063)	-0.053 (0.067)	-0.034 (0.083)	-0.039 (0.065)
	N/6	0.033 (0.049)	-0.003 (0.061)	-0.004 (0.062)	-0.013 (0.062)	-0.012 (0.050)	-0.015 (0.052)	-0.047 (0.067)	-0.024 (0.068)	-0.035 (0.054)
	N/8	0.038 (0.043)	0.009 (0.059)	-0.004 (0.054)	-0.004 (0.049)	-0.014 (0.046)	-0.018 (0.051)	-0.038 (0.058)	-0.025 (0.061)	-0.027 (0.042)
	N/10	0.041 (0.035)	0.020 (0.052)	0.002 (0.056)	-0.006 (0.048)	-0.013 (0.041)	-0.016 (0.043)	-0.037 (0.046)	-0.022 (0.056)	-0.024 (0.039)
8	N/2	-0.014 (0.122)	-0.033 (0.159)	-0.024 (0.117)	-0.045 (0.129)	-0.069 (0.108)	-0.068 (0.095)	-0.068 (0.099)	-0.037 (0.130)	-0.061 (0.084)
	N/4	0.020 (0.070)	-0.018 (0.086)	-0.023 (0.072)	-0.024 (0.081)	-0.035 (0.091)	-0.041 (0.064)	-0.054 (0.068)	-0.035 (0.084)	-0.040 (0.066)
	N/6	0.032 (0.050)	-0.004 (0.062)	-0.004 (0.063)	-0.014 (0.064)	-0.012 (0.051)	-0.016 (0.053)	-0.048 (0.068)	-0.025 (0.069)	-0.036 (0.055)
	N/8	0.037 (0.044)	0.008 (0.061)	-0.005 (0.056)	-0.004 (0.051)	-0.014 (0.048)	-0.018 (0.052)	-0.039 (0.060)	-0.026 (0.062)	-0.028 (0.043)
	N/10	0.040 (0.036)	0.019 (0.054)	0.001 (0.058)	-0.007 (0.050)	-0.014 (0.042)	-0.016 (0.044)	-0.038 (0.047)	-0.022 (0.057)	-0.025 (0.039)
10	N/2	-0.015 (0.124)	-0.034 (0.161)	-0.024 (0.119)	-0.046 (0.131)	-0.070 (0.109)	-0.068 (0.096)	-0.069 (0.100)	-0.037 (0.132)	-0.062 (0.085)
	N/4	0.019 (0.071)	-0.019 (0.087)	-0.024 (0.073)	-0.025 (0.082)	-0.035 (0.093)	-0.042 (0.065)	-0.055 (0.069)	-0.035 (0.085)	-0.040 (0.067)
	N/6	0.031 (0.052)	-0.006 (0.064)	-0.005 (0.064)	-0.014 (0.066)	-0.013 (0.052)	-0.016 (0.054)	-0.049 (0.070)	-0.025 (0.070)	-0.036 (0.056)
	N/8	0.036 (0.046)	0.007 (0.063)	-0.006 (0.057)	-0.004 (0.053)	-0.015 (0.049)	-0.018 (0.054)	-0.040 (0.061)	-0.026 (0.063)	-0.029 (0.043)
	N/10	0.039 (0.038)	0.018 (0.056)	0.000 (0.059)	-0.007 (0.052)	-0.014 (0.043)	-0.017 (0.045)	-0.039 (0.049)	-0.023 (0.058)	-0.026 (0.040)

Appendix 1.13: Differenced from generated H value group means and standard deviations for each combination of n_{min}, n_{max}, and M using AFA across all generated H signal ranges when N=500 (depicted blue**)**.

Window Size			H								
Min	Max	Order	0.1	0.2	0.3	0.4	0.5	0.6	0.7	0.8	0.9
4	N/2	1	0.109 (0.048)	0.069 (0.057)	0.049 (0.058)	0.079 (0.069)	0.091 (0.109)	0.109 (0.125)	0.124 (0.124)	0.269 (0.143)	0.274 (0.192)
		2	0.125 (0.046)	0.093 (0.058)	0.068 (0.057)	0.111 (0.076)	0.130 (0.114)	0.147 (0.139)	0.179 (0.141)	0.330 (0.163)	0.322 (0.229)
	N/4	1	0.112 (0.019)	0.079 (0.031)	0.053 (0.040)	0.035 (0.053)	0.042 (0.080)	0.072 (0.077)	0.081 (0.088)	0.092 (0.142)	0.200 (0.142)
		2	0.125 (0.020)	0.098 (0.030)	0.076 (0.045)	0.049 (0.058)	0.068 (0.088)	0.101 (0.096)	0.126 (0.107)	0.130 (0.160)	0.252 (0.179)
	N/6	1	0.119 (0.018)	0.079 (0.021)	0.051 (0.033)	0.023 (0.039)	0.041 (0.061)	0.024 (0.042)	0.064 (0.095)	0.029 (0.115)	0.145 (0.126)
		2	0.135 (0.019)	0.097 (0.019)	0.072 (0.033)	0.036 (0.032)	0.062 (0.065)	0.031 (0.054)	0.107 (0.125)	0.057 (0.140)	0.195 (0.161)
	N/8	1	0.124 (0.017)	0.082 (0.021)	0.049 (0.031)	0.022 (0.034)	0.033 (0.045)	0.000 (0.036)	0.033 (0.078)	0.017 (0.094)	0.095 (0.116)
		2	0.140 (0.016)	0.098 (0.019)	0.066 (0.031)	0.034 (0.033)	0.047 (0.044)	0.001 (0.043)	0.066 (0.097)	0.040 (0.122)	0.132 (0.159)
	N/10	1	0.126 (0.015)	0.086 (0.020)	0.049 (0.026)	0.021 (0.034)	0.020 (0.041)	-0.007 (0.035)	0.011 (0.049)	0.006 (0.088)	0.064 (0.119)
		2	0.143 (0.014)	0.100 (0.018)	0.062 (0.023)	0.034 (0.039)	0.029 (0.035)	-0.003 (0.045)	0.031 (0.065)	0.032 (0.120)	0.099 (0.162)
6	N/2	1	0.108 (0.049)	0.069 (0.058)	0.049 (0.059)	0.080 (0.070)	0.093 (0.111)	0.112 (0.127)	0.128 (0.126)	0.277 (0.145)	0.281 (0.195)
		2	0.125 (0.047)	0.093 (0.059)	0.069 (0.058)	0.113 (0.077)	0.133 (0.116)	0.151 (0.142)	0.184 (0.143)	0.339 (0.166)	0.330 (0.233)
	N/4	1	0.111 (0.020)	0.078 (0.032)	0.054 (0.041)	0.036 (0.055)	0.045 (0.082)	0.077 (0.079)	0.086 (0.090)	0.099 (0.146)	0.210 (0.147)
		2	0.124 (0.021)	0.098 (0.031)	0.077 (0.046)	0.051 (0.060)	0.072 (0.090)	0.107 (0.099)	0.134 (0.110)	0.139 (0.165)	0.265 (0.184)
	N/6	1	0.117 (0.018)	0.079 (0.022)	0.051 (0.034)	0.025 (0.041)	0.045 (0.063)	0.029 (0.044)	0.072 (0.099)	0.036 (0.119)	0.159 (0.131)
		2	0.134 (0.019)	0.097 (0.020)	0.073 (0.034)	0.039 (0.033)	0.068 (0.068)	0.037 (0.056)	0.117 (0.130)	0.067 (0.146)	0.211 (0.167)
	N/8	1	0.123 (0.018)	0.081 (0.022)	0.050 (0.033)	0.024 (0.035)	0.037 (0.047)	0.006 (0.038)	0.041 (0.082)	0.026 (0.098)	0.109 (0.122)
		2	0.138 (0.017)	0.098 (0.019)	0.068 (0.033)	0.036 (0.034)	0.053 (0.046)	0.007 (0.044)	0.078 (0.102)	0.053 (0.128)	0.151 (0.167)
	N/10	1	0.124 (0.016)	0.085 (0.021)	0.050 (0.027)	0.024 (0.035)	0.025 (0.043)	-0.002 (0.037)	0.020 (0.052)	0.016 (0.093)	0.080 (0.126)
		2	0.141 (0.015)	0.100 (0.019)	0.064 (0.024)	0.038 (0.041)	0.036 (0.037)	0.005 (0.047)	0.043 (0.069)	0.046 (0.126)	0.120 (0.172)
8	N/2	1	0.108 (0.050)	0.069 (0.058)	0.049 (0.060)	0.082 (0.072)	0.095 (0.113)	0.114 (0.129)	0.131 (0.128)	0.282 (0.147)	0.287 (0.198)
		2	0.124 (0.048)	0.093 (0.060)	0.069 (0.059)	0.115 (0.078)	0.136 (0.118)	0.154 (0.144)	0.188 (0.146)	0.346 (0.169)	0.337 (0.237)
	N/4	1	0.110 (0.020)	0.078 (0.032)	0.054 (0.042)	0.037 (0.057)	0.047 (0.084)	0.080 (0.081)	0.090 (0.093)	0.105 (0.149)	0.218 (0.150)
		2	0.123 (0.021)	0.097 (0.031)	0.077 (0.047)	0.052 (0.061)	0.075 (0.093)	0.112 (0.102)	0.139 (0.113)	0.145 (0.169)	0.275 (0.189)
	N/6	1	0.116 (0.019)	0.078 (0.023)	0.051 (0.035)	0.026 (0.042)	0.047 (0.065)	0.032 (0.046)	0.077 (0.102)	0.041 (0.123)	0.168 (0.136)
		2	0.132 (0.020)	0.096 (0.020)	0.074 (0.035)	0.040 (0.034)	0.071 (0.070)	0.041 (0.058)	0.125 (0.135)	0.073 (0.150)	0.223 (0.173)
	N/8	1	0.121 (0.018)	0.080 (0.023)	0.050 (0.034)	0.025 (0.036)	0.040 (0.048)	0.009 (0.039)	0.047 (0.086)	0.032 (0.102)	0.119 (0.127)
		2	0.137 (0.017)	0.097 (0.020)	0.068 (0.034)	0.038 (0.036)	0.057 (0.048)	0.011 (0.046)	0.086 (0.106)	0.061 (0.133)	0.164 (0.174)
	N/10	1	0.122 (0.017)	0.085 (0.022)	0.050 (0.028)	0.025 (0.037)	0.028 (0.045)	0.002 (0.038)	0.026 (0.054)	0.023 (0.097)	0.091 (0.132)
		2	0.139 (0.015)	0.099 (0.019)	0.064 (0.025)	0.040 (0.043)	0.040 (0.038)	0.009 (0.049)	0.051 (0.072)	0.056 (0.131)	0.134 (0.181)
10	N/2	1	0.107 (0.051)	0.068 (0.059)	0.049 (0.060)	0.083 (0.073)	0.097 (0.115)	0.116 (0.131)	0.133 (0.130)	0.287 (0.149)	0.291 (0.201)
		2	0.123 (0.049)	0.093 (0.060)	0.069 (0.059)	0.116 (0.080)	0.138 (0.120)	0.157 (0.146)	0.191 (0.148)	0.351 (0.171)	0.342 (0.241)
	N/4	1	0.109 (0.021)	0.077 (0.033)	0.054 (0.043)	0.038 (0.058)	0.048 (0.085)	0.083 (0.083)	0.094 (0.095)	0.109 (0.152)	0.225 (0.154)
		2	0.122 (0.022)	0.097 (0.032)	0.078 (0.048)	0.053 (0.063)	0.077 (0.095)	0.116 (0.104)	0.144 (0.116)	0.150 (0.173)	0.282 (0.193)
	N/6	1	0.115 (0.019)	0.078 (0.023)	0.051 (0.036)	0.026 (0.043)	0.050 (0.067)	0.035 (0.047)	0.081 (0.105)	0.045 (0.127)	0.175 (0.140)
		2	0.131 (0.021)	0.096 (0.021)	0.074 (0.036)	0.041 (0.035)	0.074 (0.072)	0.044 (0.060)	0.131 (0.139)	0.078 (0.154)	0.233 (0.179)
	N/8	1	0.120 (0.019)	0.080 (0.023)	0.050 (0.035)	0.026 (0.037)	0.043 (0.050)	0.011 (0.040)	0.051 (0.089)	0.036 (0.106)	0.127 (0.132)
		2	0.135 (0.018)	0.096 (0.021)	0.069 (0.035)	0.039 (0.037)	0.060 (0.050)	0.014 (0.047)	0.092 (0.110)	0.066 (0.137)	0.174 (0.181)
	N/10	1	0.121 (0.017)	0.084 (0.022)	0.050 (0.029)	0.026 (0.038)	0.031 (0.046)	0.005 (0.039)	0.030 (0.057)	0.028 (0.100)	0.099 (0.138)
		2	0.137 (0.016)	0.098 (0.020)	0.064 (0.026)	0.041 (0.045)	0.043 (0.039)	0.012 (0.050)	0.058 (0.075)	0.063 (0.136)	0.144 (0.189)

Appendix 1.14: Differenced from generated H value group means and standard deviations for each combination of n_{min}, n_{max}, and M using AFA across all generated H signal ranges when N=1000 (depicted green**)**.

Window Size			H								
Min	Max	Order	0.1	0.2	0.3	0.4	0.5	0.6	0.7	0.8	0.9
4	N/2	1	0.152 (0.036)	0.138 (0.079)	0.064 (0.056)	0.111 (0.125)	0.100 (0.126)	0.099 (0.153)	0.060 (0.118)	0.216 (0.241)	0.215 (0.268)
		2	0.180 (0.036)	0.169 (0.080)	0.080 (0.059)	0.152 (0.130)	0.141 (0.137)	0.137 (0.163)	0.105 (0.131)	0.261 (0.273)	0.252 (0.290)
	N/4	1	0.164 (0.026)	0.117 (0.034)	0.071 (0.053)	0.039 (0.047)	0.051 (0.104)	0.033 (0.084)	0.033 (0.122)	0.031 (0.161)	0.106 (0.187)
		2	0.190 (0.028)	0.135 (0.034)	0.100 (0.058)	0.067 (0.051)	0.071 (0.124)	0.050 (0.096)	0.061 (0.159)	0.056 (0.193)	0.131 (0.219)
	N/6	1	0.174 (0.021)	0.114 (0.033)	0.064 (0.044)	0.029 (0.049)	0.012 (0.073)	0.016 (0.088)	0.017 (0.125)	-0.036 (0.142)	0.054 (0.188)
		2	0.198 (0.024)	0.133 (0.035)	0.085 (0.040)	0.046 (0.039)	0.027 (0.078)	0.042 (0.101)	0.048 (0.157)	-0.025 (0.171)	0.068 (0.244)
	N/8	1	0.178 (0.022)	0.109 (0.026)	0.063 (0.038)	0.025 (0.043)	-0.009 (0.063)	0.002 (0.088)	-0.014 (0.101)	-0.061 (0.113)	0.017 (0.178)
		2	0.198 (0.022)	0.125 (0.024)	0.083 (0.037)	0.037 (0.041)	-0.002 (0.069)	0.027 (0.105)	0.002 (0.127)	-0.052 (0.141)	0.024 (0.234)
	N/10	1	0.179 (0.024)	0.106 (0.023)	0.064 (0.031)	0.020 (0.039)	-0.021 (0.058)	-0.015 (0.081)	-0.042 (0.103)	-0.088 (0.086)	-0.020 (0.166)
		2	0.197 (0.023)	0.120 (0.021)	0.082 (0.035)	0.030 (0.043)	-0.015 (0.068)	-0.001 (0.096)	-0.034 (0.132)	-0.089 (0.110)	-0.012 (0.214)
6	N/2	1	0.151 (0.038)	0.140 (0.083)	0.065 (0.058)	0.117 (0.131)	0.107 (0.131)	0.108 (0.161)	0.069 (0.125)	0.235 (0.255)	0.234 (0.282)
		2	0.180 (0.038)	0.172 (0.084)	0.082 (0.062)	0.160 (0.137)	0.151 (0.144)	0.149 (0.171)	0.117 (0.139)	0.284 (0.288)	0.275 (0.306)
	N/4	1	0.164 (0.029)	0.119 (0.036)	0.073 (0.056)	0.044 (0.050)	0.060 (0.112)	0.045 (0.090)	0.048 (0.130)	0.050 (0.173)	0.132 (0.201)
		2	0.191 (0.030)	0.138 (0.036)	0.105 (0.062)	0.076 (0.055)	0.084 (0.134)	0.064 (0.103)	0.081 (0.170)	0.082 (0.207)	0.163 (0.234)
	N/6	1	0.175 (0.022)	0.117 (0.035)	0.068 (0.048)	0.035 (0.053)	0.023 (0.079)	0.031 (0.095)	0.037 (0.137)	-0.015 (0.156)	0.088 (0.206)
		2	0.200 (0.026)	0.137 (0.038)	0.091 (0.044)	0.056 (0.043)	0.041 (0.085)	0.063 (0.110)	0.076 (0.174)	0.003 (0.188)	0.108 (0.267)
	N/8	1	0.179 (0.025)	0.111 (0.028)	0.068 (0.042)	0.033 (0.048)	0.001 (0.070)	0.020 (0.097)	0.008 (0.112)	-0.037 (0.126)	0.056 (0.199)
		2	0.201 (0.024)	0.130 (0.026)	0.090 (0.041)	0.049 (0.046)	0.012 (0.076)	0.054 (0.116)	0.033 (0.142)	-0.018 (0.159)	0.072 (0.262)
	N/10	1	0.180 (0.026)	0.108 (0.024)	0.069 (0.035)	0.030 (0.045)	-0.009 (0.065)	0.005 (0.091)	-0.017 (0.116)	-0.060 (0.098)	0.025 (0.188)
		2	0.201 (0.026)	0.125 (0.024)	0.092 (0.040)	0.044 (0.049)	0.002 (0.077)	0.029 (0.108)	0.000 (0.148)	-0.052 (0.126)	0.043 (0.244)
8	N/2	1	0.150 (0.039)	0.141 (0.087)	0.065 (0.061)	0.122 (0.137)	0.113 (0.136)	0.114 (0.168)	0.075 (0.131)	0.250 (0.266)	0.247 (0.295)
		2	0.179 (0.039)	0.174 (0.088)	0.082 (0.065)	0.167 (0.143)	0.158 (0.150)	0.157 (0.179)	0.125 (0.146)	0.301 (0.301)	0.291 (0.320)
	N/4	1	0.163 (0.031)	0.119 (0.038)	0.075 (0.060)	0.047 (0.053)	0.067 (0.120)	0.052 (0.096)	0.057 (0.138)	0.063 (0.184)	0.150 (0.213)
		2	0.190 (0.032)	0.139 (0.037)	0.107 (0.065)	0.080 (0.058)	0.092 (0.143)	0.073 (0.110)	0.093 (0.181)	0.098 (0.221)	0.184 (0.247)
	N/6	1	0.175 (0.024)	0.117 (0.038)	0.069 (0.051)	0.039 (0.057)	0.029 (0.086)	0.041 (0.101)	0.050 (0.149)	-0.002 (0.168)	0.110 (0.221)
		2	0.200 (0.028)	0.138 (0.041)	0.093 (0.047)	0.061 (0.047)	0.049 (0.093)	0.077 (0.117)	0.094 (0.189)	0.020 (0.204)	0.135 (0.287)
	N/8	1	0.180 (0.027)	0.111 (0.030)	0.069 (0.046)	0.038 (0.052)	0.007 (0.077)	0.033 (0.105)	0.023 (0.122)	-0.021 (0.138)	0.083 (0.218)
		2	0.201 (0.026)	0.130 (0.029)	0.093 (0.045)	0.055 (0.051)	0.019 (0.083)	0.071 (0.126)	0.052 (0.155)	0.002 (0.175)	0.104 (0.288)
	N/10	1	0.181 (0.029)	0.109 (0.026)	0.072 (0.039)	0.036 (0.049)	-0.003 (0.072)	0.020 (0.100)	-0.002 (0.127)	-0.044 (0.109)	0.055 (0.209)
		2	0.200 (0.028)	0.126 (0.026)	0.096 (0.044)	0.051 (0.055)	0.009 (0.085)	0.047 (0.119)	0.021 (0.163)	-0.030 (0.141)	0.081 (0.272)
10	N/2	1	0.149 (0.041)	0.143 (0.090)	0.065 (0.063)	0.126 (0.143)	0.117 (0.141)	0.120 (0.175)	0.079 (0.137)	0.262 (0.277)	0.258 (0.307)
		2	0.178 (0.041)	0.176 (0.091)	0.082 (0.067)	0.172 (0.149)	0.164 (0.155)	0.163 (0.186)	0.130 (0.152)	0.315 (0.313)	0.302 (0.333)
	N/4	1	0.162 (0.033)	0.120 (0.040)	0.075 (0.063)	0.050 (0.056)	0.072 (0.127)	0.058 (0.101)	0.064 (0.146)	0.074 (0.193)	0.163 (0.224)
		2	0.189 (0.034)	0.139 (0.039)	0.109 (0.069)	0.084 (0.061)	0.098 (0.151)	0.079 (0.117)	0.101 (0.191)	0.110 (0.233)	0.199 (0.260)
	N/6	1	0.174 (0.025)	0.118 (0.040)	0.070 (0.055)	0.042 (0.061)	0.033 (0.092)	0.048 (0.108)	0.061 (0.160)	0.008 (0.180)	0.127 (0.236)
		2	0.199 (0.030)	0.139 (0.044)	0.094 (0.050)	0.065 (0.050)	0.054 (0.100)	0.087 (0.123)	0.108 (0.205)	0.032 (0.219)	0.154 (0.307)
	N/8	1	0.180 (0.029)	0.112 (0.031)	0.070 (0.050)	0.042 (0.056)	0.011 (0.083)	0.043 (0.112)	0.034 (0.132)	-0.010 (0.150)	0.103 (0.236)
		2	0.201 (0.028)	0.130 (0.031)	0.094 (0.048)	0.060 (0.055)	0.024 (0.090)	0.084 (0.135)	0.066 (0.170)	0.017 (0.192)	0.128 (0.313)
	N/10	1	0.181 (0.031)	0.109 (0.027)	0.073 (0.042)	0.041 (0.054)	0.000 (0.079)	0.031 (0.108)	0.009 (0.139)	-0.032 (0.121)	0.078 (0.230)
		2	0.200 (0.030)	0.125 (0.028)	0.098 (0.048)	0.057 (0.061)	0.013 (0.093)	0.061 (0.130)	0.035 (0.180)	-0.015 (0.158)	0.108 (0.301)

Appendix 1.15: Differenced from generated H value group means and standard deviations for each combination of n_{min}, n_{max}, and M using AFA across all generated H signal ranges when N=2500 (depicted yellow**)**.

Window Size			H								
Min	Max	Order	0.1	0.2	0.3	0.4	0.5	0.6	0.7	0.8	0.9
4	N/2	1	0.130 (0.041)	0.089 (0.049)	0.072 (0.053)	0.049 (0.101)	0.093 (0.111)	0.097 (0.088)	0.084 (0.149)	0.210 (0.186)	0.226 (0.197)
		2	0.154 (0.047)	0.106 (0.044)	0.101 (0.060)	0.087 (0.105)	0.126 (0.116)	0.153 (0.096)	0.130 (0.163)	0.251 (0.214)	0.273 (0.208)
	N/4	1	0.127 (0.028)	0.086 (0.031)	0.059 (0.048)	0.037 (0.067)	0.027 (0.070)	0.055 (0.082)	0.079 (0.094)	0.078 (0.143)	0.129 (0.133)
		2	0.152 (0.027)	0.106 (0.032)	0.078 (0.051)	0.065 (0.069)	0.045 (0.069)	0.082 (0.092)	0.125 (0.103)	0.106 (0.170)	0.158 (0.164)
	N/6	1	0.138 (0.022)	0.086 (0.025)	0.049 (0.032)	0.038 (0.034)	0.021 (0.043)	0.033 (0.067)	0.054 (0.066)	0.022 (0.122)	0.102 (0.144)
		2	0.162 (0.021)	0.104 (0.023)	0.063 (0.032)	0.063 (0.034)	0.037 (0.050)	0.055 (0.075)	0.092 (0.079)	0.040 (0.151)	0.122 (0.180)
	N/8	1	0.145 (0.019)	0.088 (0.022)	0.043 (0.023)	0.031 (0.025)	0.013 (0.038)	0.019 (0.062)	0.028 (0.066)	0.019 (0.110)	0.086 (0.134)
		2	0.165 (0.018)	0.105 (0.021)	0.058 (0.023)	0.048 (0.032)	0.028 (0.046)	0.029 (0.075)	0.055 (0.087)	0.044 (0.139)	0.111 (0.168)
	N/10	1	0.148 (0.020)	0.090 (0.021)	0.045 (0.023)	0.025 (0.023)	0.004 (0.030)	0.000 (0.061)	0.010 (0.066)	0.010 (0.102)	0.068 (0.120)
		2	0.166 (0.021)	0.106 (0.019)	0.059 (0.026)	0.037 (0.031)	0.016 (0.034)	0.006 (0.078)	0.029 (0.090)	0.031 (0.130)	0.092 (0.153)
6	N/2	1	0.130 (0.042)	0.089 (0.050)	0.073 (0.055)	0.051 (0.104)	0.097 (0.114)	0.101 (0.090)	0.089 (0.153)	0.220 (0.192)	0.237 (0.203)
		2	0.153 (0.049)	0.106 (0.046)	0.103 (0.062)	0.089 (0.108)	0.131 (0.119)	0.160 (0.098)	0.137 (0.168)	0.263 (0.220)	0.285 (0.214)
	N/4	1	0.126 (0.029)	0.086 (0.033)	0.060 (0.049)	0.039 (0.070)	0.031 (0.073)	0.062 (0.085)	0.088 (0.098)	0.089 (0.149)	0.142 (0.139)
		2	0.152 (0.028)	0.106 (0.033)	0.080 (0.053)	0.068 (0.072)	0.051 (0.071)	0.091 (0.096)	0.138 (0.108)	0.120 (0.178)	0.175 (0.171)
	N/6	1	0.137 (0.024)	0.085 (0.026)	0.050 (0.033)	0.041 (0.036)	0.026 (0.045)	0.041 (0.071)	0.066 (0.069)	0.035 (0.130)	0.120 (0.152)
		2	0.161 (0.022)	0.105 (0.024)	0.065 (0.034)	0.069 (0.036)	0.044 (0.053)	0.066 (0.080)	0.108 (0.083)	0.056 (0.161)	0.144 (0.190)
	N/8	1	0.143 (0.020)	0.088 (0.023)	0.044 (0.025)	0.035 (0.026)	0.020 (0.040)	0.029 (0.066)	0.041 (0.070)	0.035 (0.117)	0.109 (0.144)
		2	0.164 (0.019)	0.105 (0.022)	0.060 (0.024)	0.054 (0.035)	0.037 (0.049)	0.042 (0.080)	0.074 (0.093)	0.066 (0.149)	0.139 (0.179)
	N/10	1	0.146 (0.021)	0.089 (0.023)	0.046 (0.024)	0.029 (0.024)	0.011 (0.032)	0.011 (0.065)	0.025 (0.070)	0.029 (0.111)	0.094 (0.129)
		2	0.166 (0.022)	0.107 (0.020)	0.062 (0.027)	0.044 (0.033)	0.026 (0.037)	0.020 (0.084)	0.050 (0.096)	0.057 (0.141)	0.124 (0.166)
8	N/2	1	0.129 (0.043)	0.089 (0.051)	0.073 (0.056)	0.052 (0.106)	0.100 (0.117)	0.105 (0.093)	0.093 (0.156)	0.227 (0.197)	0.244 (0.207)
		2	0.152 (0.050)	0.106 (0.047)	0.104 (0.063)	0.091 (0.110)	0.135 (0.122)	0.165 (0.101)	0.142 (0.172)	0.271 (0.226)	0.293 (0.219)
	N/4	1	0.124 (0.030)	0.085 (0.034)	0.061 (0.051)	0.041 (0.073)	0.034 (0.075)	0.067 (0.088)	0.095 (0.102)	0.097 (0.155)	0.151 (0.143)
		2	0.150 (0.029)	0.105 (0.034)	0.081 (0.055)	0.071 (0.075)	0.054 (0.074)	0.097 (0.100)	0.147 (0.112)	0.130 (0.184)	0.186 (0.177)
	N/6	1	0.135 (0.025)	0.085 (0.028)	0.050 (0.035)	0.043 (0.038)	0.030 (0.047)	0.047 (0.074)	0.074 (0.073)	0.043 (0.136)	0.132 (0.159)
		2	0.160 (0.023)	0.104 (0.026)	0.065 (0.035)	0.072 (0.038)	0.048 (0.055)	0.074 (0.083)	0.120 (0.087)	0.066 (0.169)	0.158 (0.199)
	N/8	1	0.142 (0.021)	0.087 (0.024)	0.044 (0.026)	0.037 (0.028)	0.024 (0.042)	0.035 (0.070)	0.051 (0.073)	0.045 (0.124)	0.123 (0.152)
		2	0.162 (0.020)	0.104 (0.023)	0.060 (0.025)	0.057 (0.036)	0.042 (0.052)	0.051 (0.084)	0.087 (0.097)	0.080 (0.158)	0.157 (0.190)
	N/10	1	0.144 (0.022)	0.088 (0.024)	0.046 (0.025)	0.031 (0.025)	0.016 (0.034)	0.018 (0.068)	0.036 (0.074)	0.041 (0.119)	0.111 (0.138)
		2	0.164 (0.024)	0.105 (0.021)	0.062 (0.028)	0.047 (0.034)	0.031 (0.039)	0.029 (0.088)	0.064 (0.101)	0.074 (0.150)	0.146 (0.177)
10	N/2	1	0.128 (0.044)	0.088 (0.053)	0.074 (0.057)	0.053 (0.108)	0.103 (0.120)	0.108 (0.095)	0.096 (0.160)	0.233 (0.201)	0.249 (0.211)
		2	0.152 (0.051)	0.105 (0.048)	0.105 (0.065)	0.092 (0.113)	0.138 (0.125)	0.169 (0.103)	0.146 (0.176)	0.278 (0.231)	0.300 (0.223)
	N/4	1	0.123 (0.031)	0.085 (0.035)	0.061 (0.053)	0.041 (0.076)	0.036 (0.078)	0.070 (0.091)	0.100 (0.105)	0.102 (0.160)	0.158 (0.148)
		2	0.149 (0.030)	0.105 (0.036)	0.081 (0.057)	0.072 (0.078)	0.056 (0.076)	0.102 (0.103)	0.154 (0.116)	0.137 (0.191)	0.193 (0.183)
	N/6	1	0.133 (0.026)	0.084 (0.029)	0.050 (0.036)	0.045 (0.040)	0.032 (0.049)	0.052 (0.077)	0.081 (0.075)	0.048 (0.142)	0.140 (0.165)
		2	0.158 (0.024)	0.103 (0.027)	0.065 (0.037)	0.074 (0.040)	0.051 (0.058)	0.080 (0.087)	0.129 (0.090)	0.073 (0.177)	0.168 (0.208)
	N/8	1	0.140 (0.022)	0.086 (0.025)	0.044 (0.027)	0.039 (0.029)	0.027 (0.044)	0.041 (0.073)	0.058 (0.076)	0.053 (0.131)	0.134 (0.159)
		2	0.161 (0.021)	0.103 (0.024)	0.060 (0.026)	0.060 (0.038)	0.046 (0.054)	0.057 (0.088)	0.097 (0.101)	0.091 (0.167)	0.170 (0.200)
	N/10	1	0.142 (0.023)	0.087 (0.025)	0.046 (0.026)	0.033 (0.026)	0.019 (0.035)	0.024 (0.071)	0.044 (0.078)	0.051 (0.126)	0.124 (0.146)
		2	0.161 (0.025)	0.104 (0.022)	0.061 (0.029)	0.049 (0.036)	0.036 (0.041)	0.036 (0.093)	0.076 (0.106)	0.087 (0.160)	0.162 (0.188)

Appendix 1.16: Differenced from generated H value group means and standard deviations for each combination of n_{min}, n_{max}, and M using AFA across all generated H signal ranges when N=5000 (depicted red**)**.

Window Size			H								
Min	Max	Order	0.1	0.2	0.3	0.4	0.5	0.6	0.7	0.8	0.9
4	N/2	1	0.109 (0.048)	0.069 (0.057)	0.049 (0.058)	0.079 (0.069)	0.091 (0.109)	0.109 (0.125)	0.124 (0.124)	0.269 (0.143)	0.274 (0.192)
		2	0.125 (0.046)	0.093 (0.058)	0.068 (0.057)	0.111 (0.076)	0.130 (0.114)	0.147 (0.139)	0.179 (0.141)	0.330 (0.163)	0.322 (0.229)
	N/4	1	0.112 (0.019)	0.079 (0.031)	0.053 (0.040)	0.035 (0.053)	0.042 (0.080)	0.072 (0.077)	0.081 (0.088)	0.092 (0.142)	0.200 (0.142)
		2	0.125 (0.020)	0.098 (0.030)	0.076 (0.045)	0.049 (0.058)	0.068 (0.088)	0.101 (0.096)	0.126 (0.107)	0.130 (0.160)	0.252 (0.179)
	N/6	1	0.119 (0.018)	0.079 (0.021)	0.051 (0.033)	0.023 (0.039)	0.041 (0.061)	0.024 (0.042)	0.064 (0.095)	0.029 (0.115)	0.145 (0.126)
		2	0.135 (0.019)	0.097 (0.019)	0.072 (0.033)	0.036 (0.032)	0.062 (0.065)	0.031 (0.054)	0.107 (0.125)	0.057 (0.140)	0.195 (0.161)
	N/8	1	0.124 (0.017)	0.082 (0.021)	0.049 (0.031)	0.022 (0.034)	0.033 (0.045)	0.000 (0.036)	0.033 (0.078)	0.017 (0.094)	0.095 (0.116)
		2	0.140 (0.016)	0.098 (0.019)	0.066 (0.031)	0.034 (0.033)	0.047 (0.044)	0.001 (0.043)	0.066 (0.097)	0.040 (0.122)	0.132 (0.159)
	N/10	1	0.126 (0.015)	0.086 (0.020)	0.049 (0.026)	0.021 (0.034)	0.020 (0.041)	-0.007 (0.035)	0.011 (0.049)	0.006 (0.088)	0.064 (0.119)
		2	0.143 (0.014)	0.100 (0.018)	0.062 (0.023)	0.034 (0.039)	0.029 (0.035)	-0.003 (0.045)	0.031 (0.065)	0.032 (0.120)	0.099 (0.162)
6	N/2	1	0.108 (0.049)	0.069 (0.058)	0.049 (0.059)	0.080 (0.070)	0.093 (0.111)	0.112 (0.127)	0.128 (0.126)	0.277 (0.145)	0.281 (0.195)
		2	0.125 (0.047)	0.093 (0.059)	0.069 (0.058)	0.113 (0.077)	0.133 (0.116)	0.151 (0.142)	0.184 (0.143)	0.339 (0.166)	0.330 (0.233)
	N/4	1	0.111 (0.020)	0.078 (0.032)	0.054 (0.041)	0.036 (0.055)	0.045 (0.082)	0.077 (0.079)	0.086 (0.090)	0.099 (0.146)	0.210 (0.147)
		2	0.124 (0.021)	0.098 (0.031)	0.077 (0.046)	0.051 (0.060)	0.072 (0.090)	0.107 (0.099)	0.134 (0.110)	0.139 (0.165)	0.265 (0.184)
	N/6	1	0.117 (0.018)	0.079 (0.022)	0.051 (0.034)	0.025 (0.041)	0.045 (0.063)	0.029 (0.044)	0.072 (0.099)	0.036 (0.119)	0.159 (0.131)
		2	0.134 (0.019)	0.097 (0.020)	0.073 (0.034)	0.039 (0.033)	0.068 (0.068)	0.037 (0.056)	0.117 (0.130)	0.067 (0.146)	0.211 (0.167)
	N/8	1	0.123 (0.018)	0.081 (0.022)	0.050 (0.033)	0.024 (0.035)	0.037 (0.047)	0.006 (0.038)	0.041 (0.082)	0.026 (0.098)	0.109 (0.122)
		2	0.138 (0.017)	0.098 (0.019)	0.068 (0.033)	0.036 (0.034)	0.053 (0.046)	0.007 (0.044)	0.078 (0.102)	0.053 (0.128)	0.151 (0.167)
	N/10	1	0.124 (0.016)	0.085 (0.021)	0.050 (0.027)	0.024 (0.035)	0.025 (0.043)	-0.002 (0.037)	0.020 (0.052)	0.016 (0.093)	0.080 (0.126)
		2	0.141 (0.015)	0.100 (0.019)	0.064 (0.024)	0.038 (0.041)	0.036 (0.037)	0.005 (0.047)	0.043 (0.069)	0.046 (0.126)	0.120 (0.172)
8	N/2	1	0.108 (0.050)	0.069 (0.058)	0.049 (0.060)	0.082 (0.072)	0.095 (0.113)	0.114 (0.129)	0.131 (0.128)	0.282 (0.147)	0.287 (0.198)
		2	0.124 (0.048)	0.093 (0.060)	0.069 (0.059)	0.115 (0.078)	0.136 (0.118)	0.154 (0.144)	0.188 (0.146)	0.346 (0.169)	0.337 (0.237)
	N/4	1	0.110 (0.020)	0.078 (0.032)	0.054 (0.042)	0.037 (0.057)	0.047 (0.084)	0.080 (0.081)	0.090 (0.093)	0.105 (0.149)	0.218 (0.150)
		2	0.123 (0.021)	0.097 (0.031)	0.077 (0.047)	0.052 (0.061)	0.075 (0.093)	0.112 (0.102)	0.139 (0.113)	0.145 (0.169)	0.275 (0.189)
	N/6	1	0.116 (0.019)	0.078 (0.023)	0.051 (0.035)	0.026 (0.042)	0.047 (0.065)	0.032 (0.046)	0.077 (0.102)	0.041 (0.123)	0.168 (0.136)
		2	0.132 (0.020)	0.096 (0.020)	0.074 (0.035)	0.040 (0.034)	0.071 (0.070)	0.041 (0.058)	0.125 (0.135)	0.073 (0.150)	0.223 (0.173)
	N/8	1	0.121 (0.018)	0.080 (0.023)	0.050 (0.034)	0.025 (0.036)	0.040 (0.048)	0.009 (0.039)	0.047 (0.086)	0.032 (0.102)	0.119 (0.127)
		2	0.137 (0.017)	0.097 (0.020)	0.068 (0.034)	0.038 (0.036)	0.057 (0.048)	0.011 (0.046)	0.086 (0.106)	0.061 (0.133)	0.164 (0.174)
	N/10	1	0.122 (0.017)	0.085 (0.022)	0.050 (0.028)	0.025 (0.037)	0.028 (0.045)	0.002 (0.038)	0.026 (0.054)	0.023 (0.097)	0.091 (0.132)
		2	0.139 (0.015)	0.099 (0.019)	0.064 (0.025)	0.040 (0.043)	0.040 (0.038)	0.009 (0.049)	0.051 (0.072)	0.056 (0.131)	0.134 (0.181)
10	N/2	1	0.107 (0.051)	0.068 (0.059)	0.049 (0.060)	0.083 (0.073)	0.097 (0.115)	0.116 (0.131)	0.133 (0.130)	0.287 (0.149)	0.291 (0.201)
		2	0.123 (0.049)	0.093 (0.060)	0.069 (0.059)	0.116 (0.080)	0.138 (0.120)	0.157 (0.146)	0.191 (0.148)	0.351 (0.171)	0.342 (0.241)
	N/4	1	0.109 (0.021)	0.077 (0.033)	0.054 (0.043)	0.038 (0.058)	0.048 (0.085)	0.083 (0.083)	0.094 (0.095)	0.109 (0.152)	0.225 (0.154)
		2	0.122 (0.022)	0.097 (0.032)	0.078 (0.048)	0.053 (0.063)	0.077 (0.095)	0.116 (0.104)	0.144 (0.116)	0.150 (0.173)	0.282 (0.193)
	N/6	1	0.115 (0.019)	0.078 (0.023)	0.051 (0.036)	0.026 (0.043)	0.050 (0.067)	0.035 (0.047)	0.081 (0.105)	0.045 (0.127)	0.175 (0.140)
		2	0.131 (0.021)	0.096 (0.021)	0.074 (0.036)	0.041 (0.035)	0.074 (0.072)	0.044 (0.060)	0.131 (0.139)	0.078 (0.154)	0.233 (0.179)
	N/8	1	0.120 (0.019)	0.080 (0.023)	0.050 (0.035)	0.026 (0.037)	0.043 (0.050)	0.011 (0.040)	0.051 (0.089)	0.036 (0.106)	0.127 (0.132)
		2	0.135 (0.018)	0.096 (0.021)	0.069 (0.035)	0.039 (0.037)	0.060 (0.050)	0.014 (0.047)	0.092 (0.110)	0.066 (0.137)	0.174 (0.181)
	N/10	1	0.121 (0.017)	0.084 (0.022)	0.050 (0.029)	0.026 (0.038)	0.031 (0.046)	0.005 (0.039)	0.030 (0.057)	0.028 (0.100)	0.099 (0.138)
		2	0.137 (0.016)	0.098 (0.020)	0.064 (0.026)	0.041 (0.045)	0.043 (0.039)	0.012 (0.050)	0.058 (0.075)	0.063 (0.136)	0.144 (0.189)

Appendix 1.17: Percent difference of data group means and standard deviations for each combination of $n_{min,}$ and n_{max} using DFA across all generated H signal ranges when N=500 (depicted blue**)**.

Window Sizes		H								
Min	Max	0.1	0.2	0.3	0.4	0.5	0.6	0.7	0.8	0.9
4	N/2	91.7 (61.0)	42.6 (31.8)	27.5 (22.4)	27.6 (33.3)	21.9 (15.1)	16.4 (13.1)	19.5 (11.1)	16.2 (16.9)	14.7 (13.5)
	N/4	62.1 (44.2)	32.8 (23.2)	28.1 (14.5)	18.7 (17.8)	17.7 (15.0)	11.3 (8.7)	9.8 (8.5)	13.6 (12.9)	9.4 (7.2)
	N/6	65.5 (45.0)	34.0 (25.6)	25.4 (14.7)	14.0 (12.1)	13.0 (8.8)	9.0 (8.0)	8.0 (6.2)	11.4 (9.6)	7.9 (6.8)
	N/8	62.9 (45.8)	28.6 (23.3)	22.4 (12.2)	12.3 (9.1)	10.8 (8.8)	8.4 (7.4)	6.1 (4.9)	9.8 (8.4)	7.6 (6.2)
	N/10	65.3 (42.5)	28.1 (24.3)	20.4 (14.8)	10.1 (7.1)	10.6 (8.3)	6.4 (8.2)	5.8 (5.0)	9.5 (7.8)	7.1 (6.3)
6	N/2	97.8 (66.4)	44.9 (34.4)	29.9 (23.7)	29.7 (35.5)	23.2 (15.8)	17.5 (13.9)	20.9 (11.8)	16.8 (17.8)	15.4 (14.3)
	N/4	63.0 (45.7)	35.2 (24.6)	30.0 (16.5)	20.8 (19.7)	19.3 (16.3)	12.5 (9.2)	10.6 (9.3)	14.5 (13.9)	9.9 (7.6)
	N/6	64.9 (45.8)	38.3 (28.2)	27.2 (16.7)	15.7 (14.1)	14.4 (9.4)	10.0 (8.9)	8.7 (6.8)	12.0 (10.6)	8.5 (7.3)
	N/8	59.7 (46.1)	31.9 (25.8)	24.3 (12.2)	14.7 (10.3)	12.2 (9.6)	9.5 (7.8)	6.7 (5.2)	10.5 (9.4)	8.3 (6.6)
	N/10	57.0 (46.0)	32.1 (26.4)	21.2 (15.7)	12.1 (8.0)	11.9 (9.2)	7.5 (8.7)	6.2 (5.6)	10.5 (8.5)	7.7 (6.9)
8	N/2	103.7 (72.4)	47.1 (37.1)	32.0 (24.8)	31.7 (37.1)	24.2 (16.5)	18.5 (14.7)	22.1 (12.5)	17.3 (18.6)	16.0 (14.9)
	N/4	65.9 (48.1)	37.5 (25.9)	31.9 (18.4)	22.3 (21.2)	20.7 (17.5)	13.5 (9.6)	11.4 (10.1)	15.3 (14.7)	10.4 (7.9)
	N/6	67.5 (46.5)	42.2 (30.8)	29.6 (17.6)	17.0 (15.5)	15.8 (10.3)	10.9 (9.9)	9.5 (7.4)	12.7 (11.6)	8.9 (7.7)
	N/8	59.1 (49.5)	35.7 (28.0)	26.4 (13.3)	16.3 (11.6)	13.7 (10.7)	10.8 (8.1)	7.4 (5.6)	11.3 (10.4)	8.9 (7.0)
	N/10	57.9 (42.9)	37.0 (29.1)	22.3 (18.0)	13.2 (8.8)	12.9 (11.0)	8.8 (9.5)	7.1 (6.0)	11.5 (9.6)	8.3 (7.7)
10	N/2	109.3 (78.2)	48.8 (40.0)	33.8 (26.0)	33.5 (38.6)	25.2 (17.0)	19.5 (15.6)	23.1 (13.1)	17.8 (19.2)	16.4 (15.4)
	N/4	68.1 (50.5)	39.1 (26.8)	33.8 (20.1)	23.7 (22.6)	21.9 (18.4)	14.6 (9.9)	11.8 (10.7)	16.0 (15.4)	10.7 (8.0)
	N/6	68.7 (47.8)	45.3 (32.7)	32.2 (18.5)	18.6 (16.8)	17.0 (10.9)	11.6 (11.0)	10.1 (7.6)	13.3 (12.2)	9.1 (7.8)
	N/8	59.7 (49.9)	38.8 (29.7)	28.6 (14.3)	18.3 (13.2)	15.0 (11.4)	11.1 (8.5)	7.5 (6.0)	11.8 (11.1)	9.1 (7.1)
	N/10	56.7 (41.1)	41.1 (29.8)	23.3 (20.1)	14.9 (9.6)	14.2 (11.8)	9.1 (10.3)	7.4 (5.8)	12.1 (10.4)	8.5 (7.8)

Appendix 1.18: Percent difference of data group means and standard deviations for each combination of $n_{min,}$ and n_{max} using DFA across all generated H signal ranges when N=1000 (depicted green**)**.

Window Sizes		H								
Min	Max	0.1	0.2	0.3	0.4	0.5	0.6	0.7	0.8	0.9
4	N/2	80.3 (58.1)	34.1 (28.8)	28.3 (18.8)	26.2 (17.4)	19.8 (21.9)	21.1 (17.8)	18.7 (14.4)	14.1 (10.8)	10.5 (9.5)
	N/4	75.1 (50.1)	33.0 (28.9)	24.9 (14.7)	10.7 (10.2)	16.7 (9.6)	13.8 (11.3)	9.2 (7.8)	12.0 (6.2)	8.5 (7.0)
	N/6	76.4 (47.8)	26.3 (20.0)	18.8 (12.4)	11.3 (10.2)	13.8 (8.9)	11.1 (8.4)	8.1 (5.0)	10.1 (5.6)	6.8 (5.2)
	N/8	78.6 (37.5)	27.1 (22.8)	17.3 (12.4)	8.6 (6.5)	11.4 (6.7)	10.9 (6.9)	7.0 (5.4)	8.7 (6.0)	5.7 (4.0)
	N/10	85.6 (34.9)	27.1 (23.4)	15.7 (11.8)	8.8 (5.9)	9.4 (7.7)	9.3 (6.5)	6.8 (4.7)	7.8 (6.6)	5.0 (3.0)
6	N/2	84.6 (60.4)	35.6 (30.2)	29.5 (19.7)	27.5 (18.2)	20.5 (22.9)	22.2 (18.4)	19.5 (15.1)	14.6 (11.4)	10.8 (9.9)
	N/4	77.1 (51.7)	34.3 (30.7)	26.5 (15.7)	11.5 (10.8)	17.6 (10.1)	14.4 (12.0)	9.6 (8.1)	12.4 (6.5)	8.8 (7.5)
	N/6	76.6 (49.5)	26.9 (21.0)	20.0 (13.8)	12.3 (11.2)	14.8 (9.7)	11.7 (8.9)	8.5 (5.3)	10.6 (5.9)	7.1 (5.8)
	N/8	75.6 (40.2)	27.1 (24.2)	18.5 (13.7)	9.4 (7.0)	12.5 (7.2)	11.7 (7.5)	7.4 (5.8)	9.1 (6.3)	6.0 (4.5)
	N/10	81.3 (40.2)	26.9 (24.7)	17.3 (12.4)	9.4 (6.8)	10.5 (8.1)	10.0 (6.9)	7.3 (4.9)	8.3 (7.0)	5.2 (3.4)
8	N/2	88.3 (62.4)	37.2 (31.3)	30.5 (20.6)	28.6 (18.9)	21.2 (23.8)	23.1 (18.9)	20.1 (15.7)	15.0 (11.9)	11.1 (10.1)
	N/4	79.4 (53.3)	35.7 (32.3)	27.8 (16.7)	12.2 (11.4)	18.4 (10.6)	14.9 (12.6)	10.0 (8.3)	12.8 (6.7)	9.1 (8.0)
	N/6	78.0 (50.5)	27.9 (22.0)	21.2 (14.6)	13.2 (12.2)	15.7 (10.3)	12.3 (9.3)	8.8 (5.5)	11.0 (6.1)	7.4 (6.2)
	N/8	74.1 (42.1)	28.2 (25.2)	19.6 (14.8)	10.1 (7.6)	13.5 (7.5)	12.2 (8.2)	7.6 (6.0)	9.5 (6.5)	6.2 (4.8)
	N/10	79.2 (42.6)	28.4 (25.3)	18.7 (13.1)	10.1 (7.6)	11.4 (8.4)	10.5 (7.5)	7.5 (5.2)	8.6 (7.3)	5.3 (3.7)
10	N/2	91.6 (64.8)	38.6 (32.5)	31.4 (21.3)	29.6 (19.5)	21.7 (24.6)	24.0 (19.4)	20.6 (16.2)	15.3 (12.3)	11.4 (10.4)
	N/4	82.1 (56.0)	36.9 (33.9)	29.0 (17.8)	12.9 (12.1)	19.1 (11.2)	15.3 (13.1)	10.2 (8.5)	13.2 (7.0)	9.3 (8.4)
	N/6	80.2 (52.5)	29.0 (22.9)	22.2 (15.5)	14.2 (13.3)	16.6 (10.9)	12.7 (9.6)	9.0 (5.7)	11.4 (6.3)	7.7 (6.5)
	N/8	74.3 (44.0)	29.5 (25.7)	20.8 (15.6)	10.8 (8.3)	14.4 (7.9)	12.6 (8.8)	7.7 (6.3)	9.8 (6.8)	6.4 (5.2)
	N/10	78.5 (45.8)	29.2 (26.3)	19.9 (13.9)	10.8 (8.1)	12.3 (8.7)	10.8 (7.9)	7.7 (5.4)	9.0 (7.8)	5.5 (3.9)

Appendix 1.19: Percent difference of data group means and standard deviations for each combination of $n_{min,}$ and n_{max} using DFA across all generated H signal ranges when N=2500 (depicted yellow**)**.

Window Sizes		H								
Min	Max	0.1	0.2	0.3	0.4	0.5	0.6	0.7	0.8	0.9
4	N/2	61.1 (46.6)	39.2 (25.5)	22.8 (17.9)	26.2 (20.4)	24.0 (20.2)	19.1 (13.2)	17.7 (13.1)	13.4 (12.7)	14.6 (12.8)
	N/4	62.2 (48.0)	30.0 (18.7)	15.4 (13.2)	17.9 (15.5)	12.8 (12.2)	12.5 (9.0)	9.3 (8.8)	7.7 (5.7)	10.1 (8.4)
	N/6	54.9 (29.9)	27.4 (11.9)	11.8 (9.4)	14.1 (10.0)	9.1 (9.5)	9.9 (7.2)	8.9 (6.2)	6.9 (6.2)	7.6 (6.1)
	N/8	48.8 (26.5)	19.8 (14.1)	11.3 (8.1)	11.3 (8.9)	9.4 (7.2)	8.4 (6.6)	8.5 (5.3)	6.1 (4.5)	5.9 (4.9)
	N/10	45.5 (30.1)	18.8 (11.6)	11.2 (7.2)	11.0 (8.9)	8.3 (6.3)	7.0 (5.6)	7.7 (4.8)	5.3 (4.0)	5.5 (4.3)
6	N/2	62.9 (48.2)	40.4 (26.4)	23.4 (18.4)	26.8 (21.1)	24.6 (20.6)	19.5 (13.6)	18.1 (13.4)	13.7 (13.1)	14.9 (13.1)
	N/4	64.2 (50.0)	30.9 (19.4)	15.9 (14.0)	18.6 (16.2)	13.2 (12.6)	12.9 (9.3)	9.6 (9.1)	8.0 (5.9)	10.4 (8.7)
	N/6	57.7 (29.7)	28.3 (12.5)	12.3 (9.9)	14.9 (10.5)	9.4 (9.9)	10.4 (7.5)	9.3 (6.5)	7.1 (6.5)	7.9 (6.5)
	N/8	49.8 (26.9)	20.4 (14.7)	11.7 (8.6)	12.1 (9.4)	9.8 (7.6)	8.8 (7.0)	8.9 (5.6)	6.3 (4.7)	6.1 (5.2)
	N/10	45.1 (30.6)	18.8 (12.4)	11.6 (7.7)	11.8 (9.6)	8.7 (6.6)	7.3 (5.9)	8.1 (5.1)	5.5 (4.3)	5.8 (4.6)
8	N/2	64.3 (49.5)	41.5 (27.1)	23.9 (18.8)	27.3 (21.6)	25.1 (21.1)	19.9 (13.9)	18.5 (13.7)	14.0 (13.4)	15.2 (13.4)
	N/4	66.0 (52.0)	31.9 (20.1)	16.5 (14.6)	19.2 (16.8)	13.6 (13.1)	13.3 (9.6)	9.8 (9.3)	8.1 (6.1)	10.7 (9.0)
	N/6	60.2 (30.4)	29.2 (13.0)	12.7 (10.4)	15.5 (11.0)	9.8 (10.3)	10.7 (7.7)	9.5 (6.7)	7.2 (6.8)	8.1 (6.7)
	N/8	50.8 (28.2)	21.0 (15.5)	12.2 (9.0)	12.7 (9.8)	10.3 (7.9)	9.1 (7.3)	9.2 (5.8)	6.5 (4.8)	6.3 (5.4)
	N/10	45.0 (32.1)	19.0 (13.3)	12.1 (8.1)	12.5 (10.2)	9.2 (7.0)	7.6 (6.1)	8.4 (5.3)	5.7 (4.4)	5.9 (4.8)
10	N/2	65.8 (50.5)	42.5 (27.8)	24.3 (19.2)	27.8 (22.1)	25.6 (21.5)	20.2 (14.2)	18.9 (13.9)	14.2 (13.6)	15.4 (13.6)
	N/4	67.6 (53.9)	32.7 (20.8)	16.9 (15.1)	19.7 (17.4)	13.9 (13.4)	13.6 (9.8)	10.0 (9.6)	8.3 (6.2)	10.9 (9.2)
	N/6	62.5 (31.3)	30.1 (13.6)	13.1 (10.8)	16.1 (11.4)	10.1 (10.6)	11.0 (7.9)	9.8 (6.8)	7.4 (7.0)	8.2 (7.0)
	N/8	52.0 (29.4)	21.6 (16.2)	12.7 (9.5)	13.2 (10.2)	10.6 (8.2)	9.4 (7.5)	9.5 (6.0)	6.6 (5.0)	6.4 (5.6)
	N/10	45.5 (33.0)	19.3 (14.1)	12.7 (8.4)	13.0 (10.7)	9.5 (7.3)	7.8 (6.3)	8.7 (5.4)	5.8 (4.6)	6.1 (4.9)

Appendix 1.20: Percent difference of data group means and standard deviations for each combination of $n_{min,}$ and n_{max} using DFA across all generated H signal ranges when N=5000 (depicted red**)**.

Window Sizes		H								
Min	Max	0.1	0.2	0.3	0.4	0.5	0.6	0.7	0.8	0.9
4	N/2	89.2 (75.5)	56.6 (53.1)	28.2 (25.6)	28.6 (15.4)	18.8 (16.0)	15.1 (11.1)	14.2 (8.3)	10.9 (12.1)	7.6 (8.3)
	N/4	59.7 (33.9)	27.5 (30.4)	18.8 (14.2)	16.9 (9.9)	15.1 (10.1)	10.6 (5.6)	10.0 (6.4)	7.9 (7.6)	6.0 (5.6)
	N/6	46.6 (34.4)	21.7 (19.1)	16.6 (10.5)	11.3 (10.1)	8.1 (5.5)	7.2 (4.6)	8.7 (7.1)	6.5 (5.9)	5.5 (4.2)
	N/8	46.5 (32.6)	23.1 (17.0)	12.5 (12.1)	8.4 (8.2)	7.9 (4.7)	7.4 (4.2)	7.6 (5.7)	6.1 (5.1)	4.2 (3.3)
	N/10	46.1 (29.1)	23.4 (13.5)	12.9 (12.0)	9.5 (6.5)	7.3 (3.7)	6.2 (3.9)	6.3 (5.0)	5.6 (4.5)	3.8 (3.0)
6	N/2	90.8 (77.2)	57.6 (54.1)	28.7 (26.0)	29.1 (15.8)	19.1 (16.2)	15.3 (11.3)	14.4 (8.5)	11.1 (12.3)	7.7 (8.4)
	N/4	61.1 (33.9)	28.4 (31.3)	19.3 (14.6)	17.4 (10.1)	15.5 (10.4)	10.9 (5.7)	10.2 (6.5)	8.0 (7.7)	6.1 (5.7)
	N/6	46.8 (34.8)	22.5 (19.7)	17.2 (10.7)	11.8 (10.4)	8.3 (5.7)	7.4 (4.8)	8.9 (7.3)	6.6 (6.0)	5.6 (4.3)
	N/8	46.5 (32.5)	23.8 (17.5)	13.0 (12.4)	8.8 (8.5)	8.1 (5.0)	7.7 (4.4)	7.9 (5.9)	6.2 (5.2)	4.3 (3.4)
	N/10	45.0 (29.6)	24.0 (13.7)	13.4 (12.5)	9.9 (6.8)	7.5 (3.9)	6.4 (4.0)	6.5 (5.2)	5.8 (4.6)	3.9 (3.2)
8	N/2	92.2 (78.6)	58.4 (55.0)	29.2 (26.4)	29.6 (16.0)	19.4 (16.5)	15.5 (11.5)	14.6 (8.6)	11.2 (12.4)	7.8 (8.5)
	N/4	62.3 (34.2)	29.1 (32.0)	19.7 (14.9)	17.9 (10.4)	15.9 (10.6)	11.1 (5.8)	10.4 (6.6)	8.1 (7.9)	6.2 (5.8)
	N/6	47.3 (35.1)	23.2 (20.2)	17.6 (10.9)	12.2 (10.7)	8.5 (5.9)	7.5 (5.0)	9.1 (7.5)	6.7 (6.1)	5.7 (4.4)
	N/8	47.0 (32.5)	24.6 (17.9)	13.4 (12.7)	9.1 (8.8)	8.3 (5.1)	7.9 (4.5)	8.1 (6.1)	6.4 (5.3)	4.4 (3.5)
	N/10	44.4 (30.3)	24.6 (14.0)	13.7 (13.0)	10.3 (7.1)	7.7 (4.1)	6.6 (4.1)	6.7 (5.4)	5.9 (4.7)	4.0 (3.3)
10	N/2	93.5 (79.9)	59.2 (55.8)	29.6 (26.8)	30.0 (16.3)	19.6 (16.7)	15.7 (11.6)	14.8 (8.7)	11.3 (12.6)	7.9 (8.6)
	N/4	63.5 (34.5)	29.8 (32.6)	20.1 (15.2)	18.3 (10.6)	16.3 (10.8)	11.2 (5.9)	10.6 (6.7)	8.2 (8.0)	6.3 (5.9)
	N/6	47.9 (35.4)	23.8 (20.7)	18.1 (11.0)	12.6 (11.0)	8.7 (6.1)	7.7 (5.1)	9.3 (7.7)	6.8 (6.2)	5.8 (4.5)
	N/8	47.5 (32.7)	25.3 (18.3)	13.7 (13.0)	9.4 (9.1)	8.4 (5.3)	8.1 (4.6)	8.3 (6.2)	6.5 (5.4)	4.5 (3.6)
	N/10	44.1 (31.1)	25.2 (14.3)	14.1 (13.4)	10.6 (7.4)	7.8 (4.2)	6.7 (4.2)	6.9 (5.6)	6.0 (4.7)	4.0 (3.3)

Appendix 1.21: Percent difference of data group means and standard deviations for each combination of $n_{min,}$ n_{max}, and M using AFA across all generated H signal ranges when N=500 (depicted blue**)**.

Window Size			H								
Min	Max	Order	0.1	0.2	0.3	0.4	0.5	0.6	0.7	0.8	0.9
4	N/2	1	108.9 (48.1)	36.7 (25.5)	17.4 (18.2)	20.3 (16.5)	22.3 (17.3)	22.6 (15.4)	20.7 (13.8)	33.7 (17.8)	31.1 (20.3)
		2	125.3 (46.4)	46.9 (28.4)	23.1 (18.5)	28.1 (18.3)	27.0 (21.6)	28.3 (18.0)	27.1 (17.9)	41.3 (20.4)	36.4 (24.5)
	N/4	1	112.0 (19.4)	39.3 (15.3)	19.3 (11.0)	11.6 (10.8)	13.3 (11.9)	14.5 (9.7)	12.4 (11.7)	15.3 (14.4)	23.2 (14.2)
		2	125.2 (20.0)	48.8 (14.9)	26.0 (13.7)	13.7 (13.1)	16.4 (14.9)	19.0 (13.3)	18.1 (15.1)	19.7 (16.4)	29.3 (17.8)
	N/6	1	118.8 (17.7)	39.7 (10.7)	18.1 (8.6)	8.5 (7.4)	11.6 (8.8)	6.0 (5.4)	11.8 (11.3)	9.8 (10.9)	16.5 (13.6)
		2	134.7 (18.8)	48.6 (9.6)	23.9 (10.9)	9.9 (6.7)	13.4 (12.0)	7.6 (7.0)	17.3 (15.9)	13.8 (12.7)	22.3 (16.9)
	N/8	1	124.2 (17.1)	40.8 (10.5)	17.1 (9.2)	7.2 (6.9)	8.7 (6.7)	4.3 (4.1)	8.7 (8.3)	8.3 (8.4)	13.5 (9.6)
		2	139.7 (16.1)	49.0 (9.3)	22.1 (10.4)	9.4 (7.0)	9.7 (8.6)	5.5 (4.3)	11.8 (11.8)	11.6 (10.9)	19.4 (12.0)
	N/10	1	125.8 (15.3)	42.9 (9.9)	16.5 (8.1)	7.7 (6.3)	6.9 (5.8)	4.1 (4.2)	5.1 (5.0)	8.7 (6.5)	12.1 (8.7)
		2	142.8 (13.9)	49.9 (8.9)	20.7 (7.7)	9.9 (8.4)	6.7 (6.1)	5.5 (4.9)	7.6 (6.9)	12.6 (8.6)	17.4 (11.5)
6	N/2	1	108.2 (49.1)	36.6 (25.9)	17.5 (18.4)	20.7 (16.8)	22.8 (17.7)	23.2 (15.8)	21.3 (14.2)	34.6 (18.2)	31.8 (20.8)
		2	124.7 (47.3)	47.0 (28.8)	23.3 (18.8)	28.7 (18.6)	27.6 (22.0)	29.0 (18.5)	27.8 (18.3)	42.4 (20.8)	37.2 (25.1)
	N/4	1	110.8 (19.9)	39.1 (15.8)	19.5 (11.3)	12.0 (11.2)	13.8 (12.3)	15.2 (10.3)	13.1 (12.1)	16.1 (14.9)	24.3 (14.8)
		2	124.1 (20.6)	48.8 (15.3)	26.4 (14.0)	14.3 (13.5)	17.1 (15.4)	19.9 (13.8)	19.2 (15.6)	20.7 (17.0)	30.7 (18.5)
	N/6	1	117.5 (18.3)	39.5 (11.0)	18.4 (8.9)	8.9 (7.8)	12.2 (9.3)	6.6 (5.7)	12.5 (12.0)	10.4 (11.5)	17.8 (14.3)
		2	133.5 (19.4)	48.6 (9.9)	24.4 (11.3)	10.5 (7.1)	14.3 (12.6)	8.3 (7.5)	18.5 (16.8)	14.5 (13.6)	24.0 (17.8)
	N/8	1	122.7 (17.8)	40.5 (11.0)	17.4 (9.5)	7.6 (7.3)	9.4 (7.2)	4.5 (4.3)	9.5 (8.9)	8.8 (9.0)	14.8 (10.5)
		2	138.4 (16.7)	49.0 (9.7)	22.7 (10.9)	10.0 (7.4)	10.8 (9.1)	5.7 (4.6)	12.9 (12.9)	12.4 (11.8)	21.0 (13.2)
	N/10	1	124.0 (16.0)	42.6 (10.4)	16.8 (8.3)	8.2 (6.7)	7.4 (6.5)	4.3 (4.2)	5.5 (5.6)	9.2 (7.1)	13.3 (9.6)
		2	141.4 (14.6)	50.0 (9.3)	21.3 (8.1)	10.7 (9.0)	7.7 (6.7)	5.9 (5.0)	8.6 (7.8)	13.4 (9.7)	19.2 (12.8)
8	N/2	1	107.5 (49.9)	36.5 (26.2)	17.7 (18.6)	21.1 (17.0)	23.2 (18.0)	23.6 (16.0)	21.7 (14.5)	35.3 (18.4)	32.4 (21.1)
		2	124.0 (48.2)	46.9 (29.1)	23.3 (19.1)	29.1 (18.9)	28.1 (22.4)	29.5 (18.8)	28.3 (18.7)	43.2 (21.1)	37.9 (25.6)
	N/4	1	109.8 (20.4)	38.9 (16.1)	19.7 (11.4)	12.3 (11.4)	14.2 (12.6)	15.7 (10.7)	13.6 (12.4)	16.7 (15.3)	25.2 (15.2)
		2	122.8 (21.1)	48.6 (15.6)	26.6 (14.3)	14.6 (13.8)	17.6 (15.9)	20.7 (14.3)	19.9 (16.1)	21.5 (17.5)	31.8 (19.0)
	N/6	1	116.2 (18.8)	39.1 (11.4)	18.5 (9.1)	9.1 (8.0)	12.6 (9.8)	7.1 (6.0)	13.2 (12.6)	10.8 (12.0)	18.8 (14.9)
		2	132.0 (20.0)	48.2 (10.2)	24.6 (11.5)	10.8 (7.4)	15.0 (13.1)	8.8 (7.9)	19.4 (17.5)	15.1 (14.2)	25.3 (18.6)
	N/8	1	121.3 (18.4)	40.1 (11.4)	17.6 (9.8)	7.9 (7.6)	10.0 (7.6)	4.7 (4.5)	10.0 (9.5)	9.2 (9.5)	15.7 (11.1)
		2	136.6 (17.4)	48.6 (10.0)	22.8 (11.3)	10.4 (7.7)	11.5 (9.5)	6.1 (4.8)	13.9 (13.6)	13.0 (12.6)	22.2 (14.2)
	N/10	1	122.3 (16.7)	42.3 (10.8)	17.0 (8.5)	8.5 (7.1)	7.9 (6.9)	4.5 (4.3)	5.8 (6.2)	9.6 (7.6)	14.4 (10.3)
		2	139.4 (15.2)	49.6 (9.6)	21.4 (8.4)	11.1 (9.4)	8.4 (7.0)	6.4 (5.0)	9.4 (8.4)	14.0 (10.7)	20.5 (13.8)
10	N/2	1	107.0 (50.7)	36.4 (26.5)	17.8 (18.7)	21.3 (17.3)	23.6 (18.3)	24.0 (16.3)	22.0 (14.7)	35.9 (18.7)	32.9 (21.4)
		2	123.4 (48.9)	46.9 (29.4)	23.4 (19.3)	29.4 (19.2)	28.5 (22.8)	30.0 (19.1)	28.8 (19.0)	43.9 (21.4)	38.5 (26.0)
	N/4	1	108.8 (20.8)	38.7 (16.5)	19.8 (11.6)	12.6 (11.7)	14.5 (12.9)	16.1 (11.0)	14.1 (12.8)	17.3 (15.6)	25.9 (15.5)
		2	121.6 (21.6)	48.4 (16.0)	26.8 (14.5)	14.8 (14.2)	18.0 (16.2)	21.3 (14.7)	20.6 (16.5)	22.2 (17.9)	32.6 (19.4)
	N/6	1	115.0 (19.2)	38.8 (11.7)	18.6 (9.3)	9.4 (8.3)	13.0 (10.2)	7.4 (6.2)	13.7 (13.1)	11.2 (12.4)	19.6 (15.4)
		2	130.6 (20.5)	47.9 (10.4)	24.8 (11.6)	11.0 (7.6)	15.5 (13.6)	9.2 (8.2)	20.2 (18.2)	15.6 (14.7)	26.3 (19.2)
	N/8	1	120.0 (19.0)	39.8 (11.7)	17.7 (10.0)	8.1 (7.9)	10.4 (8.0)	5.0 (4.7)	10.6 (10.0)	9.5 (10.0)	16.5 (11.7)
		2	134.9 (17.9)	48.2 (10.3)	22.9 (11.6)	10.6 (8.0)	12.1 (9.9)	6.4 (5.0)	14.6 (14.3)	13.5 (13.2)	23.3 (15.0)
	N/10	1	120.7 (17.3)	41.9 (11.1)	17.1 (8.6)	8.8 (7.4)	8.4 (7.2)	4.7 (4.5)	6.2 (6.7)	10.0 (8.1)	15.3 (10.8)
		2	137.5 (15.8)	49.1 (10.0)	21.4 (8.7)	11.5 (9.8)	9.0 (7.3)	6.8 (5.1)	10.2 (8.9)	14.5 (11.5)	21.7 (14.7)

Appendix 1.22: Percent difference of data group means and standard deviations for each combination of $n_{min,}$ n_{max}, and M using AFA across all generated H signal ranges when N=1000 (depicted green**)**.

Window Size			H								
Min	Max	Order	0.1	0.2	0.3	0.4	0.5	0.6	0.7	0.8	0.9
4	N/2	1	152.3 (35.5)	69.1 (39.5)	22.1 (17.5)	29.5 (29.3)	24.1 (20.9)	24.7 (17.2)	14.9 (11.4)	28.4 (28.8)	28.5 (25.1)
		2	180.2 (35.6)	84.4 (39.8)	29.0 (16.2)	38.7 (31.4)	28.5 (27.2)	27.5 (22.1)	19.5 (13.6)	35.4 (31.0)	32.3 (27.6)
	N/4	1	164.3 (26.3)	58.4 (17.2)	23.7 (17.3)	12.4 (8.6)	14.7 (17.6)	12.7 (7.6)	14.4 (10.3)	13.7 (15.0)	17.9 (15.5)
		2	189.8 (27.5)	67.5 (16.8)	33.3 (19.2)	18.3 (10.3)	19.7 (20.3)	15.3 (8.9)	19.1 (14.5)	17.0 (18.2)	21.6 (17.9)
	N/6	1	174.3 (20.5)	57.1 (16.5)	21.4 (14.7)	11.8 (7.5)	11.1 (9.4)	11.4 (9.2)	14.8 (9.6)	14.0 (11.5)	16.6 (13.5)
		2	197.9 (23.8)	66.5 (17.3)	28.4 (13.5)	12.9 (7.9)	12.5 (10.3)	13.0 (12.6)	19.1 (13.0)	16.2 (13.8)	22.3 (16.4)
	N/8	1	178.1 (22.4)	54.3 (12.8)	21.1 (12.6)	9.8 (7.5)	9.6 (8.2)	10.5 (9.9)	11.3 (8.9)	13.9 (7.5)	16.7 (10.2)
		2	198.4 (21.5)	62.5 (11.8)	27.6 (12.4)	10.6 (8.9)	10.4 (8.7)	12.6 (12.7)	13.5 (11.8)	15.7 (9.8)	21.8 (13.4)
	N/10	1	178.7 (23.9)	52.8 (11.3)	21.3 (10.5)	9.1 (6.1)	10.2 (6.7)	10.4 (8.7)	13.4 (8.1)	12.8 (8.3)	15.5 (9.7)
		2	196.9 (23.3)	60.2 (10.7)	27.4 (11.7)	9.8 (8.4)	10.4 (8.9)	11.7 (10.7)	15.9 (10.7)	14.3 (10.2)	19.9 (12.2)
6	N/2	1	151.4 (37.5)	70.3 (41.2)	22.6 (18.2)	31.2 (30.9)	25.5 (22.1)	26.3 (18.2)	16.0 (12.3)	30.7 (30.5)	30.5 (26.7)
		2	180.1 (37.7)	86.1 (41.9)	29.8 (16.9)	40.9 (33.2)	30.4 (28.6)	29.3 (23.6)	21.1 (14.7)	38.1 (33.0)	34.8 (29.4)
	N/4	1	163.9 (28.5)	59.3 (18.2)	24.7 (18.4)	13.6 (9.4)	16.4 (19.3)	14.1 (8.6)	15.9 (11.3)	15.0 (16.6)	19.8 (17.7)
		2	190.5 (29.7)	69.0 (17.8)	35.0 (20.6)	20.3 (11.3)	22.2 (22.2)	17.3 (10.1)	21.4 (15.8)	19.3 (19.7)	23.8 (20.6)
	N/6	1	174.9 (22.2)	58.3 (17.7)	22.5 (16.0)	13.2 (8.5)	12.5 (10.5)	12.4 (10.8)	16.9 (10.6)	14.4 (12.8)	18.7 (15.9)
		2	200.1 (26.0)	68.6 (18.9)	30.4 (14.7)	15.2 (9.0)	14.4 (11.9)	15.2 (14.4)	22.1 (14.9)	17.3 (15.4)	25.6 (18.4)
	N/8	1	179.3 (24.5)	55.4 (13.9)	22.5 (14.0)	11.3 (8.9)	10.2 (9.4)	11.0 (12.1)	11.9 (10.4)	13.6 (8.7)	19.0 (12.2)
		2	201.4 (23.7)	64.9 (13.1)	30.1 (13.7)	13.2 (10.5)	11.3 (10.3)	15.1 (14.8)	15.2 (13.7)	15.8 (11.7)	24.9 (16.1)
	N/10	1	180.4 (26.4)	54.1 (12.2)	23.1 (11.8)	10.6 (8.1)	10.5 (7.8)	10.5 (10.6)	12.9 (10.3)	11.9 (7.7)	17.4 (11.3)
		2	200.6 (25.6)	62.7 (11.9)	30.6 (13.3)	12.6 (10.5)	10.8 (10.5)	12.9 (13.2)	15.4 (14.0)	13.3 (10.2)	22.5 (15.0)
8	N/2	1	150.4 (39.3)	71.2 (42.6)	22.9 (18.7)	32.5 (32.3)	26.6 (23.1)	27.7 (19.0)	16.9 (13.0)	32.5 (32.0)	32.1 (28.0)
		2	179.2 (39.4)	87.0 (43.8)	30.1 (17.4)	42.5 (34.8)	31.8 (29.7)	30.8 (24.7)	22.3 (15.6)	40.2 (34.6)	36.6 (30.8)
	N/4	1	163.0 (30.7)	59.6 (19.1)	25.3 (19.3)	14.5 (10.0)	17.8 (20.7)	15.3 (9.5)	17.1 (12.3)	16.1 (17.9)	21.3 (19.3)
		2	189.7 (31.7)	69.4 (18.7)	35.9 (21.7)	21.6 (12.0)	24.0 (23.8)	18.7 (11.2)	23.2 (16.9)	21.2 (21.1)	25.6 (22.5)
	N/6	1	174.7 (23.7)	58.7 (18.9)	23.0 (17.1)	14.3 (9.3)	13.9 (11.3)	13.5 (11.9)	18.7 (11.8)	15.2 (14.1)	20.8 (17.6)
		2	199.8 (28.1)	69.2 (20.4)	31.1 (15.7)	16.6 (9.8)	16.0 (13.2)	17.0 (15.7)	24.8 (16.5)	18.3 (17.3)	28.3 (20.3)
	N/8	1	179.6 (26.5)	55.7 (14.9)	23.1 (15.3)	12.5 (9.9)	11.0 (10.4)	11.9 (13.6)	13.4 (11.2)	13.9 (10.1)	21.0 (14.5)
		2	201.1 (26.0)	65.2 (14.3)	31.0 (14.9)	14.7 (11.6)	12.6 (11.3)	17.3 (16.4)	17.3 (15.4)	16.9 (13.4)	27.6 (19.0)
	N/10	1	181.0 (28.8)	54.3 (13.1)	24.0 (12.8)	11.9 (9.5)	11.3 (8.8)	11.4 (12.3)	13.3 (11.9)	12.2 (7.9)	19.8 (12.9)
		2	200.1 (27.9)	62.8 (13.0)	31.9 (14.6)	14.4 (11.9)	12.1 (11.7)	14.8 (15.2)	16.2 (16.7)	14.0 (11.0)	25.9 (17.2)
10	N/2	1	149.5 (41.0)	72.0 (43.9)	23.2 (19.2)	33.7 (33.5)	27.5 (23.9)	28.9 (19.7)	17.7 (13.6)	34.0 (33.3)	33.4 (29.2)
		2	178.4 (40.9)	87.8 (45.4)	30.3 (18.0)	43.8 (36.2)	33.0 (30.7)	32.0 (25.7)	23.3 (16.3)	42.0 (36.1)	38.1 (32.1)
	N/4	1	162.1 (32.7)	60.0 (19.8)	25.7 (20.1)	15.2 (10.6)	19.0 (21.9)	16.2 (10.3)	18.1 (13.3)	17.2 (18.9)	22.6 (20.6)
		2	188.8 (33.7)	69.6 (19.4)	36.6 (22.6)	22.6 (12.6)	25.5 (25.2)	19.9 (12.2)	24.7 (18.0)	22.8 (22.3)	27.1 (24.0)
	N/6	1	174.4 (25.1)	59.1 (19.9)	23.3 (18.0)	15.2 (10.0)	15.1 (12.0)	14.7 (12.8)	20.5 (12.8)	16.1 (15.2)	22.6 (19.0)
		2	199.4 (30.2)	69.5 (21.8)	31.4 (16.7)	17.7 (10.3)	17.5 (14.2)	18.7 (16.6)	27.3 (17.9)	19.5 (19.1)	30.6 (22.0)
	N/8	1	179.8 (28.5)	55.9 (15.7)	23.5 (16.5)	13.6 (10.9)	12.0 (11.3)	13.1 (14.9)	15.1 (11.9)	14.8 (11.2)	23.1 (16.3)
		2	200.7 (28.3)	65.1 (15.4)	31.5 (16.0)	16.0 (12.6)	13.7 (12.4)	19.2 (18.0)	19.4 (17.0)	18.4 (14.9)	30.4 (21.1)
	N/10	1	181.4 (31.0)	54.4 (13.7)	24.7 (13.7)	13.1 (10.7)	12.1 (9.8)	12.5 (13.8)	14.0 (13.7)	12.7 (8.7)	22.3 (14.5)
		2	199.5 (30.3)	62.5 (14.0)	32.6 (16.0)	16.0 (13.0)	13.4 (12.8)	16.7 (16.9)	17.3 (19.3)	15.3 (12.1)	29.1 (19.5)

Appendix 1.23: Percent difference of data group means and standard deviations for each combination of $n_{min,}$ n_{max}, and M using AFA across all generated H signal ranges when N=2500 (depicted yellow**)**.

Window Size			H								
Min	Max	Order	0.1	0.2	0.3	0.4	0.5	0.6	0.7	0.8	0.9
4	N/2	1	130.4 (40.7)	44.4 (24.3)	24.7 (16.7)	21.5 (17.6)	23.5 (16.6)	18.6 (11.0)	20.3 (13.0)	30.1 (17.8)	28.0 (17.9)
		2	153.6 (47.5)	52.9 (22.1)	33.8 (20.0)	26.3 (21.2)	27.9 (19.6)	26.8 (13.5)	25.1 (15.6)	34.5 (22.3)	32.3 (20.2)
	N/4	1	127.1 (27.6)	43.1 (15.6)	20.3 (15.1)	13.0 (13.8)	10.5 (10.4)	12.8 (10.1)	13.7 (10.8)	13.2 (15.3)	15.7 (13.2)
		2	152.5 (27.2)	52.9 (15.9)	26.0 (17.0)	16.2 (17.2)	11.9 (11.1)	16.2 (12.5)	19.2 (12.9)	15.8 (19.3)	20.1 (15.2)
	N/6	1	138.0 (22.4)	43.0 (12.4)	16.7 (9.9)	10.7 (6.7)	7.4 (5.9)	10.0 (7.2)	10.4 (6.1)	11.1 (10.6)	14.9 (12.6)
		2	161.7 (20.5)	52.2 (11.6)	21.1 (10.7)	15.9 (8.4)	9.9 (7.3)	12.1 (9.6)	14.3 (9.6)	13.1 (14.2)	18.5 (15.3)
	N/8	1	144.8 (18.8)	44.1 (10.8)	14.5 (7.6)	8.2 (5.5)	6.2 (5.0)	8.0 (7.2)	8.2 (5.9)	10.7 (8.5)	13.3 (11.6)
		2	164.7 (17.9)	52.4 (10.3)	19.3 (7.7)	12.9 (6.6)	8.4 (6.5)	10.0 (8.8)	11.4 (9.2)	13.6 (11.8)	17.5 (13.6)
	N/10	1	147.7 (19.8)	44.9 (10.6)	14.9 (7.6)	7.1 (4.5)	4.4 (4.0)	6.7 (7.4)	7.5 (5.7)	9.3 (8.6)	11.9 (9.4)
		2	166.2 (21.1)	53.0 (9.4)	19.6 (8.5)	10.5 (5.9)	5.2 (5.5)	8.6 (9.7)	10.2 (8.5)	12.0 (11.2)	16.5 (10.7)
6	N/2	1	129.7 (41.8)	44.5 (24.9)	25.0 (17.1)	22.1 (18.1)	24.4 (17.1)	19.4 (11.4)	21.0 (13.5)	31.2 (18.5)	29.1 (18.5)
		2	153.2 (48.8)	52.9 (22.8)	34.4 (20.6)	27.1 (21.8)	29.0 (20.3)	28.0 (14.0)	26.0 (16.3)	35.9 (23.2)	33.5 (20.9)
	N/4	1	125.5 (28.7)	42.9 (16.3)	20.8 (15.6)	13.6 (14.6)	11.1 (11.1)	13.9 (10.6)	15.0 (11.3)	14.3 (16.2)	16.9 (14.1)
		2	151.6 (28.3)	53.0 (16.6)	26.7 (17.7)	17.1 (18.1)	12.8 (11.9)	17.6 (13.2)	21.0 (13.6)	17.0 (20.7)	21.8 (16.1)
	N/6	1	136.6 (23.7)	42.7 (13.1)	17.1 (10.4)	11.6 (7.2)	8.2 (6.4)	10.9 (8.0)	11.8 (6.7)	12.0 (11.4)	16.4 (13.8)
		2	161.1 (21.7)	52.4 (12.2)	21.7 (11.2)	17.2 (9.0)	10.8 (8.4)	13.4 (10.8)	16.2 (10.8)	14.6 (15.2)	20.6 (16.5)
	N/8	1	143.4 (20.0)	43.9 (11.5)	14.8 (7.9)	9.1 (5.9)	6.9 (5.6)	9.0 (7.8)	9.2 (6.8)	11.6 (9.7)	15.0 (13.1)
		2	164.1 (18.9)	52.6 (10.9)	20.0 (8.0)	14.4 (7.1)	9.4 (7.7)	11.3 (9.9)	12.9 (10.8)	14.9 (13.6)	19.8 (15.3)
	N/10	1	146.2 (21.0)	44.6 (11.3)	15.3 (8.0)	8.1 (4.8)	5.2 (4.2)	7.3 (8.0)	8.2 (6.7)	10.4 (9.6)	13.6 (11.2)
		2	165.6 (22.5)	53.3 (9.9)	20.5 (9.0)	12.0 (6.3)	6.4 (6.2)	8.8 (11.2)	11.9 (9.7)	13.4 (13.2)	19.0 (12.7)
8	N/2	1	129.0 (42.8)	44.5 (25.3)	25.3 (17.5)	22.6 (18.5)	25.1 (17.6)	20.1 (11.7)	21.6 (13.8)	32.2 (19.1)	29.9 (19.0)
		2	152.5 (50.0)	52.8 (23.4)	34.8 (21.1)	27.7 (22.3)	29.8 (20.8)	28.8 (14.3)	26.8 (16.8)	37.0 (23.8)	34.4 (21.5)
	N/4	1	123.9 (29.7)	42.6 (17.0)	21.2 (15.9)	14.1 (15.2)	11.6 (11.6)	14.7 (11.0)	16.0 (11.7)	15.1 (16.9)	17.8 (14.7)
		2	150.2 (29.3)	52.7 (17.2)	27.0 (18.3)	17.7 (18.8)	13.4 (12.3)	18.6 (13.7)	22.2 (14.3)	18.1 (21.5)	22.9 (16.8)
	N/6	1	134.9 (25.0)	42.3 (13.8)	17.3 (10.8)	12.2 (7.6)	8.7 (6.8)	11.7 (8.5)	12.8 (7.3)	12.8 (12.1)	17.5 (14.6)
		2	159.6 (22.8)	51.9 (12.8)	21.8 (11.7)	18.0 (9.5)	11.5 (9.0)	14.5 (11.4)	17.6 (11.6)	15.8 (16.0)	22.0 (17.4)
	N/8	1	141.6 (21.0)	43.4 (12.1)	14.9 (8.1)	9.7 (6.2)	7.5 (6.0)	9.9 (8.2)	10.1 (7.6)	12.3 (10.8)	16.4 (14.2)
		2	162.4 (19.8)	52.0 (11.4)	20.0 (8.4)	15.2 (7.6)	10.3 (8.4)	12.2 (10.7)	14.3 (11.8)	16.2 (14.9)	21.7 (16.4)
	N/10	1	144.3 (22.2)	44.1 (11.9)	15.3 (8.3)	8.7 (5.1)	5.8 (4.5)	7.9 (8.5)	9.0 (7.4)	11.4 (10.5)	15.3 (12.2)
		2	163.5 (23.6)	52.6 (10.5)	20.6 (9.4)	12.8 (6.6)	7.3 (6.7)	9.2 (12.3)	13.3 (10.6)	14.6 (14.8)	21.0 (14.1)
10	N/2	1	128.4 (43.7)	44.5 (25.7)	25.5 (17.9)	23.1 (18.8)	25.7 (18.0)	20.6 (12.0)	22.1 (14.2)	33.0 (19.6)	30.6 (19.4)
		2	151.8 (51.2)	52.6 (24.0)	35.0 (21.5)	28.3 (22.7)	30.5 (21.3)	29.6 (14.6)	27.4 (17.2)	37.9 (24.4)	35.2 (21.9)
	N/4	1	122.5 (30.7)	42.4 (17.6)	21.5 (16.3)	14.6 (15.7)	12.0 (12.0)	15.3 (11.4)	16.8 (12.1)	15.7 (17.6)	18.5 (15.2)
		2	148.9 (30.3)	52.4 (17.8)	27.1 (18.9)	18.1 (19.5)	13.9 (12.8)	19.5 (14.2)	23.2 (14.8)	19.0 (22.3)	23.8 (17.4)
	N/6	1	133.4 (26.1)	41.8 (14.4)	17.4 (11.2)	12.6 (8.0)	9.2 (7.2)	12.4 (8.9)	13.6 (7.7)	13.5 (12.7)	18.4 (15.3)
		2	158.1 (23.8)	51.4 (13.3)	21.8 (12.2)	18.6 (9.9)	12.2 (9.4)	15.5 (12.0)	18.9 (12.2)	16.8 (16.8)	23.3 (18.1)
	N/8	1	140.0 (22.1)	42.9 (12.7)	14.9 (8.3)	10.1 (6.5)	8.0 (6.5)	10.7 (8.6)	10.8 (8.3)	13.0 (11.7)	17.5 (15.0)
		2	160.6 (20.6)	51.3 (11.8)	19.8 (8.6)	15.7 (8.0)	11.0 (9.0)	13.2 (11.4)	15.4 (12.8)	17.4 (16.0)	23.2 (17.5)
	N/10	1	142.5 (23.2)	43.5 (12.5)	15.2 (8.7)	9.0 (5.3)	6.3 (4.9)	8.5 (9.0)	9.9 (7.9)	12.3 (11.4)	16.7 (13.0)
		2	161.4 (24.7)	51.9 (10.9)	20.5 (9.8)	13.4 (6.9)	8.1 (7.1)	10.0 (13.1)	14.5 (11.5)	15.9 (16.0)	22.8 (15.2)

Appendix 1.24: Percent difference of data group means and standard deviations for each combination of n_{min}, n_{max}, and M using AFA across all generated H signal ranges when N=5000 (depicted red**)**.

Window Size			H								
Min	Max	Order	0.1	0.2	0.3	0.4	0.5	0.6	0.7	0.8	0.9
4	N/2	1	108.9 (48.1)	36.7 (25.5)	17.4 (18.2)	20.3 (16.5)	22.3 (17.3)	22.6 (15.4)	20.7 (13.8)	33.7 (17.8)	31.1 (20.3)
		2	125.3 (46.4)	46.9 (28.4)	23.1 (18.5)	28.1 (18.3)	27.0 (21.6)	28.3 (18.0)	27.1 (17.9)	41.3 (20.4)	36.4 (24.5)
	N/4	1	112.0 (19.4)	39.3 (15.3)	19.3 (11.0)	11.6 (10.8)	13.3 (11.9)	14.5 (9.7)	12.4 (11.7)	15.3 (14.4)	23.2 (14.2)
		2	125.2 (20.0)	48.8 (14.9)	26.0 (13.7)	13.7 (13.1)	16.4 (14.9)	19.0 (13.3)	18.1 (15.1)	19.7 (16.4)	29.3 (17.8)
	N/6	1	118.8 (17.7)	39.7 (10.7)	18.1 (8.6)	8.5 (7.4)	11.6 (8.8)	6.0 (5.4)	11.8 (11.3)	9.8 (10.9)	16.5 (13.6)
		2	134.7 (18.8)	48.6 (9.6)	23.9 (10.9)	9.9 (6.7)	13.4 (12.0)	7.6 (7.0)	17.3 (15.9)	13.8 (12.7)	22.3 (16.9)
	N/8	1	124.2 (17.1)	40.8 (10.5)	17.1 (9.2)	7.2 (6.9)	8.7 (6.7)	4.3 (4.1)	8.7 (8.3)	8.3 (8.4)	13.5 (9.6)
		2	139.7 (16.1)	49.0 (9.3)	22.1 (10.4)	9.4 (7.0)	9.7 (8.6)	5.5 (4.3)	11.8 (11.8)	11.6 (10.9)	19.4 (12.0)
	N/10	1	125.8 (15.3)	42.9 (9.9)	16.5 (8.1)	7.7 (6.3)	6.9 (5.8)	4.1 (4.2)	5.1 (5.0)	8.7 (6.5)	12.1 (8.7)
		2	142.8 (13.9)	49.9 (8.9)	20.7 (7.7)	9.9 (8.4)	6.7 (6.1)	5.5 (4.9)	7.6 (6.9)	12.6 (8.6)	17.4 (11.5)
6	N/2	1	108.2 (49.1)	36.6 (25.9)	17.5 (18.4)	20.7 (16.8)	22.8 (17.7)	23.2 (15.8)	21.3 (14.2)	34.6 (18.2)	31.8 (20.8)
		2	124.7 (47.3)	47.0 (28.8)	23.3 (18.8)	28.7 (18.6)	27.6 (22.0)	29.0 (18.5)	27.8 (18.3)	42.4 (20.8)	37.2 (25.1)
	N/4	1	110.8 (19.9)	39.1 (15.8)	19.5 (11.3)	12.0 (11.2)	13.8 (12.3)	15.2 (10.3)	13.1 (12.1)	16.1 (14.9)	24.3 (14.8)
		2	124.1 (20.6)	48.8 (15.3)	26.4 (14.0)	14.3 (13.5)	17.1 (15.4)	19.9 (13.8)	19.2 (15.6)	20.7 (17.0)	30.7 (18.5)
	N/6	1	117.5 (18.3)	39.5 (11.0)	18.4 (8.9)	8.9 (7.8)	12.2 (9.3)	6.6 (5.7)	12.5 (12.0)	10.4 (11.5)	17.8 (14.3)
		2	133.5 (19.4)	48.6 (9.9)	24.4 (11.3)	10.5 (7.1)	14.3 (12.6)	8.3 (7.5)	18.5 (16.8)	14.5 (13.6)	24.0 (17.8)
	N/8	1	122.7 (17.8)	40.5 (11.0)	17.4 (9.5)	7.6 (7.3)	9.4 (7.2)	4.5 (4.3)	9.5 (8.9)	8.8 (9.0)	14.8 (10.5)
		2	138.4 (16.7)	49.0 (9.7)	22.7 (10.9)	10.0 (7.4)	10.8 (9.1)	5.7 (4.6)	12.9 (12.9)	12.4 (11.8)	21.0 (13.2)
	N/10	1	124.0 (16.0)	42.6 (10.4)	16.8 (8.3)	8.2 (6.7)	7.4 (6.5)	4.3 (4.2)	5.5 (5.6)	9.2 (7.1)	13.3 (9.6)
		2	141.4 (14.6)	50.0 (9.3)	21.3 (8.1)	10.7 (9.0)	7.7 (6.7)	5.9 (5.0)	8.6 (7.8)	13.4 (9.7)	19.2 (12.8)
8	N/2	1	107.5 (49.9)	36.5 (26.2)	17.7 (18.6)	21.1 (17.0)	23.2 (18.0)	23.6 (16.0)	21.7 (14.5)	35.3 (18.4)	32.4 (21.1)
		2	124.0 (48.2)	46.9 (29.1)	23.3 (19.1)	29.1 (18.9)	28.1 (22.4)	29.5 (18.8)	28.3 (18.7)	43.2 (21.1)	37.9 (25.6)
	N/4	1	109.8 (20.4)	38.9 (16.1)	19.7 (11.4)	12.3 (11.4)	14.2 (12.6)	15.7 (10.7)	13.6 (12.4)	16.7 (15.3)	25.2 (15.2)
		2	122.8 (21.1)	48.6 (15.6)	26.6 (14.3)	14.6 (13.8)	17.6 (15.9)	20.7 (14.3)	19.9 (16.1)	21.5 (17.5)	31.8 (19.0)
	N/6	1	116.2 (18.8)	39.1 (11.4)	18.5 (9.1)	9.1 (8.0)	12.6 (9.8)	7.1 (6.0)	13.2 (12.6)	10.8 (12.0)	18.8 (14.9)
		2	132.0 (20.0)	48.2 (10.2)	24.6 (11.5)	10.8 (7.4)	15.0 (13.1)	8.8 (7.9)	19.4 (17.5)	15.1 (14.2)	25.3 (18.6)
	N/8	1	121.3 (18.4)	40.1 (11.4)	17.6 (9.8)	7.9 (7.6)	10.0 (7.6)	4.7 (4.5)	10.0 (9.5)	9.2 (9.5)	15.7 (11.1)
		2	136.6 (17.4)	48.6 (10.0)	22.8 (11.3)	10.4 (7.7)	11.5 (9.5)	6.1 (4.8)	13.9 (13.6)	13.0 (12.6)	22.2 (14.2)
	N/10	1	122.3 (16.7)	42.3 (10.8)	17.0 (8.5)	8.5 (7.1)	7.9 (6.9)	4.5 (4.3)	5.8 (6.2)	9.6 (7.6)	14.4 (10.3)
		2	139.4 (15.2)	49.6 (9.6)	21.4 (8.4)	11.1 (9.4)	8.4 (7.0)	6.4 (5.0)	9.4 (8.4)	14.0 (10.7)	20.5 (13.8)
10	N/2	1	107.0 (50.7)	36.4 (26.5)	17.8 (18.7)	21.3 (17.3)	23.6 (18.3)	24.0 (16.3)	22.0 (14.7)	35.9 (18.7)	32.9 (21.4)
		2	123.4 (48.9)	46.9 (29.4)	23.4 (19.3)	29.4 (19.2)	28.5 (22.8)	30.0 (19.1)	28.8 (19.0)	43.9 (21.4)	38.5 (26.0)
	N/4	1	108.8 (20.8)	38.7 (16.5)	19.8 (11.6)	12.6 (11.7)	14.5 (12.9)	16.1 (11.0)	14.1 (12.8)	17.3 (15.6)	25.9 (15.5)
		2	121.6 (21.6)	48.4 (16.0)	26.8 (14.5)	14.8 (14.2)	18.0 (16.2)	21.3 (14.7)	20.6 (16.5)	22.2 (17.9)	32.6 (19.4)
	N/6	1	115.0 (19.2)	38.8 (11.7)	18.6 (9.3)	9.4 (8.3)	13.0 (10.2)	7.4 (6.2)	13.7 (13.1)	11.2 (12.4)	19.6 (15.4)
		2	130.6 (20.5)	47.9 (10.4)	24.8 (11.6)	11.0 (7.6)	15.5 (13.6)	9.2 (8.2)	20.2 (18.2)	15.6 (14.7)	26.3 (19.2)
	N/8	1	120.0 (19.0)	39.8 (11.7)	17.7 (10.0)	8.1 (7.9)	10.4 (8.0)	5.0 (4.7)	10.6 (10.0)	9.5 (10.0)	16.5 (11.7)
		2	134.9 (17.9)	48.2 (10.3)	22.9 (11.6)	10.6 (8.0)	12.1 (9.9)	6.4 (5.0)	14.6 (14.3)	13.5 (13.2)	23.3 (15.0)
	N/10	1	120.7 (17.3)	41.9 (11.1)	17.1 (8.6)	8.8 (7.4)	8.4 (7.2)	4.7 (4.5)	6.2 (6.7)	10.0 (8.1)	15.3 (10.8)
		2	137.5 (15.8)	49.1 (10.0)	21.4 (8.7)	11.5 (9.8)	9.0 (7.3)	6.8 (5.1)	10.2 (8.9)	14.5 (11.5)	21.7 (14.7)

Appendix B: Additional Heatmaps: Heatmaps depicting differences between the generated Hurst exponent (generated intrinsically into the fBm signals) and the estimated Hurst exponent using DFA and AFA.

Appendix 2.1: Heatmap showing overall percent difference depiction of DFA for all parameters investigated.

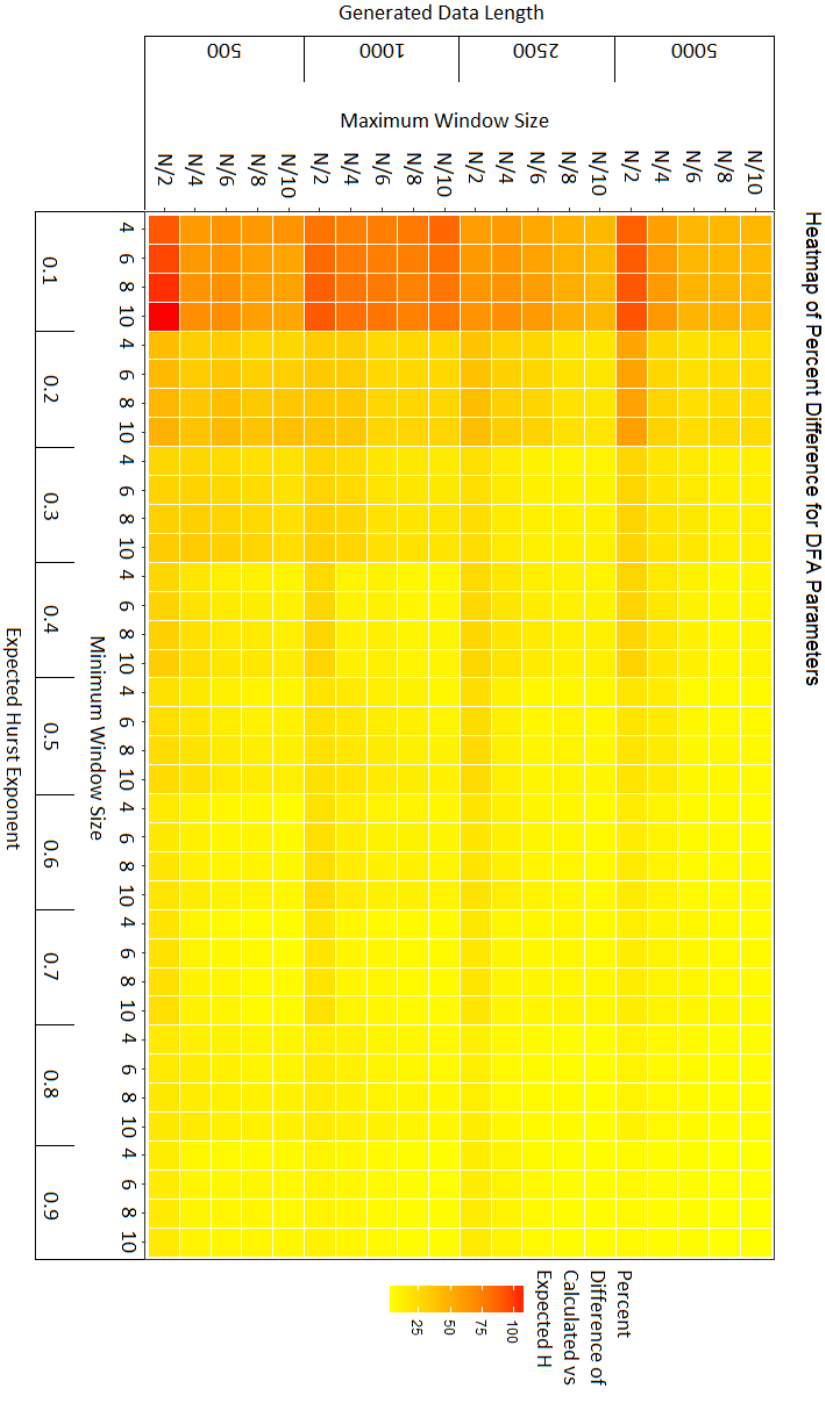

Appendix 2.2: Heatmap showing overall percent difference depiction of AFA for all investigated parameters while *M*=1.

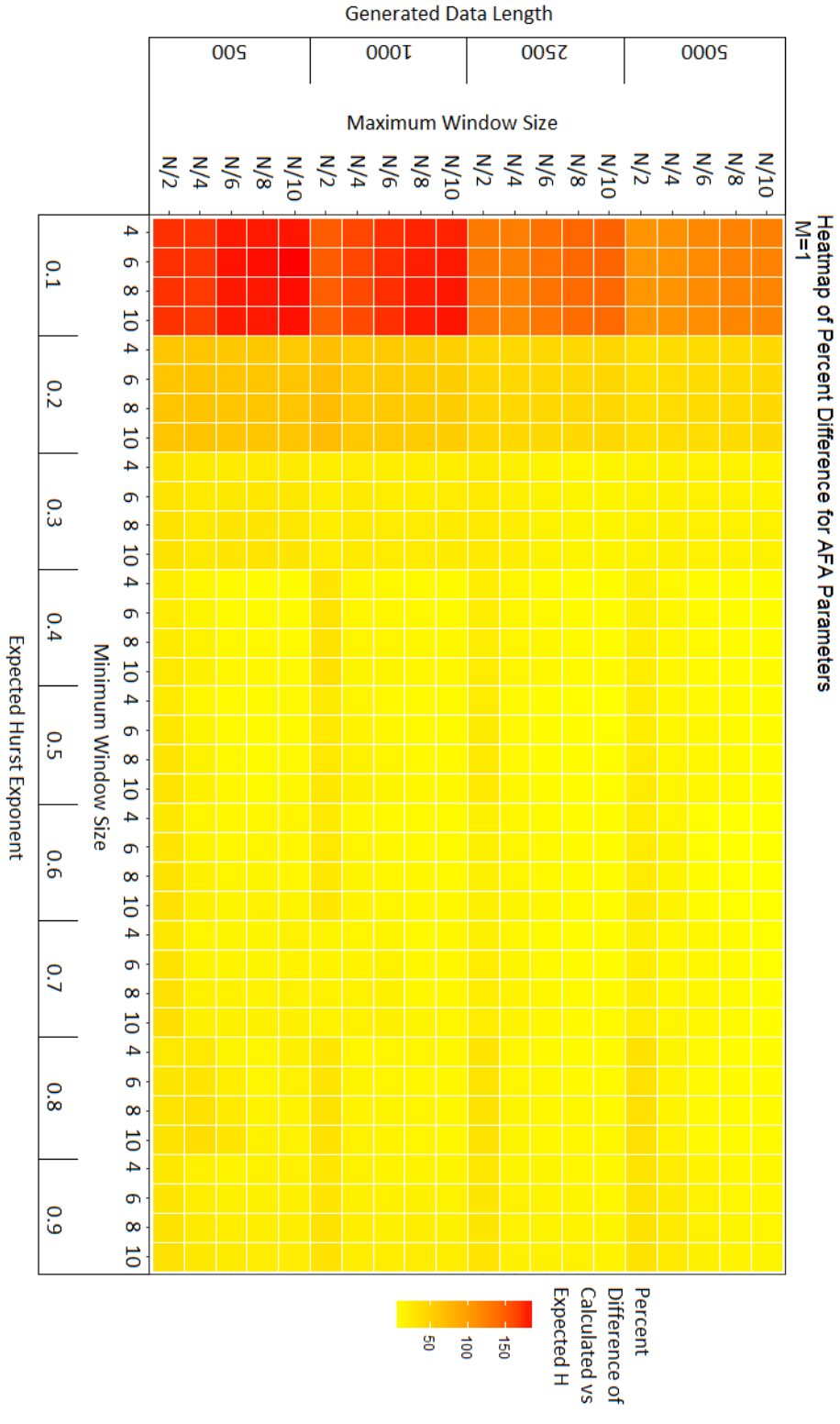

Appendix 2.3: Heatmap showing overall percent difference depiction of AFA for all investigated parameters while *M*=2.

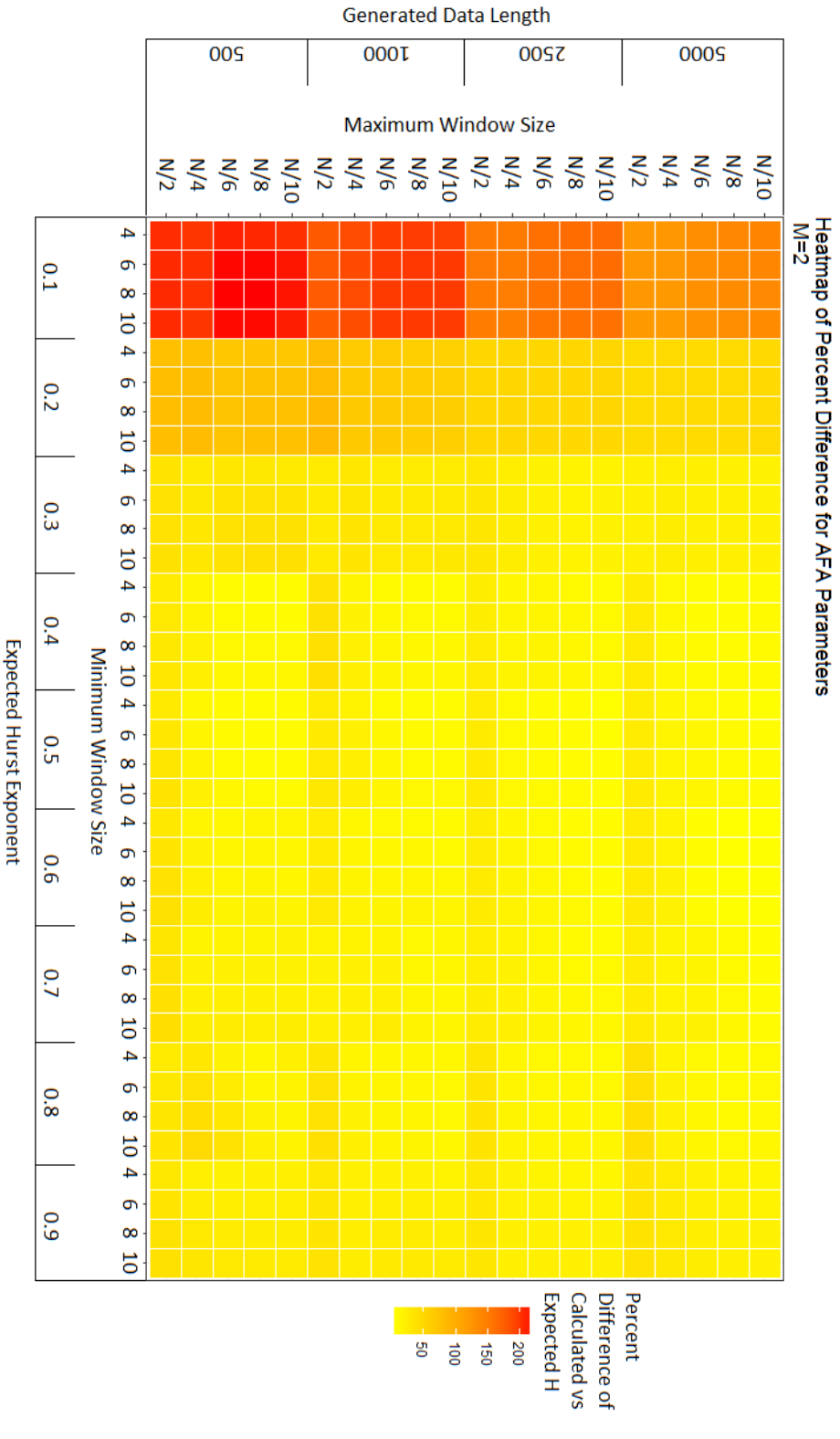

Appendix 2.4: Heatmap showing differences of DFA across all parameters investigated.

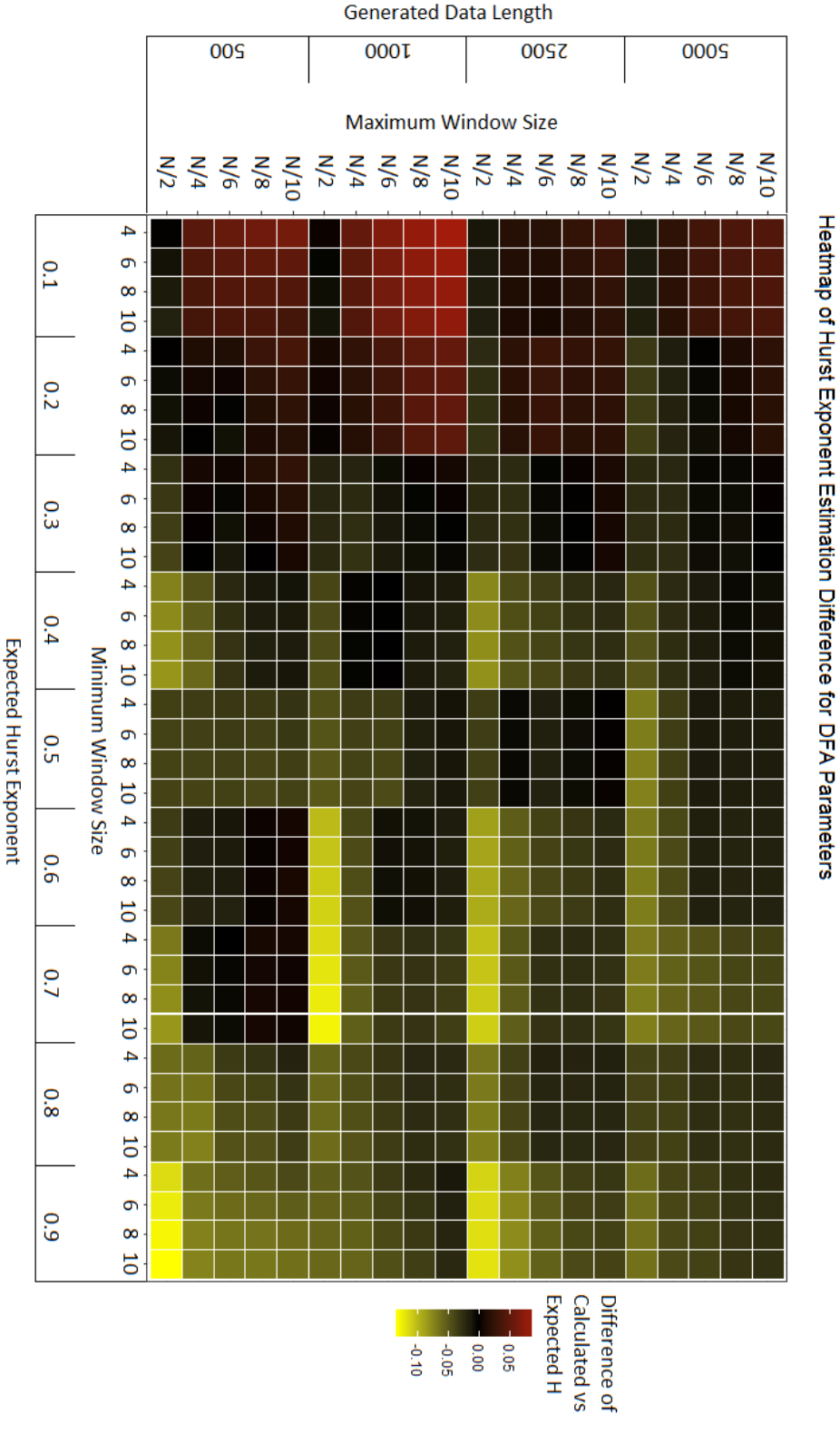

Appendix 2.5: Heatmap showing differences of AFA across all parameters investigated while *M*=1.

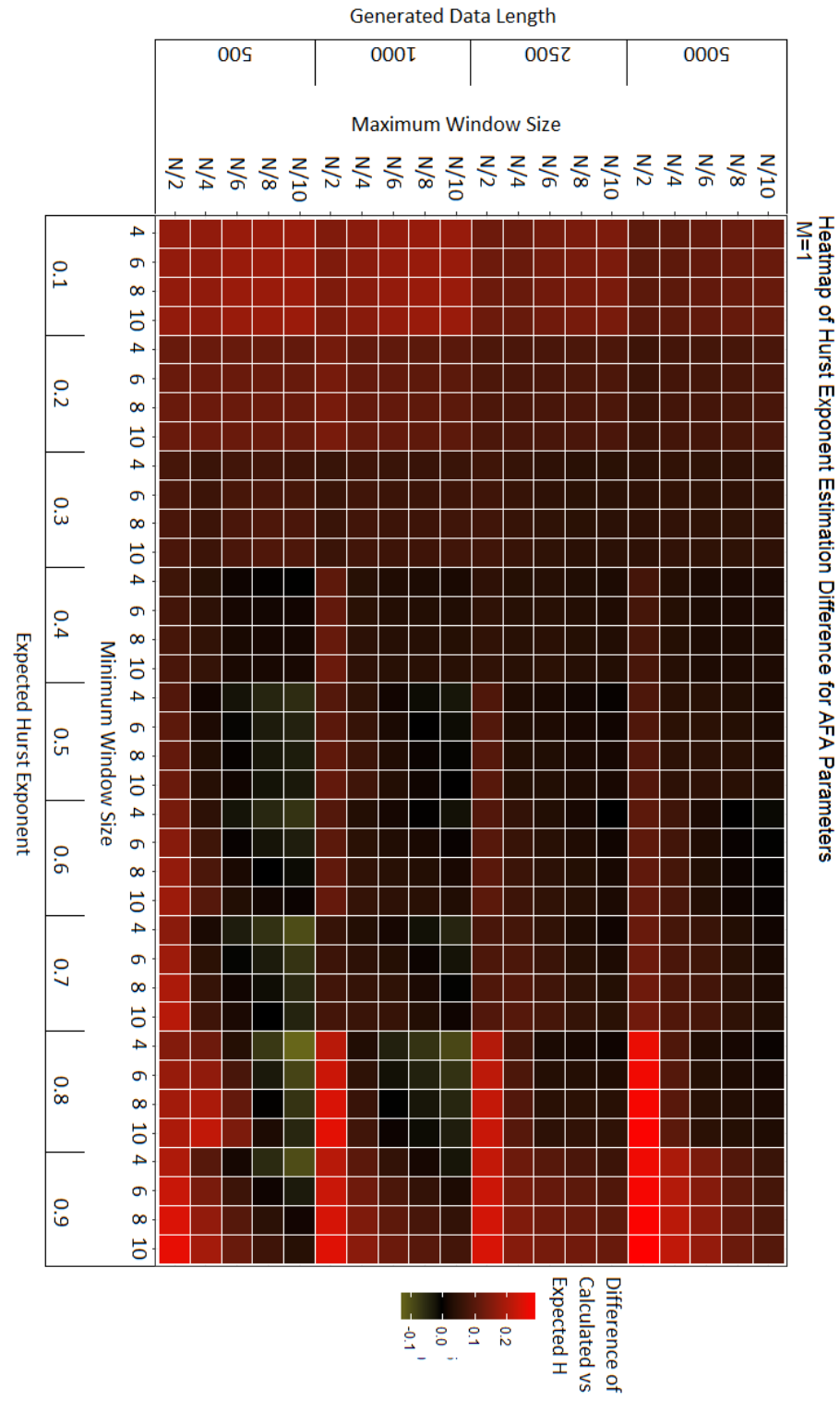

Appendix 2.6: Heatmap showing differences of AFA across all parameters investigated while *M*=2.

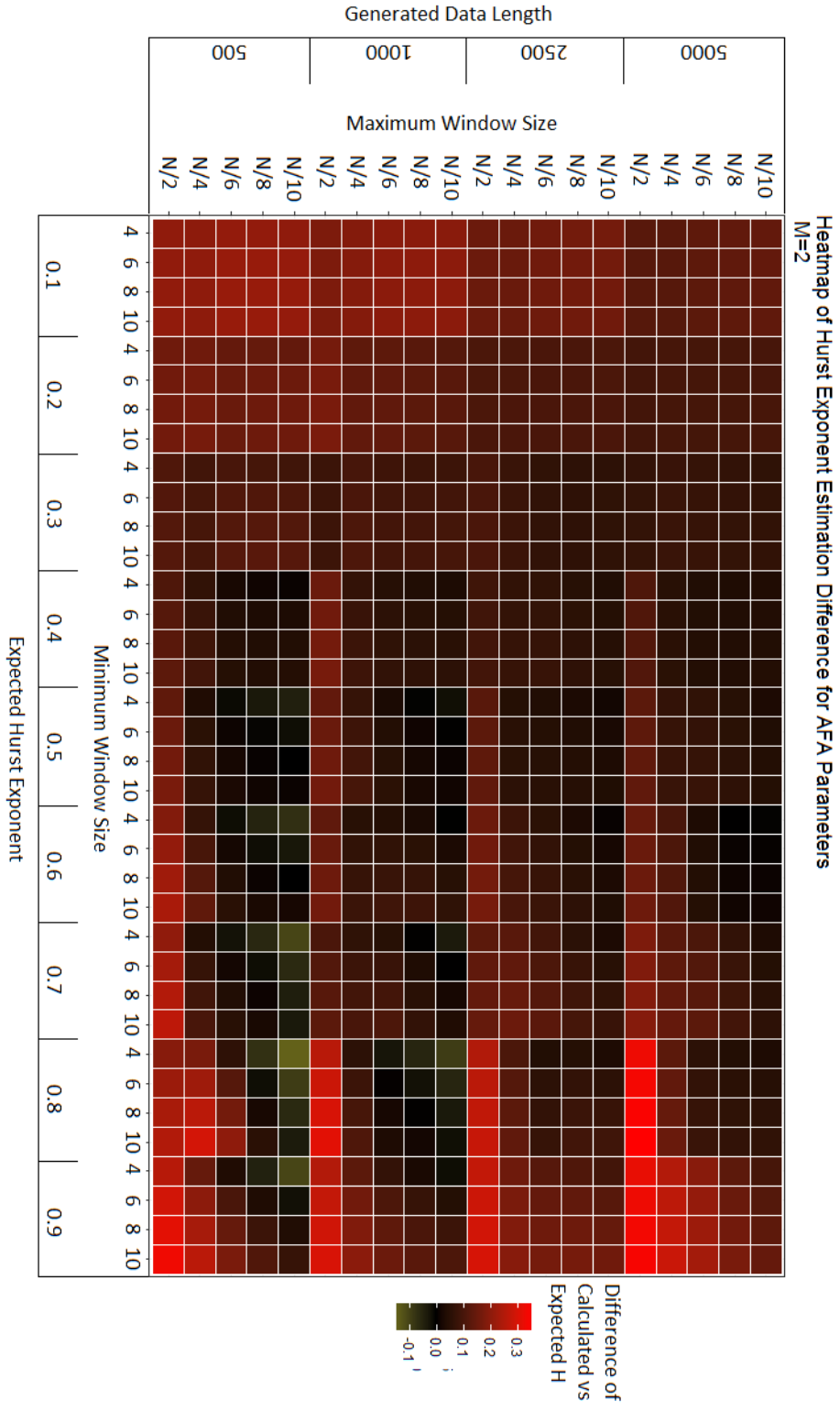

Appendix C: MATLAB Code for Chapter 3 Analysis

i. Generation of Simulated fBm Data

The file “generator.m” uses the function “SimfBm.m”, generated in collaboration with Dr. Jarod Hart to use stochastic integral approximations to input a desired data length and Hurst exponent and output data that exhibits that fractal trend.

```
%Melanie Weilert
%Biodynamics Lab
clear all; clc

%Generation of Simulated Data:
%(1) Generate a data set of N+500 samples [8 iterations]
%(2) Cut off first 500 samples to allow dynamics of simulation to stabilize
%(3) Repeat steps 1 and 2 for H=0.05:0.05:1 [20 iterations]
%(4) Repeat this 100 times.
%(5) For each iteration, save the simulated data

%Set input values:
N=[50,100,250,500,1000,2500,5000,10000];
H=0.05:0.05:1;

for i=8   %Number of variations of N.
    itxt=num2str(i);
    for j=16:20  %Number of variations of H.
        jtxt=num2str(j);
        for k=1:100   %Number of repetitions of this.
            ktxt=num2str(k);
            [data] = SIMfBm(N(i),H(j)); %%FUNCTION
            %%%%%%%%%%%%%%%%%%%%%%%%%%%%%%%%%%%%%%%%%%%%%%%%%%
            %FUNCTION CONTENT
     % Author:      Jarod Hart and Melanie Weilert
% Date:        5/11/2016

% Description:  This is a function that generates a fractional Brownian
% motion signal.  The inputs n and H indicate the length of the desired
% simulated signal and the desired Hurst exponent.  The method comes from
% approximating a stochastic integral from the work of Mandelbrat and Van
% Ness.

% Inputs:
%      n       - An integer, the desired length of the output signal
%      H       - A real number 0<H<=1, the desired Hurst exponent of the
%                output signal.

% Outputs:
%      fBm     - An n x 1 vector, simulated fractional Brownian motion
%                with Hurst exponent H.

% Resources:    This code was adapted from the following paper:

%              "Simulation and identification of the fractional Brownian
%              motion: a bibliographical and comparative study" by
```

```
%           Jean-Francois Coerujolly.  Available at:
%              www.jstatsoft.org/article/view/v005i07/simest.pdf

%           The origins of this method go back to the work of
%           Mandelbrot and Van Ness:

%           "Fractional Brownian motions, fractional noises and
%           applications," SIAM review, Vol. 10, pp. 422-437.


function [fBm] = SIMfBm(n,H)

dB1=normrnd(0,1,1,n);
borne=floor(n^1.5);
dB2=normrnd(0,1,1,borne);
fBm=zeros(1,n);
CH=( gamma(2*H+1)*sin(pi*H) )^.5/gamma(H+1/2);

ind1=(1:1:n).^(H-1/2);
ind2=(1:1:(borne+n)).^(H-1/2);

for i=2:1:n
   I1=dB1(i-1:-1:1).*ind1(1:1:i-1);
   I2=( ind2(i+1:1:i+borne)-ind2(1:1:borne) ) .* dB2;
   fBm(i)=sum(I1)+sum(I2);
end
fBm=fBm*n^(-H)*CH;
fBm(1)=0;
end

%%%%%%%%%%%%%%%%%%%%%%%%%%%%%%%%%%%%%%%%%%%%%%%%%%%%%%%%%%%%%%%%%%%%%%%%%%%%%%%
          filename=['generated_data/' itxt '_' jtxt '_' ktxt '.mat'];
          save(filename, 'data')
       end
   end
end
```

ii. AFA and DFA Analysis on Generated fBm Data

The file "Sim6.m" calculates AFA and DFA on data for every combination iteration that is pre-defined in the code. It uses the functions "afa_sim.m" (and its sub-function: "afa_window.m") and "dfa_sim.m" (and its subfunctions: "dfa_my.m" and "dfa_fluct_my.m") in order to accomplish this.

```
%Melanie Weilert
%Biodynamics Lab
% clear all
% clc

%Sim 6: Run a parameter investigation through my simulated data.
   %edit1:Added a parallel run loop to speed things up.
   %edit2:Breaking up the workspace in order to save data.
   %edit3:Elminated structure in order to try a multi-dimensional matrix instead.
   %edit4: Eliminated st as a param and set the number of iterations to
   %20, also switched H to increments of .1
   %edit5:reset the st to only 1 and then reoriented the matrix to:
   %     NEW:      afa_h(nmin,nmax,iteration,order)
   %     OLD:      afa_h(iteration,nmin,nmax,order)

%Input Parameters:
size_code=input('Which size of data do you want to analyze? ');
sizetxt=num2str(size_code);
st=1;     %Size of increment increase

%Upload data into giant 3D matrix.  rows(data)xcols(iterations)x3d(Hsim)

for i=1:20
Htxt=num2str(i);
   for j=1:20  %iteration
   iterationtxt=num2str(j);

      %Load the appropriate data.
      filename=['generated_data/' sizetxt '_' Htxt '_' iterationtxt '.mat'];
      load (filename)

      %Store the data into a big matrix.
      data_store(j,:,i) = data(:);

   end

end
Ntxt=num2str(length(data_store(j,:,i)));

itcounter=1;
counter=1;
```

```
AFA_H=NaN(5,5,20,2);
AFA_SSE=NaN(5,5,20,2);
AFA_R2=NaN(5,5,20,2);
DFA_H=NaN(5,5,20);
DFA_SSE=NaN(5,5,20);
DFA_R2=NaN(5,5,20);
%Begin loops

for Hloop=2:2:20   %For every level of H
Hlooptxt=num2str(Hloop);
clear AFA_H AFA_SSE AFA_R2 DFA_H DFA_SSE DFA_R2 data_store2
   data_store2(:,:)= data_store(:,:,Hloop);
   for iteration=1:20 %For every iteration of each combo

      %Size the data.
      N=length(data_store2(iteration,:));

      counter_nmin=1;
      for n_min=[2,4,6,8,10]
         counter_nmax=1;
         for n_max=floor([N/2,N/4,N/6,N/8,N/10])
            %Insert a check for n_min/max appropriate selection.
            if n_min>=n_max              %Do nothing, skip this combo
            else                         %Run the rest of the code.

                  counter_order=1;
                  for order=1:2          %AFA only investigation

%AFA_____________________________________________________________________
[afa_H, afa_SSE, afa_R2]=afa_sim(data_store2(iteration,:)', N, n_max, n_min, st, order);

%%%%%%%%%%%%%%%%%%%%%%%%%%%%%%%%%%%%%%%%%%%%%%%%%%%
%FUNCTION CONTENT

%This function will run my AFA code given the proper inputs and spit out
%the values I need (H, SSE, and R^2).

function [lF_AFA, lw_AFA, afa_H, afa_SSE, afa_R2]=afa_sim(data, n_max, n_min, st, order)
N=length(data);
%Open up new paths for running functions.
currentPath = fileparts(mfilename('fullpath'));
addpath(fullfile(currentPath, 'afa_functions'))
counter=1;
%Break data into each window INCREMENT
for i=0:st:n_max-n_min
%Break the data into windows j=
   window_size=n_min+i;              %How big are the windows?

%Calculate AFA
   [F_val,w_val]=afa_window(data, N, window_size, order);

%%%%%%%%%%%%%%%%%%%%%%%%%%%%%%%%%%%%%%%%%%%%%%%%%%%
%FUNCTION CONTENT

%Purpose: Takes in the data, data length, and respective window size.
%%%%%%%%%%%%%%%%%%Calculates ?
```

```
function [F_val,w_val]=afa_window(y, N, w,order)
y_global = zeros(N, 1);          %Create new matrix to clear the old one.

n = floor((w - 1) / 2);          %Determines n from w in integers
   M = floor(N / (w)); %+1));         %# of windows
   L = 1 : n + 1;                %L as defined by Riley (pg 3, eqn1): length of window OVERLAP
   w1 = 1 - (L - 1) / n;           %weighted 1 ratios
   w2 = (L - 1) / n;              %weighted 2 ratios

   for j = 1 : M                 %Calculates for each window ITSELF (within size Increments)
      switch(j)
         case 1
            t1 = 1 : w;                %Window of w#1
            t2 = n + 2 : w + n + 1;         %Window of w#2
            d1 = polyfit(t1',y(t1),order);  %Polyfit of w1
            d2 = polyfit(t2',y(t2),order);  %Polyfit of w2
            stitch_d1 = polyval(d1,t1);     %Curve 1 plot points of stitch
            stitch_d2 = polyval(d2,t2);     %Curve 2 plot points of stitch
            y_global(L) = stitch_d1(L);        %v(i)'s first segment
            if rem(w,2)~=0
               y_global(L + (n)) = w1 .* stitch_d1(L + n)+ w2 .* stitch_d2(L); %the '+1' is the result of flooring
consistencies
            else
               y_global(L + (n+1)) = w1 .* stitch_d1(L + n)+ w2 .* stitch_d2(L); %the '+1' is the result of flooring
consistencies
            end
         case M
            index = find(y_global, 1, 'last');
            y_global(L + index) = w1 .* mid_stitch(L + n) + w2 .* stitch_d1(L);

         otherwise
            index = find(y_global, 1, 'last');
            t1 = (j - 1) * w + 1 : j * w + 1;
            t2 = (j - 1) * w + 1 + (n + 1) : j * w + 1 + (n + 1);
            d1 = polyfit(t1',y(t1),order);
            d2 = polyfit(t2',y(t2),order);
            stitch_d1 = polyval(d1,t1);
            stitch_d2 = polyval(d2,t2);
            y_global(L + index) = w1 .* mid_stitch(L + n) + w2 .* stitch_d1(L);
            if rem(w,2)~=0
               y_global(L + index + (n)) = w1 .* stitch_d1(L + n)+ w2 .* stitch_d2(L);
            else
               y_global(L + index + (n+1)) = w1 .* stitch_d1(L + n)+ w2 .* stitch_d2(L);
            end
      end
      mid_stitch = stitch_d2;
   end

   y_global(y_global == 0) = [];
   %Depending on the parameters, you have to resize your matrices.

   if length(y_global)> length(y)
      N_new = length(y);
   else
      N_new = length(y_global);
   end
```

```
    yy = (y(1:N_new) - y_global(1:N_new));                    %u(i)-v(i)
    F_val= sqrt((1 / N_new) * sum(yy .^ 2));  %# of windows examined
    w_val= w;
end

%%%%%%%%%%%%%%%%%%%%%%%%%%%%%%%%%%%%%%%%%%%%%%%%%%%%%%%%%%%%%%%%%%%


%Store the values
    F(counter,1)=F_val;
    w(counter,1)=w_val;

counter=counter+1;
end

%Convert to log plots.
lF_AFA = log2(F);
lw_AFA = log2(w);

%AFA
    p_AFA=polyfit(lw_AFA,lF_AFA,1);
    yfit_AFA=polyval(p_AFA, lw_AFA);
    yresid_AFA=lF_AFA-yfit_AFA;
    SSE_AFA=sum(yresid_AFA.^2);
    SStotal_AFA=(length(lF_AFA)-1*var(lF_AFA));
    rsq_AFA= 1-SSE_AFA/SStotal_AFA;

afa_H=p_AFA(1);
afa_SSE=SSE_AFA;
afa_R2=rsq_AFA;

end

%%%%%%%%%%%%%%%%%%%%%%%%%%%%%%%%%%%%%%%%%%%%%%%%%%%%%%%%%%%%%%%%%%%%%%

%Create a 5D matrix that will store everything.
AFA_H(counter_nmin,counter_nmax,iteration,counter_order)=afa_H;
AFA_SSE(counter_nmin,counter_nmax,iteration,counter_order)=afa_SSE;
AFA_R2(counter_nmin,counter_nmax,iteration,counter_order)=afa_R2;

                counter_order=counter_order+1;
            end

%DFA________________________________________________________________________
[dfa_H, dfa_SSE, dfa_R2]=dfa_sim(data_store2(iteration,:), n_max, n_min, st);

%%%%%%%%%%%%%%%%%%%%%%%%%%%%%%%%%%%%%%%%%%%%%%%%%%%%%%%%%%%%%%%%%%%
%FUNCTION CONTENT

%This function will run my DFA code given the proper inputs and spit out
%the values I need (H, SSE, and R^2).

function [lF_DFA, lw_DFA, dfa_H, dfa_SSE, dfa_R2]=dfa_sim(data, n_max, n_min, st)

 %Open up new paths for running functions.
currentPath = fileparts(mfilename('fullpath'));
```

```
addpath(fullfile(currentPath, 'dfa_functions'))

[F_DFA, w_DFA] = dfa_my(data, n_min, n_max, st);

%%%%%%%%%%%%%%%%%%%%%%%%%%%%%%%%%%%%%%%%%%%%%
%FUNCTION CONTENT

 %DFA Code: Original code obtained at the Nonlinear Analysis Workshop run by the Biomechanics Department
and Dr. Nick Stergiou in Summer of 2017. Code is restructured and edited for my purposes of a parameter study.

function [F, w] = dfa_my(data, n_min, n_max, st)
% DFA Given time series, returns detrended fluctuation analysis scaling exponent
%
% ts:        input time series
% n_min:      minimum box size (default n_min = 16)
% n_max:      maximum box size (default n_max = N/9)
% n_length:   number of points to sample best fit
% plotOption: plot log F vs. log n? (default true)
%
% a:         DFA scaling exponent
% r2:        r^2 value for best fit line
%
% References:
%
% Damouras, S., Chang, M. D., Sejdi, E., & Chau, T. (2010). An empirical
% examination of detrended fluctuation analysis for gait data. Gait &
% posture, 31(3), 336-340.
%
% Mirzayof, D., & Ashkenazy, Y. (2010). Preservation of long range
% temporal correlations under extreme random dilution. Physica A:
% Statistical Mechanics and its Applications, 389(24), 5573-5580.
%
% Peng, C. K., Havlin, S., Stanley, H. E., & Goldberger, A. L. (1995).
% Quantification of scaling exponents and crossover phenomena in
% nonstationary heartbeat time series. Chaos: An Interdisciplinary Journal
% of Nonlinear Science, 5(1), 82-87.

%My revisions to this in order to have parameters: nmin, nmax, st, length
counter=1;
%Break data into each window INCREMENT
for i=0:st:n_max-n_min
%Break the data into windows j=
   window_size=n_min+i;               %How big are the windows?

%Calculate DFA
   [F_val,w_val] = dfa_fluct_my(data, window_size);

%%%%%%%%%%%%%%%%%%%%%%%%%%%%%%%%%%%%%%%%%%%%%
%FUNCTION CONTENT

%Extracts F from the time series (ts) of window size.

function  [F_val,w_val] = dfa_fluct_my(data, window_size)
%DFA_FLUCT Returns average detrended fluctuations in time series as a function of box size
%
% Deals with outlier and NaN values by removing them from the
% analysis while preserving the temporal order, essentially leaving a
```

```
% 'hole' in the data, rather than truncating the time series. This method
% is shown in Mirzayof and Ashkenazy (2010) to preserve alpha in
% experimental data even under extreme (>90%) dilution.
%
% ts:   input time series
% n/window_size:    vector of box sizes
% F:    vector of fluctuations
%
% Requires INPAINT_NANS by John D'Errico

currentPath = fileparts(mfilename('fullpath'));
addpath(fullfile(currentPath, 'Inpaint_nans', 'Inpaint_nans'));

% References:
%
% Mirzayof, D., & Ashkenazy, Y. (2010). Preservation of long range
% temporal correlations under extreme random dilution. Physica A:
% Statistical Mechanics and its Applications, 389(24), 5573-5580.
%
% Peng, C. K., Havlin, S., Stanley, H. E., & Goldberger, A. L. (1995).
% Quantification of scaling exponents and crossover phenomena in
% nonstationary heartbeat time series. Chaos: An Interdisciplinary Journal
% of Nonlinear Science, 5(1), 82-87.

if size(data, 1) > size(data, 2) % ts should be row vector
   data = data';
end

zero_th = .000001; % F < this value is equivalent to F = 0
num_boxes = floor(length(data)/window_size); %number of boxes

clear B y y_n;
B = data(1:num_boxes*window_size);
N = length(B); %Resizes it without the extra tail-end data

   % "the ... time series (of total length N) is first
   % integrated, y(k) = sum(i=1:k)(B(i) - B_ave), where B(i) is the ith
   % [value of the time series] and B_ave is the average [value]"
   B_ave = nanmean(B);
   B_nonan = inpaint_nans(B); % deal with NaN values for integration step (see inpaint_nans comments for details)
   y_nonan = cumsum(B_nonan - B_ave);
   y = y_nonan;
   y(isnan(B)) = NaN; % replace NaN values in integrated series

% "the integrated time series is divided into boxes of equal length, n"
   for k = 0: num_boxes - 1

      % "in each box of length n, a least-squares line is fit to the data
      % (representing the trend in that box) ... denoted by y_n(k)"
      clear X Y;
      X = k*window_size + 1:(k + 1)*window_size;
      Y = y_nonan(X); % fit using interpolated series
      m_b = polyfit(X, Y, 1);
      y_n(X) = polyval(m_b, X);
   end

   % "detrend the integrated time series, y(k), by subtracting the local
```

```
    % trend, y_n(k) .... The root-mean-square fluctuation ... is calculated
    % by [Equation 1]"
F2 = nanmean((y - y_n).^2); % ignores NaN values
F_val = sqrt(F2);

% "This computation is repeated over all time scales (box sizes)"
% "the fluctuations can be characterized by a scaling exponent a, the slope
% of the line relating log F(n) to log n"
F_val(F_val < zero_th) = NaN; % removes F = 0 from linear fit
w_val=window_size;
end

%%%%%%%%%%%%%%%%%%%%%%%%%%%%%%%%%%%%%%%%%%%%%%%%%%%%%%%%%%%%%%%%%%%%%%%
%Store the values
    F(counter,1)=F_val;
    w(counter,1)=w_val;

counter=counter+1;
end
end
%%%%%%%%%%%%%%%%%%%%%%%%%%%%%%%%%%%%%%%%%%%%%%%%%%%%%%%%%%%%%%%%%%%%%%%

lF_DFA=log10(F_DFA);
lw_DFA=log10(w_DFA);

%Compare the results regarding linear regression.
%DFA
    p_DFA=polyfit(lw_DFA,lF_DFA,1);
    yfit_DFA=polyval(p_DFA, lw_DFA);
    yresid_DFA=lF_DFA-yfit_DFA;
    SSE_DFA=sum(yresid_DFA.^2);
    SStotal_DFA=(length(lF_DFA)-1*var(lF_DFA));
    rsq_DFA= 1-SSE_DFA/SStotal_DFA;

dfa_H=p_DFA(1);
dfa_SSE=SSE_DFA;
dfa_R2=rsq_DFA;
 end
%%%%%%%%%%%%%%%%%%%%%%%%%%%%%%%%%%%%%%%%%%%%%%%%%%%%%%%%%%%%%%%%%%%%%%%
%Create a structure that will store everything.
DFA_H(counter_nmin,counter_nmax, iteration)=dfa_H;
DFA_SSE(counter_nmin,counter_nmax,iteration)=dfa_SSE;
DFA_R2(counter_nmin,counter_nmax,iteration)=dfa_R2;


            end %if check
            counter_nmax=counter_nmax+1;
          end %nmax
          counter_nmin=counter_nmin+1;
       end %nmin
       itcounter=itcounter+1
    end %iteration
    counter=1+counter;
    %Specify saving the N__ _ H___
    filename_ws=['N' Ntxt '_H' Hlooptxt];
    save(filename_ws,'AFA_H','AFA_SSE','AFA_R2','DFA_H','DFA_SSE','DFA_R2')
end %H level
```

Appendix D: MATLAB Code for Chapter 4 Analysis

i. Extraction and Preparation of Participant Data

The file "Extraction_Code.m" is code that extracts PD COP data from a force plate, analyzes and calculates desired sway parameters, and saves these calculated values into an excel sheet and .m files. "Extraction_Code.m" is a combination of these functions: "sway_info_mild.m", "sway_info_mod.m", "calb3364a.m", "calb3477a.m", "combineFP_KUMC.m", "combineFP_Lawrence", "COP_gen.m", "sway.m", "radius.m", and "derivative.m". This code was originally created by Dr. Carl Luchies and derived from the dissertation of Annaria Barnds, a member of the Biodynamics Lab in Lawrence, KS. It was repurposed to meet the needs of this study.

```
%Melanie Weilert
%Biodynamics Lab
%September 26th, 2016

%Extraction Code: Extract all 2007/2009 PD data and exports
%them into .mat files for analysis.

clear
clc
istart = 1:6;

num_trials = 6;  %total # of sway trials performed
mm2m = 1/1000;
m2mm = 1000;
N2lbs = 0.224808942443;
%Prompt for user to input Subject Number to be analyzed
studytype = input('What Study Do You Want To Upload?');
% 1 == mild study
% 2 == moderate study

subjectnum=input('What Subject Numbers Do You Want To Analyze (enter 0 to run all)?');
if studytype == 1 && subjectnum == 0
   subjectnum = [1001 1003 1006 1007 1008 1009 1010 1011 1012 1013 1014 3001 3002 3003 3004 3005 3006
3008 3009 3010 3011 3013 3014];
elseif studytype == 2 && subjectnum == 0
   subjectnum = [1001 1002 1003 1004 1005 1006 1007 1008 1009 1010 4001 4002 4004 4005 4006 4007 4008
4009 4010 4011 4012];
end

loopcount = 1;
dwnsmpl_freq = 100;
trial_time = 30;
t_dwnsmpl = 1/dwnsmpl_freq : 1/dwnsmpl_freq : trial_time;
```

```
isubj = 1;

for i = 1:length(subjectnum)
   itxt =int2str(subjectnum(i));
   ktxt = int2str(studytype);

   for j = 1:num_trials
      jtxt = int2str(j);

      if studytype ==1

         fsample_an = 1080;  %sampling frequency, Hz
         dt_an = 1/fsample_an;
         tsample = 30;   %sampling time, sec
         t_an = dt_an:dt_an:tsample;
         %upload order of sway trials (EO = 1, EC = 2) and other data
         [trial_order, age, gender, yrs_since_diag, effected_side, falling,sensory, activities_daily_living, posture,
postural_instab,motor_exam, total_UPDRS, schwab, PIGD, height,leg_length, foot_length, weight, thigh_length,
calf_length, ankle_height, foot_width] = sway_info_mild(subjectnum(i));

         datacheck = [ktxt,'_',itxt, '_', jtxt];
         %path(path, 'C:\Users\Annaria\Documents\Annaria Research\Sway MATLAB Analysis');
         %path(path, 'C:\Users\nardonea\Desktop\Annnaria_Research\Sway_MATLAB_Analysis');
         A = exist([ktxt,'_',itxt, '_', jtxt,'.mat']);
         if A ==2
            load([ktxt,'_',itxt, '_', jtxt,'.mat']);

         else
            %upload the sway trials for selected subject numbers
            datapath_an = ['Sway_Data_Files\Mild\s',itxt,'\sway',jtxt '.txt'];

            if subjectnum(i)== 1009 && j ==1
               %this is necessary because the subject steps off the plate
               %at the very end of the trial
               data_an = dlmread(datapath_an,'\t',1,0);
               data_an = data_an(1:30000,:);
               data_an = downsample(data_an,10);

               filename = [ktxt,'_',itxt, '_', jtxt];


            elseif subjectnum(i)== 3013
               %this is necessary because there is a header for subject
               %3013 that is not there for any other subjects
               data_an = dlmread(datapath_an,'\t',8,0);
               data_an = downsample(data_an,10);
               data_an= resample(data_an,9260,1000);
               data_an = downsample(data_an,10);

               filename = [ktxt,'_',itxt, '_', jtxt];

            else
               %this is the "general" upload that ensure only 30 seconds
               %of data are uploaded
               data_an = dlmread(datapath_an,'\t',1,0);

               data_an = data_an(1:32400,:);
```

```
            data_an = downsample(data_an,10);
            data_an= resample(data_an,9260,1000);
            data_an = downsample(data_an,10);

            filename = [ktxt,'_',itxt, '_', jtxt];

        end
    end

elseif studytype ==2

    fsample_an = 1000;          %sampling frequency, Hz
    dt_an = 1/fsample_an;
    tsample = 30; %sampling time, sec
    t_an = dt_an:dt_an:tsample;
    %upload order of sway trials (EO = 1, EC = 2) and the zero trial
    [trial_order, zeros, age, gender, yrs_since_diag, effected_side, falling,sensory, activities_daily_living,
posture, postural_instab, motor_exam, total_UPDRS, schwab, PIGD, height, leg_length, foot_length, weight,
thigh_length, calf_length, ankle_height, foot_width] = sway_info_mod(subjectnum(i));

    zeros = mean(zeros);

    datacheck = [ktxt,'_',itxt, '_', jtxt];
    %path(path, 'C:\Users\Annaria\Documents\Annaria Research\Sway MATLAB Analysis\Saved Sub Mfiles');
    A = exist([ktxt,'_',itxt, '_', jtxt,'.mat']);
    if A ==2
        load([ktxt,'_',itxt, '_', jtxt,'.mat']);

    else

        %upload the sway trials for selected subject numbers
        datapath_an = ['Sway_Data_Files\Moderate\s',itxt,'\sway',jtxt];
        data_an = dlmread(datapath_an,'\t',0,0);
        data_an = downsample(data_an,10);

        filename = [ktxt,'_',itxt, '_', jtxt];
    end
end

%calibrate and zero force plate data for FP 1 and 2 (only 2 active
%FPs for this experiement)
%forceplate that has the right foot on it for sway task (upper R
%looking at bulls eye in lab)
if studytype ==1
    fp_left = data_an(:,10:15);
    fp_right = data_an(:,16:21);

elseif studytype ==2
    %convert units to N and Nm
    fp_right = calb3364a(data_an(:,1:6),zeros(:,1:6), istart);

%%%%%%%%%%%%%%%%%%%%%%%%%%%%%%%%%%%%%%%%%%%%%%%%%%%%%
%FUNCTION CONTENT

function force=calb3364a(volt,zero,istart);
%
% %This file calibrates the data for the SN#3364 Force Plate
```

```
%
%%%%%%%%%%%%%%%%%%%%%%%%%%%%%%%%%%%%%%%%%%%%%%%%%%%%%%%%%%%%%%%%%%%%%%%%%%%%%%%%%%%%%%%%%%%%%%%%%%%%%%%%%%%%%%%%%%%%%%%%%%%

% User must input volt which is the array to be processed along with
% a zeros row vector and the forceplate gain (fpgain).
% The transpose of the cal. matrix is neccessary.
%   volt is the data in volts
%   zero is a row vector of zeros
%   gain_fp is the force plate amp gain
%   istart contains the column of the volt matrix with fp1 data

% KU Biomechanics Lab Force Plate - FP1 SN#3364
gain_fp = 1000;
SIcalmat=[1.506  .003  .01  -.003 -.013  .006;
        -.012 1.513 -.01   .01   .001  .009;
         .001  .002 5.895 -.002  .008  .017;
        -.001  .0    .0    .732 -.002 -.001;
         .0    .0    .0    .001  .732  .003;
         .001  .004 -.02  -.001 -.001  .385];

% SUBTRACT OFF THE ZEROS FROM THE FORCEPLATE MEASUREMENTS

[m,n]=size(volt);
zeross=(zero'*ones(1,m))';
volt(:,istart)=volt(:,istart) - zeross(:,istart);

% USING THE CALIBRATION MATRIX, CONVERT FROM VOLTS TO N AND Nm
% EXTRACT THE FP DATA, CONVERT, THEN PUT IT BACK INTO THE ORIGINAL MATRIX

fp=volt(:,istart);
GF=(1.e6)/(gain_fp*10);
%fp=fp.*1.e6./gain_fp./10;
fp=GF.*fp*SIcalmat';

force=fp;

%%%%%%%%%%%%%%%%%%%%%%%%%%%%%%%%%%%%%%%%%%%%%%%%%%%%%%%%

          fp_left = calb3477a(data_an(:,7:12),zeros(:,7:12), istart);

%%%%%%%%%%%%%%%%%%%%%%%%%%%%%%%%%%%%%%%%%%%%%%%%%%%%%%%%
%FUNCTION CONTENT

function[force] = calb3477a(volt,zero,istart);
%
gain_fp = 1000;

SIcalmat=[1.498  -.002   .004    .003    -.006   .011;
    .006   1.500   .001    -.014   .003    .015;
    -.002  .016    5.930   -.001   .003    .000
    .001   -.001   .0      .740    -.003   -.001;
    -.001  .0      .0      .002    .740    .001;
    .0     .003    -.002   .0      .001    .383];
% SUBTRACT OFF THE ZEROS FROM THE FORCEPLATE MEASUREMENTS
```

```
[m,n]=size(volt);
zeross=(zero'*ones(1,m))';
volt(:,istart)=volt(:,istart) - zeross(:,istart);

% USING THE CALIBRATION MATRIX, CONVERT FROM VOLTS TO N AND Nm
% EXTRACT THE FP DATA, CONVERT, THEN PUT IT BACK INTO THE ORIGINAL MATRIX

fp=volt(:,istart);
GF=(1.e6)/(gain_fp*10);
%fp=fp.*1.e6./gain_fp./10;
fp=GF.*fp*SIcalmat';

force=fp;

%%%%%%%%%%%%%%%%%%%%%%%%%%%%%%%%%%%%%%%%%%%%%%%%%%%%%%%%%%%%%%%%%%%%%%%
        fp_left = FP_m2mm(fp_left, m2mm);

%%%%%%%%%%%%%%%%%%%%%%%%%%%%%%%%%%%%%%%%%%%%%%%%%%%%%%%%%%%%%%%%%%%%%%%
%FUNCTION CONTENT

function[FP_in_mm] = FP_m2mm(FP_in_mm, m2mm);

FP_in_mm(:,1) = FP_in_mm(:,1);
FP_in_mm(:,2) = FP_in_mm(:,2);
FP_in_mm(:,3) = FP_in_mm(:,3);

FP_in_mm(:,4) = FP_in_mm(:,4).*m2mm;
FP_in_mm(:,5) = FP_in_mm(:,5).*m2mm;
FP_in_mm(:,6) = FP_in_mm(:,6).*m2mm;

%%%%%%%%%%%%%%%%%%%%%%%%%%%%%%%%%%%%%%%%%%%%%%%%%%%%%%%%%%%%%%%%%%%%%%%
        fp_right = FP_m2mm(fp_right, m2mm);
    end

    if studytype ==1
        %where x points anterior, y points 'lateral' (to the right)
        FP = combineFP12_KUMC(fp_left, fp_right);
%%%%%%%%%%%%%%%%%%%%%%%%%%%%%%%%%%%%%%%%%%%%%%%%%%%%%%%%%%%%%%%%%%%%%%%
%FUNCTION CONTENT

%Annaria N. Barnds
%started: August 2012
%this function combines the analog data of force plates 1 and 2 into an
%equivalent combined force-moment system
function[FP] = combineFP12_KUMC(fp_left_f, fp_right_f)
%where:
%fp_right_f is the calibrated analog data of FP 1 (3364)
%fp_left_f is the calibrated analog data of FP 2 (3477)
d = 231.5;



    %combined Fx components
        FP(:,1) = fp_left_f(:,1) + (-fp_right_f(:,1));
        %combined Fy components
        FP(:,2) =fp_left_f(:,2) + (-fp_right_f(:,2));
        %combined Fz components
```

```
        FP(:,3) =fp_left_f(:,3) + (fp_right_f(:,3));
        %combined Mx components
        FP(:,4) =fp_left_f(:,4) + (-fp_right_f(:,4) +...
           d*(fp_left_f(:,3)+fp_right_f(:,3)));
        %combined My components
        FP(:,5) =fp_left_f(:,5) + (-fp_right_f(:,5));
        %combined Mz components
        FP(:,6) =fp_left_f(:,6) + (fp_right_f(:,6)+...
           -d*(fp_left_f(:,1) + fp_right_f(:,1)));


%          %new coordinate system

%          x
%          ^
%          |
%          |
%          |
%          |
%          - - - - - - > y
%


%%%%%%%%%%%%%%%%%%%%%%%%%%%%%%%%%%%%%%%%%%%%%%%%%%%%%%%%%%%%%%%%%%%%%%%%
      elseif studytype ==2
         %where x points 'lateral' (to R), y points posterior
         FP= combineFP12_Lawrence(fp_right, fp_left);
      end
 %%%%%%%%%%%%%%%%%%%%%%%%%%%%%%%%%%%%%%%%%%%%%%%%%%%%%%%%%%%%%%%%%%%%%%%%
%FUNCTION CONTENT

%Annaria N. Barnds
%started: August 2012
%this function combines the analog data of force plates 1 and 2 into an
%equivalent combined force-moment system
function[data_calb_FP12] = combineFP12_Lawrence(data_calb_FP1, data_calb_FP2)
%where:
%data_calb_FP1 is the calibrated analog data of FP 1 (3364)
%data_calb_FP2 is the calibrated analog data of FP 2 (3477)

% in mm, distance from center of FP to the edge of FP
d = 232;


%combined Fx components
data_calb_FP12(:,1) = data_calb_FP1(:,1) + data_calb_FP2(:,1);
%combined Fy components
data_calb_FP12(:,2) = data_calb_FP1(:,2) + data_calb_FP2(:,2);
%combined Fz components
data_calb_FP12(:,3) = data_calb_FP1(:,3) + data_calb_FP2(:,3);
%combined Mx components
data_calb_FP12(:,4) = data_calb_FP1(:,4) + data_calb_FP2(:,4);
%combined My components
data_calb_FP12(:,5) = data_calb_FP1(:,5) + data_calb_FP2(:,5)+...
   data_calb_FP2(:,3).*d - data_calb_FP1(:,3).*d;
%combined Mz components
data_calb_FP12(:,6) = data_calb_FP1(:,6) + data_calb_FP2(:,6)+...
```

```
   data_calb_FP1(:,2).*d - data_calb_FP2(:,2).*d;


%          %new coordinate system

%          - - - - - - > x
%          |
%          |
%          |
%          |
%          |
%          y

%%%%%%%%%%%%%%%%%%%%%%%%%%%%%%%%%%%%%%%%%%%%%%%%%%%%%%%%%%%%%%%%%%%%%%%

      %calculate COP in the x and y direction for trial duration in mm
      % WHERE:
      %+x = anterior, -x = posterior
      %+y = lateral (to R), +y = medial (to L)
      %COP_gen function makes the KUMC and Lawrence studies now have the
      %same coordinate system
      [COP_x, COP_y] = COP_gen(FP,studytype);

%%%%%%%%%%%%%%%%%%%%%%%%%%%%%%%%%%%%%%%%%%%%%%%%%%%%%%%%%%%%%%%%%%%%%%%
%FUNCTION CONTENT

function[COP_x,COP_y, COP] = COP_gen(data_calb, studytype)
%This file finds the COP in the x and y direction
%data_calb = calibrated data for which you want to find COP x and y
%COP_x = location of COP in x for each trial
%COP_y = location of COP in y for each trial
%studytype == 1 is mild study; ==2 is moderate study
%%%%%%%%%%%%%%%%%%%%%%%%%%%%%%%%%%%%%%%%%%%%%%%%%%%%%%%%%%%%%%%%%%%%%%%
%%%%%%%%%%%%%%%%%%
dz = .038;
idata = size(data_calb);
for j=1:idata
   if    studytype == 1
      COP_x(j,:) =(-(data_calb(j,5)+data_calb(j,1)*dz)./data_calb(j,3));
      COP_y(j,:) = (data_calb(j,4)-data_calb(j,2)*dz)./ data_calb(j,3);
   elseif studytype ==2
      COP_y(j,:) = (-(data_calb(j,5)+data_calb(j,1)*dz)./data_calb(j,3)); %calculating location of center of pressure
in x
      COP_x(j,:) =-(data_calb(j,4)-data_calb(j,2)*dz)./ data_calb(j,3);    %calculating location of center of pressure in
y
   end

   COP(j,:) = sqrt(COP_x(j,:).^2+COP_y(j,:).^2);
end
%coordinate system
%          x (anterior is positive)
%          ^
%          |
%          |
%          |
%          _____________> y (lateral is positive)
```

```
%%%%%%%%%%%%%%%%%%%%%%%%%%%%%%%%%%%%%%%%%%%%%%%%%%

    COP = sqrt( COP_x.^2 + COP_y.^2);
    %normalizing data so COP trajectory starts at (0,0)
    COP_x_zeroed = COP_x -mean(COP_x(1:5));
    COP_y_zeroed = COP_y -mean(COP_y(1:5));
    NNN= size(COP_x);
    %plot(1:3001, COP_x_zeroed)
    %       COP quality check (commented out below)
    %       %%%%see below for plot code to insert here

%       length_data = length(data_an);
%       indices = 1:length_data;
%       figure
%       plot(indices,COP_x-mean(COP_x(1:10,:)))
    %       %COP PATH FIGURE (commented out below)
    %       %%%%see below for plot code to insert here

    %SWAY CALCULATIONS
    [COP_tot_dist, COPx_tot_dist, COPy_tot_dist, COP_range_AP, COP_range_ML, radius_enc, sway_area,
RMS_COP,RMS_COP_x, vel_mean, vel_mean_x, vel_mean_y,acc_mean, acc_mean_x,
acc_mean_y,peak_COP_speed, peak_COP_speed_x, peak_COP_speed_y, med_freq_AP, peak_COP_acc,
peak_COP_acc_x, peak_COP_acc_y, vel, vel_x, vel_y] = sway(COP_x,COP_y,dt_an, trial_time);

%%%%%%%%%%%%%%%%%%%%%%%%%%%%%%%%%%%%%%%%%%%%%%%%%%
%FUNCTION CONTENT


%this function calculates the total distance that the COP as well as the
%total distance traveled in the x (typically AP) and y (typically ML)
%
%%%%%%%%%%%%%%%%%%%%%%%%%%%%%%%%%%%%%%%%%%%%%%%%%%%%%%%%%%%
%%%%%%%%%%%%%%%%%%%%%%%%%

function [COP_tot_dist, COPx_tot_dist, COPy_tot_dist, COP_range_AP, COP_range_ML, radius_enc, sway_area,
RMS_COP,RMS_COP_x, vel_mean, vel_mean_x, vel_mean_y,acc_mean, acc_mean_x,
acc_mean_y,peak_COP_speed, peak_COP_speed_x, peak_COP_speed_y, med_freq_AP, peak_COP_acc,
peak_COP_acc_x, peak_COP_acc_y, vel, vel_X, vel_Y] = sway(COPx,COPy,dt_an,trial_time)

[m n]=size(COPx);

COPx_dist=COPx(2:m)-COPx(1:m-1);
COPy_dist=COPy(2:m)-COPy(1:m-1);

distance_tot=sqrt(COPx_dist.^2 + COPy_dist.^2);
distance_x=sqrt(COPx_dist.^2);
distance_y=sqrt(COPy_dist.^2);
%COP distance (ap, ml, total)
COP_tot_dist=sum(distance_tot);
COPx_tot_dist = sum(distance_x);
COPy_tot_dist = sum(distance_y);

%SWAY RANGE
COPx_max      = max(COPx);
COPx_min      = min(COPx);
COPy_max      = max(COPy);
```

```
COPy_min        = min(COPy);
COP_range_AP   = COPx_max - COPx_min;
COP_range_ML   = COPy_max - COPy_min;

%SWAY AREA
%Function: radius, calculates the radius encompassing COP data and sway area defined
%by area of the convex hulls surrounding the COP data
[radius_enc] = radius(COPx, COPy);

%%%%%%%%%%%%%%%%%%%%%%%%%%%%%%%%%%%%%%%%%%%%%%%%%%%%%%%%%%%%%%%%%%%%%%%%%%%%%%%
%FUNCTION CONTENT
function[radius_enc] = radius(xdata, ydata)
%this function calculates the radius that encompasses a set of x and y data
%xdata = data in x direction
%ydata = data in y direction
%radius_enc = radius that encompasses x and y data
%%%%%%%%%%%%%%%%%%%%%%%%%%%%%%%%%%%%%%%%%%%%%%%%%%%%%%%%%%%%%%%%%%%%%%%%%%%%%%%
%%%%%%%%%%%%%%%%%%%%

%%


%average COP values needed to calculate encompassing radius
xm     = mean(xdata(:,:));
ym    = mean(ydata(:,:));
idata = size(xdata);
for l= 1:idata
   radius(l) = sqrt( (xdata(l,:)-xm).^2 + (ydata(l,:)-ym).^2);
end
radius_enc  = max(radius);

%%%%%%%%%%%%%%%%%%%%%%%%%%%%%%%%%%%%%%%%%%%%%%%%%%%%%%%%%%%%%%%%%%%%%%%%%%%%%%%

[K,sway_area] = convhull(COPx, COPy);

%RMS OF COP ERROR

COP = sqrt(COPx.^2+COPy.^2);
COP_dist_center_sway = COP - mean(COP);
abs_COP_dist_center_sway =sqrt(COP_dist_center_sway.^2);
RMS_COP = mean(abs_COP_dist_center_sway);



COP_dist_center_sway_x = COPx - mean(COPx);
abs_COP_dist_center_sway_x =sqrt(COP_dist_center_sway_x.^2);
RMS_COP_x = mean(abs_COP_dist_center_sway_x);

a=2; %order of the derivative
%Function: derivative, takes the deriv
[vel_AP] = derivative(COPx,a,dt_an);

%%%%%%%%%%%%%%%%%%%%%%%%%%%%%%%%%%%%%%%%%%%%%%%%%%%%%%%%%%%%%%%%%%%%%%%%%%%%%%%
%FUNCTION CONTENT

function [vel,acc] = derivative(x,a,dt)
%This is taken from blackboard:
```

```
% DERIVATIVE.M   Differentiation program to calculate the first and second
%               derivatives of numerical data.  Select either a
%               second (a=1) or fourth (a=2) order accurate scheme.
%   These parameters must be defined before calling this function:
%   dt = time step
%   a = 1 or 2 to chose second or fourth order of accuracy respectively
%%%%%%%%%%%%%%%%%%%%%%%%%%%%%%%%%%%%%%%%%%%%%%%%%%%%%%%%%%%%
%%%%%%%%%%%%%%%%%%%%%%%%%

[m,n] = size(x);

x0  = x(3:m-2,:);
xp1 = x(4:m-1,:);
xp2 = x(5:m,:);
xm1 = x(2:m-3,:);
xm2 = x(1:m-4,:);

%SECOND ORDER ACCURATE VELOCITY SCHEME
if a==1

c0 = 2;
c1 = 0;
c2 = -1;
c3 = 0;
c4 = 1;
c5 = 0;

%FOURTH ORDER ACCURATE VELOCITY
elseif a==2

c0 = 12;
c1 = 1;
c2 = -8;
c3 = 0;
c4 = 8;
c5 = -1;
end

DX = (c1*xm2 + c2*xm1 + c3*x0 + c4*xp1 +c5*xp2)/c0;
vel(3:m-2,:) = DX/dt;

clear c0 c1 c2 c3 c4 c5 DX

%SECOND ORDER ACCURATE ACCELERATION SCHEME
if a==1

c0 = 1;
c1 = 0;
c2 = 1;
c3 = -2;
c4 = 1;
c5 = 0;

%FOURTH ORDER ACCURATE ACCELERATION SCHEME
elseif a==2

c0 = 12;
```

```
c1 = -1;
c2 = 16;
c3 = -30;
c4 = 16;
c5 = -1;
end

DDX = (c1*xm2 + c2*xm1 + c3*x0 + c4*xp1 +c5*xp2)/c0;
acc(3:m-2,:) = DDX/(dt*dt);

% USE FORWARD FORMULAS FOR INITIAL POINTS AND BACKWARD FORMULAS FOR END POINTS
% VEL AND ACC BEING SECOND AND FIRST ORDER ACCURATE RESPECTIVELY

vel(1,:)     = (-3*x(1,:)+4*x(2,:)-x(3,:))/2/dt;
vel(2,:)     = (-3*x(2,:)+4*x(3,:)-x(4,:))/2/dt;

acc(1,:)     = (x(1,:)-2*x(2,:)+x(3,:))/(dt*dt);
acc(2,:)     = (x(2,:)-2*x(3,:)+x(4,:))/(dt*dt);

vel(m-1,:) = (x(m-3,:)-4*x(m-2,:)+3*x(m-1,:))/2/dt;
vel(m,:) = (x(m-2,:)-4*x(m-1,:)+3*x(m,:))/2/dt;

acc(m-1,:) = (x(m-3,:)-2*x(m-2,:)+x(m-1,:))/(dt*dt);
acc(m,:) = (x(m-2,:)-2*x(m-1,:)+x(m,:))/(dt*dt);

%%%%%%%%%%%%%%%%%%%%%%%%%%%%%%%%%%%%%%%%%%%%%%

vel_mean_AP = mean(abs(vel_AP));
med_freq_AP = vel_mean_AP / (2*pi*mean(abs(COPx)));

%MAX VELOCITY AND ACCELERATION
%calculates the derivative to find velocity in x and y; and max vel

[vel, acc] = derivative(COP,a,dt_an);
[vel_X, acc_x] = derivative(COPx,a,dt_an);
[vel_Y, acc_y] = derivative(COPy,a,dt_an);
vel_mag = (sqrt( vel_X.^2 + vel_Y.^2 ));
acc_mag = (sqrt( acc_x.^2 + acc_y.^2 ));

vel_mean = mean(vel_mag);
vel_mean_x = mean(abs(vel_X));
vel_mean_y = mean(abs(vel_Y));
% vel_mean = COP_tot_dist/trial_time;
%vel_mean_x = COPx_tot_dist/trial_time;
%vel_mean_y = COPy_tot_dist/trial_time;


peak_COP_speed = (max(vel_mag));
peak_COP_speed_x = (max(abs(vel_X)));
peak_COP_speed_y = (max(abs(vel_Y)));


acc_mean = mean(acc_mag);
acc_mean_x = mean(abs(acc_x));
acc_mean_y = mean(abs(acc_y));

peak_COP_acc = (max(acc_mag));
```

```
peak_COP_acc_x = (max(abs(acc_x)));
peak_COP_acc_y = (max(abs(acc_y)));


%%%%%%%%%%%%%%%%%%%%%%%%%%%%%%%%%%%%%%%%%%%%%%%

    COP_SD = std(COP);
    COP_SD_AP = std(COP_x);
    COP_SD_ML = std(COP_y);
    vel_SD = std (vel);
    vel_SD_AP = std(vel_x);
    vel_SD_ML = std(vel_y);

    %[median_freq,ff,mx] = Spectral_analysis(100,COP);

    if studytype == 1 && subjectnum(i) <3000 && trial_order(j) ==1
        counter = 1;
    elseif studytype ==1 && subjectnum(i) <3000 && trial_order(j) ==2
        counter = 2;
    elseif studytype ==1 && subjectnum(i) >3000 && trial_order(j) ==1
        counter = 3;
    elseif studytype ==1 && subjectnum(i) >3000 && trial_order(j) ==2
        counter = 4;
    elseif studytype ==2 && subjectnum(i) <3000 && trial_order(j) ==1
        counter = 5;
    elseif studytype ==2 && subjectnum(i) <3000 && trial_order(j) ==2
        counter = 6;
    elseif studytype ==2 && subjectnum(i) == 4009 && trial_order(j) ==1
        counter = 3;
    elseif studytype ==2 && subjectnum(i) == 4009 && trial_order(j) ==2
        counter = 4;
    elseif studytype ==2 && subjectnum(i) >3000 && trial_order(j) ==1
        counter = 7;
    elseif studytype ==2 && subjectnum(i) >3000 && trial_order(j) ==2
        counter = 8;

    end
    if counter == 1 || counter == 5
        fallgroup = 1; % HC EO
    elseif counter == 2 || counter == 6
        fallgroup = 2; %HC EC
    elseif counter ==3 && falling == 0 || counter ==7 && falling == 0
        fallgroup = 3; %NF EO
    elseif counter ==4 && falling == 0 || counter == 8 && falling == 0
        fallgroup = 4; %NF EC
    elseif counter ==3 && falling == 1 || counter == 7 && falling == 1
        fallgroup = 5; %F EO
    elseif counter ==4 && falling == 1 || counter == 8 && falling == 1
        fallgroup = 6; %F EC
    end

    %calc_leg_length = thigh_length+calf_length+ankle_height;
    output(loopcount,:) = [counter, fallgroup, subjectnum(i), age, height, gender, weight, thigh_length, calf_length,
ankle_height, foot_length, foot_width ];

    extraction_filename=['E_',ktxt,'_',itxt, '_', jtxt];
    save(extraction_filename)
```

```
        loopcount = loopcount+1;
    end

    isubj = isubj+1;
end
col_header = {'counter', 'fallgroup', 'subjectnum', 'age', 'height', 'gender', 'weight', 'thigh_length', 'calf_length',
'ankle_height','foot_length','foot_width'};
output_by_counter = sortrows(output,1);

if studytype == 1
    xlswrite('results_2007.xls',col_header, 'Sheet1', 'A1');
    xlswrite('results_2007.xls',output_by_counter, 'Sheet1', 'A2');
elseif studytype == 2
    xlswrite('results_2010.xls',col_header,'Sheet1',  'A1');
    xlswrite('results_2010.xls',output_by_counter, 'Sheet1', 'A2');
end
```

ii. Conduct AFA and DFA on Participant Data

The file “analysis.m” performs AFA and DFA on participant data. All AFA and DFA related functions (“afa_sim.m”, dfa_sim.m”, etc) can be found in Appendix C.ii.

```
%Melanie Weilert
%Biodynamics Lab

clear all; clc;
%Analysis code that runs AFA and DFA through each trial.

list=dir('Data/'); %List all files

for i=3:length(list) %264 trials total
   filename1=['Data/' list(i).name]; %Assign each trial to a name
   load(filename1) %Load the trial into MATLAB

   data=COP_x_zeroed; %Switch data to what you want to analyze.

   [lF_AFA, lw_AFA, afa_H, afa_SSE, afa_R2]=afa_sim(data, 300, 4, 1, 1);  %AFA results
   [lF_DFA, lw_DFA, dfa_H, dfa_SSE, dfa_R2]=dfa_sim(data, 300, 4, 1);     %DFA results

   ick=str2num(filename(end));
   ack=trial_order(ick);

   if ack==1 %Eyes open
      filename2=['Data2/' datacheck '_EO'];
      save(filename2)
   else %Eyes closed
      filename3=['Data2/' datacheck '_EC'];
      save(filename3)
   end

end
```

iii. Develop Breakpoints and Test SICc

The files "breakpoints_1slope_v2.m", "breakpoints_2slope.m", and "breakpoints_3slope.m" test the SICc values to determine what the most appropriate scaling region to assign to each trial of participant data is. Associated functions "bp2.m" and "bp3.m" are included in the body of the code.

File: "breakpoints_1slope_v2.m"

```
%Melanie Weilert
%Biodynamics Lab

clear all; clc;
%Slope analysis: Assumption of 1 slope, calculate SICc

%Mild: 11 healthy, 12 mild
mild_pt=[1001 1003 1006 1007 1008 1009 1010 1011 1012 1013 1014 3001 3002 3003 3004 3005 3006 3008 3009
3010 3011 3013 3014];
mild_count=1;
%Mod: 10 healthy, 11 mod
mod_pt=[1001 1002 1003 1004 1005 1006 1007 1008 1009 1010 4001 4002 4004 4005 4006 4007 4008 4009 4010
4011 4012];
mod_count=1;

%%

for i=1:23 %23 Mild Trials
   mild_pt_txt=num2str(mild_pt(i));
   count_eyes=1;

   for EO=1:3
      EO_txt=num2str(EO);
      filename=['Data2/1_' mild_pt_txt '_' EO_txt '_EO.mat'];
      load(filename)

      %AFA
      p_AFA=polyfit(lw_AFA,lF_AFA,1);
      yfit_AFA=polyval(p_AFA, lw_AFA);
      yresid_AFA=lF_AFA-yfit_AFA;
      SSE_AFA=sum(yresid_AFA.^2);
      RSS=SSE_AFA/length(yfit_AFA);
      SICc_AFA=log(RSS/297)+((3*log(297))/(297-3-2));

      slope=p_AFA(1);
      slope_store_AFA(i, count_eyes)=slope;
      %DFA
      p_DFA=polyfit(lw_DFA,lF_DFA,1);
      yfit_DFA=polyval(p_DFA, lw_DFA);
      yresid_DFA=lF_DFA-yfit_DFA;
      SSE_DFA=sum(yresid_DFA.^2);
      RSS_d=SSE_DFA/length(yfit_DFA);
      SICc_DFA=log(RSS_d/297)+((3*log(297))/(297-3-2));

       slope=p_DFA(1);
```

```
        slope_store_DFA(i, count_eyes)=slope;
        %Store it
        storage_AFA(i,count_eyes)=SICc_AFA;
        storage_DFA(i,count_eyes)=SICc_DFA;

        count_eyes=count_eyes+1;
    end

    for EC=1:3
        EC_txt=num2str(EC);
        filename=['Data2/1_' mild_pt_txt '_' EC_txt '_EC.mat'];
        load(filename)

        %AFA
        p_AFA=polyfit(lw_AFA,lF_AFA,1);
        yfit_AFA=polyval(p_AFA, lw_AFA);
        yresid_AFA=lF_AFA-yfit_AFA;
        SSE_AFA=sum(yresid_AFA.^2);
        RSS=SSE_AFA/length(yfit_AFA);
        AICc_AFA=log(RSS/297)+((297+3)/(297-3-2));


        slope=p_AFA(1);
        slope_store_AFA(i, count_eyes)=slope;
        %DFA
        p_DFA=polyfit(lw_DFA,lF_DFA,1);
        yfit_DFA=polyval(p_DFA, lw_DFA);
        yresid_DFA=lF_DFA-yfit_DFA;
        SSE_DFA=sum(yresid_DFA.^2);
        RSS_d=SSE_DFA/length(yfit_DFA);
        AICc_DFA=log(RSS_d/297)+((297+3))/(297-3-2);

        slope=p_DFA(1);
        slope_store_DFA(i, count_eyes)=slope;

        %Store it

        storage_AFA(i,count_eyes)=SICc_AFA;
        storage_DFA(i,count_eyes)=SICc_DFA;
        count_eyes=count_eyes+1;
    end

    mild_count=mild_count+1;
end
%%
for j=1:21 %21 %Moderate Trials
    mod_pt_txt=num2str(mod_pt(j));
    count_eyes=1;

    for EO=1:3
        EO_txt=num2str(EO);
        filename=['Data2/2_' mod_pt_txt '_' EO_txt '_EO.mat'];
        load(filename)
%AFA
        p_AFA=polyfit(lw_AFA,lF_AFA,1);
        yfit_AFA=polyval(p_AFA, lw_AFA);
        yresid_AFA=lF_AFA-yfit_AFA;
```

```
    SSE_AFA=sum(yresid_AFA.^2);
    RSS=SSE_AFA/length(yfit_AFA);
    SICc_AFA=log(RSS/297)+(((297+3)))/(297-3-2);


    slope=p_AFA(1);
    slope_store_AFA(i, count_eyes)=slope;
    %DFA
    p_DFA=polyfit(lw_DFA,lF_DFA,1);
    yfit_DFA=polyval(p_DFA, lw_DFA);
    yresid_DFA=lF_DFA-yfit_DFA;
    SSE_DFA=sum(yresid_DFA.^2);
    RSS_d=SSE_DFA/length(yfit_DFA);
    SICc_DFA=log(RSS_d/297)+((3*log(297))/(297-3-2));

    slope=p_DFA(1);
    slope_store_DFA(i, count_eyes)=slope;
    %Store it
    storage_AFA(i,count_eyes)=SICc_AFA;
    storage_DFA(i,count_eyes)=SICc_DFA;
    count_eyes=count_eyes+1;
  end

  for EC=1:3
    EC_txt=num2str(EC);
    filename=['Data2/2_' mod_pt_txt '_' EC_txt '_EC.mat'];
    load(filename)

    %AFA
    p_AFA=polyfit(lw_AFA,lF_AFA,1);
    yfit_AFA=polyval(p_AFA, lw_AFA);
    yresid_AFA=lF_AFA-yfit_AFA;
    SSE_AFA=sum(yresid_AFA.^2);
    RSS=SSE_AFA/length(yfit_AFA);
    SICc_AFA=log(RSS/297)+((3*log(297))/(297-3-2));


    slope=p_AFA(1);
    slope_store_AFA(i, count_eyes)=slope;
    %DFA
    p_DFA=polyfit(lw_DFA,lF_DFA,1);
    yfit_DFA=polyval(p_DFA, lw_DFA);
    yresid_DFA=lF_DFA-yfit_DFA;
    SSE_DFA=sum(yresid_DFA.^2);
    RSS_d=SSE_DFA/length(yfit_DFA);
    SICc_DFA=log(RSS_d/297)+((3*log(297))/(297-3-2));

    slope=p_DFA(1);
    slope_store_DFA(i, count_eyes)=slope;
    %Store it
    storage_AFA(i,count_eyes)=SICc_AFA;
    storage_DFA(i,count_eyes)=SICc_DFA;
    count_eyes=count_eyes+1;
  end

  mod_count=mod_count+1;
end
```

File: “breakpoints_slope.m”

```
 %Melanie Weilert
%Biodynamics Lab

clear all; clc;
%Slope analysis: Assumption of 2 slopes, calculate SICc

%Mild: 11 healthy, 12 mild
mild_pt=[1001 1003 1006 1007 1008 1009 1010 1011 1012 1013 1014 3001 3002 3003 3004 3005 3006 3008 3009
3010 3011 3013 3014];
mild_count=1;
%Mod: 10 healthy, 11 mod
mod_pt=[1001 1002 1003 1004 1005 1006 1007 1008 1009 1010 4001 4002 4004 4005 4006 4007 4008 4009 4010
4011 4012];
mod_count=1;


%%
%Mild Trials

for i=1:23 %23 Mild Trials
    mild_pt_txt=num2str(mild_pt(i));
    count_eyes=1;

    for EO=1:3
        EO_txt=num2str(EO);
        filename=['Data2/1_' mild_pt_txt '_' EO_txt '_EO.mat'];
        load(filename)

        %AFA
        data_AFA=[lF_AFA, lw_AFA]; %[yval, xval]

        %Call a function that will calculate the slopes for you.
        [x_el_afa,y_f1_afa,y_f2_afa,y_fit_afa, slope1_afa, slope2_afa, length_s1_afa,length_s2_afa]=bp2(data_AFA);


%%%%%%%%%%%%%%%%%%%%%%%%%%%%%%%%%%%%%%%%%%%%%%%%
%FUNCTION CONTENT

%Melanie Weilert
%Biodynamics Lab

%This is a function that calls in a [yval, xval matrix].

%Function returns:  (1)location of the crossover point
%                   (2)x and y values of slope 1
%                   (3)x and y values of slope 2
%                   (4)slope1 and slope 2 values
%                   (5)length of slope1 and slope2 on log2(w)

function [x_el,y_f1,y_f2,y_fit, slope1, slope2, length_s1,length_s2]=bp2(data)

lF=data;
```

```
%Crossover points=k=[kx,ky]=[k,data(k)]
    for k=15:1:238   %5percent to 80percent of data as a crossover
        %Slope 1: y1=b1x
        b1=(data(k,1)-data(1,1))/(data(k,2)-data(1,2));    %Slope of 1
        Y1=data(1,1);         X1=data(1,2);
        a1=Y1-b1*X1;

        %Slope 2: y2=b2x
        b2=(data(end,1)-data(k,1))/(data(end,2)-data(k,2));    %Slope of 2
        Y2=data(end,1);       X2=data(end,2);
        a2=Y2-b2*X2;

        y_f1=polyval([b1 a1],data(1:k-1,2));
        y_f2=polyval([b2 a2],data(k:end,2));
        y_e=[y_f1' y_f2'];

        %Calculate Residual Sum of Squares
        RSS(k)=sum((data(:,1)-y_e').^2);
        RSS(RSS == 0) = NaN;
    end

        RSS_final=min(RSS);     %Crossover point.

        %Now to sub in the crossover point into the final actual slopes:
        x_el = find(RSS(:)==RSS_final);

        %Now estimate the slopes based off of these breakpoints.
        est_s1=polyfit(data(1:x_el,2),data(1:x_el,1),1);
        slope1=est_s1(1);
        est_s2=polyfit(data(x_el:end,2),data(x_el:end,1),1);
        slope2=est_s2(1);

        %If both slopes are great, then we want to plot them both.
          y_f1=polyval([est_s1(1) est_s1(2)],lF(1:x_el,2));
          y_f2=polyval([est_s2(1) est_s2(2)],lF(x_el+1:end,2));
          y_fit=[y_f1; y_f2];

        %Also want to produce lengths of the two slopes:
        length_s1=lF(x_el,2)-lF(1,2);
        length_s2=lF(end,2)-lF(x_el,2);
end

%%%%%%%%%%%%%%%%%%%%%%%%%%%%%%%%%%%%%%%%%%%%%%%

        yresid_AFA=lF_AFA-y_fit_afa;
        SSE_AFA=sum(yresid_AFA.^2);
        RSS=SSE_AFA/length(y_fit_afa);
        SICc_AFA=log(RSS/297)+((6*log(297))/(297-6-2));


    %DFA
    data_DFA=[lF_DFA, lw_DFA]; %[yval, xval]
    %Call a function that will calculate the slopes for you.
    [x_el_dfa,y_f1_dfa,y_f2_dfa,y_fit_dfa, slope1_dfa, slope2_dfa,
length_s1_dfa,length_s2_dfa]=bp2(data_DFA);

        yresid_DFA=lF_DFA-y_fit_dfa;
```

```
        SSE_DFA=sum(yresid_DFA.^2);
        RSS_d=SSE_DFA/length(y_fit_dfa);
        SICc_DFA=log(RSS_d/297)+((6*log(297))/(297-6-2));
per_diff_afa=abs(slope1_afa-slope2_afa)/(.5*(slope1_afa+slope2_afa))*100;
per_diff_dfa=abs(slope1_dfa-slope2_dfa)/(.5*(slope1_dfa+slope2_dfa))*100;
per_store_AFA(i,count_eyes)=per_diff_afa;
per_store_DFA(i,count_eyes)=per_diff_dfa;
    %Store it
    storage_AFA(i,count_eyes)=SICc_AFA;
    storage_DFA(i,count_eyes)=SICc_DFA;
          slope_store1_DFA(i, count_eyes)=slope1_dfa;
          slope_store1_AFA(i, count_eyes)=slope1_afa;
          slope_store2_DFA(i, count_eyes)=slope2_dfa;
          slope_store2_AFA(i, count_eyes)=slope2_afa;

          store_x_el_afa(i, count_eyes)=lw_AFA(x_el_afa);
          store_x_el_dfa(i, count_eyes)=lw_DFA(x_el_dfa);
    count_eyes=count_eyes+1;
  end

  for EC=1:3

    EC_txt=num2str(EC);
    filename=['Data2/1_' mild_pt_txt '_' EC_txt '_EC.mat'];
    load(filename)

    %AFA
    data_AFA=[lF_AFA, lw_AFA]; %[yval, xval]

    %Call a function that will calculate the slopes for you.
    [x_el_afa,y_f1_afa,y_f2_afa,y_fit_afa, slope1_afa, slope2_afa, length_s1_afa,length_s2_afa]=bp2(data_AFA);

        yresid_AFA=lF_AFA-y_fit_afa;
        SSE_AFA=sum(yresid_AFA.^2);
        RSS=SSE_AFA/length(y_fit_afa);
        SICc_AFA=log(RSS/297)+((6*log(297))/(297-6-2));

    %DFA
    data_DFA=[lF_DFA, lw_DFA]; %[yval, xval]
    %Call a function that will calculate the slopes for you.
    [x_el_dfa,y_f1_dfa,y_f2_dfa,y_fit_dfa, slope1_dfa, slope2_dfa,
length_s1_dfa,length_s2_dfa]=bp2(data_DFA);

        yresid_DFA=lF_DFA-y_fit_dfa;
        SSE_DFA=sum(yresid_DFA.^2);
        RSS_d=SSE_DFA/length(y_fit_dfa);
        SICc_DFA=log(RSS_d/297)+((6*log(297))/(297-6-2));
per_diff_afa=abs(slope1_afa-slope2_afa)/(.5*(slope1_afa+slope2_afa))*100;
per_diff_dfa=abs(slope1_dfa-slope2_dfa)/(.5*(slope1_dfa+slope2_dfa))*100;
per_store_AFA(i,count_eyes)=per_diff_afa;
per_store_DFA(i,count_eyes)=per_diff_dfa;
    %Store it
    storage_AFA(i,count_eyes)=SICc_AFA;
    storage_DFA(i,count_eyes)=SICc_DFA;
          slope_store1_DFA(i, count_eyes)=slope1_dfa;
          slope_store1_AFA(i, count_eyes)=slope1_afa;
          slope_store2_DFA(i, count_eyes)=slope2_dfa;
```

```
            slope_store2_AFA(i, count_eyes)=slope2_afa;

            store_x_el_afa(i, count_eyes)=lw_AFA(x_el_afa);
            store_x_el_dfa(i, count_eyes)=lw_DFA(x_el_dfa);
        count_eyes=count_eyes+1;
    end

    mild_count=mild_count+1;
end


%%
%Moderate Trials


for j=1:21 %21 Moderate Trials
    mod_pt_txt=num2str(mod_pt(j));
    count_eyes=1;

    for EO=1:3
        EO_txt=num2str(EO);
        filename=['Data2/2_' mod_pt_txt '_' EO_txt '_EO.mat'];
        load(filename)

        %AFA
        data_AFA=[lF_AFA, lw_AFA]; %[yval, xval]

        %Call a function that will calculate the slopes for you.
        [x_el_afa,y_f1_afa,y_f2_afa,y_fit_afa, slope1_afa, slope2_afa, length_s1_afa,length_s2_afa]=bp2(data_AFA);

            yresid_AFA=lF_AFA-y_fit_afa;
            SSE_AFA=sum(yresid_AFA.^2);
            RSS=SSE_AFA/length(y_fit_afa);
            SICc_AFA=log(RSS/297)+((6*log(297))/(297-6-2));

        %DFA
        data_DFA=[lF_DFA, lw_DFA]; %[yval, xval]
        %Call a function that will calculate the slopes for you.
        [x_el_dfa,y_f1_dfa,y_f2_dfa,y_fit_dfa, slope1_dfa, slope2_dfa,
length_s1_dfa,length_s2_dfa]=bp2(data_DFA);

            yresid_DFA=lF_DFA-y_fit_dfa;
            SSE_DFA=sum(yresid_DFA.^2);
            RSS_d=SSE_DFA/length(y_fit_dfa);
            SICc_DFA=log(RSS_d/297)+((6*log(297))/(297-6-2));
per_diff_afa=abs(slope1_afa-slope2_afa)/(.5*(slope1_afa+slope2_afa))*100;
per_diff_dfa=abs(slope1_dfa-slope2_dfa)/(.5*(slope1_dfa+slope2_dfa))*100;
per_store_AFA(i,count_eyes)=per_diff_afa;
per_store_DFA(i,count_eyes)=per_diff_dfa;
        %Store it
            slope_store1_DFA(i, count_eyes)=slope1_dfa;
            slope_store1_AFA(i, count_eyes)=slope1_afa;
            slope_store2_DFA(i, count_eyes)=slope2_dfa;
            slope_store2_AFA(i, count_eyes)=slope2_afa;

            store_x_el_afa(i, count_eyes)=lw_AFA(x_el_afa);
            store_x_el_dfa(i, count_eyes)=lw_DFA(x_el_dfa);
```

```
      storage_AFA(mod_count,count_eyes)=SICc_AFA;
      storage_DFA(mod_count,count_eyes)=SICc_DFA;

      count_eyes=count_eyes+1;
   end

   for EC=1:3

      EC_txt=num2str(EC);
      filename=['Data2/2_' mod_pt_txt '_' EC_txt '_EC.mat'];
      load(filename)

      %AFA
      data_AFA=[lF_AFA, lw_AFA]; %[yval, xval]

      %Call a function that will calculate the slopes for you.
      [x_el_afa,y_f1_afa,y_f2_afa,y_fit_afa, slope1_afa, slope2_afa, length_s1_afa,length_s2_afa]=bp2(data_AFA);

         yresid_AFA=lF_AFA-y_fit_afa;
         SSE_AFA=sum(yresid_AFA.^2);
         RSS=SSE_AFA/length(y_fit_afa);
         SICc_AFA=log(RSS/297)+((6*log(297))/(297-6-2));

      %DFA
      data_DFA=[lF_DFA, lw_DFA]; %[yval, xval]
      %Call a function that will calculate the slopes for you.
      [x_el_dfa,y_f1_dfa,y_f2_dfa,y_fit_dfa, slope1_dfa, slope2_dfa,
length_s1_dfa,length_s2_dfa]=bp2(data_DFA);

         yresid_DFA=lF_DFA-y_fit_dfa;
         SSE_DFA=sum(yresid_DFA.^2);
         RSS_d=SSE_DFA/length(y_fit_dfa);
         SICc_DFA=log(RSS_d/297)+((6*log(297))/(297-6-2));
per_diff_afa=abs(slope1_afa-slope2_afa)/(.5*(slope1_afa+slope2_afa))*100;
per_diff_dfa=abs(slope1_dfa-slope2_dfa)/(.5*(slope1_dfa+slope2_dfa))*100;
per_store_AFA(i,count_eyes)=per_diff_afa;
per_store_DFA(i,count_eyes)=per_diff_dfa;
      %Store it
      storage_AFA(mod_count,count_eyes)=SICc_AFA;
      storage_DFA(mod_count,count_eyes)=SICc_DFA;
            slope_store1_DFA(i, count_eyes)=slope1_dfa;
            slope_store1_AFA(i, count_eyes)=slope1_afa;
            slope_store2_DFA(i, count_eyes)=slope2_dfa;
            slope_store2_AFA(i, count_eyes)=slope2_afa;

            store_x_el_afa(i, count_eyes)=lw_AFA(x_el_afa);
            store_x_el_dfa(i, count_eyes)=lw_DFA(x_el_dfa);
      count_eyes=count_eyes+1;
   end

   mod_count=mod_count+1;
end
```

File: "breakpoints_3slope.m"

```
%Melanie Weilert
```

```
%Biodynamics Lab

clear all; clc;
%Slope analysis: Assumption of 2 slopes, calculate SICc

%Mild: 11 healthy, 12 mild
mild_pt=[1001 1003 1006 1007 1008 1009 1010 1011 1012 1013 1014 3001 3002 3003 3004 3005 3006 3008 3009
3010 3011 3013 3014];
mild_count=1;
%Mod: 10 healthy, 11 mod
mod_pt=[1001 1002 1003 1004 1005 1006 1007 1008 1009 1010 4001 4002 4004 4005 4006 4007 4008 4009 4010
4011 4012];
mod_count=1;


%%
%Mild Trials

for i=1:23 %23 Mild Trials
   mild_pt_txt=num2str(mild_pt(i));
   count_eyes=1;

   for EO=1:3
      EO_txt=num2str(EO);
      filename=['Data2/1_' mild_pt_txt '_' EO_txt '_EO.mat'];
      load(filename)

      %AFA
      data_AFA=[lF_AFA, lw_AFA]; %[yval, xval]

      %Call a function that will calculate the slopes for you.
      [x_el_1, x_el_3, y_f1,y_f2,y_f3, y_fit_afa, slope1, slope2, slope3,
length_s1,length_s2,length_s3]=bp3(data_AFA);

%%%%%%%%%%%%%%%%%%%%%%%%%%%%%%%%%%%%%%%%%%%%%%%FUNCTION
CONTENT

%Melanie Weilert
%Biodynamics Lab

%This is a function that calls in a [yval, xval matrix].

%Function returns:  (1)location of the crossover point
%                   (2)x and y values of slope 1
%                   (3)x and y values of slope 2
%                   (4)slope1 and slope 2 values
%                   (5)length of slope1 and slope2 on log2(w)

function [x_el_1, x_el_3, y_f1,y_f2,y_f3, y_fit, slope1, slope2, slope3, length_s1,length_s2,length_s3]=bp3(data)

half_pt=floor(length(data)/2);
lower_1=round(half_pt*0.05);
upper_1=round(half_pt*0.8);
lower_3=round(half_pt*0.05+half_pt);
upper_3=round(half_pt*0.8+half_pt);

lF=data;
```

```
for i=lower_1:upper_1
   %Slope 1: y1=b1x
        b1=(data(i,1)-data(1,1))/(data(i,2)-data(1,2));    %Slope of 1
        Y1=data(1,1);        X1=data(1,2);
        a1=Y1-b1*X1;

        %Slope 2: y2=b2x
        b2=(data(half_pt,1)-data(i,1))/(data(half_pt,2)-data(i,2));    %Slope of 2
        Y2=data(half_pt,1);       X2=data(half_pt,2);
        a2=Y2-b2*X2;

        y_f1=polyval([b1 a1],data(1:i-1,2));
        y_f2=polyval([b2 a2],data(i:end,2));
        y_e=[y_f1' y_f2'];

        %Calculate Residual Sum of Squares
        RSS_1(i)=sum((data(:,1)-y_e').^2);
        RSS_1(RSS_1 == 0) = NaN;
end
        RSS_final_1=min(RSS_1);     %Crossover point.

        %Now to sub in the crossover point into the final actual slopes:
        x_el_1 = find(RSS_1(:)==RSS_final_1);

        %Now estimate the slopes based off of these breakpoints.
        est_s1=polyfit(data(1:x_el_1,2),data(1:x_el_1,1),1);
        slope1=est_s1(1);

%%
for j=lower_3:upper_3
   %Slope 1: y1=b1x
        b1=(data(j,1)-data(half_pt,1))/(data(j,2)-data(half_pt,2));    %Slope of 1
        Y1=data(half_pt,1);        X1=data(half_pt,2);
        a1=Y1-b1*X1;

        %Slope 2: y2=b2x
        b2=(data(end,1)-data(j,1))/(data(end,2)-data(j,2));    %Slope of 2
        Y2=data(end,1);       X2=data(end,2);
        a2=Y2-b2*X2;

        y_f1_3=polyval([b1 a1],data(1:j-1,2));
        y_f2_3=polyval([b2 a2],data(j:end,2));
        y_e_3=[y_f1_3' y_f2_3'];

        %Calculate Residual Sum of Squares
        RSS_3(j)=sum((data(:,1)-y_e_3').^2);
        RSS_3(RSS_3 == 0) = NaN;
end
        RSS_final_3=min(RSS_3);     %Crossover point.

        %Now to sub in the crossover point into the final actual slopes:
        x_el_3 = find(RSS_3(:)==RSS_final_3);

        %Now estimate the slopes based off of these breakpoints.
        est_s3=polyfit(data(x_el_3:end,2),data(x_el_3:end, 1),1);
        slope3=est_s3(1);
```

```
%%
%Slope 2

est_s2=polyfit(data(x_el_1:x_el_3,2),data(x_el_1:x_el_3,1),1);
slope2=est_s2(1);


         %If both slopes are great, then we want to plot them both.
            y_f1=polyval([est_s1(1) est_s1(2)],lF(1:x_el_1-1,2));
            y_f2=polyval([est_s2(1) est_s2(2)],lF(x_el_1:x_el_3,2));
            y_f3=polyval([est_s3(1) est_s3(2)],lF(x_el_3+1:end,2));
            y_fit=[y_f1; y_f2; y_f3];

         %Also want to produce lengths of the two slopes:
         length_s1=lF(x_el_1,2)-lF(1,2);
         length_s2=lF(x_el_3,2)-lF(x_el_1,2);
         length_s3=lF(end,2)-lF(x_el_3,2);

%%%%%%%%%%%%%%%%%%%%%%%%%%%%%%%%%%%%%%%%%%%%%%%%%%%%%%%%%%%%%%%%%%%%%%%%

         yresid_AFA=lF_AFA-y_fit_afa;
         SSE_AFA=sum(yresid_AFA.^2);
         RSS=SSE_AFA/length(y_fit_afa);
         SICc_AFA=log(RSS/297)+((8*log(297))/(297-8-2));


            slope_store1_AFA(i, count_eyes)=slope1;
            slope_store2_AFA(i, count_eyes)=slope2;
            slope_store3_AFA(i, count_eyes)=slope3;
            store_x_el1_afa(i, count_eyes)=lw_AFA(x_el_1);
            store_x_el3_afa(i, count_eyes)=lw_AFA(x_el_3);

      %DFA
      data_DFA=[lF_DFA, lw_DFA]; %[yval, xval]
      %Call a function that will calculate the slopes for you.
      [x_el_1, x_el_3, y_f1,y_f2,y_f3, y_fit_dfa, slope1, slope2, slope3,
length_s1,length_s2,length_s3]=bp3(data_DFA);

         yresid_DFA=lF_DFA-y_fit_dfa;
         SSE_DFA=sum(yresid_DFA.^2);
         RSS_d=SSE_DFA/length(y_fit_dfa);
         SICc_DFA=log(RSS_d/297)+((8*log(297))/(297-8-2));

      %Store it
      storage_AFA(i,count_eyes)=SICc_AFA;
      storage_DFA(i,count_eyes)=SICc_DFA;

      count_eyes=count_eyes+1;
   end

   for EC=1:3

      EC_txt=num2str(EC);
      filename=['Data2/1_' mild_pt_txt '_' EC_txt '_EC.mat'];
      load(filename)

      %AFA
```

```
      data_AFA=[lF_AFA, lw_AFA]; %[yval, xval]

      %Call a function that will calculate the slopes for you.
      [x_el_1, x_el_3, y_f1,y_f2,y_f3, y_fit_afa, slope1, slope2, slope3,
length_s1,length_s2,length_s3]=bp3(data_AFA);

         yresid_AFA=lF_AFA-y_fit_afa;
         SSE_AFA=sum(yresid_AFA.^2);
         RSS=SSE_AFA/length(y_fit_afa);
         SICc_AFA=log(RSS/297)+((8*log(297))/(297-8-2));
                  slope_store1_AFA(i, count_eyes)=slope1;
            slope_store2_AFA(i, count_eyes)=slope2;
            slope_store3_AFA(i, count_eyes)=slope3;
            store_x_el1_afa(i, count_eyes)=lw_AFA(x_el_1);
            store_x_el3_afa(i, count_eyes)=lw_AFA(x_el_3);
      %DFA
      data_DFA=[lF_DFA, lw_DFA]; %[yval, xval]
      %Call a function that will calculate the slopes for you.
      [x_el_1, x_el_3, y_f1,y_f2,y_f3, y_fit_dfa, slope1, slope2, slope3,
length_s1,length_s2,length_s3]=bp3(data_DFA);

         yresid_DFA=lF_DFA-y_fit_dfa;
         SSE_DFA=sum(yresid_DFA.^2);
         RSS_d=SSE_DFA/length(y_fit_dfa);
         SICc_DFA=log(RSS_d/297)+((8*log(297))/(297-8-2));

      %Store it
      storage_AFA(i,count_eyes)=SICc_AFA;
      storage_DFA(i,count_eyes)=SICc_DFA;

      count_eyes=count_eyes+1;
   end

   mild_count=mild_count+1;
end


%%
%Moderate Trials


for j=1:21 %21 Moderate Trials
   mod_pt_txt=num2str(mod_pt(j));
   count_eyes=1;

   for EO=1:3
      EO_txt=num2str(EO);
      filename=['Data2/2_' mod_pt_txt '_' EO_txt '_EO.mat'];
      load(filename)

      %AFA
      data_AFA=[lF_AFA, lw_AFA]; %[yval, xval]

      %Call a function that will calculate the slopes for you.
      [x_el_1, x_el_3, y_f1,y_f2,y_f3, y_fit_afa, slope1, slope2, slope3,
length_s1,length_s2,length_s3]=bp3(data_AFA);
```

```
        yresid_AFA=lF_AFA-y_fit_afa;
        SSE_AFA=sum(yresid_AFA.^2);
        RSS=SSE_AFA/length(y_fit_afa);
        SICc_AFA=log(RSS/297)+((8*log(297))/(297-8-2));
                slope_store1_AFA(i, count_eyes)=slope1;
           slope_store2_AFA(i, count_eyes)=slope2;
           slope_store3_AFA(i, count_eyes)=slope3;
           store_x_el1_afa(i, count_eyes)=lw_AFA(x_el_1);
           store_x_el3_afa(i, count_eyes)=lw_AFA(x_el_3);
     %DFA
     data_DFA=[lF_DFA, lw_DFA]; %[yval, xval]
     %Call a function that will calculate the slopes for you.
     [x_el_1, x_el_3, y_f1,y_f2,y_f3, y_fit_dfa, slope1, slope2, slope3,
length_s1,length_s2,length_s3]=bp3(data_DFA);

        yresid_DFA=lF_DFA-y_fit_dfa;
        SSE_DFA=sum(yresid_DFA.^2);
        RSS_d=SSE_DFA/length(y_fit_dfa);
        SICc_DFA=log(RSS_d/297)+((8*log(297))/(297-8-2));

     %Store it
     storage_AFA(mod_count,count_eyes)=SICc_AFA;
     storage_DFA(mod_count,count_eyes)=SICc_DFA;

     count_eyes=count_eyes+1;
  end

  for EC=1:3

     EC_txt=num2str(EC);
     filename=['Data2/2_' mod_pt_txt '_' EC_txt '_EC.mat'];
     load(filename)

     %AFA
     data_AFA=[lF_AFA, lw_AFA]; %[yval, xval]

     %Call a function that will calculate the slopes for you.
     [x_el_1, x_el_3, y_f1,y_f2,y_f3, y_fit_afa, slope1, slope2, slope3,
length_s1,length_s2,length_s3]=bp3(data_AFA);

        yresid_AFA=lF_AFA-y_fit_afa;
        SSE_AFA=sum(yresid_AFA.^2);
        RSS=SSE_AFA/length(y_fit_afa);
        SICc_AFA=log(RSS/297)+((8*log(297))/(297-8-2));
                slope_store1_AFA(i, count_eyes)=slope1;
           slope_store2_AFA(i, count_eyes)=slope2;
           slope_store3_AFA(i, count_eyes)=slope3;
           store_x_el1_afa(i, count_eyes)=lw_AFA(x_el_1);
           store_x_el3_afa(i, count_eyes)=lw_AFA(x_el_3);
     %DFA
     data_DFA=[lF_DFA, lw_DFA]; %[yval, xval]
     %Call a function that will calculate the slopes for you.
     [x_el_1, x_el_3, y_f1,y_f2,y_f3, y_fit_dfa, slope1, slope2, slope3,
length_s1,length_s2,length_s3]=bp3(data_DFA);

        yresid_DFA=lF_DFA-y_fit_dfa;
        SSE_DFA=sum(yresid_DFA.^2);
```

```
        RSS_d=SSE_DFA/length(y_fit_dfa);
        SICc_DFA=log(RSS_d/297)+((8*log(297))/(297-8-2));

      %Store it
      storage_AFA(mod_count,count_eyes)=SICc_AFA;
      storage_DFA(mod_count,count_eyes)=SICc_DFA;

      count_eyes=count_eyes+1;
    end

    mod_count=mod_count+1;
end
```